UCL
Université
catholique
de Louvain

Faculté d'ingénierie biologique,
agronomique et environnementale

Earth and Life Institute
Environmental Sciences
Soil Science

Impact of tree species on silicon cycling in temperate soil-tree systems

Jean-Thomas Cornelis
Louvain-la-Neuve, MAI 2010

Thèse présentée en vue de l'obtention du grade de docteur en sciences agronomiques et ingénierie biologique

Membres du jury :

President	Prof. Jacques Mahillon (UCL, Belgium)
Promoteurs	Prof. Bruno Delvaux (UCL, Belgium)
	Dr. Jacques Ranger (INRA, France)
Lecteurs	Prof. Luc André (MRAC, Belgium)
	Prof. Yves Lucas (U. du Sud-Toulon, France)
	Prof. Marnik Vanclooster (UCL, Belgium)
	Prof. Dominique Weis (UBC, Canada)

A la rencontre aux antipodes de la vie,

Anna, Abigail et Nestor.

Noble Soleil qui prodigue la chaleur
Et par le même geste prodigue l'ombre qui nous abrite
Soleil qui mûrit les grappes et les corps pour la fête
Puis se retire afin que nous puissions célébrer
Soleil qui ferme les yeux sur nos excès, sur nos folies de mortels
Et qui est là le lendemain, d'humeur égale, d'égale générosité
Il n'attend de nous ni gratitude ni soumission
Noble est notre Soleil quand il se lève
Et noble quand il se couche…

La fille d'Athimar en était à ces mots lorsque Mani cessa de souffrir (un lundi, le 2 mars 274)

Remerciements

«… Les théories viennent et disparaissent rapidement. Chacune sert un moment à classer les faits connus et à stimuler la recherche de faits nouveaux. Chaque théorie manifeste à son tour son impuissance à s'accommoder avec des faits nouvellement découverts… ». Depuis 4 ans au sein du laboratoire des Sciences du Sol, c'est avec grand intérêt que je tente d'appliquer la démarche scientifique, telle que décrite ci-dessus par le philosophe-mathématicien Bertrand Russel (1872-1970). La démarche scientifique est tel un champ de bataille où la rivalité entre angoisse et initiative, désillusion et découverte, impatience et connaissance, berce sainement notre quotidien en titillant constamment notre imagination. En lisant une réflexion du philosophe-biologiste Henri Laborit (1914-1995), je me suis rendu compte de la chance que nous avions de pouvoir stimuler notre créativité à travers l'expérimentation et l'innovation : « … *Une structure sociale dont les hiérarchies de pouvoir, de consommation, de propriété, de notabilité, sont entièrement établies sur la productivité de marchandises, ne peut que favoriser la mémoire et l'apprentissage des concepts et des gestes efficaces dans les processus de la production. Elle supprime le désir et le remplace par l'envie qui stimule non la créativité, mais le conformisme bourgeois ou pseudo-révolutionnaire… ».*

Etant donné que nous ne sommes rien sans les autres, je ne pourrais clore ce chapitre de ma vie sans remercier toutes les personnes qui m'ont soutenu et m'ont permis de réaliser et vivre mes passions.

Tout d'abord, je remercie sincèrement *Bruno Delvaux* de m'avoir ouvert les portes de son laboratoire en mai 2005 pour réaliser mon mémoire et d'avoir, ensuite, accepté d'encadrer ma thèse. Malgré votre emploi du temps surchargé et vos hautes responsabilités au sein de notre *Alma Mater*, vous avez toujours mis un point d'honneur à libérer un peu de votre temps pour m'écouter, me motiver, me conseiller et me « recadrer ». Votre enthousiasme et votre passion pour les sciences, le tout dans un esprit enclin de chaleur humaine, ont été un cadre très prolifique à la réalisation de mes recherches. Pour anecdote, lors de mon arrivée à l'UCL, ma curiosité pour les vins venait tout juste d'être semée. Mais, au fur et à mesure que nos entretiens au décanat se transformaient en cours d'œnologie, votre passion pour la relation entre typicité des vins et typologie des sols a rapidement fait germer ma curiosité en véritable hobby. Je vous adresse, ici, mes plus chaleureux remerciements pour la confiance que vous m'avez accordée ; en espérant pouvoir encore voyager ensemble à travers la dégustation de grands crus.

Ma thèse n'aurait pas eu lieu sans la fructueuse collaboration mise en place avec le laboratoire de Biogéochimie des Ecosystèmes Forestiers (INRA-Champenoux). Cette collaboration m'a permis d'avoir accès à l'exceptionnel site forestier de Breuil-Chenue (Morvan, France). Je remercie tout particulièrement *Jacques Ranger*, co-promoteur de ma thèse. Merci pour votre accueil, vos encouragements, votre disponibilité et vos conseils pragmatiques dans le domaine des cycles biogéochimiques forestiers. Travailler avec une équipe aussi aimable est un réel plaisir ; merci à *Marie-Pierre Turpault*, *Pascal Bonnaud*, *Etienne Dambrinne, Dominique Gelhaye* et *Louis Mareschal.*

A travers la collaboration établie avec le Musée Royale d'Afrique Centrale (MRAC), j'ai pu découvrir le monde, tout aussi rigoureux que prometteur, de la géochimie isotopique. Je tiens à remercier *Luc André* d'avoir accepté et soutenu ce projet de recherche. Merci à toute son équipe de Géologie et Minéralogie pour son accueil (*Kathrin Abraham, Camille Delvigne, François Fripiat, Harold Hughes, Frédéric Planchon* et *Pierre-Denis Plisnier*) ; ainsi qu'à *Laurence Monin* et *Nourdine Dahkani* pour leurs bons conseils et particulièrement à *Damien Cardinal* et *Sophie Opfergelt* de m'avoir transmis leur rigueur scientifique dans le domaine de la chimie isotopique. Merci aussi à *Nadine Matielli* et *Jeroen de Jong* (ULB) pour l'accès au MC-ICP-MS, machine incroyablement performante mais tellement redoutable à dompter.

La prolifique collaboration entre ces trois groupes de recherche m'a permis d'avancer en toute sérénité durant ma thèse.

Je voudrais également remercier *Jospeh Dufey* pour ses nombreux conseils avisés lors de mes 3 derniers mois de rédaction. C'est un plaisir de pouvoir côtoyer son humour, son côté « pince sans rire » et ses anecdotes au quotidien. J'adresse aussi mes remerciements à *Hugues Titeux* qui a su me faire apprécier la pédologie à travers sa conception de la recherche et nos longues et nombreuses discussions. Merci pour tous les moments scientifiques et autres (je pense à nos sorties sur le terrain et à nos sorties chez Francis) que nous avons pu passer ensemble.

Je tiens également à remercier les membres de mon jury d'avoir consacré de leur précieux temps à juger ce travail afin d'en améliorer la qualité. J'exprime donc ma reconnaissance à Madame *Dominique Weis* et Messieurs *Luc André*, *Yves Lucas* et *Marnik Vanclooster*.

L'excellente ambiance qui règne au sein de notre laboratoire des Sciences du Sol est au niveau de la qualité du travail qui y est réalisé. Pour toutes les analyses effectuées, leurs nombreux conseils en laboratoire et sur le terrain, leur bonne humeur, leur attention et l'amitié qui en est née ; merci à *Claudine Givron*, *Anne Iserentant*, *André Lannoye* et *Patrick Populaire*. Sans vous et votre expertise, notre laboratoire rentrerait certainement dans une phase d'hibernation. Un merci particulier à *Françoise Hauwen* pour son encadrement administratif et l'attention qu'elle apporte à notre bien être. Chers collègues, les pauses café et l'imagination débordante de Monseigneur Le Hat, les activités extra-professionnelles, les congrès, les petits moments de détente en terrasse, les discussions idéologiques ou pas ont toujours été des moments très agréables à vivre en votre compagnie. A vous *Isabelle Caignet*, *Eléonore Couder*, *Séverine Delstanche*, *Océane Derzelle*, *Claudine Givron*, *Françoise Hauwen*, *Céline Henriet, Anne Iserentant*, *Lucie Kablan*, *Céline Meunier*, *Sophie Opfergelt*, *Florence Trum*, *Thomas Delfosse*, *Bruno Delvaux*, *Joseph Dufey*, *David Houben*, *André Lannoye*, *Benoît Pereira*, *Patrick Populaire*, *Hugues Titeux*, *Arnaud Schneider* et *Philippe Sonnet,* je tiens à vous dire que je suis heureux de vous avoir rencontrés et côtoyés. Je n'oublie pas l'agréable collaboration avec *Anouck Lambin, Sébastien Mauro* et *Mathijs Dumon* pour leur mémoire, *Laurence Ryelandt* (UCL-EPL) de m'avoir formé à la microscopie électronique à balayage, *Sophie Chassery* (Ut2a-Pau) et *Delphine Yeghicheyan* (SARM-CRPG) pour les analyses Ge.

La vie est aussi faite (et heureusement !) de magnifiques rencontres fortuites dont la diversité et le mystère en font la magie. L'équipe de feu l'ACFA, le groupe de recherche « Forêt, Nature & Société », mais aussi plus particulièrement, *Carine De Meyer*, *Christine Farcy*, *Anne-Laure Jacquemart*, *Mélanie Weynants*, *Caroline Vincke*, *Olivier Baudry*, *Damien Debecker*, *Tom Dedeurwaerdere*, *Hervé Dupré*, *Grégory Duveiller*, *Bernard Feltz*, *Mathieu Javaux, Mathieu Jonard*, *Eric Laloy, Pierre Lhoir, Jean-Pierre Misson*, *Alain*

Servais et *Eric Van Ranst* ; que le temps qu'ils m'ont consacré à discuter sciences et toutes autres choses soit ici salué.

Mes sincères remerciements au *FNRS* pour le mandat FRIA et le soutien financier qui m'a été octroyé afin de réaliser mes recherches dans les meilleures conditions.

Au coin d'un bar à refaire le monde ou d'un feu dans un endroit perdu, à l'occasion d'une randonnée en montagne, durant nos années de scoutisme, lors de sorties étudiantes où nous étions censés rentrer tôt, vous, chers ami(e)s, vous m'avez comblé de bonheur. En écrivant ces quelques mots, je pense à la magie et la grandeur de l'*Amitié*. A vous qui vous reconnaitrez ici, soyez remerciés pour ces moments de pur bonheur !

Outre la génétique, il est souvent reconnu que les êtres vivants évoluent à 50% de par leur environnement. Mes derniers remerciements, et pas des moindres, vont donc à ma *famille* pour tout le bien-être que je ressens à ses côtés. Merci à mes parents pour leur présence en toute circonstance, à Damien de jouer pleinement son rôle de grand frère, à mon jumeau, Mathieu, de m'avoir ouvert l'esprit sur la philosophie des sciences à travers de nombreuses discussions et à ma belle-famille (j'ai ici une pensée profonde et émue pour toi, Nestor). A toi, Florence, ma petite, quelle chance j'ai eue de te rencontrer.

TABLE OF CONTENTS

Chapter 1:

Chapter 2:

Chapter 3:

Chapter 4:

Tree species impact the terrestrial cycle of silicon through various uptakes 51

Chapter 5:

The contrasting silicon uptakes by coniferous trees: a hydroponic experiment on young seedlings 75

Chapter 6:

Distribution of amorphous silica in a temperate forest soil under three common tree species ... 89

Chapter 7:

Tracing mechanisms controlling the release of dissolved silicon in forest soil solutions using Si isotopes and Ge/Si ratios ... 107

Chapter 8:

Chapter 9:

Appendix A:

Appendix B:

Appendix C:

Appendix D:

Summary

The distribution and origin of silicon (Si) in the soil-tree system has not been thoroughly researched, despite the crucial role of the terrestrial Si cycle in major biogeochemical processes due to its close linkage with other cycles (*i.e.* N, P and C).

The PhD thesis focuses on Si cycling in temperate forest ecosystems to investigate the effect of tree species on Si distribution in soil-tree systems and the relative role of biogenic and litho/pedogenic Si pools in the release of dissolved Si (DSi) in the aqueous phase. Our field location is a forest site in Central France (Morvan) with granitic bedrock combining various tree species in identical climate and soil conditions.

Tree species clearly influence Si uptake rates and can affect Si transfer to hydrosphere since the DSi leaching from the soil profile is negatively correlated to the Si uptake by forest vegetation. In the top organic horizons, tree species impact (i) the amorphous Si (ASi) pool through contrasting Si uptake and restitution of biogenic ASi (phytoliths) to the topsoil and (ii) the litho/pedogenic Si distribution through different incorporation rates of silicate minerals by bioturbation. In underlying mineral soil horizons, pedogenic processes such as opaline sphere formation and ASi sorption onto Fe oxides can hide the impact of tree species on ASi distribution. In order to study the origin of DSi in shallow soil solutions, we measured Si isotope compositions and Ge/Si ratios in the different compartments of the soil-tree system. Relative to the granitic bedrock, clay-sized minerals are enriched in ^{28}Si and have high Ge/Si ratio while biogenic Si from phytoliths is enriched in ^{28}Si and has low Ge/Si ratio. The forest floor solutions are clearly enriched in ^{28}Si and Ge relative to granite. This finding suggests that the release of DSi in shallow soil solutions is greatly influenced by the partial dissolution of secondary clay-sized minerals incorporated by bioturbation in organic-rich horizons. In the temperate soil-tree system studied, tree species thus influence the DSi content in forest floor solutions through various bioturbation rates and, to a lesser extent, through different ways of Si biocycling. Furthermore, this study opens up new horizons to assess the relative impact of biological and pedogenic processes on the carbon dynamic in forest soils.

Résumé

La distribution et l'origine du silicium (Si) dans le système sol-arbre sont encore peu étudiées malgré le lien étroit entre le cycle terrestre du Si et les cycles biogéochimiques globaux du carbone, de l'azote et du phosphore. A travers une étude détaillée du cycle du Si dans des écosystèmes forestiers tempérés, nos recherches visent à quantifier l'impact des essences forestières sur la distribution du Si dans les systèmes sol-arbre et la contribution relative des pools de Si biogénique et litho/pédogénique à la libération de Si dissous (DSi) en phase aqueuse. Notre étude est réalisée dans un site forestier expérimental (Morvan, France) caractérisé par un matériau parental granitique combinant différentes essences forestières dans des conditions climatique et pédologique identiques.

L'absorption végétale annuelle de Si varie selon le type d'essence forestière et influence, en partie, le flux de Si vers l'hydrosphère étant donné que le lessivage de Si à partir des profils de sol est négativement corrélé au prélèvement de Si par la végétation forestière. Dans les horizons organiques de surface, le contenu en silice amorphe (ASi) est significativement différent selon le type d'essence forestière étant donné les taux de prélèvement et de restitution de Si biogénique amorphe différents. Dans ces mêmes horizons, la distribution du Si litho/pédogénique est dépendante du type d'essences forestières suite à des taux d'incorporation des minéraux du sol par bioturbation différents selon l'activité biologique du milieu. Dans les horizons minéraux, les processus pédogéniques tels que la formation de sphère d'opale et l'adsorption de ASi sur les oxides de Fe ne nous permet pas de mettre en évidence un effet caractéristique du type d'essence forestière sur la distribution de ASi. Finalement, nous avons interprété les compositions isotopiques et les rapports Ge/Si des différents compartiments du système sol-arbre afin d'étudier l'origine du DSi dans les solutions de litières forestières. Par rapport au granite, les minéraux de la fraction argileuse sont enrichis en isotopes légers du Si (^{28}Si) et ont un rapport Ge/Si élevé alors que les phytolithes (BSi) sont enrichis en ^{28}Si et ont de faibles rapports Ge/Si. Le fait que les lixiviats des horizons organiques soient enrichis en ^{28}Si et en Ge par rapport au granite révèle que la libération de DSi dans les horizons organiques de surface est fortement influencée par la dissolution partielle des minéraux secondaires de la fraction argileuse. Le type d’essence forestière influence donc le contenu en DSi des lixiviats de litière à travers différents taux de bioturbation et, dans une moindre mesure, à travers des taux de prélèvement de Si différents. Par ailleurs, cette étude ouvre de nouvelles perspectives afin d’évaluer l’impact relatif des processus biologiques et pédogéniques sur la dynamique du carbone dans les sols forestiers.

CHAPTER 1:

INTRODUCTION

1.1 Thesis context

Geological records provide evidence that natural phenomena control global climate changes throughout Earth’s history. On shorter timescales ($<10^3$ years), greenhouse gas concentrations in the atmosphere, such as carbon dioxide (CO2), have risen continually since the industrial revolution, causing an increase in the average global surface temperature of 0.6°C since the late 19th century (IPCC, 2001). Accordingly, the global C cycle plays a major role in the Earth's global balance through the control of atmospheric CO2 concentration, which is closely connected to energy demand. World energy consumption increased from 11.5×10^{18} J in 1860 to 463×10^{18} J in 2005 and 850×10^{18} J are forecast for 2050. The exponential increase in world population is the principal motor behind such a dramatic surge. Global population, reckoned a mere 3 000 people half a million years ago, stood at 1 billion in 1800, 6.0 billion in 2000, and is projected to reach 9.2 billion in 2050 before stabilizing at 10 billion by 2100 (Lal, 2010).

Through population development, industrialization and domination of the productivity concept, human beings strongly influence the environment and its homeostasis, leading to excess and/or depletion of certain (in-)organic constituents in some specific environments. As a consequence, the global biogeochemical cycles that describe the circulation of elements from non-living lithosphere to living biosphere and back to the non-living environment, are changing drastically on short timescales ($<10^3$ years), and this scenario is widely modifying global earth processes such as climate. Is this disturbance reversible? What is the relative human contribution in relation to natural processes? How can scientific hypotheses be combined to improve the environment of our planet? How to have a beneficial effect on the balance of an element without adversely affecting the balance of other constituents? Consequent to these current issues, the study of biogeochemical cycles has become increasingly relevant to the future of *Homo sapiens*, the “knowing man”.

In the biogeochemical cycles, soils play a major role as they are essential to the functioning of the terrestrial biosphere. The biogeochemical approach provides a pertinent framework for managing the environment reshaped by human beings in the best possible way. Indeed, an understanding of the dynamics of (in)-organic constituents in a soil-plant system is vital to preserve the Earth's surface environment while ensuring biomass production, which is related to the future needs of humanity.

Since 1971, the Scientific Committee on Problems of the Environment (SCOPE) has synthesized information on the complex dynamic of biogeochemical elements between various compartments of the environment. In this regard, the Scientific Committee has recently stressed the importance of the global silicon (Si) cycle (Ittekkot et al., 2006), given its close linkage with other cycles (*i.e.* N, P and C). The global Si cycle is now at the core of the Land-Ocean Nutrient Fluxes project conducted by the SCOPE of the International Council for Science (Ittekkot et al., 2006).

1.2 Thesis background

1.2.1 Global Si cycle

Si is the second most abundant element in the Earth's crust (28.8 wt%) (Wedepohl, 1995) and occurs in primary silicate minerals, secondary aluminosilicates and various forms of SiO_2, which makes it almost ubiquitous within the lithosphere. The rocks and silicate minerals undergo physical and chemical weathering that contribute to the dissolved and suspended load of materials carried by rivers. The dissolved silicon (DSi), as monosilicic acid H_4SiO_4, is a major solute of river discharge into oceans (Gaillardet et al., 1999a). Consequently, the leaching of DSi from soil to river strongly impacts the oceanic Si cycle, as land-river fluxes contribute to more than 80% of the net DSi input in the oceans (Tréguer et al., 1995). The global Si cycle presented in Figure 1.1 show the terrestrial Si cycle which feeds the marine Si cycle through dissolved and/or particulate Si transport.

On its transfer from land to oceans, a part of DSi released in aqueous phase by silicate weathering is involved in several biogeochemical dynamics processes, which would widely control the DSi fluxes to the world oceans. Considering the continental Si cycle and focusing on the soil-plant system, H_4SiO_4 can be taken up from soil solutions by the roots of terrestrial plants. Monosilicic acid is then translocated to transpiration sites where it polymerizes as amorphous biogenic opal, called phytoliths ($SiO_2.nH_2O$) (Jones and Handreck, 1965). The phytoliths (BSi) return to the topsoil through litterfall and organic matter decomposition, where they can be preserved or dissolved. Once DSi is released in aqueous phase of soil by silicate weathering and/or BSi dissolution, it can be (i) taken up by plants, (ii) adsorbed onto Fe and Al (hydr)oxides, (iii) incorporated into secondary precipitates, and (iv) leached out from the soil profile to rivers.

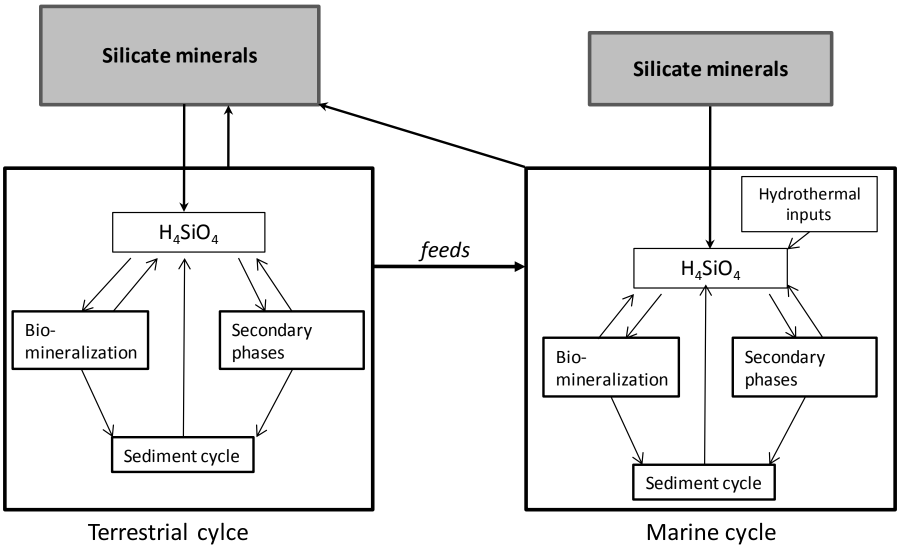

Figure 1.1 The coupled terrestrial and marine biogeochemical cycles of silicon. Silicate minerals replenishment is dependent upon geotectonic processes, such as mountain building and subduction (adapted from Exley, 1998).

In the hydrosphere, Si represents an essential nutrient for phytoplankton such as diatoms which account for 45% of total marine primary production and thus play a crucial role in the marine food chain (Mann, 1999). The ocean carbon budget is largely influenced by Si biomineralization rates since diatoms are of fundamental importance for CO_2 conversion into organic carbon on ocean surfaces by the so-called biological pump and the subsequent organic carbon export to the deep ocean (Smetacek, 1998; Ragueneau et al., 2000). Thus any perturbation in the Si land-ocean transfer by natural and/or anthropogenic factors could have a significant impact on ocean capacity to regulate atmospheric CO_2 (Ittekot et al., 2006).

Besides Si essentiality for phytoplankton CO_2-consumers (Tréguer and Pondaven, 2000), the interaction between Si and C cycles also regulates atmospheric C through silicate weathering (Berner, 1995). During the weathering of Ca and Mg-silicate minerals, atmospheric CO_2 is converted to dissolved HCO_3^- which can then be removed from the oceans in the form of carbonate minerals. On the geological timescale, the drawdown of atmospheric CO_2 is balanced by equivalent CO_2-liberating processes such as neoformation of silicates, volcanic outgassing and the burial of $CaCO_3$ and organic matter (Berner et al., 1983; Walker et al., 1981). Chemical weathering creates a crucial negative feedback to prevent the development of a runaway greenhouse or icehouse effect as CO_2 consumption by silicate weathering increases with rising temperatures. Conversely, as atmospheric CO_2 decreases, the global cooling involves a decrease in CO_2 consumption by weathering (Berner, 1995).

In addition, the beneficial effects of Si on the growth of higher plants have been reported in a wide variety of crops, including rice, wheat, barley, and cucumber (Ma et al., 2001; Korndorfer and Lepsch, 2001; Ma and Takahashi, 2002; Ma, 2004) because Si improves their biomass production under stress conditions (Epstein, 1999). Silica deposition in leaves allows them to assume a more upright position favoring light interception and promoting photosynthesis (Epstein, 1994; Marschner, 1995). Hence, the beneficial effects of Si for some terrestrial plants could indirectly regulate atmospheric CO_2 through an increase of photosynthesis and biomass production.

Finally, the formation of short-range ordered aluminosilicates in soils (*e.g.* allophane and imogolite) is widely controlled by Si and Al activities in soil solutions (Wada, 1989). As these poorly crystalline minerals largely control the amount of organic carbon stabilized in soils, Si dynamics in a soil-plant system should directly affect the sequestration of atmospheric CO_2 in soils (Basile-Doelsch et al., 2007).

As a consequence, the ongoing efforts to understand the global Si cycle are timely because of its close link with global change processes through silicate weathering, diatom growth, the beneficial Si effects on plant growth and the organic carbon storage in soils.

1.2.2 Si in soil-plant systems

In terrestrial environments, higher plants can impact the hydrological output of DSi through root-induced silicate weathering but also through Si uptake and BSi restitution *via* litterfall. Land plants and their associated microbiota directly affect silicate mineral weathering in several ways by (i) affecting the soil temperature, (ii) protecting soil against erosion, (iii) generation of chelating ligands, (iv) modifying pH through production of CO_2 and organic acids, (v) altering the soil's physical properties, and (vi) nutrient uptake (Drever, 1994; Hinsinger et al., 2001). The study by Moulton et al., (2000) confirms these findings as solute fluxes exported from vegetated areas were shown to be about four times larger than those measured in bare areas. Berner (1997) shows that the activities of rooted vascular plants during the Devonian Period (400 to 360 million years ago) resulted in enhanced weathering and enhanced removal of atmospheric CO_2.

On geological timescales, we consider that all products of weathering are ultimately transported from the continents to the oceans. On shorter timescales, part of the DSi released by mineral weathering is cycled through vegetation on the Earth's surface (Conley et al., 2006). Si biocycling should be influenced by species as plants greatly differ in their ability to accumulate Si in their aerial parts, ranging from 0.1 to 10% of dry weight (Raven, 1983; Marschner, 1995; Epstein, 1999; Hodson et al., 2005; Ma and Yamaji, 2006a). The Si accumulation also depends on factors extrinsic to the plant such as soil mineralogical composition (Klein and Geis, 1978; Henriet et al., 2008a,b), the kinetic dissolution of various Si-containing solid phases in soils (Sommer et al., 2006), transpiration rate and availability of silicic acid in the soil solution (Jones and Handreck, 1967; Hodson and Sangster, 1999).

Terrestrial plants largely contribute to the global Si pool since annual BSi production ranges from 1.7 to 5.6×10^{12} kg Si yr^{-1} (Conley, 2002) and rivals that produced by diatoms in oceans (6.7×10^{12} kg Si yr^{-1}) (Tréguer et al., 1995). In addition, the annual production of terrestrial BSi is an order of magnitude greater than DSi annual inputs to the ocean (0.14×10^{12} kg Si yr^{-1}). The DSi load to rivers is significantly impacted by BSi accumulation in vegetation as the Si uptake by terrestrial plants significantly increases the chemical weathering rate without necessarily increasing DSi leaching (Alexandre et al., 1997). Moreover the restitution of BSi on topsoil can largely contribute to H_4SiO_4 release in the aqueous phase (Farmer et al., 2005) as the solubility of phytoliths seems much greater than crystalline Si-containing minerals (Fraysse et al., 2009).

1.2.3 The biogeochemical Si cycle in forest ecosystems

In forest ecosystems, the Si biocycling is ubiquitous and trees take up a substantial amount of H_4SiO_4 from soil solutions (Bartoli, 1983; Lucas et al., 1993; Alexandre et al., 1997; Lucas, 2001; Hodson et al., 2005). In most temperate forest soils, Si concentration in the aqueous phase varies between 0.1 and 0.7 mM (Gérard et al., 2002; Fulweiler and Nixon, 2005; Wonisch et al., 2008).

On the basis of current literature (Table 1.1), Si recycling by tropical and temperate forest vegetation is shown to be in the same order of magnitude as Si outputs from soils (Sommer et al., 2006; Street-Perrott and Barker, 2008). In temperate forest ecosystems, the Si uptake varies between 2 and 44 kg Si ha^{-1} yr^{-1}, while the Si leached out from the soil profile ranges from 0.7 to 28 kg Si ha^{-1} yr^{-1} (Bartoli, 1983; Markewitz and Richter, 1998; Fulweiler and Nixon, 2005; Gérard et al., 2008). In humid tropical conditions, the recycling of Si by forest trees is evaluated at around 67 kg ha^{-1} yr^{-1} in Congo rainforest (Alexandre et al., 1997), while the DSi export does not exceed 16 kg ha^{-1} yr^{-1}. The Si input from the rainforest on topsoil through litterfall (41 kg ha^{-1} yr^{-1}) is about two to four times greater than the Si leached out of the system (11-26 kg ha^{-1} yr^{-1}) (Lucas et al., 1993; Cornu et al., 1998).

In 2005, the world's total forest area was estimated at 3952 million hectares, which corresponds to about 30% of the land area (FAO, 2006). Assuming a mean Si uptake by global forest vegetations of 40 kg Si ha^{-1} yr^{-1} (Table 1.1), the annual forest BSi production would amount to 0.15×10^{12} kg Si yr^{-1}, which represents 6.3% of the recent value of the total terrestrial Si biologically fixed as BSi (2.5×10^{12} kg Si yr^{-1}) (Laruelle et al., 2009). In addition, considering a mean Si output from forested land of 10 kg Si ha^{-1} yr^{-1} (Table 1.1), we obtain 0.04×10^{12} kg Si yr^{-1}, that is the global DSi leached from forest ecosystems, which represents 28% of the net DSi inputs in oceans (0.14×10^{12} kg Si yr^{-1}, Figure 2.2). This assessment is valuable because previously the biogeochemical Si cycle in forest ecosystem was thought to be insignificant, given that most Si biocycling studies focused on typical Si accumulator plants *i.e.* monocots.

The Si dynamics in the soil-tree system may be species-dependent since angiosperms enhance the weathering to a greater degree than gymnosperms (Moulton et al., 2000; Johnson-Maynard et al., 2005).

Table 1.1 Si fluxes (uptake, restitution and drainage) in tropical and temperate forest ecosystems.

		Si (kg ha^{-1} yr^{-1})		
		Vegetation uptake	Restitution by litter fall	Export by drainage
Equatorial forest (Ferralsols)	1		41	11-26
Equatorial forest (Ferralsols)	2	58-76	58-76	16
Temperate deciduous forest (Cambisols)	3	23	22	3
Temperate deciduous forest (Cambisols)	4	18-23	18-19	6-7
Temperate coniferous forest (Cambisols)	4	30-43	29-42	0.7-1
Temperate coniferous forest (Cambisols)	6	44	36	5
Temperate pine forest (Cambisols)	4	2.3	2.1	9.4
Temperate pine forest (Podzols)	3	6	5	28
Temperate pine forest	5	16	14	17

1. Lucas et al. (1993), Cornu et al. (1998); 2. Alexandre et al. (1997); 3. Bartoli (1983); 4. Cornelis et al. (2010), Chapter 4; 5. Markewitz and Richter (1998); 6. Gérard et al. (2008)

Furthermore, conifers, in contrast to broadleaved species, generally accumulate low amounts of Si in their shoots (Bartoli and Souchier, 1978; Klein and Geis, 1978; Hodson et al., 2005). Within conifers, Si accumulation by pine is ten times lower than in spruce (Hodson and Sangster, 1999). These findings confirm Bartoli's results (1983) in various soil and climate conditions, which estimate that 80% of DSi derives from the BSi pool in deciduous stands as against 20% in coniferous species.

Tree species could influence the continental Si cycle as recent studies demonstrate that forest vegetations exert strong biological control over Si cycling and export to rivers (Bartoli, 1983; Lucas et al., 1993; Meunier et al., 1999; Carnelli et al., 2001; Lucas, 2001; Derry et al., 2005). For instance, in a tropical rainforest affected by strong Si depletion of the mineral soils and high Si uptake rates, Derry et al. (2005) found that BSi contributes 68–90% of the DSi transported by Hawaiian stream water. In an Amazonian rainforest, Lucas et al. (1993) show that constant Si supply through litterfall on topsoil ("nutrient uplift") controls shallow soil kaolinite stability while kaolinite is weathered to gibbsite in the underlying soil with very low availability of mineral-derived Si. In a humid tropical environment, Alexandre et al. (1997) illustrate that Si release from phytolith dissolution is twice that of Si release due to silicate weathering. The few studies examining the temperate forest ecosystem show that the presence of forest trees with high productivity and significant Si concentration in leaves largely contribute to the terrestrial biogeochemical Si cycle even in temperate climates (Fulweiler and Nixon, 2005; Gérard et al., 2008).

On the one hand, the impact of tree species on the terrestrial Si cycle is poorly quantified because studies in identical soil and climate conditions are lacking. On the other hand, recent studies in specific tropical areas evidence that a large fraction of DSi released to the hydrosphere passes through the BSi pool. However, as the terrestrial biogeochemical cycle of Si is largely influenced by climate, vegetation type, and geological substratum, the observations and assumptions realized in a tropical rain forest cannot be generalized to other ecosystems.

1.3 Thesis objectives

Forest ecosystems are highly characteristic of terrestrial environments with very efficient Si biogeochemical recycling. Despite the fact that forest ecosystems are widespread on the Earth's surface and the important linkage of Si dynamics in biogeological systems with the global change processes, hardly any research has examined the impact of temperate forest vegetation on the terrestrial Si pools. For a better understanding of the terrestrial Si cycle, the biogeochemical study of Si in temperate forest ecosystems is crucial. A soil-tree system approach that entails contrasting common tree species in identical climate and soil conditions would be ideal to assess the tree-species effect on the distribution and origin of the various Si forms in forest ecosystems. The study of the origin of DSi in forest soil should also be viewed in the broad context of the control of global C fluxes, these being largely influenced by the interaction between terrestrial and oceanic Si cycles.

Our study was carried out on the experimental forest site of Breuil-Chenue, located in central France (Nièvre department, Morvan). The native mixed forest, dominated by European beech (*Fagus sylvatica* L.) and oak (*Quercus sessiliflora* Smith.) was clear-cut in 1976 and replaced by monospecific plots of different common tree species. In this well-defined soil-tree system, the impact of tree species is discernible since soil physical and chemical properties were identical between tree plots when the experimental site was set up (Bonneau et al., 1977). The combination of this forest site with very promising geochemical tracers such as stable Si isotopes and Ge/Si ratios allowed us to better assess the relative impact of specific tree species compared with pedogenic processes on Si release in forest soil solutions.

This PhD thesis focuses on Si cycling in temperate soil-tree systems and aims to (i) elucidate the effect of tree species on Si distribution in the soil-tree system, (ii) identify the major pool of Si-containing solid phases, and (iii) assess the relative contribution of biogenic and litho/pedogenic Si pools to the release of dissolved Si.

The research objectives were developed in order to answer several questions:

Q.1. Is the Si recycling by forest vegetation impacted by tree species?
Q.2. To what extent do the species impact the pool of dissolved Si?
Q.3. What factors control the Si uptake by forest vegetation?
Q.4. To what extent does the biogenic process (Si biocycling) impact the distribution of amorphous silica in forest soil, compared to pedogenic processes?
Q.5. What is the relative contribution of litho/pedogenic minerals and biogenic opal to the DSi released in forest soil solutions?
Q.6. How do various soil-plant systems influence the origin of DSi transferred towards rivers?

1.4 Thesis outline

The research results (Chapters 4 to 7) are presented in a succession of articles either published or submitted to peer review journals. This presentation has the advantage that each chapter can be easily read and understood independently. Complete and continuous reading is also possible, given the logical succession of chapters leading to an overall understanding of subject and objectives. Nevertheless, I apologize for any inconvenience the redundancies among chapters may provide.

The first part of the dissertation (***Chapter 1***) (i) gives an overview of the thesis context, (ii) explains the motivation for this study through an introduction about current knowledge on the global Si cycle, and then (iii) focuses on the thesis objectives. In ***Chapter 2***, we provide a review of the current knowledge on Si pools and fluxes in terrestrial ecosystems. ***Chapter 3*** describes the environmental features of the area researched in central France.

Chapter 4 presents the results of our field approach aimed at quantifying the Si cycling in soil-tree systems characterized by contrasting tree species. The study focuses on (i) the effect of contrasting Si uptakes by forest vegetation on the pool of dissolved Si in forest soil, and (ii) the influence of the Si recycling and the incorporation of silicate minerals by bioturbation on the origin of Si-containing solid phases in organic horizons.

Si concentration in plant shoots varies greatly between plant species. This variation is partly explained by three root-uptake modes: active, passive and rejective. When the same capacity for Si root-uptake is observed, the different accumulation of Si in leaves can be due to external environmental factors such as soil development, transpiration and H_4SiO_4 activity in soil solution. ***Chapter 5*** presents a study in hydroponics that compares the Si uptake by two coniferous species (*Pseudotsuga menziensii* and *Pinus nigra*) characterized by contrasting Si uptake in the field.

In continental ecosystems, Si recycling by forest vegetation contributes to the amorphous silica (ASi) pool in soil through amorphous BSi restitution on topsoil. ***Chapter 6*** is devoted to the quantification of ASi in soil under three common tree species to (i) highlight the impact of tree species on the ASi distribution, and (ii) identify the components of the ASi pool in temperate forest soil with granitic parental material.

Elucidation of the origin of DSi in temperate forest soil solutions by studying the relative contribution of both biogenic and litho/pedogenic Si pools to DSi release needs more consideration. In this regard, ***Chapter 7*** focuses on the use of geochemical tracers in soil-tree systems. We present the Si isotopes and Ge/Si ratios data of the aqueous and solid compartments (soil solutions, bedrock, soil fractions and phytoliths), which allow us to identify the main processes impacting the release of DSi in forest floor leachate solutions. By comparing the Ge/Si ratio to Si isotope data, we can better assess the Si pathways in a well-defined soil-tree system before its release in soil solution and *in fine* in rivers.

Chapter 8 we discuss about the origin of DSi transferred from various soil-plant systems towards hydrosphere; it combines the thesis results with the other studies on the subject.

Finally, ***Chapter 9*** explores the implications and perspectives of this doctoral research.

CHAPTER 2:

GENERAL OVERVIEW

2.1 Components involved in the soil-plant Si cycle

On Earth's surface environments, it is well known that a part of dissolved Si (H_4SiO_4) released by weathering of Si-containing solid phases is cycled by vegetation before a transfer to the hydrosphere. Given Si mainly accumulates in transpiration termini, it becomes largely mobile in soil-plant system through litterfall leading to a substantial reactive biogenic silica pool in soil that contributes to the release of DSi in soil solution. The DSi export from soil is of great interest since rivers would contribute to 80% of DSi load in oceans regulating the ocean food chain as a result of the essentiality of H_4SiO_4 for phytoplankton CO_2-consumers. DSi fluxes seem deeply influenced by climate (temperature and runoff) and soil-vegetation systems so that continental areas are characterized by various abilities to transfer DSi from soil-plant system towards rivers. Here we pay special attention to the way soil-plant systems impact Si transfer towards rivers.

2.1.1 The vegetal system

The Silicon is taken up by terrestrial plants from soil solution as uncharged monosilicic acid ($H_4SiO_4^0$), transported into the xylem (Casey et al., 2003) and deposited in transpiration sites where polymerization of hydrated amorphous silica occurs to form phyoliths ($SiO_2.nH_2O$; BSi) (Jones and Handreck, 1965; Jones and Handreck, 1967; Raven, 1983; Sangster and Hodson, 1986). SiO_2 precipitation occurs mainly in the epidermis of shoots but can also occur in the vascular system and endodermis of roots (Raven, 1983; Lux et al., 2003a,b). Phytoliths are restored on topsoil within organic residues and decomposition (Smithson, 1956). The biomineralization of phytoliths seems to be restricted to some plant families (Epstein, 1999; Hodson et al., 2005) and appear in various shapes depending on location of Si deposits and plant species (Carnelli et al., 2004). An International Code for Phytolith Nomenclature (ICPN) has been proposed to describe and name phytoliths (Madella et al., 2005), as the preservation of phytoliths in terrestrial and aquatic paleoenvironments can be used for reconstructing past environments and human activity (Piperno, 1988; Pearsall and Piperno, 1993). The amount of Si accumulated in plants is species dependent and ranges from 0.1 to 10% of dry weight (Raven, 1983; Marschner, 1995; Epstein, 1999; Hodson et al., 2005; Ma and Yamaji, 2006a). Based on active, passive or exclusive mechanisms with respect to Si uptake, plant species are classified as high-, intermediate- or non-accumulator, respectively (Takahashi et al., 1990). A classification of plant kingdom shows that the majority of Si high-accumulators (1.0-10 wt% shoots) belong to the monocotyledons (banana, bamboo, sugar cane, soybean, rice, wheat, barley, sorghum and oat), while most dicotyledons absorb Si passively (0.5-1.0 wt% shoots) and some dicots such as legumes have limited Si uptake (<0.5 wt% shoots) (Ma et al., 2001; Ma and Takahashi, 2002; Liang et al., 2007). Hodson et al. (2005) carried out a detailed data analysis of mean relative shoot Si concentration of 735 plant species. These data reveal that a high shoot Si concentration is not a general feature of monocot species and indicate that phytolith production is strongly controlled by the genetic code: the mean relative shoot Si concentration declines in the order marchantiophyta (liverworts) > equisetophyta (horsetails) > angiosperms > gymnosperms > polypdiophyta (ferns) (Table 2.1).

The transport of Si can be either active, passive or rejective. Active transport corresponds to the Si uptake in larger quantity than predicted by mass flow, while the passive transport is the Si uptake proportional to mass flow. Rejective transport is given when low plant Si concentrations indicate a Si accumulation in soil solution. For the active Si uptake, the difference in Si accumulation between plant species is commonly attributed to the density of Si transporters in roots (coded by the low-silicon genes *Lsi1* and *Lsi2*) and in shoots (*Lsi6*) (Mitani et al., 2005; Ma et al., 2006b, 2007; Yamaji et al., 2008). On another hand, for the mass-flow driven Si uptake (passive) and for a same concentration of Si in soil solution, the difference in Si accumulation between plant species could be explained by various transpiration rates (Jones and Handreck, 1967; Raven, 1983; Bartoli and Souchier, 1978; Henriet et al., 2006).

The essentiality of Si for terrestrial plants has been and is still extensively debated (Takahashi et al., 1990; Richmond and Sussman, 2003). So far only two groups of plants are known to have an absolute and quantitatively major requirement for Si: the diatoms and other members of the yellow-brown or golden algae, the Chrysophyceae and the Equisitaceae (Epstein, 1999). Si is not considered as an essential element for higher plants (Epstein, 1994; Epstein, 1999; Ma and Takahashi, 2002), but its beneficial effects on growth have been reported in a wide variety of crops,

Table 2.1 Degree of Si accumulation in plant estimated from mean relative shoot Si concentration of plant species (non-: <0.5% Si, intermediate-: 0.5-1% Si and high-accumulator: >1% Si) (Ma and Takahashi, 2002), using data analysis of Hodson et al. (2005) which adjust an average shoot Si concentration for each species across studies.

Group	Species	Common name	Si (wt%) in shoots	Degree of Si accumulation†
Marchantiophyta				
	March. polymorpha	liverworts	5.45	+
Equisetophyta				
	Equisetum arvense	Com. horsetail	3.99	+
Angiosperm				
Asteraceae				
	Helianthus annuus	sunflower	1.88	+
Cyperaceae				
	Carex cinica	sedge	2.44	+
Fabaceae				
	Glycine max	soybean	1.39	+
	Lupinus nanus	lupine	0.28	-
	Phaseolus vulgaris	bean	0.95	±
Fagaceae				
	Quercus robur	Pedunc. oak	1.54	+
	Fagus sylvatica	European beech	6.08	±
Lamiaceae				
	Mentha longifolia	mint	0.73	±
Liliaceae				
	Allium fistulosum	onion	0.31	-
Musaceae				
	Musa basjoo	banana	0.98	±
Poaceae				
	Arundin. gigantea	cane	8.77	+
	Avena sativa	oat	1.51	+
	Hordeum vulgare	barley	1.82	+
	Oryza sativa	rice	4.17	+
	Sorghum bicolor	sorghum	1.54	+
	Triticum aestivum	wheat	2.45	+
	Zea mays	maize	0.83	±
Urticacea				
	Urtica dioica	nettle	1.34	+
Gymnosperm				
Pinaceae				
	Larix decidua	Europ.larch	0.87	±
	Picea abies	Nor. spruce	1.36	+
	Picea rubens	Red spruce	0.32	-
	Pinus strobus	White pine	0.12	-
	Pseudots. menziesii	Douglas fir	0.32	-
Polypodiophyta				
Dryopteridaceae				
	Dryopt carthusiana	Buckler fern	0.18	-
Polypodiaceae				
	Polypod. vulgare	Rockcap fern	0.15	-

† -, ± and +: Si non-, intermediate- and high-accumulator

including rice, wheat, barley, and cucumber (Ma et al., 2001; Korndorfer and Lepsch, 2001; Ma and Takahashi, 2002; Ma, 2004). There is a general consensus that Si improves the plant resistance to various biotic and abiotic stresses. Silica deposition in leaves is a resistant structural component energetically cheaper to incorporate than lignin (Raven, 1983), providing a more upright position which favours light interception, therefore promoting photosynthesis (Epstein, 1994; Marschner, 1995). Moreover, biogenic silica in plant tissues creates a hard outer layer that serves as a defense against fungal and insect attacks (Bélanger et al., 2003; Sangster et al., 2001).

Finally, it is widely accepted that Si alleviates the toxicity of Al and other metal ions, such as Mn, in higher plants (Birchall, 1990; Hammond et al., 1995; Hodson and Evans, 1995; Cocker et al., 1998; Perry and Keeling-Tucker, 1998; Liang et al., 2001; Liang et al., 2007). In acidic coniferous forest, it is established that the free Al co-deposited with Si represents a defense against Al toxicity (Hodson and Sangster, 1999). The extent of silicon's role in plants appears to be species-dependent since plants that actively take up Si are the most sensitive to a Si deficit (Raven, 1983; Carnelli et al., 2001). Currently, there is no evidence showing the involvement of Si in plant metabolism (Ma et al., 2001) since no silicon bearing organic compound has been identified in higher plant so far (Knight and Kinrade, 2001). The beneficial Si effects are small under optimized growth conditions, but become obvious and more clearly expressed under stress conditions (Epstein, 1994; Bélanger et al., 1995). The Si accumulators wheat (*Triticum aestivum*) and rice (*Oryza sativa*), the premier crops for the nutrition of mankind, are exposed to a variety of diseases if the Si supply is low (Epstein, 2001). Therefore, soils intensively used for cropping are regularly fertilized with silicate amendments such as wollastonite (Korndörfer and Lepsch, 2001).

2.1.2 The solid phase in soil

The silicon is a major element in soil minerals and occurs in almost all parent materials, in which Si ranges from more than 46.5% in orthoquartzite to trace amounts in some limestones and carbonatites (Table 2.2). The silica-rich igneous rocks (granite, rhyolite) contain considerably more quartz than basic igneous rocks (basalt and gabbro).

Soils derived from parental rocks are a central reservoir between lithosphere, biosphere, hydrosphere and atmosphere, in which Si is recycled between various inorganic and biological sinks and sources. In soils, Si ranges from 46% in silcretes to 7.9% in petrocalcic horizons, and even lower in many highly weathered Oxisols (Monger and Kelly, 2002). Soils mainly contain Si as silica minerals, primary silicates and secondary silicates, especially phyllosilicates (Iler, 1979). Primary minerals, through physical and chemical weathering, are transformed into secondary Si-containing minerals crucial for soil development and fertility (McKeague and Cline, 1963a; Lindsay, 1979), in variable amounts depending on the nature of the parent material and the transformations undergone. Physical and chemical weathering produces a great variety of solid Si-fractions in soils summarized in Figure 2.1. More than one hundred relatively common crystallized silicates have been listed in soils in addition to an important

Table 2.2 Silicon content in rock expressed as Si wt% (modified from Monger and Kelly, 2002).

Rock type	**Si (wt%)**
orthoquartzite	46.5
rhyolite	34.7
arkose sandstone	33.7
volcanic ash (acidic Krakatoa ash)	32.2
granite	32.0
quartz monzonite	30.6
andesite	27.4
alkali olivine basalt	23.6
basalt	23.0
gabbro	22.5
calcareous shale	11.7
dolomite	1.5
fossiliferous limestone	0.1
carbonatite	trace

variety of amorphous forms of silica and poorly-crystalline silicates (McKeague and Cline, 1963a). Most of sand (50-2000 µm) and silt (2-50 µm) fractions is of primary origin, and thus is inherited in soils. Conversely, most clay-sized minerals are of secondary origin as a result of pedogenic processes (Allen and Hajek, 1989). As shown in Figure 2.1, the most common primary minerals from igneous rocks are olivine, pyroxene, amphibole, mica and feldspar (Schulze, 2002). Secondary minerals are mainly constituted by clay-sized phyllosilicates and Al and Fe (hydr)oxides which play a key role in the dynamic interaction between the solid and aqueous Si phases in soil.

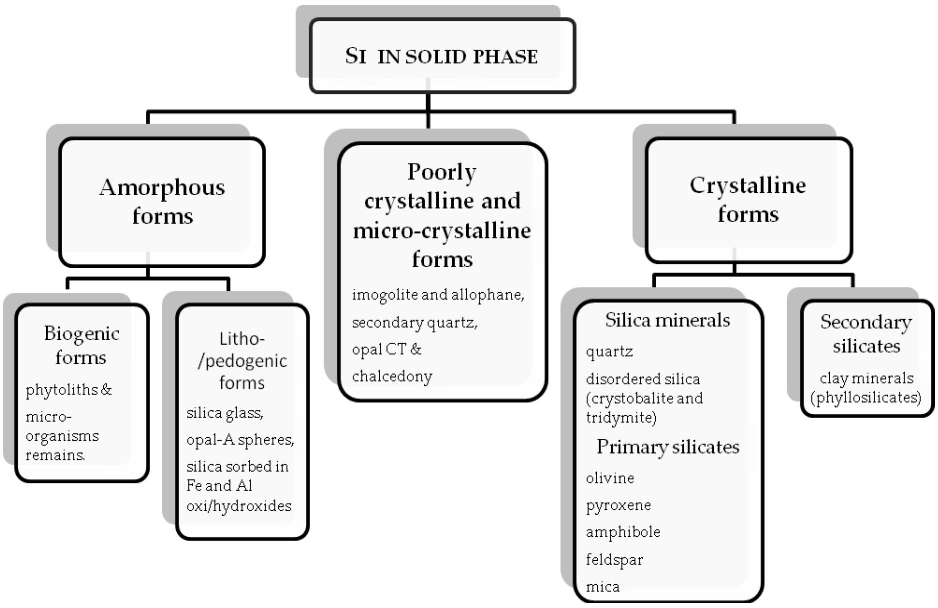

Figure 2.1 Classification of solid Si compounds in the soil (modified from Sauer et al., 2006).

Well-crystallized crystobalite and disordered crystobalite (opal-CT) are commonly associated with soil developed from volcanic rocks while tridymite is rare in soils and is usually limited to siliceous volcanic rocks. Si also occurs as poorly crystalline phases such as short-range ordered silicates (allophane and imogolite) and micro-crystalline phases such as authigenic quartz and chalcedony. Poorly ordered Al-Si compounds are likely to occur in acid soils showing a molar Si:Al ratio of 1:2 to 1:1 (Farmer et al., 1980; Buurman and Van Reeuwijk, 1984; Wada, 1989). Imogolite is mostly reported from podzols (Dahlgren and Ugolini, 1989; Lundström et al., 2000) whereas allophane mainly occurs in volcanic soils (Wada, 1989). The Si contained in amorphous silica pool of soil has both pedogenic and biogenic (BSi) origins. Pedogenic origin corresponds to the non-crystalline inorganic fraction such as opal-A formed under supersaturated soluble Si levels (Drees et al., 1989) and amorphous silica adsorbed on Fe and Al oxides/hydroxides (Dietzel, 2002; Sauer et al., 2006). The formation of amorphous silica coatings (silcretes, cements) on other mineral surfaces as a secondary product of weathering is widely recognized in soils and sediments (Dove, 1995; Basile-Doelsch et al., 2005). On another hand, biogenic pool in soil is constituted by phytoliths (opal-A) and micro-organisms remains (microbial and protozoic Si) (Sommer et al., 2006; Sauer et al., 2006; Aoki et al., 2007). Biogenic opal is a ubiquitous and significant component of soils developed under a wide range of environmental conditions, while pedogenic opal is formed only under specific physico-chemical soil conditions (Drees et al., 1989).

2.1.3 The aqueous phase in soil

The silicon is a main component of soil solution and is mainly dominated by uncharged monomeric molecule of silicic acid $H_4SiO_4^0$ in common soil pH values (Iler, 1979). The dissolution of silica polymorphs is strongly pH-dependent and undergoes hydrolysis at pH<9 by the overall reaction:

$$SiO_{2(s)} + 2H_2O = H_4SiO_4^0 \qquad \text{Eq. (2.1)}$$

Si concentrations in soil solution usually range from 0.01 to 1.99 mM Si (Karathanasis, 2002), but more commonly from 0.1 to 0.6 mM (Epstein, 2001; Faure, 1991). In most soils, the Si concentration in aqueous phase is in agreement with the mineralogical composition, which depends on the current stage of soil development influenced by climate and parent material (Rai and Kittrick, 1989; Karathanasis, 2002). Indeed, for a fixed pH, smectite stability in Vertisols is associated with a relatively high concentration of aqueous H_4SiO_4 (~1.6 mM Si) whereas kaolinite, predominantly occurring in Ferralsols, Acrisols, and Lixisols, is associated with low H_4SiO_4 concentration (0.03 mM Si) (Rai and Kittrick, 1989).

2.2 Processes controlling the H_4SiO_4 concentration in weathering environments

The aqueous chemistry of Si is regulated by a number of coupled processes (Figure 2.2): (i) dissolution of the Si-containing solid phases, (ii) precipitation and neoformation of authigenic Si-constituents, (iii) Si adsorption/desorption on various solid phases, (iv) Si absorption by vegetation and micro-organisms, (v) preservation of stable Si forms and (vi) external atmospheric inputs. In Figure 2.2, we suggest a continental Si cycle with five compartments: soil solution, groundwater, rivers, biomass and soils linked to the global Si cycle through two other compartments (oceans and atmosphere).

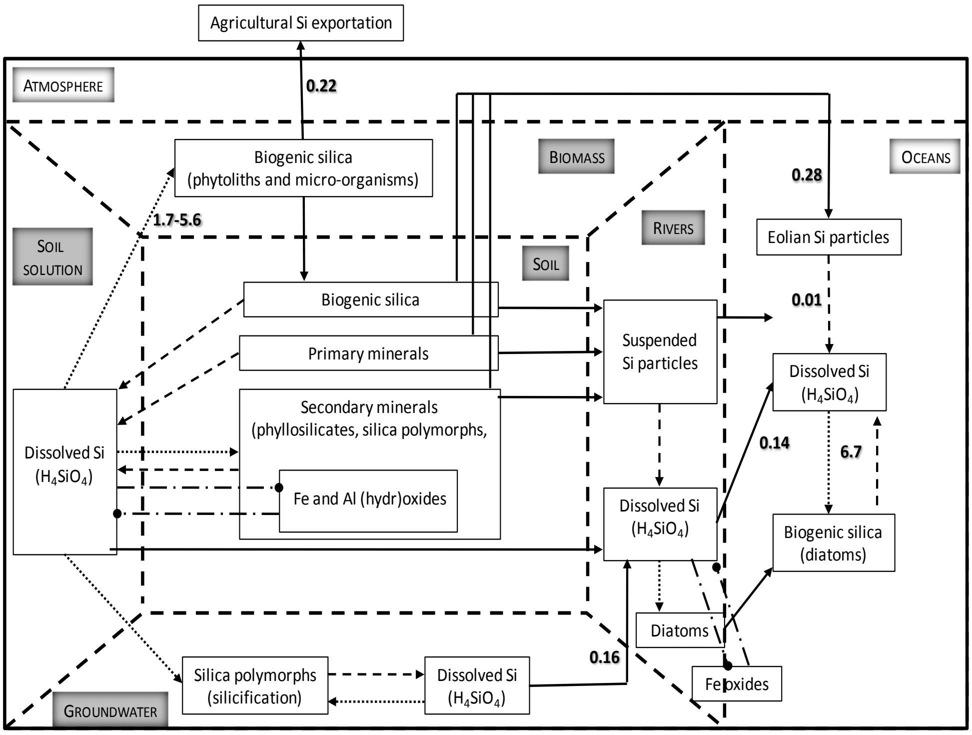

Figure 2.2 Biogeochemical Si cycle on continents (compartments modified from Basile-Doelsch et al., 2005). Solid line: Transport; dashed line: Dissolution; small dotted line: Neoformation/Precipitation; pointed-dotted line: Adsorption/Desorption. Numbers labeling arrows show interpool Si transfers in 10^{12} kg Si yr^{-1} (Tréguer et al., 1995; Matichenkov and Bocharnikova, 2001).

2.2.1 Solubility of Si-containing minerals

2.2.1.1 Silica

In soils, the solubility of amorphous silica is higher (1.8-2 mM Si) than quartz (0.10-0.25 mM Si) since solubility is a function of the packing density of the silica tetrahedral and long-range crystal order (Iler, 1979; Lindsay, 1979; Drees et al., 1989). Quartz, abundant in both residual and transported parent material, is highly stable and thermodynamically more resistant to weathering, being the last mineral to crystallize from magma (Drees et al., 1989; Monger and Kelly, 2002). Considering the biogenic silica, its solubility is equivalent to vitreous silica (1.8 mM Si) and is 17 times higher than quartz (Fraysse et al., 2006). Despite the various morphologies and different specific surface area of phytoliths, mass-normalized dissolution rates are similar among all types of plant species (horsetail, larch, elm and fern) studied by Fraysse et al. (2009) and these dissolution rates are an order of magnitude higher than those of typical soil clay minerals. On another hand, Bartoli (1985) demonstrates that the solubility of phytoliths form pine is three times lower than for beech phytoliths because of a higher Al substitution at surface. Fraysse et al. (2006) demonstrate that the Si release rate from litter is independent of cellulose hydrolysis, which suggests that phytoliths are in a pure “inorganic” pool not complexed with organic matter.

The dissolution rates of silica particles decrease with the decreasing of surface area and surface energy (Bartoli and Wilding, 1980; Drees et al., 1989). The amorphous phases have surface disordered at an atomic scale so that the transfer of SiO_4 tetrahedra to solution always leaves the surface free energy of the solid unchanged. As a consequence, dissolution rates of amorphous silica should simply increase linearly with the driving force (undersaturation). However, Dove et al., (2008) observe that the dissolution rates of amorphous silica exhibit an exponential dependence on electrolytes (alkaline or alkaline earth cations) as their crystalline counterpart, quartz. In fact the nucleated process overcomes an energy barrier to remove a surface species of lower chemical reactivity such as Q3 species (bonded to three bridging oxygens). That subsequently creates vacancy islands, each with a periphery of new surface groups enriched in the reactive Q2 species (bonded with two bridging oxygens). This model also accounts for reported demineralization rates of natural biogenic silica

(Dove et al., 2008). The solubility of silica polymorphs, both crystalline and amorphous, is essentially constant between the pH limits of 2 and 8.5, but increases rapidly near pH 9 since the weakly acidic H_4SiO_4 dissociates appreciably such that the first reaction is written (Dove et al., 1995):

$$H_4SiO_4 = H_3SiO_4^- + H^+ \qquad \text{Eq. (2.2)}$$

This reaction is an important buffer for some natural systems and, as a result, only highly unusual low-silica environments like carbonatites and serpentinites can reach a pH above the first pK of silica ($pK_{a1} = 9.82$ at 25°C). The polymeric species become stable at pH ~ 9 (Knight and Kinrade, 2001; Dietzel, 2000,2002) at which the solubility of amorphous silica increases due to the dissociation of silicic acid successively into $Si(OH)_3O^-$ ($pK_{a1} = 9.82$ at 25°C) and $Si(OH)_2O_2^{2-}$ ($pK_{a2} = 11.84$ at 25°C) (Alexander et al., 1953; Iler, 1979).

The sorption of Al and other bi- and trivalent metals (Fe^{3+}, Zn^{2+} and Cu^{2+}) affect the surface properties of the silica polymorphs and decrease their rates of dissolution (Dove et al., 1995; McKeague and Cline, 1963a).

2.2.1.2 Silicate minerals

The weathering rates of silicate minerals have a major importance in soil development, soil buffering capacities related to acidic deposition, control of carbon cycle and cycling of many inorganic elements which are important in soil fertility (White, 1995). The weathering rate of a mineral in a given environment can be considered as a function of intensity factors (temperature, moisture, pH and Eh) and capacity factors (specific surface area and nature of the mineral) (McKeague and Cline, 1963a). In Table 2.3, we present a weathering sequence for soil minerals in which primary phases and secondary clay minerals (phyllosilicates) containing iron were least stable, followed by mixed layer phyllosilicates, and smectites, and finally by phases of increasingly simpler compositions and structures (e.g. kaolinite, allophane, Al and Fe (hydr)oxides) (Nagy, 1995).

Land plants and their associated microbiota directly affect silicate minerals weathering in several ways by: (i) affecting the temperature of the soil, (ii) protecting soil against erosion, (iii) generating of chelating ligands, (iv) modifying pH through production of CO_2 and organic acids, and (v) altering the physical properties of a soil, particularly the exposed surface areas of minerals and the residence time of water (Drever, 1994; Moulton et al., 2000). The relative importance of each of these processes depends upon plant type, climate and geology (Moulton et al., 2000). Gérard et al. (2002) emphasize that soil temperature strongly influence the chemical weathering rates and may be considered as the dominant factor for seasonal variations in soil solution Si concentration.

Since a relatively large K^+, Na^+ and Ca^{2+} ions balances the charge deficit, feldspar weathers more rapidly than quartz (McKeague and Cline, 1963a; White, 1995) to give secondary clays and silicic acid:

$$2KAlSi_3O_8 + 2CO_2 + 11H_2O \rightarrow Al_2Si_2O_5(OH)_4 + 2K^+ + 2HCO_3^- + 4H_4SiO_4 \qquad \text{Eq. (2.3)}$$

The mineral weathering rate is dependent upon equilibrium and any processes consuming silicic acid produced (Eq. (2.3)) will accelerate mineral dissolution (Exley, 1998). Indeed, if some of the H_4SiO_4 produced reacts with a solute species to form a complex or is taken up by vegetation, more solid dissolves to replenish the reacted H_4SiO_4 (Dove et al., 1995; Street-Perrott and Barker, 2008).

Vegetation should also cause an increase in weathering rate through the pH effect only where the pH is below 4-5. Indeed in the circumneutral region, the rate is pH-independent and at pH values above 8, the rate increases with increasing pH (McKeague and Cline, 1963a). In addition, acidification of soil solution in Podzols and Luvisols leads to disintegration of secondary clay minerals providing a source of Si (Sommer et al., 2006). Indeed, the high concentration of low molecular organic acids in the organic horizons is likely to promote primary and secondary minerals weathering through a combined action of complexation and acid attack (Bennet et al., 1991; Barman et al., 1992; Oliva et al., 1999; Giesler et al., 2000; Gérard et al., 2002).

2.2.2 Neoformation and precipitation of Si-containing minerals

Subsequent to incongruent weathering of primary silicate minerals, the precipitation of secondary minerals, most commonly clay-sized phyllosilicates and Al and Fe (hydr)oxides, is expected to significantly influence the activity of elements in soil solutions (White, 1995).

Table 2.3 Mineral weathering sequence and type of minerals as indicators of relative degree of soil development (the higher the number, the higher the degree of soil development) (Rai and Kittrick, 1989; Nagy, 1995; Allen and Hajek, 1989).

Relative degree of soil development	Stability	Minerals†	Formula
	STABLE ↑		
13	•	Anatase	TiO_2
		RUTILE	TiO_2
		CORUNDUM	Al_2O_3
12	•	Hematite	α-Fe_2O_3
		Goethite	α-$FeOOH$
11	•	Gibbsite	$Al(OH)_3$
		Allophane	$(Al2O_3)(SiO_2)_{1.3}.2.5(H_2O)$
10	•	Kaolinite	$Si_2Al_2O_5(OH)_4$
		Halloysite	$Si_2Al_2O_5(OH)_4.2H_2O$
9	•	Smectites	$M_xSi_4(Al_{2-x}Mg_x)O_{10}(OH)_2$
8	•	Vermiculite	$(Mg,Fe,Al)_3(Al_xSi_{4-x})O_{10}(OH)_2.4H_2O$
7	•	MUSCOVITE	$KAl_2(Si_3Al)O_{10}(OH)_2$
		Illite	$K_xAl_2(Si_{4-x}Al_x)O_{10}(OH)_2$
6	•	QUARTZ	SiO_2
5	•	FELDSPARS	$KAlSi_3O_8$, $NaAlSi_3O_8$-$CaAl_2Si_2O_8$
4	•	BIOTITE	$K(Mg,Fe)_3(Si_3Al)O_{10}(OH)_2$
3	•	OLIVINE	$(Mg,Fe)_2SiO_4$
		HORNBLENDE	$Ca_2Na(Mg,Fe)_4(Al,Si)_8O_{22}(OH,F)_2$
		PYROXENE	$Ca(Mg,Fe,Al)(Si,Al)_2O_6$
2	•	CALCITE	$CaCO_3$
		DOLOMITE	$Ca,Mg(CO_3)_2$
		APATITE	$Ca_5(F,Cl,OH)(PO_4)_3$
1	•	GYPSUM	$CaSO_{4.2}H_2O$
		HALITE	$NaCl$
	UNSTABLE		

† Primary minerals are capitalized.

More particularly, Si concentrations in soil solutions strongly depend on equilibrium with secondary phases. In this regard, the weathering of plagioclase requires the aqueous release of two moles of SiO_2 for every mole incorporated with Al in kaolinite. On the other hand, three moles of

SiO_2 will be released in soil solution if gibbsite forms in soil, and less than two moles of silica will be mobilized if smectites forms (White, 1995).

The competitive condensation of H_4SiO_4 with an Al hydroxide template form hydroxialuminosilicates (HAS) which might be considered as amorphous precursors to imogolite (Exley, 1998; Doucet et al., 2001). Besides the fact that Al coatings depress the solubility of silica, the decrease of Al activity in soil solution would bring about dissolution of secondary Al-containing minerals and, hence, release of H_4SiO_4 in soil solution (McKeague and Cline, 1963a; Rai and Kittrick, 1989). In environment with very active humus, the formation of Al-organic matter complex inhibits the formation of allophane and imogolite and favours formation of opaline silica. The formation of short-range ordered Al-Si compounds occurs in horizons with pH(H_2O) values > 5.0 (Wada, 1989).

If the ecological and climatic conditions favour the evapotranspiration, the H_4SiO_4 concentration of some soil solutions might exceed the solubility of amorphous silica defined as 2.1 mM Si at 25°C (Alexander et al., 1953; Monger and Kelly, 2002). Related to that solubility, biogenic opal-A plays an important role in the genesis of the siliceous cements of hardpans and silcretes (Clarke, 2003). The dissolution of opal-A and reprecipitation of opal-CT which in turn is transformed into secondary micro-crystalline quartz may be mediated by condensation reactions of silica polymers onto metal hydroxides (Drees et al., 1989; Monger and Kelly, 2002). The partial dissolution of biogenic opal-A pool in topsoil also provides DSi for sequestration in secondary minerals (clay neoformation and Si adsorption) in upper soil horizons (Lucas et al., 1993; Lucas, 2001; Michalopoulos and Aller, 2004; Barré et al., 2009; Opfergelt et al., 2010). Moreover, Conrad et al. (2007) demonstrate the importance of nanocolloidal silica particles (<3 nm, equivalent to 300 silica monomer units) for the precipitation of SiO_2. These nanoparticles of silica can account for a portion up to ~65% of the total silica present in aqueous solutions at low pH (3-4) regardless of ionic strength. Considering duripans and silcretes soils, high H_4SiO_4 concentrations (2.1 mM Si) favour opal-A precipitation; intermediate concentrations (0.7-2.1 mM Si) favour opal-CT formation; and low $H_4SiO_4^0$ concentrations (< 0.7 $mg.l^{-1}$) favour microquartz formation (Chadwick et al., 1987). Basile-Doelsch (2005) suggests the quartz re-precipitation plays an important role in the biogeochemical cycle of Si. This pedogenic silicification is associated with arid climates, and its contribution to the Si cycle probably followed climatic variations. In addition, the polymerized silicic acid may also indicate a type of precursor material for neoformation of secondary Al-silicates (Wonisch et al., 2008).

It must be emphasized that the pedogenic formation of secondary Si-containing minerals (phyllosilicates, silica and short-range ordered aluminosilicates) is strongly influenced by Si activity in soil solution which depends on (i) parental material as the ultimate and readily source of H_4SiO_4 through the physical and chemical weathering, and (ii) climate providing water for weathering and preventing for intensive leaching of H_4SiO_4 (Jackson et al., 1948; Dove, 1995; White, 1995; Berner, 1995; Gérard et al., 2002; Monger and Kelly, 2002). The climate (mainly moisture and temperature) plays a major role in the Si distribution in soils since, across the world, there may be formation of an extraordinary range of soils from a same rock (climosequence). Moisture is influenced by the total amount, intensity, and seasonality of precipitation, humidity, evapo-transpiration, runoff and infiltration. Thermal effects, described by the Arrhenius relationship, include average air temperature, seasonal temperature variations, and thermal gradients in soils (White, 1995). Generally, we can schematize the world weathering system and the distribution of Si-containing minerals as a function of climate (Millot, 1979; Pédro, 1984; IUSS, 2006). In arid climate (mainly North Africa), the weathering of minerals is absent. In cold and humid climate, primary clays (illites and chlorites) are inherited directly from the parent material (detrital origin) without forming new minerals. There is thus no neoformation of secondary clay minerals in these two climates. In temperate climate, the rate of weathering is restricted inducing secondary clay minerals derived from limited transformation of existing minerals in rocks into new species. In Mediterranean and tropical climates, clay-rich silica such as smectites can be observed. The neoformation of authigenic phases such as secondary clay minerals (kaolinite) and oxides/hydroxides (gibbsite) is typical of tropical humid and equatorial climates.

As a consequence of the pedogenesis, the type of soils influences the form and the content of Si (McKeague and Cline, 1963a). For example, *Podzols* (IUSS, 2006), occurring mainly in temperate humid and boreal areas with siliceous rock, are characterized by a siliceous eluvial horizon with quartz as the main form of silica and by a spodic illuvial accumulation of humus complexes and secondary phases. *Cambisols* (IUSS, 2006) are recognized by their incipient soil formation with a limited degree of weathering derived from a wide range of rocks. Cambisols are particularly well represented in temperate and boreal regions with a young parent material; they cover an estimated 1.5 billion hectares worldwide. Si is commonly present as a mixture of weatherable primary silicates, quartz, and secondary clay minerals. *Ferralsols* (IUSS, 2006) represent the most highly weathered soil mainly from basic rock of the humid tropics in which the low concentrations of dissolved weathering products promote desilication (Si leaching by drainage). These soils display a mineral assemblage dominated by low activity clays (mainly kaolinite) and a high content of sesquioxides.

2.2.3 Si adsorption on solid phases

The monosilicic acid can be withdrawn from soil solution through the adsorption onto a variety of solid phases in soils (McKeague and Cline, 1963b). Although little Si adsorption has been reported onto secondary clay minerals (Siever and Woodford, 1973), Fe and Al oxides are the main soil components with a significant capacity of adsorption (Beckwith and Reeve, 1963; McKeague and Cline, 1963b).

Adsorption of monosilicic acid by oxides depends on (i) pH with an increase from pH 4 to pH 9, and (ii) metal type since aluminium oxides were more effective, weight for weight, in adsorbing monosilicic acid than iron oxides (Jones and Handreck, 1963,1965,1967; McKeague and Cline, 1963b). Delstanche et al. (2009) confirm the specific adsorption of H_4SiO_4 onto secondary oxides with higher Si amount adsorbed onto synthetic short-range ordered ferrihydrite compared to crystalline goethite. H_4SiO_4 interacts with Fe-oxide surface OH groups through ligand exchange to form silicate bi-dendate innersphere complex (Parfitt, 1978; Pokrovski et al., 2003; Hiemstra et al., 2007). At Fe oxides surfaces, Dietzel (2002) show that polysilicic acid might be formed by specific interaction with orthosilicic acid that would significantly influence the amorphous silica content in soils. As a consequence of the ubiquity of iron oxides in sediments and soils (Schwertmann and Taylor, 1989), they partly control the concentration of H_4SiO_4 in the aqueous phase (McKeague and Cline, 1963b; Opfergelt et al., 2009).

2.2.4 Si recyling by vegetation

A Si-accumulator forest (1.1% Si in leaves) with a biomass production of 16T dry weight yr^{-1} would extract 200 kg Si ha^{-1} yr^{-1} (Lovering, 1959). After 5000 years, this would be equivalent to the Si content of $1000m^3$ of basalt, so that Si-accumulator forest could convert basalt into lateritic soil rapidly at geological time scale. While the predominant role of photosynthetic plants in the Si cycle is in converting silicates to silicic acid on land and converting silicic acid to silica in the ocean, terrestrial higher plants are also involved in the conversion of silicic acid to biogenic silica (Raven, 1983; Raven, 2001). Indeed, it is well known that a part of the DSi released by mineral weathering is cycled through vegetation at the surface of the earth (Conley, 2002) before its transfer to oceans (Bartoli, 1983; Lucas et al., 1993; Alexandre et al., 1997; Markewitz and Richter, 1998; Conley, 2002; Derry et al., 2005; Fulweiler and Nixon, 2005; Blecker et al., 2006; Sommer et al., 2006; Gérard et al., 2008).

In temperate forest ecosystem, the Si uptake depends on tree species, ranging from 2 to 44 kg Si ha^{-1} yr^{-1} (Bartoli, 1983; Markewitz and Richter, 1998; Fulweiler and Nixon, 2005; Gérard et al., 2008). In humid tropical conditions, the Si recycling by forest trees is evaluated up to 67 kg ha^{-1} yr^{-1} in Congo rainforest (Alexandre et al., 1997). Blecker et al. (2006) calculate a Si uptake between 22 and 59 kg ha^{-1} yr^{-1} for various dry and humid temperate grasslands. The uptake by vegetation induced decline in H_4SiO_4 concentration in soil solution and thus has the effect of accelerating the rate of mineral weathering (see Eq. (2.3)) (Exley, 1998). Indeed, Hinsinger et al. (2001) demonstrate that Si-accumulators plants such as maize and banana accelerated the dissolution of basalt. The Si is largely mobile in the soil-plant cycle through litterfall since Si seems to be unavailable for retranslocation to other parts of the plant once amorphous $SiO_2.nH_2O$ polymerizes in aerial parts of the plants, thereby limiting the quantity of H_4SiO_4 available for export (Raven, 1983). Thus, the Si recycling by vegetation strongly controls the amount of Si restituted on topsoil. Reported values indicate litterfall to be the most important Si flux from vegetation to soil, followed by throughfall (Sommer et al., 2006). Even with a lower biomass, the Si restitution on topsoil through litterfall by grasses is comparable to forests, since grasslands are characterized by higher Si concentrations and turnover (Blecker et al., 2006).

The DSi load to rivers is significantly reduced when significant amounts of BSi accumulate in vegetation. The uptake of Si by terrestrial ecosystems significantly increases the chemical weathering rate without necessarily increasing the measured denudation rate (Alexandre et al., 1997; Street-Perrott and Barker, 2008). The Si uptake by forest vegetation is negatively correlated with the amount of DSi leached out from soil profile (see Chapter 4). This observation is confirmed by the significant increases in the transport of DSi by rivers with deforestation (Saccone et al., 2008). Indeed, Conley et al. (2008) show that in a temperate forest ecosystem the increase DSi leaching to the hydrosphere with deforestation can be attributed to the dissolution of the amorphous BSi which was restituted on topsoil.

On another hand, the highly soluble BSi pool returning on topsoil through litterfall (Van Cappellen et al., 2003; Fraysse et al., 2009) is an ubiquitous and substantial component of soil (Drees et al., 1989; Saccone et al., 2007) which will contribute to Si release in soil solution (Farmer et al., 2005). However, a quantitative assessment of the actual amount of ASi, whether from biogenic or pedogenic origin, in the soil is difficult to obtain (Sauer et al., 2006; Saccone et al., 2007).

The global agricultural Si exportation is estimated at 0.22×10^{12} kg Si yr^{-1} (Matichenkov and Bocharnikova, 2001; Figure 2.2), which is the same order of magnitude as the total dissolved Si transferred from continents to oceans by rivers (0.14×10^{12} kg Si yr^{-1}) (Tréguer et al., 1995). When Si accumulators such as rice and wheat are cultivated, their biomass exported from the field represents a net loss of Si from the soil-plant system (Meunier et al., 2008). As a consequence, man activity, through intensive cropping of Si-accumulator plants (rice and sugar cane), is responsible for a significant decrease of Si in soils within a few decades (Meunier, 2003).

2.2.5 Biogenic Si preservation

If the restitution rate of phytoliths on topsoil is higher than their dissolution rate, they may accumulate in soil, as described on the volcanic island of La Réunion under Si-accumulating bamboos (Meunier, 1999). The phytolith is an adsorptive surface and is implicated in the removal of metal ions, such as Al, from the soil solution (Epstein, 2001). These adsorptive processes tend to stabilize a part of phytoliths from dissolution (Bartoli and Wilding, 1980) and thereby reduce the amount of silicic acid returning to the biosphere through the preservation in soil profile (Alexandre et al., 1997). In an equatorial rainforest, 8% of the BSi input (4-6 kg Si ha^{-1} yr^{-1}) supplies a stable pool of phytoliths with a lower turnover (Alexandre et al., 1997). In temperate deciduous and coniferous forest, the preservation of phytoliths represents respectively 0 and 1 kg Si ha^{-1} yr^{-1} (Bartoli, 1983), while the storage of BSi in grasslands ecosystem ranges from 4 to 16 kg Si ha^{-1} yr^{-1} (Blecker et al., 2006). In this regard, Wilding and Drees (1974) have shown that forest BSi is about 10-15 times more soluble than grass BSi, owing to its greater specific surface area. In Podzols, Bartoli and Souchier (1978) calculated a residence time of 30 years for beech phytoliths and of 300 years for pine phytoliths. Amount of amorphous silica in soils, essentially composed by BSi, commonly ranges from <1 to 30 mg g^{-1} on a total soil basis (Drees et al., 1989).

If preserved in soil, phytoliths will be dissolved and/or exported to rivers (see Figure 2.2). Where the vegetation is highly productive and the erosion of top soils is significant, the phytolith loads as suspended particles will be substantial. In the Nyong basin (Cameroon), phytoliths originating from the soil erosion contribute to more than 90% of BSi pool in Nyong River suspended load and can account for 4% of the total suspended load (Cary et al., 2005).

2.2.6 Atmospheric Si input

The atmospheric dust inputs in the biogeosphere must be taken into account in biogeochemical studies. In highly weathered soils, Chadwick et al. (1999) show that inputs of elements from the atmosphere (marine aerosols and dusts) can sustain the productivity of Hawaiian rainforest. In addition to the DSi transfer by rivers, the eolian erosion of the land surface is a potentially important pathway for transport of Si to the oceans. Airborne particles enter the surface ocean (0.28×10^{12} kg Si yr^{-1}) where a small fraction dissolves (0.01×10^{12} kg Si yr^{-1}) (Tréguer et al., 1995) (Figure 2.2).

Depending on its mineralogy, the impact of dust on the soil genesis and, *in fine*, on terrestrial biogeochemical cycle of Si varies greatly by region (Simonson, 1995). Street-Perrott and Barker (2008) show that atmospheric Si input in temperate and tropical forests ranges from 0.04 to 2 kg Si ha^{-1} $year^{-1}$. Dry Si deposition is highest near the sources of the African, Arabian, Asian and Australian deserts (Tegen et al., 2002). In East African, savanna fires would be a significant source of atmospheric phytolith particles (Street-Perrott and Barker, 2008). In most intensely weathered soils, wind-blown dust becomes the dominant source of Si on topsoil: near-surface horizons of Hawaiian soils contain as much as 30% quartz, a mineral absent from local parent material (Kurtz et al., 2001). In soil derived from basaltic ash (Cameroon), Opfergelt et al. (2010) estimate that the content of quartz from saharian dust deposition on topsoil ranges from 2-8% depending on soil localization. In Northeast Sweden, Engström et al. (2008) suggest that Si content in tree leaves originates both from Si plant uptake and from local airborne particulate material, quantifying this exogenous Si contribution between 1 and 70%. The minerals identified in the exogenous material on shoots include NaCl, $CaSO_4$, $CaCO_3$, SiO_2 and silicates (Wyttenbach and Tobler, 1998). Precipitations can also sustain Si to the soil-plant system, such as in a rice field in Camargue (France) where the annual precipitation flux give a DSi input of 3±2 kg Si ha^{-1} yr^{-1} (Desplanques et al., 2006). Similarly, in two amazonian forest environments in Brazil, the inputs of Si on topsoil from the rain and from dust were small but not negligible: 0.6 kg Si ha^{-1} yr^{-1} (Cornu et al., 1998). Finally, in humid climates, most values of annual Si inputs through rainfall are <1.4 kg Si ha^{-1} yr^{-1} (Sommer et al., 2006). More generally, atmospheric inputs were estimated at <1, 1.5 and 2 kg Si ha^{-1} yr^{-1} (Alexandre et al., 1997; Bartoli, 1983; Blecker et al., 2006, respectively). The atmospheric Si supply in biogeosphere is thus ubiquitous but very low compared to other Si inputs in the soil-plant system (Street-Perrott and Barker, 2008).

2.3 Transfer of dissolved Si from soil-plant systems towards hydrosphere

The DSi concentrations in rivers can be useful to quantify chemical weathering rates and CO_2 consumption (Gaillardet et al., 1997,1999a,b; Oliva et al., 1999; Vuai and Tokuyama, 2007). However, values can be misinterpreted if the part of H_4SiO_4 polymerized in higher plants and in phytoplankton as BSi is neglected (Bormann et al., 1998; Meunier, 2003; Street-Perrott and Barker, 2008). Indeed, the mass-balance of Si at watershed scale has to be evaluated taking into account the pathways of Si between lithosphere and biosphere (recycling, immobilization, exportation and restitution of Si by vegetation) before its transfer to rivers. Moreover, before its transfer to oceans, dissolved and particulate rivers loads can be deposited and DSi can be extracted by grasses and stored in phytoliths (Wüst and Bustin, 2003; Ding et al., 2004) or taken up by phytoplankton and stored in frustules (Ragueneau et al., 2006). Struyf et al. (2009) confirm that wetlands, as biological Si sink, control the fluxes of both DSi and ASi along the land-ocean continuum. Most watershed studies, which have estimated soil weathering rates, assume that surface discharge chemistry reflects the soil water chemistry. However significant discrepancies between soil and surface chemistries are apparent in some cases and could be explained by rapid surface runoff (DSi in surface discharge < DSi in soil water) and weathering at a narrow interface between the bedrock and soil zone in saprolite (DSi in surface discharge > DSi in soil water) (White, 1995).

The average DSi concentration in freshwater at global scale displays huge variations relative to geographical regions (Table 2.4). The low DSi concentration of Australian freshwater reflects the intensely weathered soils in this region (Exley, 1998). In boreal and arctic rivers, the concentration of DSi, 30-50% lower than the global average, seems to be mainly controlled by the soil and vegetation through the production of organic acids since there is a positive correlation between total organic carbon and DSi in these rivers (Humborg et al., 2006). The huge variations in DSi concentrations are closely linked to the weathering status of the immediate geology (Exley, 1998).

However, the DSi concentration alone does not provide clues on the sources and processes affecting riverine fluxes of DSi (Jennerjahn et al., 2006). In weathering-limited systems, transport processes remove products of weathering faster than the neoformation and precipitation of secondary phases. In contrast, in transport-limited systems, river load depends on the availability of water as a transporting agent (Drever, 1988). This will induce variations in DSi transfer towards rivers between geographical regions. Because minerals weathering (temperature and physical denudation) and transport conditions (runoff) exert major control on processes governing the DSi inputs to rivers (Meybeck, 1979; Anderson et al., 1997; Gaillardet et al., 1999a; Turner et al., 2003; Fulweiler and Nixon, 2005; Jennerjahn et al., 2006; Gislason et al., 2009), DSi fluxes will be discussed separately in tropical and non-tropical rivers, following the

Table 2.4 The DSi concentration of freshwater at global scale (modified from Exley, 1998).

	DSi (µmol l^{-1})
Australia	65
Europe	126
North America	151
Asia	196
South America	200
Africa	389
Global average[a]	150

[a] Estimation of discharge-weighted average silicic acid concentration in rivers (Tréguer et al., 1995)

various geographical regions as compiled by Jennerjahn et al. 2006 (Table 2.5).

Currently, the average global DSi flux is two to three times higher in tropical than in non-tropical rivers according to Tréguer et al. (1995): 74% of the total annual DSi input by rivers into the oceans is from tropical region (0.12×10^{12} kg Si yr^{-1}) and 20% is from temperate region (0.03×10^{12} kg Si yr^{-1}). This distribution could vary as precipitations increase in most of the Northern hemisphere (0.5-1%/decade) and decrease in sub-tropical land areas (0.3%/decade) (Lal, 2004).

The *tropical* ecosystems represent 33% of the land mass (Meunier et al., 2001) and are responsible for the major part of the DSi transfer from continents to oceans. Indeed, the river basins with the largest total CO_2 consumption fluxes are all located in the humid tropics (Gaillardet et al., 1999b). Tropical rivers in Asia and Oceania display high DSi fluxes that match the optimum weathering and transport conditions (Jennerjhan et al., 2006).

These tropical environments are characterized by young geology, active tectonism in the circum-Pacific ring of fire, high runoff and high silicate weathering rates (Milliman and Meade, 1983; Milliman and Syvitski, 1992; Sommer et al., 2006). The model predictions of Beusen et al. (2009) also give strong indication that DSi fluxes depend on the precipitation and the occurrence of volcanic rocks.

Table 2.5 Average DSi fluxes and load per continent and per latitude (tropical or not). Data are from Jennerjahn et al. (2006) and represent only the large tropical rivers.

	DSi flux (kg Si ha^{-1} yr^{-1})	DSi load (10^9 kg Si yr^{-1})
Tropical rivers		
Africa	11.3	8.9
South America	21.9	24.3
Asia	23.6	11.5
Oceania	95.1	1.4
Non-tropical rivers		
Oceania	0.2	0.2
Africa	0.6	0.3
North America	7.5	5.4
Asia	7.9	12.9
Europe	7.9	1.6
South America	32.0	6.6
Total Load		74.5[a]

[a] This estimation of DSi load from rivers into oceans represents 50% of the total riverine DSi load calculated by Tréguer et al. (1995) (see Figure 2.2) since this table only represents half of the world river discharge (37400 km^3 yr^{-1}).

Despite its restricted spatial distribution, basalts are eight times more soluble than granites (Dupré et al., 2003) and contain a high proportion of ferromagnesian minerals susceptible to chemical weathering by higher plants (Cochran and Berner, 1996). The conversion of forest to agricultural field of rice (Si-accumulator) may reduce DSi fluxes in tropical rivers despite high weathering rates because of Si storage in biomass exported (Jennerjahn et al., 2006).

The *non-tropical* rivers generally display much lower relative silicate weathering rates and DSi fluxes (Jennerjahn et al., 2006). Especially the Siberian and Canadian rivers contribute to 10% of the total DSi input into oceans (Gordeev et al., 1996). With low temperature and runoff in weathering-limited temperate region, DSi fluxes should be driven by soil and vegetation (Humborg et al., 2006) through (i) the high supply of organic protons lowering pH in topsoils (ii) the high Si recycling rates by vegetation compared to DSi fluxes in rivers, and (iii) the production of reactive phytoliths on topsoil. All of these phenomena accelerate the silicate mineral weathering rates. In a granitic forested ecosystem, the river DSi concentrations exhibit a strong seasonal signal that did not vary in a regular way with water discharge or water temperature. In this study, the spring decline in river DSi concentration should be due to Si uptake by terrestrial vegetation (Fulweiler and Nixon, 2005). According to the low DSi fluxes and loads in non-tropical rivers, we can conclude that these biological processes are less efficient in transferring DSi from continents to oceans than the high weathering rates observed in tropical regions (Jennerjahn et al., 2006; Humborg et al., 2006). The vegetation and soil may also impact the DSi fluxes in highly weathered tropical watersheds (Sommer et al., 2006) since the DSi flux in poorly developed soils under subarctic climate (Anderson et al., 1997,2000) is the same order than strongly developed soils of tropical climate (Oliva et al., 1999).

The relatively high DSi flux from non-tropical South America could be explain by the physical denudation in mountainous aeras combined with high runoff and temperature which provide ideal conditions for high chemical weathering rates and high DSi transport (Milliman and Syvitski, 1992, Gaillardet et al., 1999a). Indeed, physical weathering and erosion in areas of high relief enhance weathering by continually exposing freshmineral surfaces (Summerfield and Hulton, 1994; Street-Perrott and Barker, 2008). However, physical weathering in high-latitude watersheds seems to lead mostly to the formation of clay minerals but does not immediately lead to higher DSi fluxes as observed for tropical regions with active tectonics (Anderson et al., 2000; Humborg et al., 2006).

In summary, a hierarchy of driving variables can be established to control Si fluxes from continents to oceans. At global scale, runoff is the main driver of Si fluxes, followed by temperature. At regional scale, DSi fluxes are a function of (1) the catchment lithology (content of weatherable minerals), (2) the hydrological conditions (discharge), (3) the soil development in the catchment (Sommer et al., 2006), and (4) the biological processes.

CHAPTER 3:

ENVIRONMENTAL SETTINGS OF THE EXPERIMENTAL SITE

3.1 Historical context

The behavior of human society and its socio-economic evolution have often caused a decrease in forest area through overexploitation. In France, the forest area was 40 Mha after the last glaciation (de Monza, 1991) and fell to 8.5 Mha in the mid-19th century (Cinotti, 1996). Given the deficit in the forestry wood chain, high production coniferous species were planted after the Second World War to reach a forest area currently at 14.5 Mha. These coniferous species, translocated within Europe and imported from North America, are thought to have a significant effect on the physical, chemical and biological characteristics of topsoil, with a potential negative impact on the environment (Augusto et al., 2002). The effect of tree species should not affect the soil fertility as long as the processes of the ecosystem which are modified do not become limiting factors on the trees and other parts of the ecosystem (Binkley and Giardina, 1998). We know that in forest management, the concept of soil resiliency is of great importance in order to estimate the amount of wood production the ecosystem can sustain. However, the effect of fast-growing species with elevated nutrient export is thought to be considerable because these species are largely planted on poor soils in Europe. The intensity of the species effect is estimated in diverse ways, due to the variations in pedological conditions between the study sites (Binkley, 1995). During the 1970s, environmental awareness and the concept of sustainable management led the scientific community to assess the impact of coniferous species on the ecosystem.

In this regard, the experimental site of Breuil-Chenue is part of a global project to quantify the effect of the substitution of tree species, both coniferous and broadleaved, on the biogeochemical and biological stability of the soil-tree system (Bonneau et al., 1977; Ranger et al., 2004). In this unique natural laboratory, the impact of tree species is clearly discernible since soil physical and chemical properties were identical between tree plots (Bonneau et al., 1977). The contrasting tree species planted in identical soil and climate conditions provide an excellent opportunity to study the terrestrial Si biogeochemical cycle in various temperate forest ecosystems.

The forest of Breuil-Chenue has always been forested. In the past, the native forest was a royal forest, which then became an estate forest in

1789. The native forest has not been harvested since the second half of the last century (Mareschal, 2008). The native mixed forest was a 150 year-old Coppice with Standards (CwS) stand dominated by European beech (*Fagus sylvatica* L.) and oak (*Quercus sessiliflora* Smith.). It was clear-cut in 1976 and replaced by monospecific plantations distributed in plots of 0.1 ha: oak (*Quercus sessiliflora* Smith), European beech (*Fagus sylvatica* L.), Norway spruce (*Picea abies* Karst.), Douglas fir (*Pseudotsuga menziesii* Franco) and Black pine (*Pinus nigra* Arn. *Ssp laricio* Poiret var corsicana). Trees were 4 years old at planting. The plantation density was 1600 trees.ha^{-1} for coniferous trees and 15000 trees.ha^{-1} for broadleaved trees. The experimental site is divided into two adjacent blocs with replicated stands. The parcels of native forests are not control plots since they have not been set up by swathing (Bloc 1) or burning (Bloc 2) (Figure 3.1). In our study, the forest floor horizons and soil layers were collected in November 2006 in Bloc 2 from three selected points at the core of each of the following stands: Douglas fir, Norway spruce, Black pine, European beech and oak (Figure 3.1). For some specific experiments, we used soil samples collected in Bloc 1 by the INRA-Nancy research team working on the Biogeochemistry of forest ecosystems.

3.2 Geography and climate

The experimental site is located in the estate forest of Breuil-Chenue in Nièvre department in the Morvan natural park (central France: 47°18’10”N; 4°4’44”E) (Figure 3.2), on a plateau at 638 m asl, slightly inclined towards the south (Figure 3.3).

According to the Köpper-Geiger climate map of Europe, the climate is Cfb, i.e. a temperate climate without dry season and with a warm summer (Peel et al., 2007). The main climatic characteristics, observed at the nearby meteorological station of Château-Chinon, are as follows: (i) the mean annual rainfall is 1212 mm with a marked seasonal pattern of higher rains in winter and lower ones in April and July and (ii) the mean annual temperature is 9°C with a mean monthly minimum of 5.4°C and a mean monthly maximum of 12.5°C. The Morvan mid-mountains, watered by rains from the West, have a dense river network, feeding the basin of the Seine and the Loire in France.

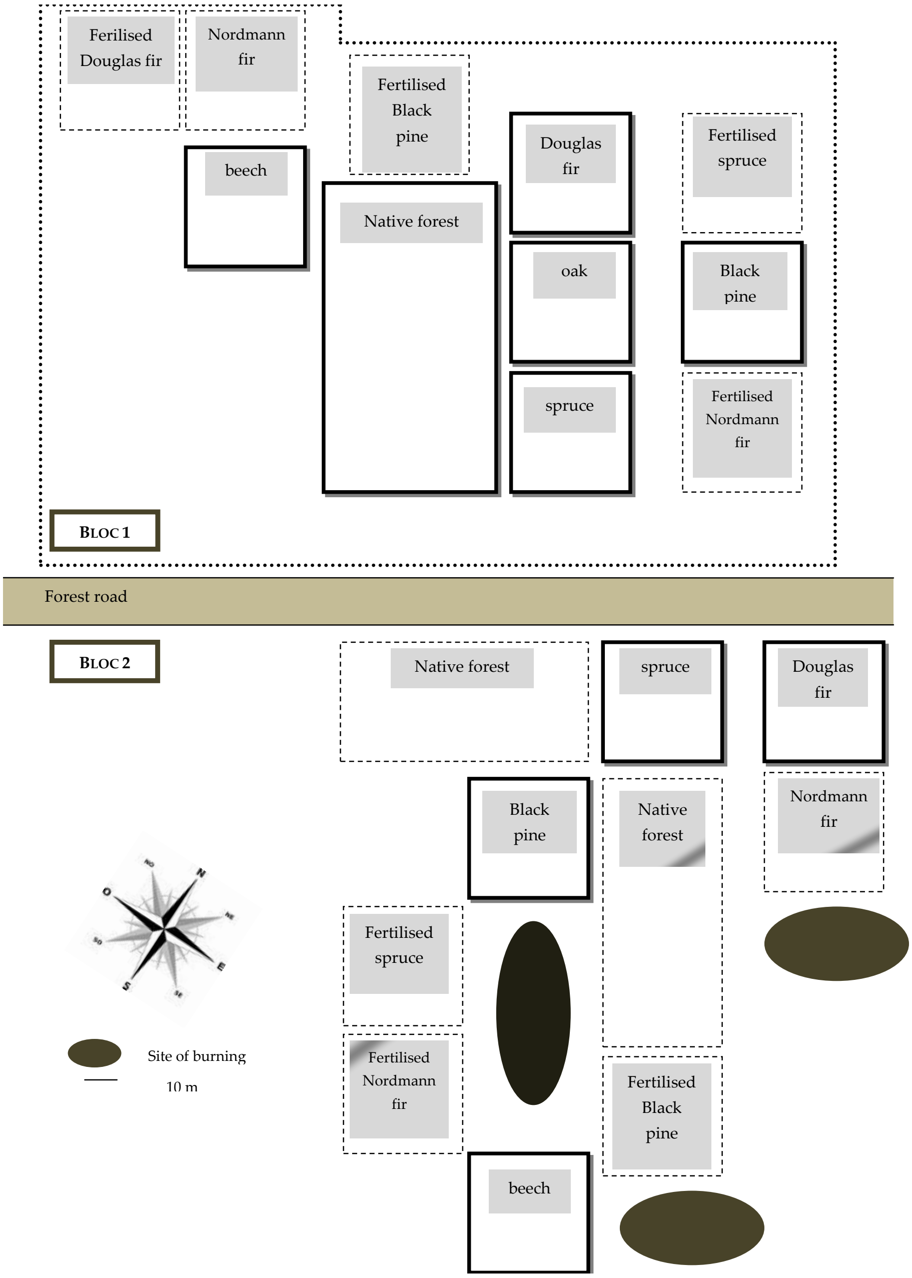

Figure 3.1 Description of the experimental site at Breuil-Chenue forest; it is divided into two blocs (1 and 2). The samplings of organic and mineral soils as well as soil solutions were carried out in the boxes printed in bold type; there was no sampling in dotted boxes.

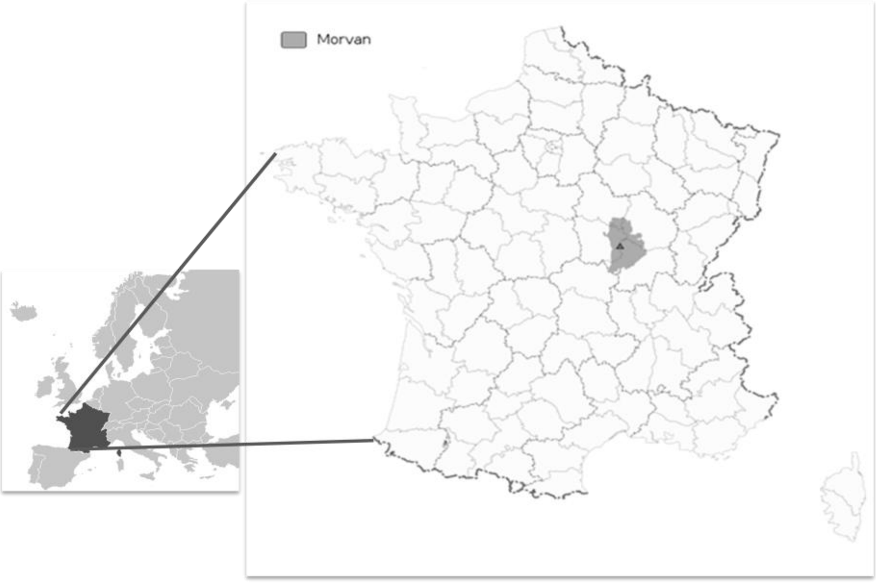

Figure 3.2 Map of France showing the location of the natural Morvan park.

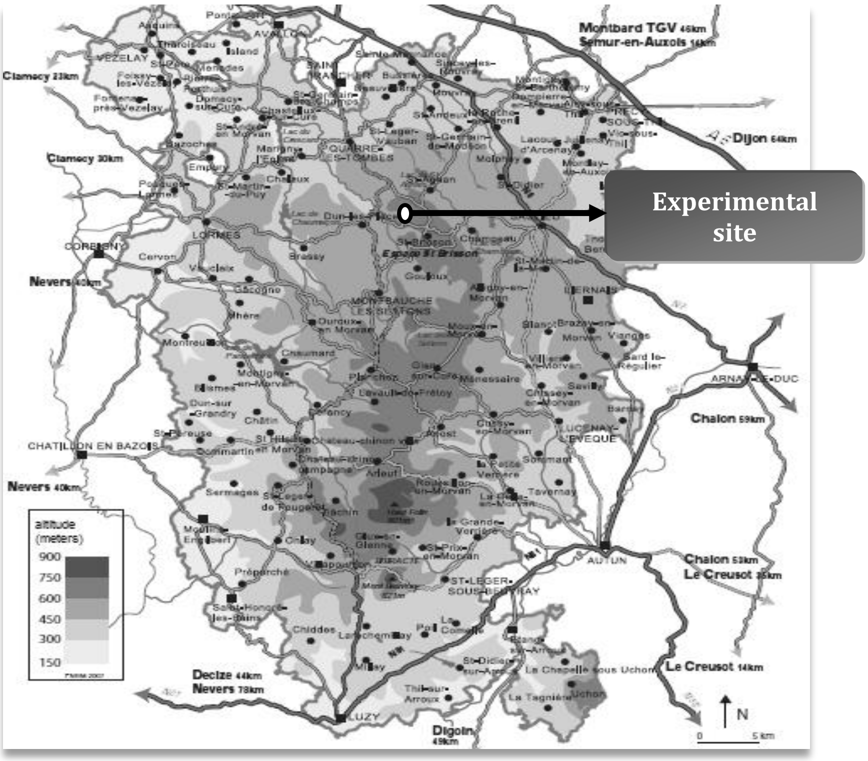

Figure 3.3 Map of Morvan showing the location of the experimental site (www.parcdumorvan.org).

3.3 Geological context

The geological substrate is the granite of La Pierre-qui-Vire (Seddoh, 1973) covered by a thin layer of cryoturbated quaternary loess (Aurousseau, 1976). The 2-micas granitic block la Pierre-qui-Vire is located in the region between Saint Brisson, Quarré-le-Tombes, La Roche-en-Breuil and Saulieu (Figure 3.4) and it extends 20 km east-west and 10 km north-south to include the experimental site of Breuil-Chenue in the south of the granitic block. According to Dejou's observations (1966), the transition between the 3 facies constituting the granite (coarse, medium and fine grains) is gradual and the crystal size increases gradually. Their situation seems to show that magma cooling was (i) rapid on the edge of batholith leading to finer facies and (ii) slower at the center of the igneous intrusive rock leading to coarse facies. Geochronological results show that 2-mica granite is 295±5 million years, which is the most recent Morvan granite (Vialette, 1965).

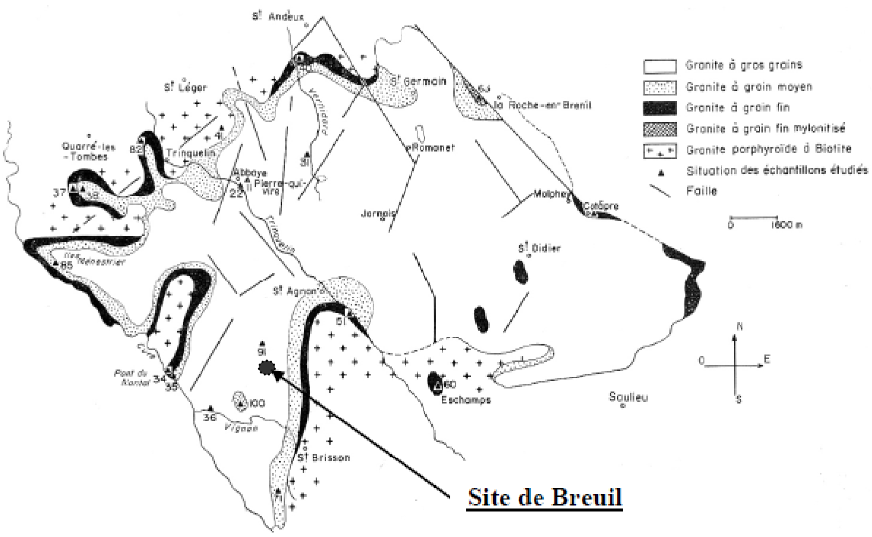

Figure 3.4 Mapping of the facies of 2-mica granite (Dejou, 1966; adapted from Mareschal, 2008).

The medium-grained granite is almost exclusively located in Bloc 2 and the coarse-grained granite in Bloc 1. The granite has the following mineralogical composition for coarse and medium facies respectively (Mareschal, 2008; Ranger et al., 2004): 34 and 35% quartz, 24.2 and 23.8%

feldspars, 31.1 and 30.3% albite, 8.9 and 8.1% muscovite, 1.2 and 2.2% biotite, 0.5 and 0.8% chlorite, leading to mean total concentrations of 0.17% MgO, 0.34% CaO, 4.69% K_2O and 75.8% SiO_2 (Table 3.1). The granite of La Pierre-qui-Vire is an acid rock containing more than 75% silica and represents a low potential source of alkaline earth cations.

Table 3.1 Total concentrations (% wt) of medium (M) and coarse (C) grains of the 2-micas granite collected in Bloc 2 (M) and Bloc 1 (C) (Mareschal, 2008).

	SiO_2	Al_2O_3	Fe_2O_3	MnO	MgO	CaO	Na_2O	K_2O	TiO_2	P_2O_5
	--------------------------------------%--									
M	75.46	14.15	1.22	0.05	0.21	0.37	3.32	3.32	0.10	0.13
C	76.07	13.55	1.26	0.05	0.13	0.31	3.51	3.51	0.07	0.08

3.4 Pedological context

The acid brown soil is well-drained and classified as Alumnic Cambisol (IUSS, 2006) with depths ranging from 120 to 140 cm. This Cambisol could also be classified as a Dystri-Alumnic Cambisol since the forest soil is characterized by a base saturation of less than 50% in at least some part between 20 and 100 cm from the soil surface and by 50% or more Al-saturation in at least some part of the subsurface horizon between 50 and 100 cm from the soil surface (IUSS, 2006). A typical Breuil-Chenue forest soil profile is described in Appendix A.

The major soil properties at the experimental site are presented in Table 3.2 and 3.3. The soil is sandy loam with 55% sand and less than 20% clay. The soil is acid with pH ranging from 3.8 to 4.6 and a small base saturation, which is less than 10% and decreases with depth (Table 3.2). The cation exchange capacity (CEC) is small and mainly occupied by Al (Mareschal et al., 2010).

As estimated from their total reserve in bases (TRB = sum of total Ca, Mg, K, and Na contents expressed in $cmol_c\ kg^{-1}$) (Herbillon, 1986), the content of weatherable minerals slightly increases to a depth of 70cm, with a mean value of 164 $cmol_c\ kg^{-1}$ for the first soil depth and 169 $cmol_c\ kg^{-1}$ at greater depth (Table 3.3). Then, TRB contents decrease significantly near the granitic parental material. The Ca and Mg concentrations are negligible. Alkaline cations, especially K, are present at greater concentrations. On average, Ca, Mg, Na and K represent <1, 14, 22 and 62% respectively of the TRB. The total stock of SiO_2 on the Breuil site is considerable (10236 $T.ha^{-1}$) in comparison with the alkaline and alkaline earth elements that correspond well with the acidity of bedrock.

Given the temperate climate and the bedrock very poor in alkaline and alkaline earth cations, organic matter accumulates at the soil surface as humus (> 2cm). The humus form is a moder with a medium rate of decomposition (Brethes et al., 1995) in the native forest. In Breuil-Chenue forest, most of the root biomass occurs within the first 70 cm (Mareschal 2008). The carbon (C) concentration is 7.3% in the Ah horizon (~0-5cm) and then decreases with depth (Mareschal et al., 2010). Ranger et al. (2004) and Mareschal (2008) observed that organic acids produced by humus lead to a crypto-podzolisation at the surface and to a re-distribution of free Fe_o in the shallow soil (5-10cm) (Table 3.4). Through the XRD patterns and chemical analyses performed on Breuil-Chenue forest soil, Mareschal (2008) and Calvaruso et al. (2009) identified the following (i) primary minerals: K-feldspar, muscovite, biotite, albite and quartz, and (ii) secondary minerals, mainly identified in the clay fraction: kaolinite, vermiculite, smectite, gibbsite, iron oxide and complex interstratified minerals. The clay-sized fraction in the shallow soil consists of the following distribution of minerals: kaolinte (30%) ~ illite (30%) > quartz (20%) > vermiculite (11%) > smectite (4%) > gibbsite (3%) > Fe oxides (2.5%) (Mareschal, 2008). The specific surface area of the soil is between 48 and 57 $m^2.g^{-1}$ of fine earth fraction. The clay fraction contributes between 78 and 84% of the total specific surface area, depending on horizons (Mareschal, 2008).

Table 3.2 Soil properties of the original native forest (CwS) at the experimental site (Mareschal, 2008; Mareschal et al., 2010).

Depth	pH [a] (H_2O)	pH (KCl)	C	N	Clay	Silt	Sand	[b] Ca^{2+}	Mg^{2+}	K^+	Na^+	Al_{tit}	CEC [c]	BS [d]
cm			$g\ kg^{-1}$	$g\ kg^{-1}$	------------- % --------------			--------------------------$cmol_c\ kg^{-1}$--------------------------						%
0-5	3.8	3.1	73.4	3.9	17.1	25.2	57.7	0.15	0.27	0.39	0.03	7.3	9.2	9.1
5-10	4.2	3.7	37.9	2.0	18.4	26.6	55.0	0.05	0.12	0.21	0.01	6.7	6.9	5.6
10-15	4.6	4.1	31.6	1.7	16.2	23.8	60.0	0.02	0.06	0.12	0.01	4.8	5.2	4.0
15-25	4.6	4.3	19.1	1.0	18.8	25.2	56.0	nd	0.03	0.09	0.01	3.3	3.4	3.8
25-40	4.5	4.3	13.2	0.7	19.6	26.9	53.5	0.02	0.02	0.08	nd	2.5	2.7	4.4
40-55	4.5	4.3	nd [e]	nd	17.7	23.1	59.2	0.02	0.02	0.08	0.01	2.6	2.7	4.8
55-70	4.5	4.3	nd	nd	19.0	24.0	57.0	0.02	0.02	0.08	0.01	2.4	2.7	4.8

[a] The pH of soil samples was measured in both 1M KCl and in distilled water, with a soil to solution ratio of 1:5

[b] Exchangeable cations in soil samples were extracted, using either 1M KCl for Mg^{2+}, Ca^{2+}, Na^+, Fe^{3+} and Mn^{2+} or a 1M NH_4Cl for K^+. The 1M KCl soil extract was also titrated to assess exchangeable H^+ and Al_{tit} (Mareschal et al., 2010)

[c] Cation exchange capacity (CEC) = (Mg^{2+} +Ca^{2+} +K^+ + Na^+ +Fe^{3+} +Mn^{2+} +H^+ +Al_{tit})

[d] BS, base saturation = ($(Na, K, Ca, Mg)_{exch}$*100)/CEC

[e] nd = not determined

Table 3.3 Total elemental contents and total reserve in bases (Mareschal, 2008; Mareschal et al., 2010).

Depth	SiO_2	Al_2O_3	Fe_2O_3	MnO	MgO	CaO	Na_2O	K_2O	TRB[a]
cm	------------------------------- Total contents (%)							--------------------	$cmol_c.kg^{-1}$
0-5	74.3	15.4	2.4	0.0	0.3	LD	1.4	4.9	164
5-10	72.6	15.9	2.6	0.0	0.3	LD	1.4	4.9	164
10-15	73.0	16.1	2.5	0.1	0.4	LD	1.4	4.8	167
15-25	70.9	16.5	2.6	0.1	0.4	LD	1.4	4.7	165
25-40	69.1	17.3	2.8	0.1	0.5	0.1	1.4	4.5	169
40-55	67.7	17.2	2.7	0.1	0.5	0.1	1.5	4.4	169
55-70	69.7	16.2	2.5	0.1	0.4	0.1	1.5	4.6	169
70-100	66.8	18.6	2.9	0.1	0.5	LD	0.9	4.5	134
100-140	66.0	21.1	1.5	0.0	0.2	LD	0.3	5.3	132
Total stock ($T\ ha^{-1}$)	10236	2793	344	7	56	5	142	727	

[a] TRB = total reserve in bases. TRB is the sum of the total contents of the four alkaline and alkaline-earth cations (Na^+, K^+, Ca^{2+}, Mg^{2+}) and characterizes the fertility level in the Breuil forest site

Table 3.4 presents the specific Al and Fe extractions. The higher Fe_d/Fe_t ratio in deep soil layers shows that the content of Fe-bearing minerals (Fe_t) is lower in the deep soil. This finding confirms the lower TRB content at a depth of between 70 and 140 cm, and this reveals the high weathering rates of primary minerals in deep soil (Mareschal, 2008). Fe_d/Fe_t ratio slightly increases from 70 cm deep to surface organic-rich horizons. Such a trend matches the weak decrease in TRB and bears out increasing weathering accompanied by the release of Fe. The pedogenic formation of iron oxides is frequently associated with the weathering process of brunification in humid temperate environments (Schwertmann and Cornell, 1991). Fe_o contents increase from the deep mineral layers up to the surface. The increase in Fe_o/Fe_d ratios towards the surface points to the weak crystallinity of extractable Fe. As we know organic substances affect the formation of crystalline iron compounds in surface horizons (Schwertmann and Cornell, 1991; Brahy et al., 2000a).

Table 3.4 Extractable Fe and Al in dithionite-citrate-bicarbonate (DCB) (d) and oxalate (o), Fe_d/Fe_t and Fe_o/Fe_d ratios. Fe and Al are extracted in dithionite citrate bicarbonate (d) and acid ammonium oxalate at pH 3 (o) and are described by Mareschal (2008).

Depth	Fe_d [a]	Al_d [a]	Fe_o [b]	Al_o [b]		
cm	----------------------	%	----------------------		Fe_d/Fe_t	Fe_o/Fe_d
0-5	0.81	0.27	0.32	0.18	0.48	0.39
5-10	0.98	0.45	0.40	0.35	0.54	0.41
10-15	0.87	0.56	0.32	0.49	0.50	0.37
15-25	0.96	0.57	0.35	0.57	0.53	0.36
25-40	0.92	0.44	0.28	0.41	0.47	0.30
40-55	0.81	0.36	0.25	0.37	0.43	0.31
55-70	0.85	0.36	0.23	0.33	0.48	0.27
70-100	1.19	0.31	0.21	0.26	0.58	0.18
100-140	0.67	0.14	0.05	0.11	0.64	0.07

[a] DCB digestion releases Fe from crystallized iron oxides. The content of Fe-bearing minerals is evaluated by $Fe_t - Fe_d$. Fe_t represents the total Fe contents

[b] Oxalate digestion releases Al from organic complexes and dissolves allophane, imogolite and poorly crystalline hydrous Fe oxides

The DSi concentrations in forest floor leachate solutions range from 0.02 to 0.06 mM and are tree species-dependent (Figure 3.5). The DSi concentrations in soil solutions show a very similar trend under each tree species: an increase of DSi concentration from the humus layer to a depth of 15 cm (0.08-0.14 mM) and a slight decrease at a depth of 15 to 60 cm (0.06-0.08 mM). The Si concentrations in soil solutions are also tree species-dependent and vary between 0.06 and 0.14 mM (Jaffrain, 2006).

DSi concentrations in forest floor leachates vary by a factor of four over the annual cycle, with a minimum of about 0.5-1.5 mg.l^{-1} in late spring and early summer and a maximum of about 1.5-3.0 mg.l^{-1} during autumn and winter (Figure 3.6). Under oak and Norway spruce, we observe an increase of DSi concentrations (4.0 mg.l^{-1}) in September and November, respectively. Besides the decrease of DSi concentrations in late spring, the seasonal variability does not seem constant between tree species. In solution collected at 60 cm soil depth, we observe a slight seasonal variability, with a minium of about 1.5 mg.l^{-1} during spring and summer and a maximum of about 2-2.7 mg.l^{-1} during autumn and winter (Figure 3.7).

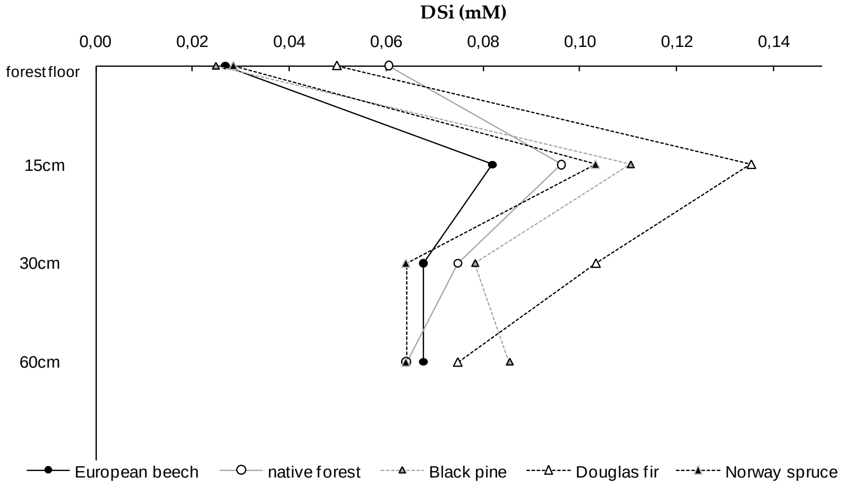

Figure 3.5 Mean DSi concentrations (mM) in soil solutions collected by zero tension plate lysimeter made of polypropylene (forest floor leachate solutions) and by ceramic cup lysimeter (soil solutions) between 2001 and 2006 in the forest site of Breuil-Chenue.

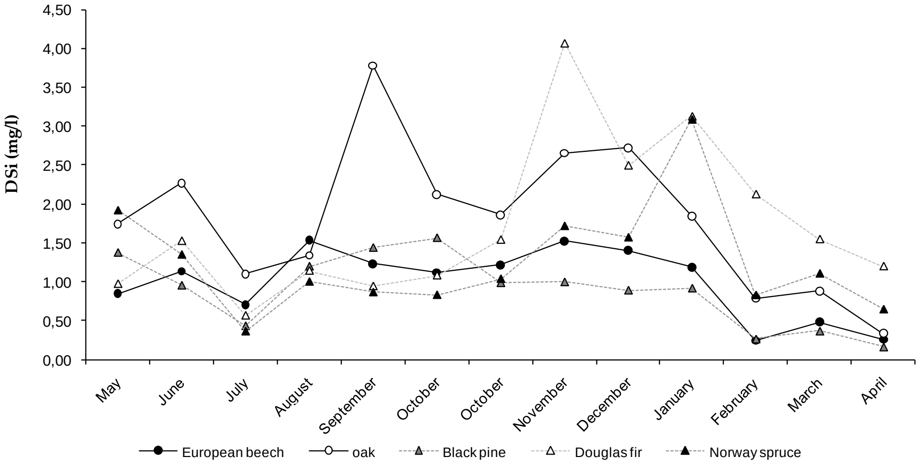

Figure 3.6 Dissolved Si concentrations in forest floor leachates as a function of time (May 2006-April 2007) and of tree species in the forest site of Breuil-Chenue.

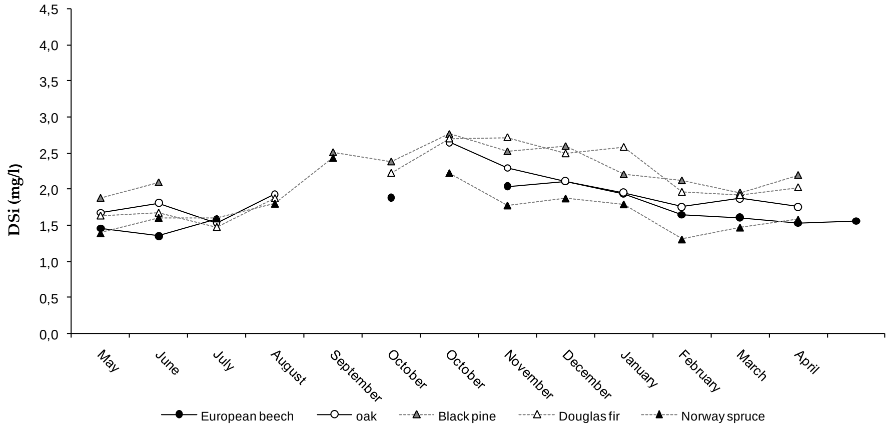

Figure 3.7 Dissolved Si concentrations in soil solutions (60 cm depth) as a function of time (May 2006-April 2007) and of tree species in the forest site of Breuil-Chenue.

At the Breuil forest site, the chemical composition of forest floor leachate solutions seems mainly controlled by (i) organic matter mineralization (NO_3, alkaline and alkaline earth cations), (ii) organo-metallic complexes and transport of secondary organo-mineral phases (Al, Fe, dissolved organic carbon, Si) and (iii) atmospheric deposit (Na, Cl , SO_4) (Jaffrain, 2006). In forest floor leachates, the content of DSi in aqueous phase seems influenced by DOC content. Indeed H_4SiO_4 can be adsorbed onto Fe and Al (hydr)oxides which are associated with the colloidal fraction of DOC. Organic ligands could promote chemical weathering and increase DSi concentration in the upper soil layers. An activity diagram (Figure 3.8) relevant to the Al-Si system show that Breuil site solutions are undersaturated with respect to amorphous $Al(OH)_3$ and amorphous silica (Wonisch et al., 2008). Moreover, solutions are mostly supersaturated with respect to poorly-crystallized and well-crystallized kaolinite, but also mostly undersaturated with respect to ITM (imogolite type material). As illustrated in the stability diagram, forest soil solutions on the Breuil site are supersaturated with quartz.

This is consistent with soil mineralogy since kaolinite is detected in our forest soil (Mareschal, 2008). As suggested by Jaffrain (2006), the lack of a linear relationship for log (Al^{3+}) + 3pH on log (H_4SiO_4) with Al-Si containing solids demonstrates that the formation of these solid phases may not be responsible for the Si sink at a depth of 30 cm (Figure 3.8).

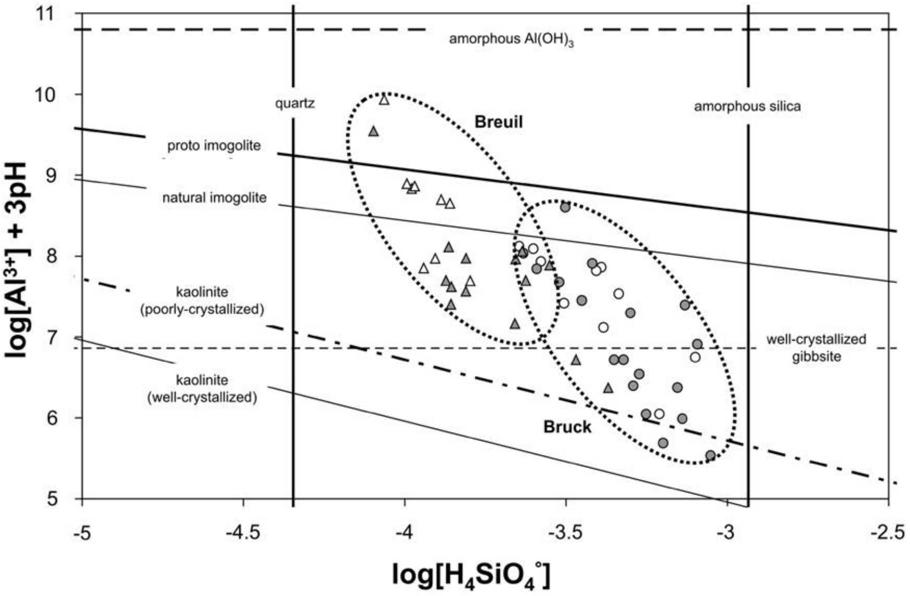

Figure 3.8 The activities of Al^{3+}, H^+ and $H_4SiO_4^0$ and solubility lines for Al-Si containing solids. Open and closed symbols denote solutions containing solely monosilicic acid and additional polymerized silicic acid, respectively. Triange symbols: solutions from the Breuil forest site (France); circle symbols: solutions from Bruck site (Austria) (adapted from Wonisch et al., 2008).

CHAPTER 4:

TREE SPECIES IMPACT THE TERRESTRIAL CYCLE OF SILICON THROUGH VARIOUS UPTAKES*

---

* Adapted from Cornelis JT., Ranger J., Iserentant A. and Delvaux B. (2010) Tree species impact the terrestrial cycle of silicon through various uptakes. *Biogeochemistry* 97:231-245.

A laboratory experiment on ceramic cup lysimeter is presented in Appendix B.

Abstract

The quantification of silicon (Si) uptake by tree species is a mandatory step to study the role of forest vegetations in the global cycle of Si. Forest tree species can impact the hydrological output of dissolved Si (DSi) through root induced weathering of silicates but also through Si uptake and restitution *via* litterfall. Here, monospecific stands of Douglas fir, Norway spruce, Black pine, European beech and oak established in identical soil and climate conditions were used to quantify Si uptake, immobilization and restitution. We measured the Si contents in various compartments of the soil-tree system and we further studied the impact of the recycling of Si by forest trees on the DSi pool. Si is mainly accumulated in leaves and needles in comparison with other tree compartments (branches, stembark and stemwood). The immobilization of Si in tree biomass represents less than 15% of the total Si uptake. Annual Si uptake by oak and European beech stands is respectively 18.5 and 23.3 kg ha^{-1} yr^{-1}. Black pine has a very low annual Si uptake (2.3 kg ha^{-1} yr^{-1}) in comparison with Douglas fir (30.6 kg ha^{-1} yr^{-1}) and Norway spruce (43.5 kg ha^{-1} yr^{-1}). The recycling of Si by forest trees plays a major role in the continental Si cycle since tree species greatly influence the uptake and restitution of Si. Moreover, we remark that the annual tree uptake is negatively correlated with the annual DSi output at 60 cm depth. The land-ocean fluxes of DSi are certainly influenced by geochemical processes such as weathering of primary minerals and formation of secondary minerals but also by biological processes such as root uptake.

4.1 Introduction

Silicon (Si) is a major solute of river discharge into oceans (Gaillardet et al., 1999a). It plays a crucial role in major global biogeochemical processes such as the nutrition of both marine and terrestrial biota (Smetacek, 1999; Epstein, 1999), and the regulation of atmospheric carbon dioxide (Volk, 1987; Berner, 1997; Sommer et al., 2006) through the buffering of proton fluxes during silicate dissolution (Rai and Kittrick, 1989). Plants can exert a strong imprint on the Si continental cycle through the uptake and restitution of Si (Derry et al., 2005; Street-Perrott and Barker, 2008). Plants greatly differ in their ability to accumulate Si, a non-essential but beneficial element (Richmond and Sussman, 2003; Ma and Yamaji, 2006; Liang et al., 2007). They can accumulate Si in a similar extent as some major macronutrients: 0.1% to 10% of dry weight (Epstein, 1999). Most studies of Si uptake in the higher plants were focusing on monocots which are typical Si-accumulators (Ma and Takahashi, 2002). Taken up as aqueous monosilicic acid ($H_4SiO_4^0$), Si is translocated to transpiration sites (Jones and Handreck, 1965) where it polymerizes as amorphous biogenic opal called phytolith (BSi), which returns to the soil within organic residues (Smithson, 1956). Thus, in terrestrial ecosystems, BSi is distributed between plant and soil. In forest ecosystems, the BSi recycling is one of the major processes to control the hydrological output of aqueous monosilicic acid (Bartoli, 1983; Alexandre et al., 1997; Markewitz and Richter, 1998; Meunier et al., 1999; Lucas, 2001; Watteau and Villemin, 2001; Farmer et al., 2005). The quantity of Si recycled within the soil-tree cycle may be species-dependent since angiosperms enhance the weathering to a greater degree than gymnosperms (Moulton et al., 2000; Johnson-Maynard et al., 2005). Relative to broadleaved species, conifers generally accumulate low amounts of Si in their shoots (Geis, 1973; Bartoli and Souchier, 1978; Klein and Geis, 1978; Carnelli et al., 2001; Hodson et al., 2005). Within conifers, Si accumulation by pine is ten times below than spruce (Hodson and Sangster 1999). In tropical conditions, Si uptake by forest vegetations is significant in comparison with weathering Si input and hydrologic Si output (Lucas et al., 1993; Alexandre et al., 1997; Conley, 2002; Derry et al., 2005; Ziegler et al., 2005a). In temperate forests, Bartoli (1983) has estimated that 80% of dissolved Si (DSi) derives from the BSi pool in deciduous stands against 20% in coniferous ones. Yet, the impact of tree species on Si uptake and Si output to the hydrosphere is poorly known because studies in identical soil and climate conditions are lacking. The influence of soil type is, indeed, crucial, as the accumulation of BSi in the soil-plant system is directly governed by soil mineralogical compositions (Henriet et al., 2008a,b). The climate also impacts the BSi accumulation through plant transpiration (Raven, 1983).

Here, we study, on a quantitative basis, the recycling of Si by various monospecific forest stands established in the same soil and climate conditions. We compare three coniferous and two broadleaved forest stands. Our study aims at answering two questions: (1) Is the tree uptake of

Si impacted by tree species? (2) If it does, how large does the species effect impact the pool of dissolved Si?

4.2 Materials and methods

4.2.1 Experimental site

The experimental site is located at Breuil-Chenue (Nièvre-Morvan, France, latitude 47°18'10"N; longitude 4°4'44"E), on a plateau at 638 m asl. Over the period 2001-2006, the mean annual rainfall and temperature are respectively 1212 mm and 9°C. According to the Köpper-Geiger climate map of Europe, the climate is Cfb, i.e. a temperate climate without dry season and with a warm summer (Peel et al., 2007). Table 3.2 and 3.3 present the major soil characteristics at the experimental site. The humus form is a moder with 42.0% of C and a pH of about 4.0. It is an acid brown soil, classified as an Alumnic Cambisol (IUSS, 2006), developed from granite very poor in major cations (0.1% MgO, 0.3% CaO and 3.5% K_2O). The native forest mixes trees dominated by European beech (*Fagus sylvatica* L.) and oak (*Quercus sessiliflora* Smith.). It was cleared in 1976 and replaced by six monospecific plantations. Out of these, we selected five forest stands: Douglas fir (*Pseudotsuga menziesii* Franco), Norway spruce (*Picea abies* Karsten), Black pine (*Pinus nigra* Arn. *Ssp laricio* Poiret var corsicana.), European beech (*Fagus syslvatica* L.) and oak (*Quercus sessiliflora* Smith.).

Since surface runoff is negligible at the site (Ranger et al., 2004) and tree species have no effect on the available water capacity of soil below 10 cm depth (Levrel and Ranger, 2006), the mean annual drainage over the period 2001-2006 (Table 4.1) was calculated by the following mass balance model:

$$\text{Drainage (mm yr}^{-1}\text{)} = P - In - T - E_u \pm \varepsilon \qquad \text{Eq. (4.1)}$$

where P is the mean annual rainfall, In the mean annual rainfall interception, T the mean annual tree transpiration, E_u the mean annual evaporation from understorey vegetation and soil and ε the structural error (corresponding to the not calculated flow). P and In were measured in the experimental site between 2001 and 2006. T was estimated from the relation between leaf area index (*LAI*) and the ratio of stand transpiration to the potential evapotranspiration (*PET*) (Granier et al., 1999). *LAI* was estimated from Breda et al. (2002). *PET* was measured in the experimental site between 2001 and 2006 using data from a weather station. E_u is proportional to the available energy below trees and it is calculated from the Beer-Lambert function and a light coefficient of extinction (0.5) (Granier et al., 1999).

Table 4.1 Mean annual drainage (mm yr^{-1}) estimated for each forest stand at the experimental site (Eq (4.1)). The mean annual rainfall (*P*), the mean annual rainfall interception (*In*), the mean annual tree transpiration (*T*) and mean annual evaporation from understorey vegetation and soil (*Eu*) were calculated over the period 2001-2006. The underestimated standard deviation, calculated by the method of the propagation of uncertainty, is given in parentheses and corresponds to inter-annual variations.

Flux (mm yr^{-1})	Douglas fir	Norway spruce	Black pine	European beech	oak
P	1212	1212	1212	1212	1212
In	545	557	327	351	351
T	567	567	283	432	432
E_u	41	41	181	67	67
Drainage	59 (73)	47 (72)	421 (81)	362 (81)	362 (81)

4.2.2 Materials

Tree compartments

Ten trees were harvested in each stand in 2001 to collect branches, stemwood and stembark samples. Leaves and needles were collected between 2001 and 2006 from 5 litter-traps per stand to estimate the mean annual Si restitution in solid form on topsoil. Needles were also collected from coniferous trees to evaluate the mean accumulation of Si.

Forest floor horizons

We define the forest floor by the whole set of organic horizons (Oln, Olv, Of and Oh) above the organo-mineral horizon (Ah). Under each forest stand, three replicates of organic horizons were sampled in November 2006 according to the forest humus classification (Brethes et al., 1995): Oln (plant remains), Olv (poorly fragmented), Of (fragmented) and Oh (dark humified organic matter).

Soil organo-mineral and mineral layers

Under each forest stand, 16 soil profiles were sampled in May 2001 at the following systematic depths (cm), which do not correspond to specific horizons: 0-5; 5-10; 10-15; 15-25; 25-40; 40-55 and 55-70.

Solutions

In each forest stand, we collected the solutions under the forest floor by using two replicates of sets of 9 zero tension plate lysimeters made of polypropylene (Jaffrain et al., 2007). At 15, 30 and 60 cm depth, ceramic cup lysimeters were introduced into the soil profile (5 replicates per forest stand). The ceramic cup lysimeters were connected to a vacuum pump which maintained a constant suction of -400hPa. Rainfall was collected outside the forest stand by a daily collector system. Throughfall was collected every month by double gutters (3 replicates per forest stand).

4.2.3 Biomass evaluation

The evaluation of tree biomass was done according to procedures described by Ranger et al. (1995) and Saint-André et al. (2005). It involved four steps. (i) The circumference of all trees was measured at 1.30m height, $C_{1.30}$. (ii) Ten trees, representing the whole range of $C_{1.30}$ values, were selected to sample branches, stemwood and stembark. (iii) The weighed allometric relationships fitted for each individual compartment were calculated according to Sicard et al. (2005) for coniferous species and Ranger et al. (2004) for broadleaved species. (iv) Tree biomass (branches, stemwood and stembark) was quantified per hectare by applying fitted equations to the stand inventory. The uncertainty for tree biomass values varied between 3 and 10% (Sicard et al., 2005).

4.2.4 Analytical methods

Si contents in tree compartments

The total Si contents in tree compartments were determined after calcination at 450°C followed by borate fusion (Chao and Sanzolone, 1992). Briefly, a crushed sample of 150 mg of the ignition residue was melted at 1000°C for 5 minutes in a graphite crucible in the presence of 0.4 g Li-tetraborate and 1.6 g Li-metaborate. After dissolution of fusion beads in 10% HNO_3, Si content was determined by inductively coupled plasma atomic emission spectrometry (ICP-AES). The concentrations of the major elements were previously measured (Ranger et al., 2004). In this study, we express Si concentrations of tree compartments as SiO_2 percent.

For the extraction of phytoliths, *i.e.* biogenic silica (BSi), leaves and needles were washed successively with deionized water, HCl 1M, 70% ethanol and rinsed again with deionized water in order to avoid aeolian contamination (Kelly, 1990). About 5 to 10 g of dry matter was grinded and digested at 120°C in a concentrated HNO_3 (70%) / H_2O_2 (30%) mixture until the reaction ceased (~10 days). BSi was filtered through a preweighed 0.2 µm filter and rinsed with deionized water. BSi concentrations were measured gravimetrically (Kelly, 1990; Carnelli et al., 2001). Here, we express BSi concentrations as SiO_2 percent.

Si contents in organic horizons

The total Si contents in forest floor horizons were determined after calcination at 450°C (Oln and Olv) and 950°C (Of and Oh) followed by borate fusion, as described here above.

The extraction of amorphous silica (ASi) was carried out following the heavy liquid method adapted from Kelly (1990). This method includes silt and sand-sized particles having a density below 2.3 g cm^{-3}, thereby involving silt- and sand-sized particles of BSi (2-2000 µm), other poorly crystallized alumino-silicates and some crystallized minerals as revealed by X-ray diffraction, but excluding clay-sized particles (<2 µm). First, clay, silt and sand fractions were separated from fragmented (Of) and humified (Oh) organic horizons by dispersion with Na^+ resins (Rouiller et al., 1972; Bartoli et al., 1991). Silt and sand fractions were then treated by H_2O_2 5% (pH fixed at 5.5) at 70°C until full oxidation of organic matter, and subsequently by DCB to extract free iron compounds (Mehra and Jackson, 1960). Finally, a second dispersion with sodium hexametaphosphate (Na-HMP) was necessary to eliminate the clay contamination.

To recover ASi by densimetric separation, 0.5-2 g of either sand or silt fraction were mixed with 20 cm^3 of zinc bromide solution ($ZnBr_2$, density = 2.3 g cm^{-3}) and centrifuged at 4000rpm for 10 minutes. The supernatant containing the floating ASi was carefully removed with a pipette and filtered through a preweighed 2.0 µm teflon filter (PTFE) soaked with ethanol and rinsed with HCl 1M and deionized water. The operation was repeated four times to remove most of the ASi from the sample (Kelly, 1990; Herbauts et al., 1994; Carnelli et al., 2001). The filter was dried at 105°C for gravimetrical quantification. Here, we express ASi concentrations as SiO_2 percent.

Si contents in organo-mineral and mineral layers

The total Si contents in organo-mineral and mineral layers were determined after calcination at 950°C followed by borate fusion, as described here above. Briefly, sand fraction [>50 µm] was separated from fine earth (<2 mm) by ultrasonic dispersion and wet sieving. Clay [0-2 µm] and silt [2-50 µm] fractions were then collected by gravimetric sedimentation. We used the same methodology described here above to recover ASi from the silt and sand fractions. For the 16 soil profiles sampled under each tree-species, we extracted ASi from 4 samples of the first soil layer [0-5 cm] to study the variability of the ASi distribution.

Si contents in solution

Solutions of forest floor, soil, rainfall, stemflow and throughfall were filtered at 0.45µm, maintained at 4°C and analysed. The Si contents in the solutions were measured by ICP-AES.

Microscopic analysis

Morphological features and chemical content of BSi and ASi particles were respectively examined by scanning electron microscopy (SEM:Leica Stereoscan 260) and energy dispersive X-ray analysis (EDX: EDAX system).

Determination of Al and Ti contents in selected samples

After calcination and borate fusion, the total Al and Ti contents were measured by ICP-AES (Al in leaves, needles, branches, throughfall, stemflow and forest floor solutions; Ti in leaves, needles, forest floor horizons, 0-5 cm and 55-70 cm layers).

4.2.5 Statistical analyses

Statistical analyses consisted in comparisons of means. They were performed with the SAS System (version 9.1, SAS Institute, Cary, NC, USA). Means were compared based on least significant differences (LSD Fisher).

Means with various letters are significantly different at the 95% level of confidence.

4.3 Results

4.3.1 Si contents in the various compartments of the soil-tree system

Tree parts

As shown in Table 4.2, the mean content of SiO_2 in leaves and needles significantly decreased in the sequence European beech (1.59%) > oak (1.17%) > Douglas fir (1.13%) > Norway spruce (0.97%) > Black pine (0.05%). The concentrations of SiO_2 in old needles, as collected in litter traps (Norway spruce = 2.55%, Douglas fir = 2.05% and Black pine = 0.13%) (not shown), were higher than the ones of old and young needles collected from trees. In each specific stand, the SiO_2 concentrations were larger in leaves and needles than in other compartments (branches, stembark and stemwood).

Table 4.2 Mean SiO_2 concentration in tree compartments (data expressed as percent of dry matter); when considering tree species, means with various letters are significantly different at the 95% level of confidence (n=3).

	Total SiO_2 content (% wt)				
	Douglas fir	Norway spruce	Black pine	European beech	oak
Leaves/needles[a]	1.13 c	0.97 d	0.05 e	1.59 a	1.17 b
Branches	0.04 c	0.06 b	0.03 c	0.07 a	0.01 d
Stem bark	0.04 b	0.04 b	0.02 c	0.32 a	0.02 c
Stem wood	0.01 ab	0.01 a	0.01 ab	0.004 b	0.004 b

[a] Concentration of Si in the leaves collected in litter-traps and in the old and young needles collected from coniferous trees (November 2006)

Organic horizons and soil layers

The BSi concentrations of leaves and needles ranged from 0.02% (Black pine) to 1.93% (European beech) (Table 4.3). In leaves and needles, the total SiO_2 concentration did not exactly correspond to the BSi concentration as measured gravimetrically. However, the former was correlated with the total SiO_2 content in falling litter Oln ($r = 0.97$) but not with that in the humified organic horizon Oh ($r = 0.1$).

In the Oh horizon, the relative proportion of [BSi + ASi] on the total SiO_2 content ranged between 0.3 and 3% depending on tree species. The relative standard deviation (RSD) (not shown) exhibited a large variability of the [BSi + ASi] distribution in the first soil layer (0-5 cm), as it ranged between 40 and 61 % according to tree species. The concentrations of [BSi + ASi] in soil layers varied between 0.42 and 4.77 % and were the largest at soil depth between 0 and 15 cm, and decreased from 15 to 40 cm in each stand (Table 4.3). The concentrations of [BSi + ASi] determined by heavy liquid method were similar to the ones calculated by Saccone et al. (2007) in forest soils with alkaline methods (on average 1.2 – 2 %). Assuming 10% water content in [ASi + BSi] and 5% content of other elements than Si (Bartoli and Wilding, 1980; Drees et al., 1989), the relative proportion of [BSi + ASi] on the total SiO_2 concentration in soil ranged between 0.5 and 5% depending on tree species. These values were very similar to the ones (1-3 %) calculated by Blecker et al. (2006) in grasslands.

Solutions

The mean concentrations of DSi and DAl, as measured between April 2006 and April 2007 in throughfall and stemflow, forest floor and soil solutions, are presented in Table 4.4. They both increased in the sequence: throughfall ~ stemflow < forest floor leachate. They ranged from 0.86 to 1.81 mg l^{-1} for DSi and from 0.54 to 1.74 mg l^{-1} for DAl in forest floor leachates.The DSi content was the largest in the soil solution collected at 15 cm depth, and tended to decrease beneath in all forest stands.

Table 4.3 Mean total SiO_2 content (n=3), biogenic SiO_2 content (BSi) and amorphous SiO_2 content (ASi) in leaves/needles, forest floor and soil layers.

	Total SiO_2 (% wt)					**[BSi + ASi] (SiO_2 % wt)**				
	Douglas fir	Norway spruce	Black pine	European beech	oak	Douglas fir	Norway spruce	Black pine	European beech	oak
Organic horizons										
Leaves	1.13	0.97	0.05	1.59	1.17	0.96	0.54	0.02	1.93	1.13
Oln	0.99	0.77	0.05	1.54	1.30	[a] nd	nd	nd	nd	nd
Olv	2.30	2.07	0.35	2.97	1.46	nd	nd	nd	nd	nd
Of	6.44	4.38	11.40	13.51	5.71	1.22	1.10	0.08	0.21	0.49
Oh	20.88	12.06	38.06	39.43	44.01	0.43	0.45	0.11	0.12	0.39
Soil layers (cm)										
0-5	61.94	68.49	64.08	61.12	63.17	2.63	2.43	3.16	1.53	0.42
5-10	66.35	68.38	68.87	64.51	67.84	2.65	2.42	1.33	3.70	2.17
10-15	66.45	70.55	71.05	65.78	71.32	2.84	0.79	1.14	1.70	4.77
15-25	66.50	70.94	70.84	64.71	65.89	0.58	0.57	nd	1.31	1.14
25-40	67.65	72.27	73.02	65.55	69.42	0.63	0.61	nd	0.76	0.90

[a] nd: no data

Table 4.4 Mean dissolved Si and Al contents in various solutions as measured between April 2006 and April 2007 (unpublished data, INRA-Champenoux, Nancy); the error associated with the mean (n=number of replicates) is given in parentheses (standard error).

	Douglas fir	Norway spruce	Black pine	European beech	oak
Si content in solution (mg l^{-1})					
Rainfall (n=12)	0.01 (0.01)	0.01 (0.01)	0.01 (0.01)	0.01 (0.01)	0.01 (0.01)
Throughfall (n=3)	0.05 (0.02)	0.03 (0.02)	0.01 (0.01)	0.07 (0.07)	0.05 (0.05)
Stemflow (n=3)	0.07 (0.05)	0.01 (0.14)	0.06 (0.06)	0.08 (0.05)	0.13 (0.11)
Forest floor (n=2)	1.54 (1.04)	1.50 (1.13)	0.86 (0.44)	0.97 (0.43)	1.81 (0.90)
-15 cm (n=5)	3.53 (0.65)	3.10 (0.37)	3.22 (0.48)	1.80 (0.57)	2.40 (1.13)
-30 cm (n=5)	2.67 (0.34)	1.73 (0.30)	2.16 (0.28)	1.79 (0.28)	2.34 (0.34)
-60 cm (n=5)	2.02 (0.40)	1.71 (0.32)	2.27 (0.29)	1.69 (0.25)	1.88 (0.30)
Al content in solution (mg l^{-1})					
Throughfall (n=3)	0.04 (0.02)	0.03 (0.02)	0.02 (0.02)	0.01 (0.02)	0.02 (0.02)
Stemflow (n=3)	0.11 (0.27)	0.07 (0.05)	0.13 (0.14)	0.01 (0.01)	0.04 (0.03)
Forest floor (n=2)	0.54 (0.08)	0.60 (0.28)	1.74 (0.56)	0.74 (0.25)	1.07 (0.41)

4.3.2 BSi and ASi particles morphologies

From Figure 4.1, BSi particles from the various tree species could be identified. We observed other siliceous amorphous substances (ASi) and other shaped BSi particles like “bilobate short cell”, “cylindrical polylobate”, “globular” and “favose”, probably inherited from the herbaceous understorey vegetation. BSi from conifers and broad-leaved tree species were characterized by elongate and circular shape. The Phytoliths of *Picea* *abies* and *Pinus nigra* seemed very similar to the ones of *Picea rubens* and *Pinus strobes* (Klein and Geis, 1978) and *Pinus mugo* (Carnelli et al., 2001). The surface of *Pseudotsuga menziesii* phytolith was smooth. The *Fagus sylvatica* phytolith was furrowed. Most of the *Quercus sessiliflora* phytoliths were long and smooth. Following ICPN names (Madella et al., 2005), the phytoliths of *Picea abies* and *Pinus nigra* are called "cylindric lacunose"; the phytoliths of *Fagus sylvatica* are called "cylindric sulcate" or "laminate tracheid"; the phytoliths of *Quercus sessiliflora* and *Pseudotsuga menziesii* are called "elongate long cell". Phytoliths extracted from humus and soil layers exhibited dissolution features, as compared to the ones from leaves and needles. EDX analysis revealed the large dominance of Si (98%) in BSi particles isolated from leaf/needle materials. As compared to the former, ASi particles extracted from forest floor horizons and soil layers exhibited a larger Al content, likely because of Al adsorption onto the surfaces of siliceous amorphous compounds (Bartoli and Wilding, 1980; Bartoli, 1985).

Table 4.5 Total Al and Ti contents in selected tree and soil compartments; when considering tree species, means with various letters are significantly different at the 95% level of confidence (n=3).

	Douglas fir	Norway spruce	Black pine	European beech	oak
Total Al content (% wt)					
Leaves /needles	0.054 a	0.050 b	0.054 a	0.020 c	0.019 c
Branches	0.018 b	0.010 c	0.022 a	0.003 d	0.002 d
Total Ti content (% wt)					
Leaves/needles	0.001 ab	0.002 a	0.001 b	0.001 b	0.001 b
Olv	0.003 b	0.001 d	0.002 c	0.012 a	0.002 c
Of	0.018 d	0.009 e	0.049 b	0.062 a	0.024 c
Oh	0.08 c	0.04 d	0.14 b	0.16 a	0.130 b
0-5 cm soil layer	0.18 a	0.20 a	0.17 a	0.19 a	0.170 a
55-70 cm soil layer	0.23 a	0.21 a	0.24 a	0.21 a	0.240 a

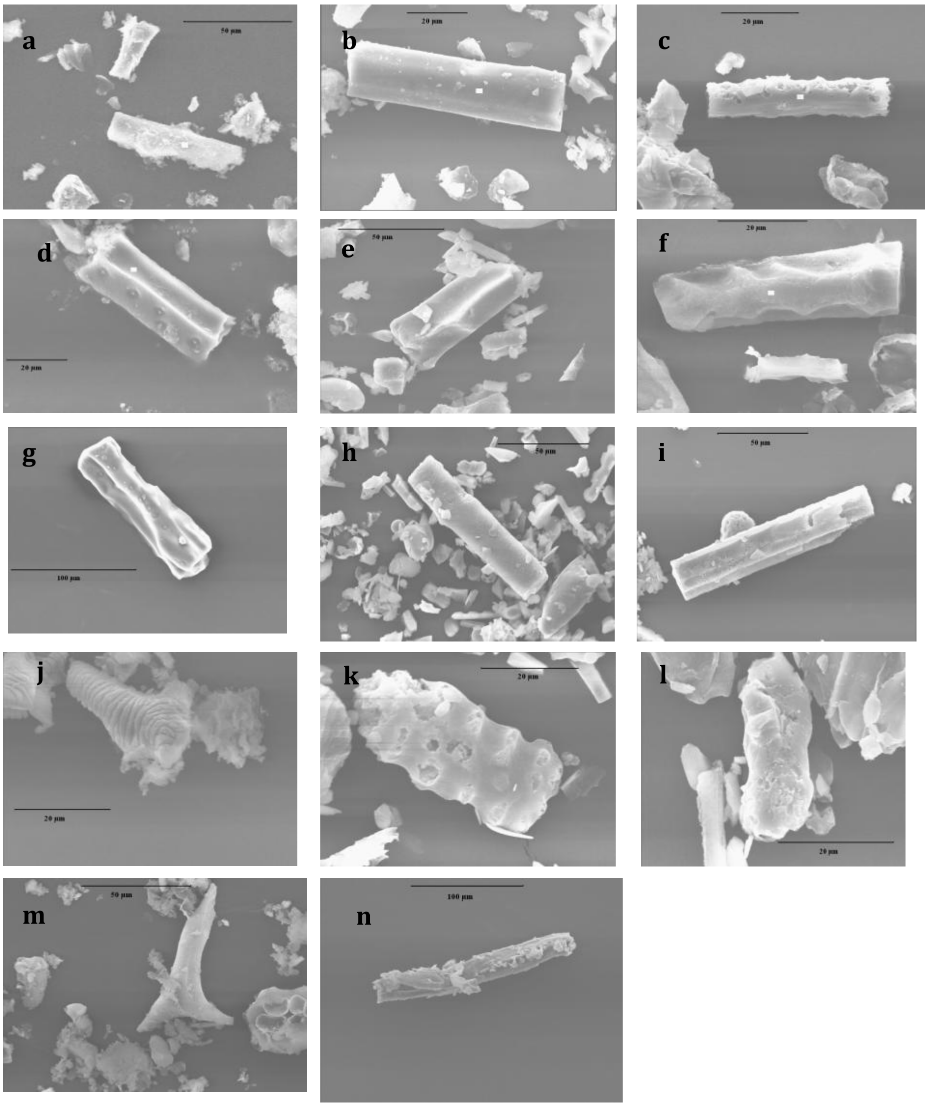

Figure 4.1 Scanning electron micrographs of BSi (phytolith) from leaves/needles and ASi from humus and soil layers. a. BSi isolates from *Pseudotsuga menziesii* needles. b. ASi isolates from Oh under *Pseudotsuga menziesii*. c. ASi isolates from soil (25-40 cm) under *Pseudotsuga menziesii*. d. BSi isolates from *Picea abies* needles. e. ASi isolates from Oh under *Picea abies*. f. ASi isolates from soil (10-15 cm) under *Picea abies*. g. BSi isolates from *Pinus nigra* needles. h. ASi isolates from Oh under *Pinus nigra*. i. ASi isolates from soil (10-15 cm) under *Pinus nigra*. j. BSi isolates from *Fagus syslvatica* leaves. k. ASi isolates from Oh under *Fagus syslvatica*. l. ASi isolates from soil (10-15 cm) under *Fagus syslvatica*. m. BSi isolates from *Quercus sessiliflora* leaves. n. ASi isolates from soil (25-40 cm) under *Quercus sessiliflora.*

4.3.3 Total Al and Ti in the selected samples

As shown in Table 4.5, the total Al content of leaves (0.02-0.05%) was smaller than the total Si content in all tree species (0.45-0.74%); except in Black pine (0.02%). The total Al content in leaves/needles and branches was significantly larger in coniferous than in deciduous species. The total Ti content increased in the sequence Olv << Of < Oh < 0-5 cm < 55-70 cm.

4.4 Discussion

4.4.1 Si uptake by forest trees

The recycling of Si by forest trees can be described considering a steady state system. Thus, the current Si annual uptake is estimated as follows (Ranger and Bonneau, 1984; Ranger et al., 1997; Markewitz and Richter, 1998):

$$\text{Uptake (kg ha}^{-1}\text{ yr}^{-1}\text{)} = \text{Immobilization} + \text{Restitution} \qquad \text{Eq. (4.2)}$$

where the annual Si restitution into soil is computed from Eq. (4.3):

$$\text{Restitution (kg ha}^{-1}\text{ yr}^{-1}\text{)} = \text{Litterfall} + \text{Crown leaching} \qquad \text{Eq. (4.3)}$$

The total Si concentration of the ligneous biomass (branches, stemwood and stembark) was multiplied by the current annual biomass increment (averaged between 2001 and 2006; Sicard et al., 2005; Ranger et al., 2004) to compute the current annual immobilization of Si. The total Si concentration in leaves/needles and branches collected in litter traps was multiplied by the mean annual litterfall mass (averaged between 2001 and 2006; unpublished data, INRA-Champenoux, Nancy) to compute the annual restitution of Si in solid form. The concentrations of Si in throughfall and rainfall (Table 4.4) were used to calculate the concentration of Si leached by rainfall from tree crown (throughfall – rainfall = crown leaching + dry deposition); that concentration was further multiplied by the computed amount of crown leaching ($P - In$, Eq. (4.1)). Here, only the contribution of the above-ground phytomass is considered, since the calculated Si-mass contained in tree-roots represents no more than 1% of the total uptake (Gérard et al., 2008).

Table 4.6 Mean annual values of Si immobilization, Si restitution through litterfall and crown leaching measured between 2001 and 2006; annual uptake of Si is deduced from Eq. (4.2); annual output of Si is deduced from Eq. (4.1) The standard deviation, calculated by the method of the propagation of uncertainty, is given in parentheses and corresponds to inter-annual variations.

	Si (kg ha^{-1} yr^{-1})				
	Douglas fir	Norway spruce	Black pine	European beech	oak
Immobilization	1.4 (0.2)	1.2 (0.3)	0.2 (0.1)	3.5 (1.5)	0.4 (0.1)
Litterfall	29.0 (8.0)	42.2 (14.1)	2.1 (0.8)	19.3 (6.4)	17.8 (5.3)
Crown leaching	0.2 (0.2)	0.1 (0.2)	0 (0.1)	0.5 (0.6)	0.3 (0.4)
Uptake	30.6 (8.0)	43.5 (14.1)	2.3 (0.9)	23.3 (6.5)	18.5 (5.3)
Si soil water output	1.1 (1.5)	0.7 (1.2)	9.4 (2.2)	6.0 (1.6)	6.7 (1.9)
Litterfall/Uptake	0.95	0.97	0.91	0.83	0.96

From Table 4.6, the relative proportion of Si immobilization on Si uptake decreases as the following sequence: European beech (15%) > Black pine (8.7%) > Douglas fir (4.5%) > Norway spruce (2.7%) > oak (2.1%). The maximum contribution of Si crown leaching to the total restitution of Si into soil is 2.5%. Our computations show that, at least, 83% of the Si uptake is annually recycled on topsoil throughout litterfall (Litterfall/Uptake: Table 4.6), whatever the species. These results accord with the fact that Si is deposited at the termini of the transpiration stream, mainly in the outer walls of the epidermal cells on both surfaces of the leaves (Marschner, 1995).

As computed from Eq. (4.2), the mean annual Si uptake is clearly dependent on tree species (Table 4.6), and decreases as the following sequence: Norway spruce (43.5±14.1 kg ha^{-1} yr^{-1}) > Douglas fir (30.6±8.0 kg ha^{-1} yr^{-1}) > European beech (23.3±6.5 kg ha^{-1} yr^{-1}) > oak (18.5±5.3 kg ha^{-1} yr^{-1}) >>> Black pine (2.3±0.9 kg ha^{-1} yr^{-1}). The concentration of Si in plants is controlled by soil properties, climate and plant species (Jones and

Handreck, 1967; Raven, 1983). Here, we isolate the impact of tree species on the uptake of Si since soil physical and chemical properties were nearly identical between trees plots when the experimental site was set up (Bonneau et al., 1977).

Our uptake values are very similar to the ones computed previously in temperate climate: 8-44 kg ha^{-1} yr^{-1} in coniferous forests (Bartoli, 1983; Markewitz and Richter, 1998; Gérard et al., 2008), 10.8-32.3 kg ha^{-1} yr^{-1} in mixed broadleaved-coniferous forests (Fulweiler and Nixon, 2005; Garvin et al., 2006) and 26 kg ha^{-1} yr^{-1} in a broadleaved forest (Bartoli, 1983). In humid tropical conditions, the recycling of Si by forest trees is evaluated up to 67 kg ha^{-1} yr^{-1} in Congo rainforest (Alexandre et al., 1997).

The relatively low concentration of Si in branches, stembark and stemwood (Table 4.2) confirms the relatively low transport of Si through the phloem to other plant parts (Raven, 1983). As old needles accumulate more Si than young ones, needle age may influence Si accumulation (Bartoli and Souchier, 1978). Considering the mean concentration of Si in young needles (Table 4.2), conifers accumulate less Si in comparison with the broad-leaved trees (Hodson et al., 2005).

4.4.2 DSi output

Most of the root uptake occurs within the first 50 cm of the soil (Drénou, 2006). For instance, 93% of fine root length of Norway spruce is distributed between 0 and 50 cm depth in an acid brown soil (Puhe, 2003). Based on literature data, Jackson et al. (1996) suggest that the rooting profile is shallower in temperate deciduous forest than in temperate coniferous forest, with respectively, 75% and 50% of roots in the uppermost 30 cm of the soil. In temperate and tropical forests, 78% of roots are distributed in the top 50 cm of the soil (Jackson et al., 1996). In our experimental site, the distribution of roots strongly decreases from 70 cm depth as suggested by field observations (Ranger et al., 2004). Thus, it is reasonable to expect that a major part of DSi is leached out from soil at 60 cm depth, and readily contributes to the hydrological output of Si.

The amount of DSi leached out from soil at 60 cm depth (Table 4.6) was computed by multiplying the mean annual drainage (Eq. (4.1), Table 4.1) and the average Si concentration in solution collected at 60 cm depth between April 2006 and April 2007 (Table 4.4). We calculated the standard deviation on the flux by method of the propagation of uncertainty. The mean DSi output (kg ha^{-1} yr^{-1}) decreases as the following sequence: Black pine (9.4±2.2) > oak (6.7±1.9) > European beech (6.0±1.6) > Douglas fir (1.1±1.5) > Norway spruce (0.7±1.2).

4.4.3 Origins of Si in organic horizons

The Si content is mostly controlled by biological recycling in the recent litter layer (Oln), and by bioturbation in the humified Oh horizon. Bioturbation mixes up silicate minerals from mineral horizons beneath through the action of living organisms (Giesler et al., 2000), and can be estimated through the fate of poorly mobile elements (Al, Ti).

Al is not essential, but toxic to plants. Rustad and Cronan (1995) observed that DAl leached from the O-horizons is much larger than the aboveground Al input (litterfall + throughfall + stemflow). It suggests a contribution of Al incorporated from the mineral layers beneath. From Table 4.7, the contribution of DAl released from weathering of soil minerals incorporated in the O-horizons is larger under Black pine (8.9 kg ha^{-1} yr^{-1}), oak (7.3 kg ha^{-1} yr^{-1}) and European beech (5.1 kg ha^{-1} yr^{-1}) in comparison with Douglas fir (0.7 kg ha^{-1} yr^{-1}) and Norway spruce (1.1 kg ha^{-1} yr^{-1}).

Table 4.7 Aboveground Al inputs into forest floor, as computed from the concentration of Al in litterfall (Table 4.5), throughfall and stemflow (Table 4.4), mean annual litterfall mass and mean annual rainfall under canopy; amount of DAl released from the forest floor, as computed from the concentration of aqueous Al in forest floor solution (Table 4.4) and the estimation of drainage (Eq. (4.1), Table 4.1); Al released from weathering of silicate minerals incorporated into forest floor is the difference between Al inputs and Al output (Rustad and Cronan, 1995).

	Douglas fir	Norway spruce	Black pine	European beech	oak
Al (kg ha^{-1} yr^{-1})					
Al inputs in forest floor	2.7	2.5	3.3	0.8	1.2
Al output from forest floor	3.4	3.6	12.2	5.9	8.5
Al released from weathering	0.7	1.1	8.9	5.1	7.3

Table 4.8 “Titanium ratio”, defined here as the Ti content in specific horizons (Oln - 0-5 cm soil layer) divided by the Ti content in the mineral soil at 55-70 cm depth, considered as reference horizon; when considering tree species, means with various letters are significantly different at the 95% level of confidence.

	Douglas fir	Norway spruce	Black pine	European Beech	oak
$[Ti_{horizon} / Ti_{reference}] * 10^2$					
Leaves	0.56	0.43	0.40	0.48	0.38
	a	a	a	a	a
Olv	1.56	0.44	0.88	5.90	0.87
	b	d	c	a	c
Of	7.74	4.38	20.44	29.81	10.12
	d	e	b	a	c
Oh	36.97	20.72	57.26	78.20	54.99
	c	d	b	a	b
0-5 cm soil layer	78.29	86.5	73.26	89.1	70.09
	bc	a	c	ab	c

Plants take up very small quantities of Ti, which seems poorly mobile in soils (Fitzpatrick and Chittleborough, 2002). The titanium ratio is defined as follows:

$$\text{Ti ratio} = \left[\frac{Ti_{horizon}}{Ti_{reference}}\right]*10^2 \qquad \text{Eq. (4.4)}$$

where $Ti_{horizon}$ is Ti content in each specific individual horizon (Oln - 0-5 cm soil layer), and $Ti_{reference}$ is Ti content in 55-70 cm soil layer.

From Table 4.8, Ti ratio increases from 0.38-0.56 in Oln to 70-89 in 0-5 cm soil layer, in parallel with the increase of mineral content. Under fir, Ti ratio increases from 7.7 in Of to 37 in Oh, and then abruptly to 78.3 in 0-5 cm soil layer (2.1-fold increase). Under spruce, Ti ratio increases from 4.4 in Of to 20.7 in Oh, and then abruptly to 86.5 in 0-5 cm soil layer (4.2-fold increase). Under the other forest stands (pine, beech and oak), Ti ratio increases from 10-29.8 in Of to 55-78.2 in Oh and slightly rises to 70.1-89.1 in 0-5 cm soil layer (1.1-1.3-fold increase). The increase of the Ti ratio is thus less abrupt in the latter tree stands, denoting less bioturbation in the two former ones.

Both Al and Ti bioturbation indexes show that the incorporation of soil minerals into organic horizons is less important under Douglas fir and

Norway spruce than under Black pine, European beech and oak. This accords with the values of the concentration of SiO_2 inherited from soil minerals in Oh, which is lower in Norway spruce (11.6% wt) and Douglas fir (20.4% wt), in comparison with Black pine (37.9% wt), European beech (39.3% wt) and oak (43.6% wt) (Table 3.4). We can thus assume that the DSi concentrations in forest floor leachate result from a dynamic balance between (i) dissolution processes involving silicate minerals incorporated into O-horizon as well as BSi particles returned to topsoil through litterfall, and (ii) neoformation of clay minerals, adsorption of Si onto iron and/or aluminium oxides as well as polymerization of BSi through the recycling of DSi by trees. Giesler et al. (2000) also suggested that DSi concentration in forest floor leachate might be controlled directly by the weathering of silicate minerals incorporated into forest floor (low pH and high concentration of low molecular organic acids) and indirectly by root uptake.

In this respect, phytolith solubility is partly influenced by the specific surface area of the particle (Bartoli and Wilding, 1980). As illustrated in Figure 4.1, the morphology of BSi particles clearly differs within tree species. Thus, we can expect various dissolution rates of BSi particles in forest floor. Wilding and Drees (1974) have shown that phytoliths dissolution rates are a function of the phytoliths morphology: forest BSi is about 10-15 times more soluble than grass BSi, due to the higher specific surface area of the former.

4.4.4 Budget of Si in the soil-tree system

From Figure 4.2, the annual Si uptake is negatively correlated with the annual DSi output at 60 cm depth. Under Norway spruce and Douglas fir, Si uptake is respectively sixty and thirty times larger than the amount of DSi leached out from soil. Under European beech and oak stands, Si uptake is about three times larger than the amount of DSi leached out from soil. In contrast, the uptake of Si by Black pine is about four times lower than the amount of DSi leached out from soil. Except for pine, Si uptake and restitution are largely significant in comparison with the annual leaching of Si. Using a numerical model, Gérard et al. (2008) suggest that the annual Si output (5.1 kg $ha^{-1}yr^{-1}$) is very small in comparison to Si uptake by Douglas fir (44.4 kg $ha^{-1}yr^{-1}$). In tropical conditions, the annual Si restitution into soil (41 kg ha^{-1} yr^{-1}) is also significant in comparison with annual Si leaching (11 kg ha^{-1} yr^{-1}) (Lucas et al., 1993).

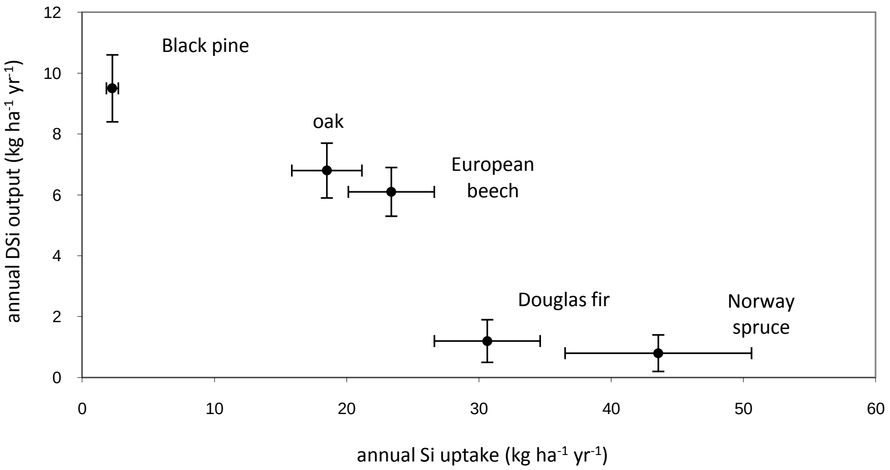

Figure 4.2 Relationship between the annual Si uptake by forest stands and the annual DSi output at 60 cm depth.

Under Black pine, the DSi output exceeds the Si uptake because DSi released by mineral dissolution does not readily contribute to the BSi pool of the vegetation. Considering all species, this reveals that the decrease of DSi in soil solution through clay formation is less important than the decrease of DSi in soil solution through root uptake, as argued by Farmer et al. (2005). The fact that BSi pool of the vegetation acts as a sink for DSi is largely recognized in other studies of forest ecosystems (Bartoli and Souchier, 1978; Bartoli, 1983; Lucas et al., 1993; Alexandre et al., 1997; Giesler et al., 2000; Gérard et al., 2008). Consequently, the decrease of DSi content beneath 15 cm depth could be largely influenced by the active root uptake as suggested by Gérard et al. 2008. The Si cycling by plants can impact the clay mineral stability or formation. This phenomenon called “nutrient uplift” or “element translocation” can counteract the geochemical trend of Si leaching, and may account for the stability of clay mineral in upper soil horizons (Lucas et al., 1993; Lucas, 2001; Kleber et al., 2007; Barré et al., 2009). If plants are rapidly cycling nutrients, the incorporation of BSi, that is more soluble than primary silicates, likely decreases the rate of primary silicates weathering (Kelly et al., 1998). On the other hand, Lucas (2001) suggests that Si uptake by plants directly impacts soil formation through the dissolution of primary minerals and/or the formation of secondary clays. The importance of biological uptake does not exclude the impact of geological processes on the decrease of DSi concentrations from 15 cm to 60 cm depth (Table 4.4; Figure 3.5). As suggested by Blecker et al. (2006), clay formation would deplete the concentration of DSi in soil solution. Besides, the reaction of silicic acid with aluminium to form hydroxyaluminosilicates (HAS) is also a Si sink which could influence DSi concentration through the weathering (Exley, 1998). The increase of DSi concentration between 0 and 15 cm depth results from a combined effect of (i) the increase of mineral weathering driven by organic ligands (Gérard et al., 2008), proton excretion and cations uptake by roots (Drever, 1994; Kelly et al., 1998), and (ii) the dissolution of phytoliths returned on topsoil through litterfall (Lucas, 2001). The DSi released by the dissolution of phytoliths could be immobilized through formation of clay minerals beneath (Lucas et al., 1993), and thus does not contribute to the leaching of DSi to the hydrosphere. Accordingly, our results can not provide direct evidence about the impact of various tree uptakes on the leaching of DSi from land to the ocean and cannot prove the origin of DSi (geochemical or biological). However, since our data were performed in identical climate and soil conditions, we clearly demonstrate that tree species directly impact on Si uptake, immobilization and restitution and, consequently, on the DSi concentration in soil solution.

4.4.5 Implications

Plants largely contribute to the terrestrial Si reservoir since annual BSi production by plants ranges between 60 and 200 Tmol year^{-1} (Conley, 2002) and rivals that produced by diatoms in oceans (240 Tmol year^{-1}) (Tréguer et al., 1995). The dissolution of BSi pool and release of DSi in the soil solution would strongly increase DSi output to oceans following deforestation (dissolution of terrestrial BSi pool and no Si uptake) (Conley et al., 2008). The leaching of aqueous Si from soil to rivers strongly impacts the oceanic biogeochemical cycle, as land-ocean flux contributes to more than 80% of the input of DSi to the oceans (Tréguer et al., 1995). The drainage losses of Si and the amount of Si recycled by forest trees are still poorly quantified. The results presented here show that forest tree species can strongly influence the Si cycling. Thus, tree species must be taken into account in further studies concerning both mineral weathering and DSi fluxes to the hydrosphere. Forest ecosystems are usually considered as open systems, meaning that matter and energy are continuously transferred across their boundaries. In this paper, we clearly demonstrate the impact of tree species on the retention of Si by the soil-tree system, as Si is conserved within the system through Si uptake by forest trees. Without considering Si retention by the soil-tree system, forest trees can enhance the release of DSi from soil mineral through weathering of silicate minerals. The recycling of Si by forest trees generates a BSi pool in soil, more soluble than the silicate minerals (Fraysse et al., 2006; Fraysse et al., 2009), and thus promotes the leaching of DSi to the hydrosphere. Considering Si retention by the soil-tree system, the hydrological output of Si is reduced when a large amount of Si is taken up by forest trees (terrestrial BSi pool). For calcium, Likens et al. (1977) also suggest that the quantities circulating within the ecosystem are much greater than those lost by leaching. The recycling of Si by forest trees is thus an important mechanism of Si conservation in the soil-tree system (Alexandre et al., 1997; Street-Perrott and Barker, 2008). Indeed, during the growing season, Si released by mineral and [BSi + ASi] dissolution is largely taken up by forest vegetations and is concentrated in the BSi-plant pool before returning to soil. When plant uptake decreases during winter, DSi is much more leached from the soil profile (Gérard et al., 2002; Farmer et al., 2005; Figure 3.6, 3.7). That increase of DSi output is mainly controlled by the decrease of Si uptake (Fulweiler and Nixon, 2005), as weathering processes decline with a decrease of temperature (Farmer et al., 2005). Thus, on the basis of our data, we believe that the Si leaching from soil are liable to dominate over retention and recirculation of Si in the soil-tree system when root uptake is limited.

4.5 Conclusions

Our results provide clear answers to the questions raised in the Introduction section. (1) The tree species influence the uptake and restitution of Si to soil through litterfall. (2) Among other processes, the recycling of Si by tree species impacts the leaching of DSi from forest soils.

Si is mainly accumulated in leaves and needles. Consequently, Si becomes largely mobile in the soil-tree cycle through litterfall. The Si soil-tree cycle is clearly modulated by tree-species as shown by the distinct uptake, immobilization and restitution rates of Si. Moreover, our data show that the amount of DSi released from soil at 60 cm depth is negatively correlated with the uptake of Si by forest trees. As geochemical processes, tree species can also strongly impact on the content of DSi in the soil solution and, consequently, could influence the land-ocean fluxes of DSi.

It is now fundamental to understand the mechanisms responsible of various Si uptakes by tree species and to quantify the respective contribution of the non biogenic and BSi mineral dissolution to the DSi pool. Ge:Si ratio (Derry et al., 2005) and stable Si isotopes (Ziegler et al., 2005a,b; Opfergelt et al., 2008,2010) seem to be relevant tools to investigate the origin of DSi, in order to clear up the biologic control on the Si export to the hydrosphere.

CHAPTER 5:

THE CONTRASTING SILICON UPTAKES BY CONIFEROUS TREES: A HYDROPONIC EXPERIMENT ON YOUNG SEEDLINGS[*]

---

[*] Adapted from Cornelis JT., Delvaux B. and Titeux H. The contrasting silicon uptakes by coniferous trees: a hydroponic experiment on young seedlings. Accepted with minor revisions in *Plant and Soil*

Abstract

Silicon uptake by terrestrial plants impacts the Si land-ocean fluxes, therefore inducing significant modifications for biogeochemical cycle of Si. Understanding the mechanisms that control Si uptakes by forest vegetation is of great interest for the study of the global Si cycle as the world's total forest area corresponds to about 30% of the land area. Our study compares Si uptake in controlled conditions by two coniferous species (*Pseudotsuga menziensii* and *Pinus nigra*) exhibiting contrasting Si uptake in the field. For this purpose, seedlings were grown for 11 weeks under controlled conditions in hydroponics with different Si concentrations (0.2 to 1.6 mM) in nutrient solutions. The Si concentrations were greater in Douglas fir leaves as compared with Black pine leaves and increased, depending on the Si concentration in the nutrient solution. According to mass balance, Si absorption seems to have been driven by passive Si transport at 0.2 mM Si (realistic concentration for forest soil solutions) and was rejective at higher Si concentrations in nutrient solution for both species. For this reason, we attributed the higher Si concentration in Douglas fir leaves to the greater cumulative transpiration of these seedlings. We suggest that contrasting transpiration rates may also play a key role in controlling Si accumulation in leaves at field scale.

5.1 Introduction

Silicon (Si) influences global biogeochemical processes on long timescales as a result of CO_2 neutralization by silicate weathering (Berner, 1997) and the essentiality of dissolved silicon (DSi) for phytoplankton CO_2 consumers (Conley et al., 1993). On shorter timescales, part of the DSi released by mineral weathering is cycled through vegetation on the earth's surface (Conley, 2002; Derry et al., 2005) before its land-ocean transfer, which contributes to 80% of the ocean's DSi load (Tréguer et al., 1995). Si is released in soil solutions as monosilicic acid ($H_4SiO_4^0$), which is then translocated to the transpiration sites where polymerization of hydrated amorphous silica occurs to form phytoliths (Jones and Handreck, 1965; Casey et al., 2003). Higher plants can accumulate Si, a non-essential but beneficial element, as phytoliths (BSi) to a similar degree as some major macronutrients: 0.1-10% (Epstein, 1999). In keeping with active, passive or exclusive mechanisms with respect to Si uptake, plant species are classified as high-, intermediate-, or non-accumulators respectively (Takahashi et al., 1990). Hodson et al. (2005) studied phylogenetic variations in the Si composition of plants and demonstrated that gymnosperms and angiosperms accumulate less Si in their shoots than non-vascular plant species and horsetails.

In temperate forest ecosystems, previous studies show that the Si uptake varies considerably, ranging between 2 and 44 kg Si ha^{-1} yr^{-1} (Bartoli, 1983; Markewitz and Richter, 1998; Fulweiler and Nixon 2005; Gérard et al., 2008; Cornelis et al., 2010; Chapter 4). The major part of the Si uptake returns to the topsoil through litterfall as a reactive BSi pool (Fraysse et al., 2009), this being an ubiquitous and substantial component of forest soil (Drees et al., 1989; Saccone et al., 2007; Conley et al., 2008). Thus, the study of mechanisms controlling the contrasting Si biocycling by tree species is a critical step to improve our knowledge of Si mass-balance in soil-tree systems.

In Chapter 4, we demonstrate that the annual Si uptake clearly depends on tree species since a strong difference in Si absorption rates was observed between Douglas fir and Black pine: *Pseudotsuga menziesii* (30.6±8.0 kg Si ha^{-1} yr^{-1}) >> *Pinus nigra* (2.3±0.9 kg Si ha^{-1} yr^{-1}) in identical climatic and soil conditions. The different accumulation of Si in aerial parts may be due to the varying abilities of Si root-uptake, soil mineralogical composition (Klein and Geis, 1978), transpiration rate and availability of silicic acid in soil solutions (Jones and Handreck, 1967; Hodson and Sangster, 1999). Gérard et al. (2008) suggest that Douglas fir on a forest site actively absorbs Si from the soil solution to explain the decrease in DSi concentrations with soil depth and equilibrate mass balance calculations of the Si uptake flux. However, this field study did not consider the impact of pedogenic Si-sinks (*i.e.* secondary minerals formation and Si adsorption onto Fe oxides), which can also induce a lower DSi concentration in solution. The mechanisms controlling the Si biocycling have not yet been elucidated; hence the interest of hydroponics experiment with tree species characterized by different Si uptake.

Furthermore, such a difference of Si concentration in forest vegetation could affect tree seedling growth. Although silicon is not traditionally considered to be an essential plant element (Epstein, 1999; Ma and Takahashi, 2002; Ma and Yamaji, 2006a; Liang et al., 2007), many studies have shown its beneficial effect on plant growth and yield (Korndorfer and Lepsch, 2001; Ma and Takahashi, 2002; Ma, 2004), which is more clearly expressed under stress conditions (Epstein, 1994; Bélanger et al., 1995). However, besides the study of Emadian and Newton (1989) that demonstrates the beneficial effect of Si supply on pine seedling growth under water-stress conditions, the effect of a wide range of Si supply on the Si uptake and growth of different coniferous tree seedlings in optimal conditions has never been studied.

Here, we set out to (1) understand the contrasting Si uptake between Douglas fir and Black pine and (2) measure the Si effect on the growth of tree seedlings. *Pseudotsuga menziesii* and *Pinus nigra* seedlings were therefore grown for 11 weeks in hydroponics with a wide range of Si concentrations in the nutrient solution (0.2 to 1.6 mM).

5.2 Materials and methods

5.2.1 Hydroponic growth conditions

The seeds were collected from *Pseudotsuga menziensii* Franco stands in Belgium and from *Pinus nigra* Arn. *Ssp laricio* Poiret var corsicana stands in France. Tree seeds were surface-sterilized with 5% H_2O_2 and rinsed five times with demineralized water. The seeds were germinated for 15 days in the dark at day/night temperatures of 20/18 °C. They were then weaned for 30 days in nutrient solution tanks before uniform seedlings were selected for the experiments. Batches of six seedlings were grown in separate cylindrical PVC pots containing 2.5 l of nutrient solution and placed on a perforated plate of expanded polystyrene which limits water loss by evaporation. The experiment was conducted over 11 weeks in growth chambers with a 448 µE $m^{-2}s^{-1}$ photon density flux for 8h per day, 75% relative humidity, and day/night temperatures of 20/18 °C. The nutrient solution was obtained by mixing salts, boric acid and FeEDTA to reach the following concentrations and match common tree seedling nutrient requirements (Ingestad, 1971): $Ca(NO_3)_2$ (4.8 mM), $CaSO_4$ (1.6 mM), $CaCl_2$ (1.6 mM), KCl (4.0 mM), K_2SO_4 (4.0 mM), $MgCl_2$ (0.4 mM), $MgSO_4$ (0.4 mM), NH_4Cl (3.2 mM), $(NH_4)_2SO_4$ (3.2 mM), 0.2 NaH_2PO_4 (0.2 mM), H_3BO_3 (80 µM), FeEDTA (80 µM), $MnCl_2$ (8 µM), $ZnSO_4$ (0.8 µM), CuSO4 (0.8

µM) and $(NH_4)_6Mo_7O_{24}$ (5.6 µM). Since the nutrient solution was not renewed, the ion concentrations were calculated to maintain an optimum nutrient status during the experiment. As suggested by Ingestad (1971), we used an optimum NH_4-N/NO_3-N ratio (40/60). Si was supplied at three different concentrations (0.2, 0.8 and 1.6 mM) for each tree species. Three replicates of six seedlings per pot were repeated for each concentration and for each tree species. As described by Henriet et al. (2006), Si was supplied as H_4SiO_4 obtained by dissolving sodium metasilicate in demineralized water, followed by leaching on a protonated cation-exchange resin (Amberlite® IR-120). Neither Si precipitation nor H_4SiO_4 deprotonation was expected because Si concentration was below the solubility limit (< 1.79 mM Si) and pH ranged between 5 and 6.5 (Stumm and Morgan, 1996).

5.2.2 Sampling and Si analysis

Twice a week, the volumes of the remaining solutions were weighed to estimate water loss, which was immediately balanced by adding demineralized water. Water loss through evaporation, measured in the six control pots, was 6.2 ± 1.9 $ml.day^{-1}$. Cumulative water uptake was calculated as the difference between water loss and evaporation. The potential Si uptake by mass flow (MFU) was defined by the product of water uptake and Si concentration in the nutrient solution. The MFUs were calculated for each sampling period (twice a week) and summed up for the whole period (77 days). For this purpose, two ml of the nutrient solution were sampled twice a week from each pot after mixing and Si concentration was measured by ICP-AES (inductively coupled plasma – atomic emission spectrometry). Moreover, we measured the pH of the nutrient solution at each sampling: initial pH value of nutrient solution was 5.58 ±0.06 and gradually increased to reach a value of 6.38 ±0.23 at the end of the experiment. After 11 weeks, seedlings were harvested and the different parts - roots, trunk and leaves - were cut up (Figure 5.1). Dry weight was determined after storing at 60°C for one week. The Si leaf concentrations were determined after calcination at 450°C followed by borate fusion (Chao and Sanzolone, 1992). Briefly, a crushed sample of 100 mg of the ignition residue was melted at 1000°C for 5 minutes in a graphite crucible in the presence of 0.4 g Li-tetraborate and 1.6 g Li-metaborate. After dissolution of fusion beads in 10 % HNO_3, Si content was determined by ICP-AES. Given the negligible Si concentrations in roots and trunk (Gérard et al. 2008; Cornelis et al., 2010), Si analysis have not been processed in these samples.

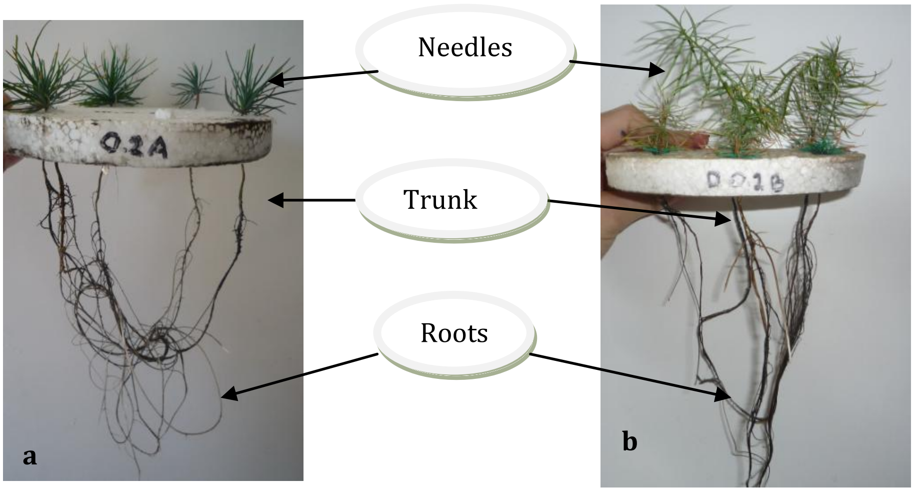

Figure 5.1 Identification of tree seedlings parts (**a.** Black pine; **b.** Douglas fir) separated for biomass calculation (roots and leaves) and Si quantification in leaves.

5.2.3 Statistical analysis

Significance levels of tree species (Douglas fir and Black pine) and Si treatments (0.2, 0.8 and 1.6 mM) effects were assessed by ANOVA2 (model : species; treatment; species×treatment). Furthermore, the effect of Si treatments was compared for each species separately with the Fisher's least significant differences test (LSD, ANOVA1). Statistics were performed with the SAS System (version 9.1, SAS Institute, Cary, NC, USA).

5.3 Results

5.3.1 Seedlings growth

Whatever the Si treatment, the mean total dry weight of leaves at the end of experiment was 82 mg for each tree species, ranging from 57 to 125 mg. We did not observe significant differences in leaf weight between Si treatments (p-value = 0.16) and tree species (p-value = 0.99) (Table 5.1). The mean dry weight of roots was lower and ranged from 8.3 to 40.6 mg, with no significant differences between tree species (p-value = 0.09). We observed that root biomass in Black pine was significantly higher for seedlings with the lowest Si concentrations in the nutrient solution.

5.3.2 Water and mass flow Si uptake

Water uptake was significantly greater for Douglas fir seedlings than for Black pine seedlings (Figure 5.2). After 11 weeks, the mean cumulative water uptake, equivalent to the transpiration, was 99 ml for Douglas fir and 25 ml for Black pine. After experiments lasting 11 weeks, the potential cumulative mass flow Si uptake (MFU) clearly increased with the Si concentration in the nutrient solution (Figure 5.3): from 0.12 to 1.07 mg of Si for Douglas fir and from 0.07 to 0.65 mg of Si for Black pine. At each Si supply and for the first two weeks of the experiments, the MFU was equivalent for Douglas fir and Black pine (i.e ~0). After 3 weeks, the MFU was markedly higher for Douglas fir than for Black pine for each Si concentration in the nutrient solution.

Table 5.1 Leaf and root biomass per seedling (in mg of dry matter) for Douglas fir and Black pine grown in nutrient solution with different Si-concentrations; standard deviation associated with the mean (n=3) is given in parentheses. The interactions between tree species and Si treatments are not significant for leaves and roots biomasses (p-value = 0.39 and 0.84, respectively). Different letters indicate significant differences between Si treatments for the same tree species (p-value < 0.05).

Si-conc in nutrient solution (mM)	Douglas fir	Black pine
	Leaves (mg)	
0.2	125.4 a (57.3)	92.2 a (36.1)
0.8	60.6 a (18.7)	57.3 a (3.4)
1.6	60.1 a (40.6)	96.5 a (64.2)
	Roots (mg)	
0.2	26.0 a (14.1)	40.6 a (16.9)
0.8	14.8 a (16.5)	23.1 ab (5.3)
1.6	8.3 a (2.5)	15.5 b (4.8)

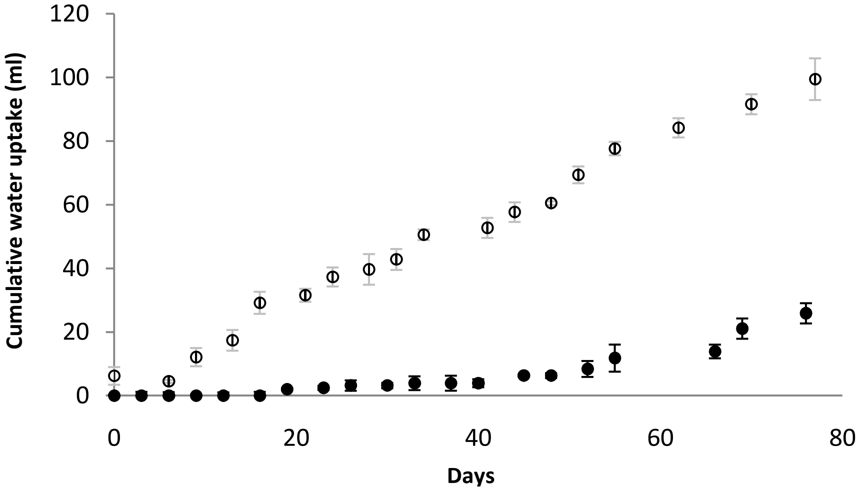

Figure 5.2 Mean cumulative water uptake per seedling (ml) for each species (white circle = Douglas fir; black circle = Black pine) grown in nutrient solutions with different Si-concentrations. The error bar (n=3) represents the standard deviation on the mean value calculated in three pots (one per Si treatment) for each species.

5.3.3 Si leaf concentrations

For each tree species, Si leaf concentration clearly increased with the increasing Si concentration in the nutrient solution (Figure 5.4 and Table 5.2): 0.76 to 3.53 mg Si g^{-1} for Douglas fir and 0.51 to 1.69 mg Si g^{-1} for Black pine. Douglas fir accumulated significantly more Si in leaves than Black pine (p-value < 0.001), except for the low Si supply where the difference was not significant.

Table 5.2 Actual Si concentrations in leaves (mg g^{-1} of dry matter) for Douglas fir and Black pine grown in nutrient solutions with different Si-concentrations; standard deviation associated with the mean (n=3) is given in parentheses. The interaction between tree species and Si treatments is not significant (p-value = 0.08). Different letters indicate significant differences between Si treatments for the same tree species (p-value < 0.05).

Si-conc in nutrient solution (mM)	Douglas fir	Black pine
	Si (mg g^{-1})	
0.2	0.76a (0.34)	0.51a (0.14)
0.8	2.76b (1.32)	1.05b (0.03)
1.6	3.53b (0.60)	1.69c (0.17)

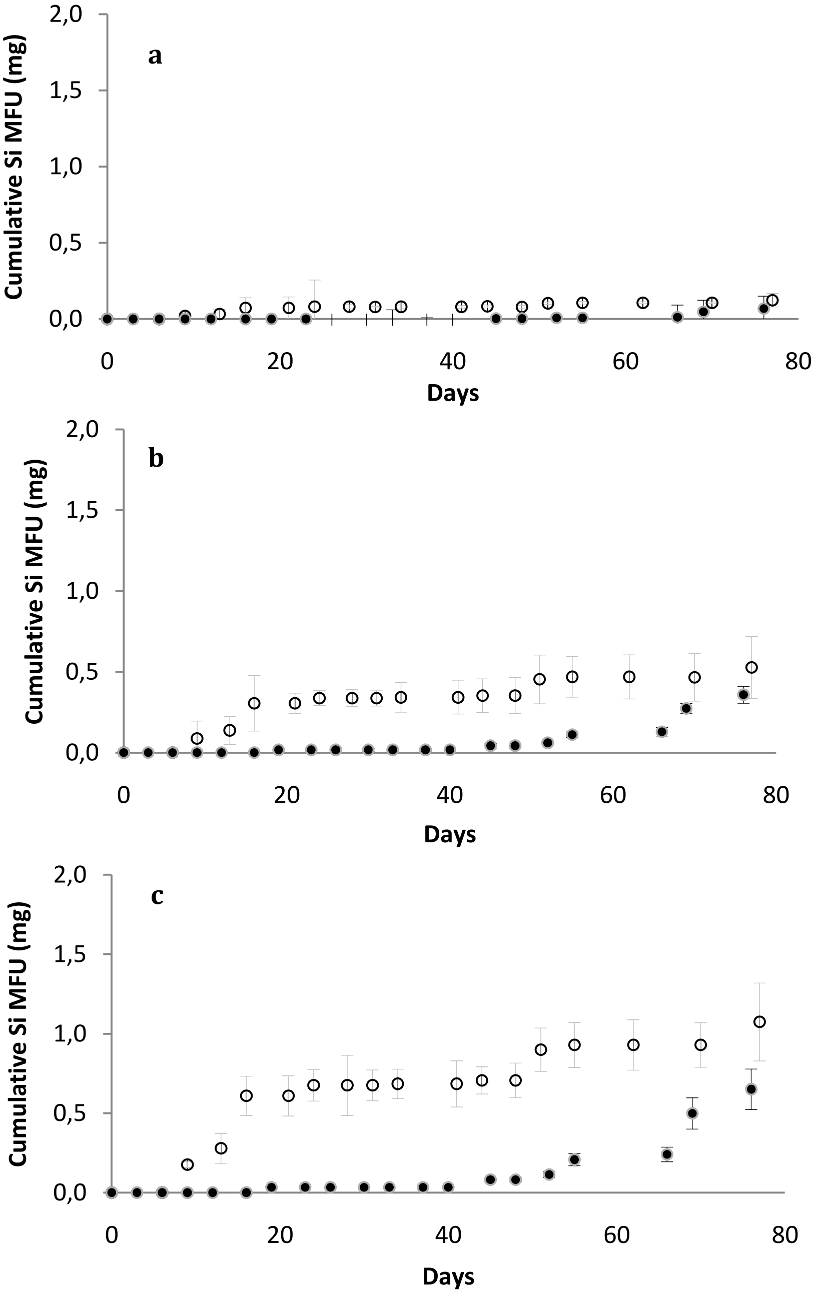

Figure 5.3 Cumulative potential mass flow Si uptake per seedling (mg) for the two tree species (white circle = Douglas fir; black circle = Black pine) grown in nutrient solutions with different Si-concentrations: **(a)** 0.2 mM Si; **(b)** 0.8 mM Si; **(c)** 1.6 mM Si. The error bar (n=3) represents the standard deviation.

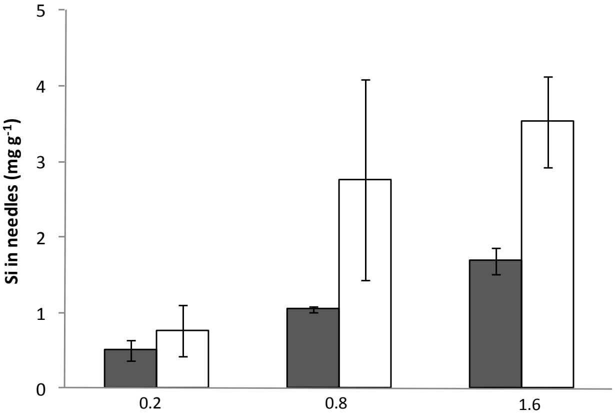

Figure 5.4 Si concentrations in leaves (mg g^{-1} of dry matter) for Douglas fir (white) and Black pine (grey) grown in nutrient solutions with different Si-concentrations: 0.2 mM Si, 0.8 mM Si and 1.6 mM Si. The error bar (n=3) represents the standard deviation associated with the mean.

5.4 Discussion

5.4.1 Si impact on tree seedling growth

The growth of fir and pine seedlings did not increase with increasing Si supply in the nutrient solution (from 0.2 to 1.6 mM): for each tree species, our results did not reveal any positive effect arising from Si supply to the leaf and root dry biomass. In addition, we observed that pine root biomass was significantly larger for seedlings cultivated in the nutrient solution with the lowest Si concentration (0.2 mM), which represents a realistic Si concentration in a temperate forest soil solution (Gérard et al., 2002; Cornelis et al., 2010; Chapter 4). These observations contradict previous studies revealing the positive effect of Si on plant growth by improving their resistance to stress, *e.g.* nutrient imbalance, mineral toxicities, water deficit, diseases and pests (Epstein, 1994; Richmond and Sussman, 2003; Ma, 2004; Liang et al., 2007). In addition, Emadian and Newton, (1989) suggest that the relative increase in pine seedling growth accompanied by a higher Si supply is clearly more important under water-stress conditions. Moreover, Henriet et al. (2006) show that Si did not affect the growth of young banana plants since stress was not imposed during the experiment. Thus, the absence, in our study, of a positive Si effect on the growth of tree seedlings could be attributed to the absence of the stress conditions, which can be attenuated by Si.

5.4.2 Mechanisms controlling Si uptake

In Table 5.3, we show the cumulated potential mass flow Si uptake (MFU) after experiments lasting 11 weeks. We also compute the potential Si concentration in leaves resulting from mass flow absorption, dividing the MFU (mg of Si) by leaf biomass (g), in order to compare this potential Si concentration to the actual Si concentrations in leaves (Table 5.2). At low Si concentration, actual Si leaf concentration was equivalent to potential Si leaf concentration (ratio "actual/potential" ~1) for the two species, suggesting a passive Si uptake, as for some other dicots (Liang et al., 2006). At intermediate and high Si concentrations in nutrient solutions, we found that the actual Si concentration in fir and pine leaves was significantly lower than the potential Si concentrations (ratio "actual/potential" ~0.2-0.3) for both species, assuming a rejective mode of uptake as for some dicots (Liang et al., 2006). Recent studies demonstrate the existence of active Si transporters in roots (*Lsi1* and *Lsi2*) and shoots (*Lsi6*), responsible for the high Si uptake capacity of rice (Ma et al., 2006b, 2007; Yamaji et al., 2008). *Lsi1* is an influx transporter of silicic acid, while *Lsi2* is an active efflux transporter of the same chemical compound. These findings imply that the active transport process operates in some places along the Si trajectory from the root to xylem loading sites. For tree seedlings, the likely passive and rejective processes allow us to assume the inhibition of such active Si transporters in roots and shoots at Si concentration used in our hydroponic experiments. However, for realistic Si concentrations observed in forest soil solutions (0.05-0.2 mM Si; Figure 3.5), we could assume that tree seedling Si uptake could be essentially driven by a combined effect of water flow (passive mode) and active Si uptake. Indeed, in hydroponic experiments, *Helianthus annuus* and *Benincase hispida* take up Si passively at high Si concentration in solution (0.85 mM) while the active uptake contributes to the total Si uptake, especially at lower Si concentration in solution (0.085 mM) (Liang et al., 2006). Therefore, we cannot exclude that both active and passive Si uptake co-exist in tree seedlings at lower Si concentrations in rhizospheric solution (0.05-0.2 mM). Moreover, the Si rejective process at high concentrations in solution should operate in roots, given the relatively low Si concentration in branches, stembark and stemwood in Douglas fir and Black pine (Chapter 4).

Table 5.3 Potential mass flow Si uptake (MFU) is calculated in mg of Si taken up for each seedling after 11 weeks in hydroponics. The estimated Si concentration in leaves is computed through the ratio between MFU and the biomass of leaves. The error associated with the mean (n=3) is given in parentheses (standard error).

Si-conc in nutrient solution	MFU Si uptake after 11 weeks	MFU-based Si concentrations in leaves	Ratio†
mM	Si (mg)	Si (mg g^{-1})	
	DOUGLAS		
0.2	0.12 (0.04)	0.96	0.8
0.8	0.53 (0.19)	8.75	0.3
1.6	1.07 (0.25)	17.80	0.2
	PINE		
0.2	0.07 (0.08)	0.76	0.7
0.8	0.36 (0.05)	6.28	0.2
1.6	0.65 (0.13)	6.74	0.2

† Ratio between the actual (Table 5.2) and potential Si concentrations in leaves

5.4.3 Effect of tree species

The higher *in-situ* Si uptake by Douglas fir as compared with Black pine (Chapter 4) is confirmed in this study of hydroponics in relation to tree seedlings. Since the ratios between actual and potential Si concentrations in leaves of both Douglas fir and Black pine are equivalent (Table 5.3), we conclude that tree species did not affect the Si uptake mechanisms, whatever the Si concentration in nutrient solution. Given the identical Si uptake mechanisms between the two species at realistic Si concentrations (0.2 mM) and the absence of an active Si uptake mode, the much lower accumulation of Si in leaves of Black pine seedlings cannot be directly explained by either a defective or absent transporter to absorb Si from cortical cells to the xylem (Ma and Yamaji, 2006a) or by a lower density of the Si transporter to absorb Si from the external solution to the cortical cells (Mitani and Ma, 2005). The contrasting Si uptake by Douglas fir and Black pine in hydroponics is likely due to the significant difference in transpiration rates. Thus, the *in situ* contrast in Si uptake in an experimental forest site with identical soil and climatic conditions (Cornelis et al., 2010; Chapter 4) could be mainly explained by different transpiration rates. This confirms the following results: (i) the major role of transpiration in Si accumulation in fir leaves (Bartoli and Souchier, 1978), (ii) the leaf area index (LAI), that strongly controls the transpiration rates in trees, is 2 times higher for fir species than for pine (Breda et al., 2002), and (iii) Si accumulates preferentially in the plant transpiration termini with greater amounts in the tip and middle of leaves (Sangster et al., 2007).

Note also a greater difference of Si concentration between fir and pine leaves collected on the forest site - 5.3 and 0.2 mg Si g^{-1} dry matter respectively - than the ones measured after our hydroponics experiment - 0.7 and 0.5 mg Si g^{-1} dry matter respectively. This could be explained by tree species impact on other processes that can influence directly or indirectly the Si uptake in the field site: (i) active uptake at Si concentrations lower than 0.2 mM in rhizospheric solution, and/or (ii) Si sinks in soil such as hydroxyaluminosilicates formation, Si sorption onto Fe oxides, opal-A precipitation and clay neoformation which influence the Si activity in rhizospheric solution.

5.5 Conclusions

This experimental study using tree seedlings in hydroponic conditions confirms the *in-situ* observation of higher Si accumulation in Douglas fir leaves as compared with those of Black pine. The mechanisms of Si uptake in hydroponics are identical between tree species: passive (mass-flow driven) uptake at realistic Si concentrations (0.2 mM) and rejective uptake at higher Si concentrations in nutrient solution. The contrasting Si accumulation in the leaves of coniferous tree seedlings could be attributed to the significant difference in the transpiration rates. The higher Si concentrations in nutrient solutions (0.8 and 1.6 mM) do not affect the growth of tree seedlings, probably because they are not subjected to stress conditions. This finding helps us to understand the mechanisms controlling the different Si uptakes by forest vegetations in order to better predict Si pathways in soil-tree systems. Besides the genetic difference controlling the transpiration rate, climatic and pedogenic factors would also influence the coniferous Si biocycling by modifying the water flow in the soil-tree system and Si activity in soil solution. Further study should be carried out in contrasting soil and climate conditions to assess the effect of various transpiration streams and pedogenic processes on Si uptake and dissolved Si transfer to hydrosphere.

CHAPTER 6:

DISTRIBUTION OF AMORPHOUS SILICA IN A TEMPERATE FOREST SOIL UNDER THREE COMMON TREE SPECIES[*]

---

[*] Adapted from Cornelis JT., Titeux H., Ranger J. and Delvaux B. Distribution of amorphous silica in a temperate forest soil under three common tree species. Submitted to *European Journal of Soil Science*

Abstract

In terrestrial ecosystems, biogenic silica (BSi) deposits are formed in leaves of plants and contribute to the amorphous silica (ASi) pool in soil through litterfall. In forests, the ASi pool is ubiquitous and a substantial component of soil, influencing the Si mass-balance at watershed scale. Here, we examined the distribution of ASi in an acid brown soil under three tree species in identical soil and climate conditions in order to understand how these species impact the ASi pool. We quantified ASi concentration in soil with alkaline extraction (Na_2CO_3 0.1M). In humus layer, we observed that the concentration of ASi (mg SiO_2 g^{-1}) significantly decreases in the sequence: Douglas fir (14.5±0.65) > European beech (11.8±0.30) > Black pine (5.4±0.31). Tree species impact the ASi pool in the humus layer through contrasting uptakes of $H_4SiO_4^0$ and accumulation of BSi in leaves. In mineral layers, pedogenic processes could hide tree species impact on ASi concentration, which decreases from the humus layer to 15 cm depth and then progressively increases from 15 to 75 cm depth under the three species. The ASi concentration is likely controlled by BSi translocation as well as by pedogenic processes such as opaline spheres formation and ASi sorption on Fe oxides. Our data demonstrate the impact of tree species on BSi stock in the soil-tree system and underline the major pedogenic mechanisms influencing the distribution of ASi pool in temperate forest soils.

6.1 Introduction

Silicon (Si) plays a major role in global biogeochemical processes since the interaction between the Si cycle and the C cycle regulates the atmospheric carbon dioxide through the chemical weathering of silicate minerals (Berner, 1995) and the nutrition of marine and terrestrial biota (Tréguer and Pondaven, 2000; Epstein, 1999). The continental cycle of Si strongly impacts the oceanic biogeochemical cycle of Si, as land-ocean fluxes contribute to more than 80% of the input of dissolved Si (DSi) in the oceans (Tréguer et al., 1995). Terrestrial plants largely contribute to the DSi pool since their annual BSi production ranges from 60 to 200 Tmol year^{-1} (Conley, 2002), which rivals BSi production of diatoms in oceans (240 Tmol year^{-1}) (Tréguer et al., 1995). In soils, besides primary crystalline silicates, secondary crystalline minerals (phyllosilicates) and secondary short-range ordered silicates (allophane and imogolite), Si also occurs as amorphous silica (ASi) (Wada, 1989; Drees et al., 1989; Sauer et al., 2006). The ASi pool have both pedogenic and biogenic (BSi) origins. Pedogenic ASi corresponds to the non-crystalline inorganic fraction such as opal formed under supersaturated soluble Si levels (Drees et al., 1989) and ASi adsorbed on pedogenic oxides (Mc Keague and Cline, 1963a,b). Biogenic pool of ASi in soil is constituted by phytoliths and micro-organisms remains (diatoms and sponge spicules). Phytoliths in terrestrial plants are hydrous amorphous silica (opal; $SiO_2.nH_2O$) which polymerize in transpiration sites and return to topsoil within organic residues (Jones and Handreck, 1965). Amount of ASi in soils commonly ranges from <1 to 30 mg g^{-1} on a total soil basis (Drees et al., 1989). As the solubility of ASi is an order of magnitude higher than crystalline silicate minerals (Bartoli and Wilding, 1980; Fraysse et al., 2009), amount of ASi in soils could influence the leaching of DSi to the hydrosphere in specific ecosystems (Bartoli, 1983; Conley et al., 2008; Struyf et al., 2009). Thus, an accurate quantification of the ASi pool in soils is a mandatory step to better understand the Si mass-balance at watershed scale. Besides the study of Saccone et al. (2008), the influence of tree species on ASi pool in soil is poorly studied and there are only few other studies where the BSi component is the only ASi component determined (Bartoli, 1983; Alexandre et al., 1997; Meunier et al., 1999). Thus, our study is aimed to: (1) Identify the different constituents of the ASi pool in an acid brown soil under three common tree species (2) Evaluate the relative impact of pedogenic and biogenic processes on the concentration of ASi in a temperate and granitic ecosystem. Therefore, we compare the distribution of different ASi fractions in an acid brown soil under different tree species (Douglas fir, Black pine and European beech). We isolate the impact of tree species on the distribution of ASi since soil physical and chemical properties were nearly identical between tree plots when the experimental site was set up (Bonneau et al., 1977).

6.2 Materials and methods

6.2.1 Experimental site

The experimental site (Breuil-Chenue) is located in Nièvre department in central France. Over the period 2001-2006, the mean annual rainfall is 1212 mm and the mean annual temperature is 9 °C. The acid brown soil is classified as an Alumnic Cambisol (IUSS, 2006) and is developed from granite with 34.5% quartz, 24.0% feldspars, 30.7% albite, 1.7% biotite, 8.5% muscovite and 0.6% chlorite, leading to total concentrations of 0.1% MgO, 0.3% CaO, 3.5% K_2O and 76.1% SiO_2 (Ranger et al., 2004; Mareschal 2008). The major soil properties at the experimental site are presented in Table 3.2 and 3.3. The native mixed forest, dominated by European beech (*Fagus sylvatica* L.) and oak (*Quercus sessiliflora* Smith.), was clear-cutted in 1976 and replaced by monospecific plots of different tree species. Here, we considered the plots of Douglas fir (*Pseudotsuga menziesii* Franco), Black pine (*Pinus nigra* Arn. *Ssp laricio* Poiret var corsicana.) and European beech (*Fagus syslvatica* L.).

6.2.2 Phytolith sampling and analysis

Leaves and needles were collected from five litter-traps per stand in the experimental site. Phytoliths (BSi) were isolated from leaves and needles by the following method: (1) leaves and needles were washed successively with deionized water, HCl 1M, 70 % ethanol and rinsed again with deionized water in order to avoid aeolian contamination (Kelly, 1990), (2) about 5 - 10 g of dry matter was grinded and digested at 120 °C in a concentrated HNO_3 (70 %) / H_2O_2 (30 %) mixture until the reaction ceased (~10 days), and (3) BSi suspension was filtered through a pre-weighed 0.2 μm filter and rinsed with deionized water. Morphological features and chemical content of BSi particles were respectively examined by scanning electron microscopy (SEM: Leica Stereoscan 260) and energy dispersive X-ray analysis (EDX: EDAX system). Phytoliths were also identified by X-ray diffraction (XRD) using CuKα radiation in a Bruker Advance diffractometer.

6.2.3 Soil samples

We defined the forest floor as the whole set of organic horizons above the organo-mineral horizon (Ah). Under each forest stand, three replicates of organic horizons were sampled in November 2006 according to the forest humus classification (Brethes et al., 1995): Oln (plant litter), Olv (poorly fragmented), Of (fragmented litter) and Oh (dark humified organic matter). In this study, we only considered the humus layer (Oh). Humus samples were immediately stored at 4°C in the dark after removing branches and living roots. At the same time, we collected three samples of soil layers under each forest stand and at each following depths (cm), which do not correspond to specific horizons: 0-7.5; 7.5-15; 15-30; 30-45; 45-60 and 60-75. Soil samples were air dried during one week, sieved at 2 mm (fine earth fraction) and stored.

6.2.4 ASi determination

Wet alkaline dissolution

The wet alkaline methods are the more popular used for the measurements of ASi in aquatic sediments as attested by an inter-laboratory comparison (Conley, 1998) and are based on the significant increase of amorphous Si solubility at pH above 9.0 (Iler, 1979). Numerous methodologies were proposed for extracting ASi from soils (Sauer et al., 2006). Saccone et al. (2007) show the validity of the wet alkaline methods to quantify ASi fraction in forest soils previously developed for measuring ASi in aquatic sediments. During the alkaline extraction, quartz is virtually insoluble, but the dissolution of clay minerals severely complicates the determination of the BSi content (Koning et al., 2002). Thus, corrections for the simultaneous dissolution of amorphous and crystalline Si using time course extractions were proposed (DeMaster, 1981). The time course Na_2CO_3 extraction is a relatively simple and accurate method which can be applied to a large number of samples. Recently, it was shown that this technique was effective for measuring the total ASi concentration in spodsols with sandy loam texture (Saccone et al., 2007; Saccone et al., 2008). In our study, the alkaline solution (Na_2CO_3 0.1 mol l^{-1}, pH = 11.2) was used to supply the hydroxyl ion needed to release DSi from ASi (Iler, 1979). Here, 30 mg of dried soil (< 2 mm) was mixed in 40 ml of alkaline solution and digested at 85 °C during 5 hours. One milliliter was removed from the extraction solution after 15, 60, 120, 180, 240 and 300 minutes and was neutralized with 9 ml of 0.022 mol l^{-1} HCl, before DSi determination by inductively coupled plasma atomic emission spectrometry (ICP-AES). Extracted SiO_2 (mg g^{-1}) was plotted versus time and ASi concentration was calculated using the correction of DeMaster (1981) assuming that (i) most ASi completely dissolved within the first 2 hours of the extraction and (ii) clay minerals released Si at a much slower and constant rate over the whole extraction time. Furthermore, we must assume the absence of short-range ordered Al-Si compounds which are more sensitive to alkaline solutions than crystalline clay minerals and are completely dissolved during the first time of extraction (Wada, 1989; Kamatani and Oku, 2000). The concentration of ASi was estimated by extrapolating the linear part of the plot to zero (intercept value on Y-axis).

Three samples collected under European beech at 60-75 cm depth were analyzed in triplicate to test the reproducibility of the alkaline method. We obtained a mean reproducibility of ± 4.0 % for the ASi content, expressed as mg SiO_2 g^{-1} of soil dry weight. In this study, for all soil layers and under each tree species, extractions were realized on three different soil samples (n = 3).

Gravimetric separation

The extraction of ASi constituents was carried out by heavy liquid method adapted from Kelly (1990) using zinc bromide solution ($ZnBr_2$, density = 2.3 g cm^{-3}). Details can be found in Chapter 4.

6.2.5 Specific extraction

The content of weakly-ordered sesquioxides and poorly crystalline constituents as allophane and imogolite was estimated on dried fine earth (<2mm) under European beech by extraction with 0.2 mol l^{-1} ammonium oxalate-oxalic acid at pH 3 (Dahlgren, 1994), followed by analysis of extracted Si, Fe and Al by ICP-AES. Oxalate digestion releases Al from organic complexes and dissolves allophane, imogolite and poorly crystalline hydrous Fe oxides but no or very little amorphous opal (BSi) (Kodama and Ross, 1991).

The pool of the so-called "plant-available Si", *i.e.* silicic acid in soil solution, was assessed by $CaCl_2$ extraction (0.01 M) (Sauer et al., 2006) and represented the ASi fraction which is readily soluble. Si concentration was measured in the $CaCl_2$ extract by ICP-AES. The specific extractions (Na_2CO_3, Oxalate and $CaCl_2$) are not sequential.

6.3 Results

6.3.1 Microscopic analysis

Tree phytoliths

The BSi particles morphologies are presented in Figure 6.1 (a,d,g) and are described in Chapter 4. *Pinus nigra* phytolith is called "cylindric lacunose"; *Fagus sylvatica* phytolith is called "cylindric sulcate" or "laminate tracheid" and *Pseudotsuga menziesii* phytolith is called "elongate long cell". The EDX analysis (Figure 6.2a) revealed the large dominance of Si (98 wt%) in BSi particles isolated from leave materials. The XRD analysis showed that the BSi particles extracted were opal-A, characterized by a diffused broad diffraction band centered at 0.4nm (Figure 6.1j) (Drees et al., 1989).

ASi from soil

Comparing phytoliths extracted from leaves and needles, BSi particles extracted from humus and soil layers exhibited dissolution features as revealed by SEM analysis (Figure 6.1c,f,i) and a larger Al adsorption onto their surfaces as shown by EDX analysis (Figure 6.2b). In addition to weathered tree phytoliths, SEM analysis revealed the presence of (i) non-biogenic amorphous particles (opaline spheres) (arrows in Figure 6.1e,h,i) and (ii) BSi particles with other shapes ("bilobate short cell", "cylindrical polylobate", "globular" and "favose") probably inherited from the herbaceous understory vegetation (cross in Figure 6.1b,h).

The XRD analysis revealed that particles extracted by the heavy liquid method from soil samples contain opal-A (typical band at 0.4nm) (Figure 6.1k), but also the following crystalline minerals: quartz (0.33 and 0.43nm), kaolinite (0.71 and 0.35nm), mica (0.99 and 0.49nm), and chlorite (1.41nm).

6.3.2 Depth distribution of ASi

The ASi concentration determined by wet alkaline method in humus and soil layers under each tree species is presented in Table 6.1 and Figure 6.3. The mean concentration of ASi in humus layer significantly decreased in the sequence: Douglas fir (14.5±0.38 mg SiO_2 g^{-1}) > European beech (11.8±0.17 mg SiO_2 g^{-1}) > Black pine (5.4±0.18 mg SiO_2 g^{-1}). In topsoil (0-7.5 cm), the concentration of ASi was significantly larger under European beech than

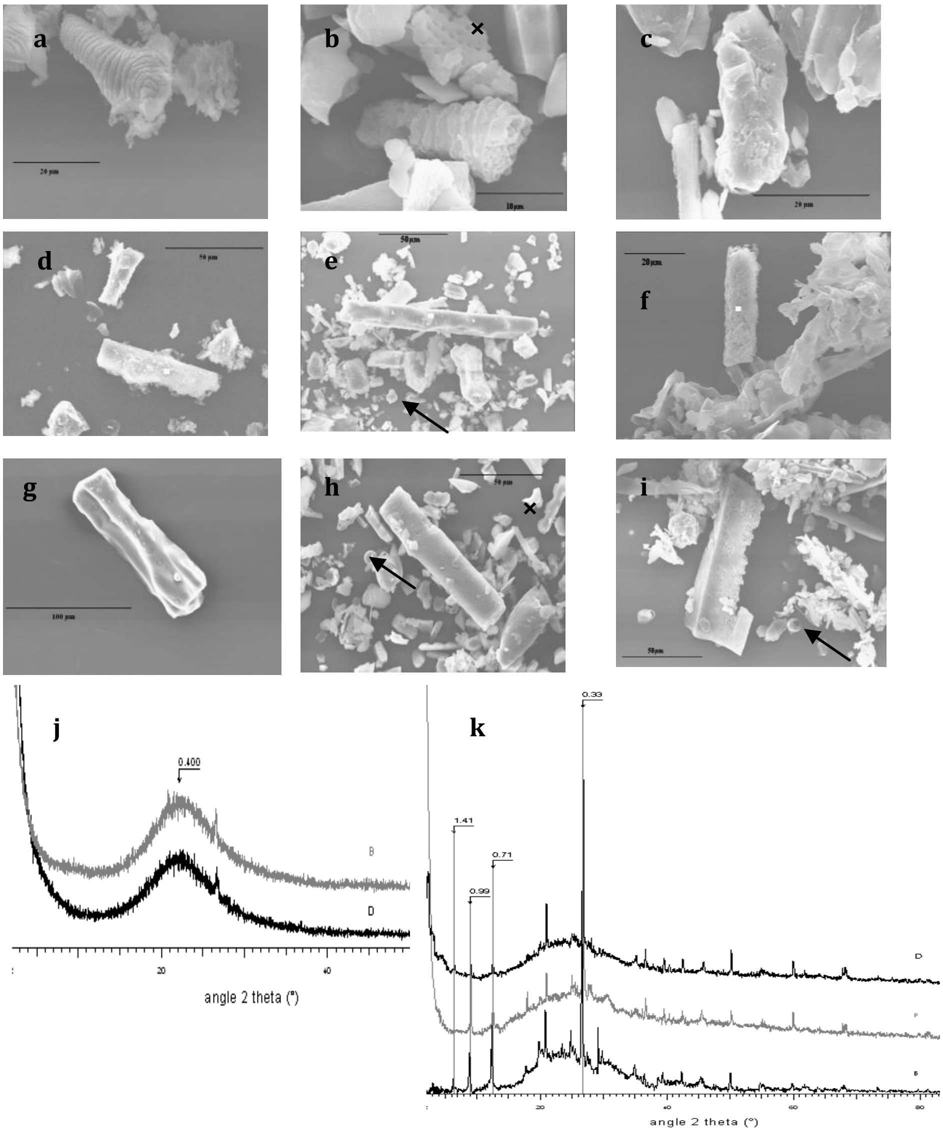

Figure 6.1 Scanning electron micrographs of BSi from leaves and ASi from humus and soil layers. -**a**- BSi isolates from *Fagus syslvatica* leaves. -**b**- ASi isolates from Oh under *Fagus syslvatica*. -**c**- ASi isolates from soil (>15 cm) under *Fagus syslvatica*. -**d**- BSi isolates from *Pseudotsuga menziesii* needles. -**e**- ASi isolates from Oh under *Pseudotsuga menziesii*. -**f**- ASi isolates from soil (>15 cm) under *Pseudotsuga menziesii*. -**g**- BSi isolates from *Pinus nigra* needles. -**h**- ASi isolates from Oh under *Pinus nigra*. -**i**- ASi isolates from soil (>15 cm) under *Pinus nigra*. -**j**- characterization of beech (B) and douglas fir (D) BSi by X-ray diffraction (XRD) spectrum with the typical 0.4nm band of opal-A. -**k**- characterization of ASi extracted by zinc bromide from soil under beech (B), pine (P) and Douglas fir (D) by XRD, which also reveals some crystalline minerals: quartz (0.33 and 0.43nm), kaolinite (0.71 and 0.35nm), mica (0.99 and 0.49nm), and chlorite (1.41nm).

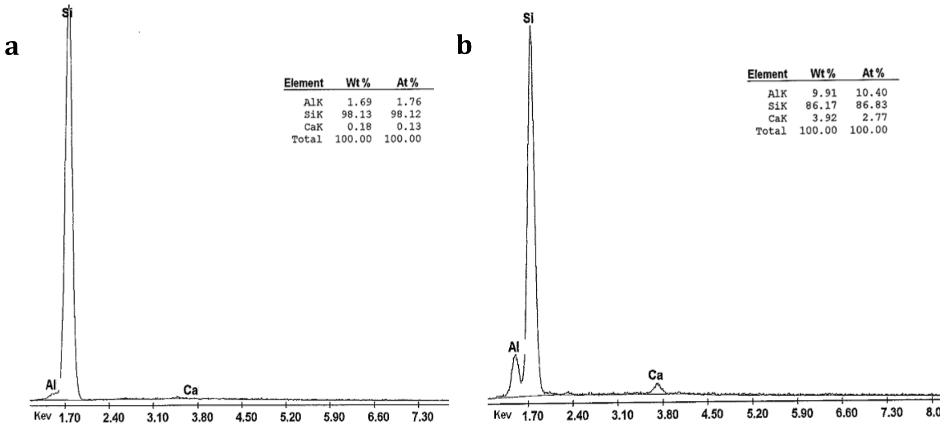

Figure 6.2 EDX analysis of (a) beech phytoliths and (b) ASi isolates form soil (10-15 cm) under *Fagus syslvatica*.

Table 6.1 Mean ASi concentration in humus and soil layers, expressed as mg of SiO_2 per g of dry matter. The Si is extracted using Na_2CO_3 0.1M alkaline solution. The error associated with the mean (n = 3) is given in parenthesis (standard error).

	ASi/ mg SiO_2 g^{-1}		
	European beech	Douglas fir	Black pine
Oh	11.8	14.5	5.4
	(0.17)	(0.38)	(0.18)
0-7.5 cm	6.4	3.2	5.3
	(0.72)	(0.65)	(0.21)
7.5-15 cm	3.6	1.3	2.0
	(0.18)	(0.34)	(0.23)
15-30 cm	4.0	2.6	2.3
	(0.41)	(0.85)	(0.35)
30-45 cm	3.6	4.0	3.2
	(0.55)	(0.48)	(0.51)
45-60 cm	4.4	4.3	3.9
	(0.21)	(0.25)	(0.33)
60-75 cm	5.7	4.5	4.5
	(0.19)	(1.40)	(1.01)

under Douglas fir and Black pine. At others soil depth, there was no significant difference between tree species. The ASi distribution with depth shows very similar trend under each tree species: a decrease of the ASi concentration from the humus layer to 15 cm depth and a slight increase from 15 to 75 cm depth.

6.3.3 Gravimetric versus alkaline methods

ASi extracted from soil by the alkaline method was compared with the ASi extracted by heavy liquid method (ASi_g) (Figure 6.4). In the humus layer, the alkaline solution extracted 3 to 10 times more ASi than the concentration evaluated by the heavy liquid method, according to tree species (Table 6.2). However, for mineral layers, ASi_g concentration was up to 15 times higher than the ones evaluated by wet alkaline method in this study.

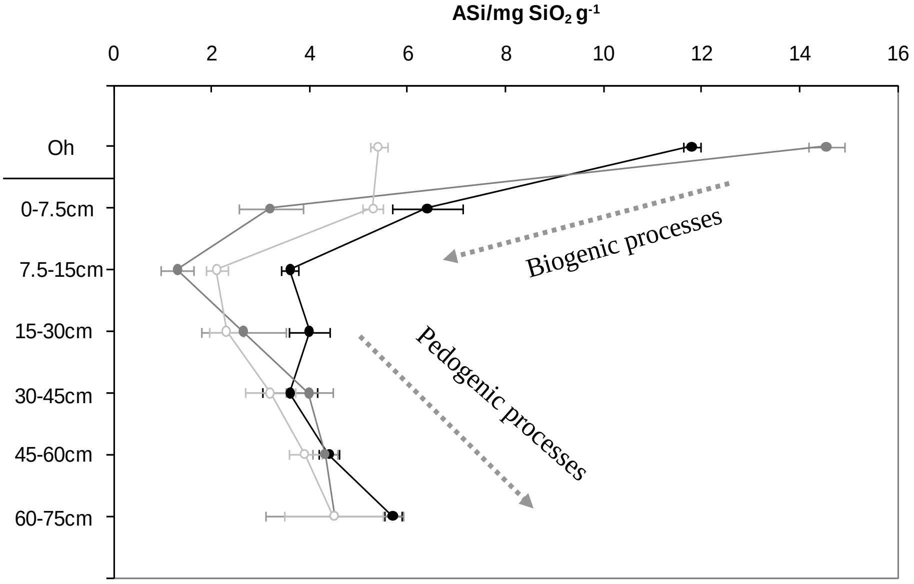

Figure 6.3 Mean ASi concentration in humus (Oh) and soil layers, expressed as mg SiO_2 g^{-1} of dry matter. The ASi concentration is evaluated by wet alkaline dissolution (Na_2CO_3 0.1 mol l^{-1}) under European beech (black), Douglas fir (grey) and Black pine (white). The error bar (n = 3) represents the standard error.

Table 6.2 Mean ASi_g concentration in humus and soil layers, expressed as mg SiO_2 g^{-1} of dry matter. The ASi_g is extracted using heavy liquid method ($ZnBr_2$). There are not replicates for this extraction; except for the 0-5 cm depth (the error associated with the mean (n = 3) is given in parentheses).

	ASi/mg SiO_2 g^{-1}		
	European beech	Douglas fir	Black pine
Oh	1.2	4.3	1.1
0-5 cm	15.3 (7.2)	26.3 (8.3)	31.6 (10.0)
5-10 cm	37	26.5	13.3
10-15 cm	17	28.4	11.4
15-25 cm	13.1	5.8	nd
25-40 cm	7.6	6.3	nd

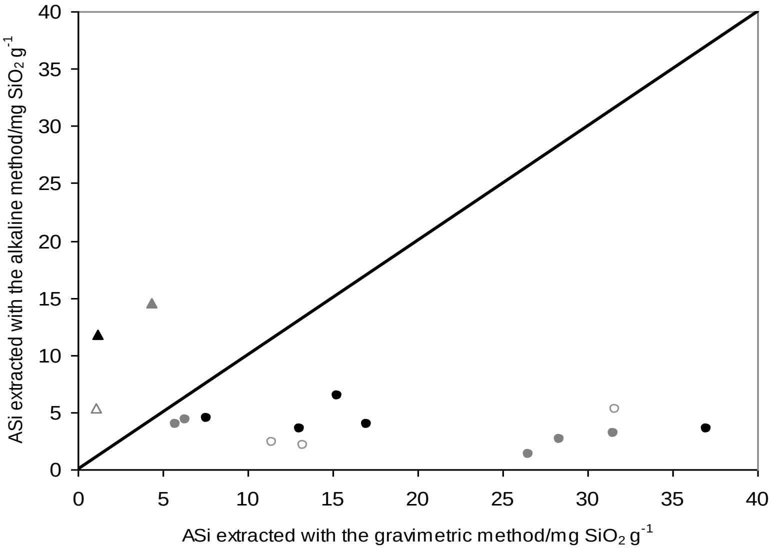

Figure 6.4 Comparison between the ASi measured with the alkaline extractions and the ASi_g measured with gravimetric separation by heavy liquid floatation. The ASi concentration is evaluated under European beech (black), Douglas fir (grey) and Black pine (white); in humus (triangle) and mineral soil layers (circle). 1:1 line is the black line.

6.3.4 Specific extraction of Si, Fe and Al

Under European beech, Si extracted with oxalate (Si_{ox}) was very low in the first soil layer (0-7.5 cm) and increased between 7.5 and 60 cm soil depth

(Table 6.3). In our forest soils, we also observed an increase of oxalate-extractable Al and Fe between 7.5 and 45 cm depth and then a decrease. Under each tree species, the $CaCl_2$-extractable Si concentrations were very low as compared to oxalate-extractable Si and ASi concentrations (Table 6.4).

Table 6.3 Mean concentration of oxalate-extractable Si, Al and Fe in soil under European beech. The error associated with the mean (n = 3) is given in parenthesis (standard error).

	Si/ mg g^{-1}	**Al/ mg g^{-1}**	**Fe/ mg g^{-1}**
Oh	0.09	1.72	2.42
	(0.002)	(0.01)	(0.04)
0-7.5 cm	0.04	2.78	4.02
	(0.01)	(0.35)	(0.38)
7.5-15 cm	0.43	3.50	3.64
	(0.06)	(0.11)	(0.31)
15-30 cm	0.35	3.59	2.93
	(0.03)	(0.10)	(0.06)
30-45 cm	0.20	3.41	2.87
	(0.03)	(0.23)	(0.19)
45-60 cm	0.29	2.80	2.38
	(0.02)	(0.09)	(0.11)
60-75 cm	0.14	2.67	2.18
	(0.01)	(0.15)	(0.09)

Table 6.4 Average values of $CaCl_2$-extractable Si concentration in soil under European beech, Douglas fir and Black pine. The error associated with the mean (n = 3) is given in parenthesis (standard error).

	$CaCl_2$-extractable Si/ mg kg^{-1}		
	European beech	Douglas fir	Black pine
Oh	42.6	28.5	31.2
	(0.3)	(1.3)	(1.2)
0-7.5 cm	13.8	15.7	17.5
	(0.4)	(1.0)	(3.0)
7.5-15 cm	18.5	16.3	18.0
	(0.7)	(2.0)	(1.4)
15-30 cm	20.6	22.1	21.3
	(1.0)	(0.5)	(0.4)
30-45 cm	20.0	24.1	26.4
	(0.4)	(0.7)	(0.3)
45-60 cm	21.8	24.4	27.8
	(0.2)	(1.3)	(1.6)
60-75 cm	20.1	22.7	20.7
	(0.3)	(1.4)	(0.3)

6.4 Discussion

6.4.1 Methodology

The ASi_g pool involves silt- and sand-sized ASi particles (2-2000 µm), other poorly crystallized alumino-silicates and some crystallized minerals, but not clay-sized BSi (<2 µm) (Herbauts et al., 1994). Gravimetric separation of ASi from soil allowed us to perform microscopic and XRD analysis, in order to identify amorphous and crystalline minerals extracted. However, for quantification, the gravimetric method (i) is not very accurate since a few clay minerals are present in the sample extracted by zinc bromide solution (Herbauts et al., 1994; Zhao and Pearsall, 1998), (ii) cannot be applied to a large number of samples since it is very time consuming and (iii) is very toxic due to the heavy liquid medium (Madella et al., 1998). We observe that the relative standard deviation of the ASi determination by alkaline extraction in the first soil layer (0-7.5 cm) is 6-28 %, which is much lower than relative standard deviation of gravimetric extraction (41-60%) (Cornelis et al., 2010; Chapter 4). Furthermore, as reported in previous works (Zhao and Pearsall, 1998), we show that the extraction of ASi_g from soil samples integrates crystallized silicates: mica, chlorite and kaolinite (Figure 6.1k). This can explain the over-estimation of ASi with the gravimetric method as compared to the wet alkaline dissolution in mineral layers. In humus layer, alkaline dissolution extracts more ASi than the heavy liquid separation. It could be explained by the exclusion of clay-sized BSi fraction in the gravimetric method (Herbauts et al., 1994). In the organic horizons, we could hypothesize that the ASi_g concentration is less impacted by the presence of crystallized minerals. Obviously, considering our experimental site and our objective, time course Na_2CO_3 extraction seems to be the more relevant procedure to determine the ASi concentration in our forest soil samples (Herbauts et al., 1994; Conley, 1998; Koning et al., 2002; Sauer et al., 2006; Saccone et al., 2007; Saccone et al., 2008), and above all, is more accurate than gravimetric procedures, which is lacking of precision because the weighed opal mass is generally very small (< 5mg) (Herbauts et al., 1994).

6.4.2 Composition of ASi

Table 6.5 summarizes the components of the ASi pool extracted with the different methods (Na_2CO_3, oxalate and $CaCl_2$). In our temperate forest soil samples, we assume that ASi fraction extracted with Na_2CO_3 solution may include: (i) micro-organisms remains as well as biogenic and pedogenic opal, (ii) ASi sorbed on Fe and Al oxides/hydroxides, short-range ordered silicates such as allophane and imogolite and ASi in exfoliated sheets of weathered clays, each extracted by oxalate and (iii) silicic acid in soil solution, extracted by $CaCl_2$.

Table 6.5 Classification of Si released from liquid, adsorbed, amorphous and poorly crystalline Si forms by specific extraction: $CaCl_2$, Oxalate and Na_2CO_3.

	Biogenic amorphous forms	**Pedogenic amorphous forms**		**Poorly crystalline forms**	**Liquid and adsorbed phases**
	Phytoliths, Micro-orgnaism remains	*Opaline spheres*	*ASi sorbed on Fe oxides,* *ASi on clay weathered surfaces*	*Allophane, Imogolite*	*Monosilicic acid, Polysilicic acid*
Na_2CO_3	────	────	────	────	────◆
Oxalate			- - - -	- - ──	────◆
$CaCl_2$					──◆

Short-range ordered silicates, which are not amorphous and are characterized by Si:Al ratio of 1:2 to 1:1, are more sensitive to alkaline solutions than crystalline clay minerals and are completely dissolved during the first 20 min of alkaline extraction (Wada, 1989; Kamatani and Oku, 2000). Thus, the quantification of ASi pool by alkaline dissolution should be interpreted with caution in soils with high concentrations of allophane and imogolite. However, we could assume that allophane, which occur mainly in volcanic soils, are excluded from our soil samples because the acidic conditions in our forest soil (pH (H_2O) = 3.8 – 4.6) likely impede the synthesis of these compounds (Wada, 1989). Furthermore, Wonisch et al. (2008) demonstrate the absence of imogolite type material and other allophane compounds in the forest site of Breuil-Chenue. Thus, in our case, we can consider that time course Na_2CO_3 extraction includes only the amorphous Si fraction but not the short-range ordered silicates. During dissolution, released Si is also chemically adsorbed on surfaces of soil constituents, like Al hydroxides and Fe oxides (Mc Keague and Cline, 1963a,b). At Fe oxides surfaces, Dietzel (2002) show that polysilicic acid might be formed by specific interaction with orthosilicic acid. Oxalate is expected to extract Si from weakly-ordered sesquioxides and short-range ordered Si-Al compounds (Wada, 1989; Kodama and Ross, 1991). As allophane and imoglite are absent from our soil, we suppose that Si_{ox} merely includes ASi adsorbed onto weakly ordered Fe and Al oxides/hydroxides. Si may also be precipitated from soil solution as pedogenic opaline spheres (Drees et al., 1989). Besides, the ASi concentration is influenced by the degree of weathering of silicates. During alteration process, Turpault and Trotignon (1994) remark that the lateral exfoliated sheets around the biotite is composed of amorphous silica. Finally, the content of micro-organism remains is likely very low as revealed by SEM analysis.

6.4.3 Effect of tree species on ASi distribution

ASi in humus layer

We assume that the ASi fraction in the humus layer mainly consists of BSi from tree and understory vegetations as revealed by SEM analysis and by the low concentration of Si extracted by oxalate digestion in topsoil (Table 6.3). Saccone et al. (2008) also show that ASi extracted from the surface of soil have mainly a biogenic origin. In the same experimental site, Cornelis et al. (2010) show that the annual Si uptake is clearly dependent on tree species, decreasing in the sequence: Douglas fir (30.6±8.0 kg ha^{-1} yr^{-1}) > European beech (23.3±6.5 kg ha^{-1} yr^{-1}) > Black pine (2.3±0.9 kg ha^{-1} yr^{-1}). This study also reveals that, at least, 83% of the Si uptake is annually recycled on topsoil through litterfall (Cornelis et al., 2010; Chapter 4). Moreover, the influence of tree species on the restitution rate of BSi on topsoil has the same trend as for concentration of ASi extracted from humus layer. Thus, tree species impacts the ASi pool in organic horizons as a result of contrasting Si uptakes and BSi restitution on topsoil.

We also observed minor amounts of pedogenic opal spheres (Figure 6.1e,h), although forest floor solutions in our experimental site are not supersaturated with respect to amorphous silica (Cornelis et al., 2010; Chapter 7). Such contradiction might be explained by Si saturation in soil microsites or during short periods, because evaporation may have a significant impact on polymerization behavior of silicic acid in soils causing elevated silicic acid in the remaining solutions quite well above the solubility limit of ASi (Wonisch et al., 2008).

ASi in soil layers

The decrease of the ASi concentration between humus layer and 15 cm depth, may be due to the translocation and dissolution of phytoliths (BSi) followed by root-uptake and/or leaching. The BSi dissolution is in agreement with the increase of DSi concentration between forest floor leachates and the solutions collected under 15 cm depth (Cornélis et al., 2010; Chapter 3). However, this increase of DSi could also be explained by silicate minerals weathering driven by low pH and high concentration of low molecular organic acids in the topsoil (Giesler et al., 2000). Between 15 and 75 cm depth, the slight increase of the ASi concentration is probably due to the translocation-accumulation of stable phytoliths and precipitation of opaline spheres, as revealed in Figure 6.1 (i). In our experimental site, the concentration of oxalate-extracted Al (Table 6.3) is dominated by organic-Al complexes as revealed by Al speciation calculations realized by Wonisch et al. (2008). In addition, these authors show that monomeric Al-Si species are present in very low amounts and all solutions are undersaturated with respect to amorphous $Al(OH)_3$. Thus, we could assume an increase of ASi sorbed on Fe oxides with depth, which is in agreement with the increase of reactive Fe oxides between 7.5 and 45 cm depth (Table 6.3). The increase of ASi sorption on Fe oxides with depth is confirmed by the increase of Si_{ox} between 15 and 60 cm depth, which represents 12-26% of total ASi concentration in soil. In comparison, the Si_{ox} in humus and 0-7.5 cm layers only represents 1-2 % of total ASi concentration. In comparison with the Si_{ox} concentrations, the $CaCl_2$-extractable Si represents a very low amount of the ASi extracted by Na_2CO_3 alkaline solution (Table 6.4). We notice a slight effect of tree species on the concentrations of readily-soluble ASi fraction in soils.

6.4.4 Implications

Saccone et al. (2008) suggest that the concentration of ASi in soil under various landscape position and under both coniferous and deciduous species is dependent on the BSi production. Our study supports the hypothesis that tree species impacts the ASi pool in the humus layer through contrasting Si recycling. Trees act both as a source (BSi restitution) and a sink (Si uptake) of dissolved Si in soil solution. Consequently, considering the impact of tree species on the ASi fraction in humus layer, the increase of DSi leaching to the hydrosphere after deforestation (Conley et al., 2008) could be influenced by tree species. On the other hand, more than 30 years after plantation, the ASi concentration in mineral soil layer is not only impacted by tree species since it is also influenced by pedogenic processes, such as BSi translocation-dissolution (Alexandre et al., 1997), pedogenic opal formation and ASi sorption on Fe oxides (Drees et al., 1989). The increase of ASi concentration with depth reveals that pedogenic processes could hide the effect of tree species.

6.5 Conclusions

In the present study, the extraction with alkaline solution seems accurate even if the proportion of ASi is low in comparison with crystalline silicates. The oxalate extraction could be used to estimate the impact of Fe oxides on the sorption of polymerized silicic acid. In our samples, the ASi fraction mainly integrates biogenic opal (BSi), pedogenic opal and ASi sorbed in pedogenic Fe oxides. Consequently, the alkaline dissolution measure ASi concentration as a whole amorphous fraction which includes BSi fraction. The extraction of ASi from forest soil samples in identical climate and soil conditions reveals that: (i) tree species impacts the concentration of ASi in the humus layer through various Si uptake and (ii) the ASi concentration in soil is influenced by the Si recycling but also by pedogenic processes such as opaline spheres precipitation and sorption on Fe oxides. Like other studies (Blecker et al., 2006; Saccone et al., 2007; Conley et al., 2008; Struyf et al., 2009), our experimental case confirms that the ASi pool, including BSi from plants, is an ubiquitous and substantial component of forest soils (0.1-1.5 %). The ASi quantification is a critical step to improve the knowledge about the Si mass-balance at watershed scale. In our temperate and granitic environment, the study of the relative contribution of small ASi pool and large crystalline silicates pool on the dissolved Si need more consideration.

CHAPTER 7:

TRACING MECHANISMS CONTROLLING THE RELEASE OF DISSOLVED SILICON IN FOREST SOIL SOLUTIONS USING SI ISOTOPES AND GE/SI RATIOS[*]

---

[*] Adapted from Cornelis JT., Delvaux B., Cardinal D., André L., Ranger J., Opfergelt S. (2010) Tracing mechanisms controlling the release of dissolved silicon in forest soil solutions using Si isotopes and Ge/Si ratios. *Geochimica et Cosmochimica Acta* (in press), doi 10.1016/j.gca.2010.04.056.
Complementary data on XRD analysis and BSi dissolution are presented in Appendix C and D, respectively.

Abstract

The terrestrial biogenic Si (BSi) pool in the soil-plant system is ubiquitous and substantial, likely impacting the land-ocean transfer of dissolved Si (DSi). Here, we consider the mechanisms controlling DSi in forest soil in a temperate granitic ecosystem that would differ from previous works mostly focused on tropical environments. This study aims at tracing the source of DSi in forest floor leachates and in soil solutions under various tree species at homogeneous soil and climate conditions, using stable Si isotopes and Ge/Si ratios. Relative to granitic bedrock, clays minerals were enriched in ^{28}Si and had high Ge/Si ratios, while BSi from phytoliths was also enriched in ^{28}Si, but had a low Ge/Si ratio. Such a contrast is useful to infer the relative contribution of silicate weathering and BSi dissolution in the shallow soil on the release of DSi in forest floor leachate solutions. The $\delta^{30}Si$ values in forest floor leachates (-1.38 to -2.05 ‰) are the lightest ever found in natural waters, and Ge/Si ratios are higher in forest floor leachates relative to mineral soil solutions. These results suggest dissolution of ^{28}Si and Ge-enriched secondary clay minerals incorporated by bioturbation in organic-rich horizons in combination with an isotopic fractionation releasing preferentially light Si isotopes during this dissolution process. Ge/Si ratios in soil solutions are governed by incongruent weathering of primary minerals and neoformation of secondary clays minerals. Tree species influence Si-isotopic compositions and Ge/Si ratios in forest floor leachates through differing incorporation of minerals in organic horizons by bioturbation and, to a lesser extent, through differing Si recycling.

7.1 Introduction

It is well established that rooted vascular plants greatly influence the terrestrial Si cycle through silicate weathering by modifying the pH value (Kelly et al., 1998; Berner, 1997) and through Si recycling (Bartoli, 1983; Alexandre et al., 1997; Cornelis et al., 2010). In a forest ecosystem, trees take up a substantial amount of monosilicic acid ($H_4SiO_4^0$) from soil solution (Bartoli, 1983; Lucas et al., 1993; Alexandre et al., 1997; Lucas, 2001; Hodson et al., 2005; Cornelis et al., 2010). $H_4SiO_4^0$ is translocated to transpiration sites where it polymerizes as phytoliths (BSi) (Jones and

Handreck, 1965) generating a significant and ubiquitous terrestrial BSi pool (Conley, 2002; Sommer et al., 2006; Henriet et al., 2008). The soil-tree system may impact on the land-ocean Si flux, which currently contributes to more than 80% of the dissolved Si (DSi) input to the oceans (Tréguer et al., 1995). Accordingly, the Si soil-tree cycle might play a major role in the global climate on a geological timescale. Indeed, the interactions between Si and C cycles regulate the atmospheric carbon dioxide through diatoms' productivity in the oceans (Smetacek, 1999) and weathering processes on the continents (Volk, 1987; Berner, 1997; Sommer et al., 2006).

As suggested by Basile-Doelsch (2006), Si can be considered as being distributed in two main pools: a primary Si-I pool (crystalline rocks and their sedimentary detrital derivatives) and a secondary Si-II pool that leaves the Si-I pool by weathering producing secondary precipitates. On continents, $H_4SiO_4^0$ is released in soil solutions where its concentration is principally influenced by mineral weathering, plant uptake, secondary clay mineral formation, adsorption onto oxides and leaching to the hydrosphere. The dissolution of litho- and pedogenic minerals as well as biogenic minerals contributes to the pool of DSi in soil solutions exported to the rivers.

Germanium (Ge) is a trace element, which is often considered as an analog to Si due to its very similar chemical properties (Azam and Volcani, 1980). The study of Ge/Si fractionation allows tracing silicate weathering and the biogeochemical cycle of Si (Kurtz et al., 2002; Derry et al., 2005; Scribner et al., 2006), as clay minerals and biogenic opal display contrasting Ge/Si ratios. Clay-sized weathering products are enriched in Ge (Murnane and Stallard, 1990; Kurtz et al., 2002; Kurtz and Derry, 2004) whereas phytoliths (BSi) are depleted in Ge relative to Si (Derry et al., 2005; Blecker et al., 2007; Delvigne et al., 2009).

Similarly, the fractionation of stable Si isotopes represents a useful tool to study the Si soil-plant cycle (Ziegler et al., 2005a; Engström et al., 2008; Opfergelt et al., 2010). The δ^{30}Si values in freshwater and seawater show enrichment in heavy Si isotope in comparison to δ^{30}Si values of magmatic and metamorphic rocks, suggesting isotopic fractionation during biogeochemical processes (De La Rocha et al., 2000; Ding et al., 2004; Alleman et al. 2005; Georg et al., 2006,2007). The neoformation of secondary precipitates as clay minerals (Ziegler et al., 2005a,b; Opfergelt at al., 2008), plant Si uptake producing biogenic opal (Douthitt, 1982; Ziegler et al., 2005a; Ding et al., 2005, 2008; Opfergelt et al., 2006a,2006b,2008), biomineralization by diatoms (De La Rocha et al., 1997) and adsorption of Si onto Fe-oxides (Delstanche et al., 2009; Opfergelt et al., 2009) are processes favoring the incorporation of light Si isotopes, generating rivers enriched in heavy Si isotopes (De La Rocha et al., 2000; Ding et al., 2004; Georg et al., 2006,2007). Silicon isotope data alone can hardly decipher these processes. Combining Ge/Si and Si isotope data may provide a better understanding of the Si pathways in a well-defined soil-tree system before its release in soil solution (Delvigne et al., 2009; Opfergelt et al., 2010; Lugolobi et al., 2010).

This study aims to assess the relative contribution of Si released from dissolution of primary and secondary minerals and from biogenic opal to soil solutions. For this purpose, δ^{30}Si and Ge/Si data are combined to investigate the soil-tree systems, which show similar acid-brown soils, climatic conditions and parental material but differ in the planted tree species. Silicon isotopic compositions and Ge/Si ratios were measured in (i) forest floor leachates and soil solutions, (ii) different soil fractions (bedrock; clay, silt, and sand fractions), and (iii) plant-related compartments of the forest ecosystem (plant BSi from phytoliths, and organic-rich horizons).

7.2 Materials and methods

7.2.1 Experimental site

The experimental site is located at Breuil-Chenue (Nièvre-Morvan, France), on a plateau at 638 m above sea level. Table 3.2 and 3.3 present the major properties of the acid brown soil. The parental material is the granite of "La Pierre-qui-Vire", which is covered by a thin layer of cryoturbated Quaternary loess (Aurousseau, 1976). The acid brown soil is classified as an Alumnic Cambisol (IUSS, 2006) and is developed from a granite with 34.5% quartz, 24% feldspars, 30.7% albite, 8.5% muscovite, 1.7% biotite and 0.6% chlorite, leading to total concentrations of 0.1% MgO, 0.3% CaO, 1.3% Fe_2O_3, 3.5% K_2O, 3.5% Na_2O, 13.5% Al_2O_3 and 76.1% SiO_2 (Ranger et al., 2004; Mareschal, 2008). The soil was sandy-loamy (55% sands and < 20% clays) and acidic (pH = 3.8 - 4.6). The native forest mixes trees dominated by European beech (*Fagus sylvatica* L.) and oak (*Quercus sessiliflora* Smith.).

It was clear-cut in 1976 and replaced by six monospecific plantations. Out of these plantations, we selected five forest stands: Douglas fir (*Pseudotsuga menziesii* Franco), Norway spruce (*Picea abies* Karsten), Black pine (*Pinus nigra* Arn. *Ssp laricio* Poiret var corsicana.), European beech (*Fagus syslvatica* L.) and oak (*Quercus sessiliflora* Smith.).

7.2.2 Sampling and physico-chemical characterization

Soil and plant samples

The sampling was conducted in November 2006 and described in Chapter 4. Briefly, leaves and needles were collected from five litter traps per stand. Three replicates of forest floor horizons were sampled under each forest stand from which we have selected the fragmented (Of) and humified (Oh) horizons above the mineral soil layers. Moreover, three replicates of soil organo-mineral and mineral layers were sampled, under each forest stand, at the following systematic depths (cm) below the organic soil horizons: 0-7.5; 7.5-15; 15-30; 30-45; 45-60; 60-75. Solid samples were then mixed to build up composite samples for each depth, and sieved at 2mm to obtain the fine earth fraction (bulk soil <2mm). Granitic bedrock buried in the soil profile was also collected from the experimental site. Soil physical and chemical properties were identical between trees plots when the experimental site was set up (Bonneau et al., 1977). Thus, we assume homogeneous soils conditions between plots of monospecific plantations.

Tree BSi was extracted from leaves and needles after digestion of organic matter in an mixture of ultrapure concentrated HNO_3 (70%) / H_2O_2 (30%). In humus (Oh) and mineral soil layers, amorphous silica fraction (ASi), which includes BSi, was extracted both by gravimetric separation using heavy liquid for all forest stands and alkaline dissolution for Douglas fir, Black pine and European beech (Chapter 6). The sand fraction [50-2000µm] was separated from the fine earth fraction [<2mm] by ultrasonic dispersion and wet sieving. Clay [0-2µm] and silt [2-50µm] fractions were then collected by gravimetric sedimentation (Rouiller et al., 1972). The separation of sand, silt and clay fractions was conducted on humus (Oh) and mineral soil layers, as it was shown that organic layers incorporated minerals from lower soil layers through bioturbation (Cornelis et al., 2010; Chapter 4). Clay fractions, treated with Na-citrate at 100°C, were saturated with K^+ and Mg^{2+} and clay minerals were identified by X-ray diffraction using CuKα radiation in a Bruker Advance diffractometer (at UCL) after saturation with ethylene glycol (EG) and heating (105, 300 and 550°C) (Robert and Tessier, 1974) (Appendix C).

Solution samples

In each forest stand, forest floor leachate solutions were collected in September 2008 by using two sets per forest stand of 9 lysimeters made of polypropylene (zero tension plate) placed just above the mineral soil (i.e. 0 cm). In addition, ceramic cup lysimeters were introduced into the soil profile at 60 cm depth and connected to a vacuum pump, which maintained a constant suction of -400hPa to collect soil solutions (5 replicates per forest stand). The solutions were filtered at 0.45 µm and maintained at 4°C.

Cations concentrations (Ca^{2+}, K^+, Na^+, Mg^{2+} and Mn^{2+}) in forest floor leachates and soil solutions were analyzed by inductively coupled plasma atomic emission spectrometry (ICP-AES). Anions concentrations (F^-, Cl^-, SO_4^{2-}, NO_2^-, NO_3^- and PO_4^{3-}) were measured by ionic chromatography (Dionex DX 300). The dissolved organic carbon (DOC) concentration was determined using a TOC-5050 Shimadzu. Concentrations represent the average of monthly measurements between April 2006 and April 2007, which were performed at the “Institut National de la Recherche Agronomique” (INRA-Champenoux, France).

7.2.3 Si and Ge analyses

Ge/Si ratios were determined from the Ge and Si concentrations in (i) granitic bedrock, (ii) sand, silt and clay fractions from the 30-45 cm mineral layer at European beech site, assuming soil homogeneity under each tree species, (iii) tree BSi, organic horizons (Of, Oh) above the mineral soil, bulk soils (0-7.5 and 30-45 cm) for the five forest stands, and (iv) forest floor leachates and soil solutions collected under the five forest stands.

Most Si and Ge analyses were performed by ICP-AES and inductively coupled plasma mass spectrometer (ICP-MS, Thermo Elemental X7), respectively, at the “Service d'Analyse des Roches et des Minéraux” (SARM, CNRS Nancy, France). Si and Ge were recovered after $LiBO_2$ fusion at 1000°C in a Pt crucible (Carignan et al., 2001). Detection limits for Ge (0.05 $\mu g.g^{-1}$ for solid samples and 2 $ng.l^{-1}$ for solutions) were calculated as six times the standard deviation of the mean plus the mean of 150 procedure blanks for solids (borate fusion) and 10 solution blanks for solutions (HNO_3 2%). The accuracy was determining by measuring six reference rock and water standards (BR, AN-G, UB-N, DR-N, GH and SLRS-4; Carignan et al., 2001; Yeghicheyan et al., 2001). The Si reproducibility was better than 5% for rocks and solutions while the Ge reproducibility was better than 15% for rocks and better than 10% for aqueous solutions in the concentration ranges obtained.

Some solid samples (leaves and needles) with low Ge concentrations were analyzed by hydride-generation ICP-MS (PerkinElmer ELAN 6100 DRC) at the Ut2A-Pau (France) following the method adapted from Mortlock and Froelich (1996). Germanium was extracted on hot plate in nitric acid and hydrogen peroxide media. The acid extract was concentrated by evaporation to a 1 ml volume and then diluted with ultrapure water at 6 ml final volume. As no certified samples were available, the accuracy was checked by spiking a sample at 2 ng.g^{-1} Ge in the solid sample (about 70 ng.l^{-1} Ge in the extract). The detection limit for Ge was 0.05 ng.g^{-1} and Ge reproducibility was better than 20%.

Germanium contents in clay minerals were measured by high resolution (HR) ICP-MS (Element 2) after borate fusion at 1000°C for 1h in Pt crucibles at the "Royal Museum for Central Africa" (RMCA, Belgium). Details about the method, reproducibility and accuracy are available in Delvigne et al. (2009).

7.2.4 Si isotope analyses

Two forest stands of contrasting tree species, Douglas fir (coniferous) and European beech (deciduous), were selected for Si isotope analyses because of the time-consuming sample preparation. The Si-isotopic compositions were determined on (i) granitic bedrock, (ii) bulk soils (0-7.5cm, 30-45cm), and separated sand, silt and clay fractions from the soil layer (30-45cm) at the European beech site (iii) tree BSi and humus layers (Oh), and (iv) forest floor leachates. Silicon was recovered from solid sample material by alkaline fusion at 1000°C. Five mg of sample were mixed with 30mg of $LiBO_2$ flux in a covered Pt crucible, and dissolved in double distilled 5% HNO_3 (Abraham et al., 2008). The dissolved Si was purified by triethylamine molybdate (TEA-moly) co-precipitation and combustion in covered Pt crucibles at 1000°C (De La Rocha et al., 1996). The combustion product was dissolved in a diluted Suprapur HF-HCl mixture (Cardinal et al., 2003). Silicon isotope compositions were determined using a Nu Plasma multicollector inductively coupled plasma mass spectrometer (MC-ICP-MS) operating in dry plasma mode, using Mg doping as an external standard to correct mass bias (Cardinal et al., 2003). The isobaric interferences, mostly $^{14}N^{16}O$ on ^{30}Si, were solved following Abraham et al. (2008). Measurements were performed using the sample-standard bracketing technique relative to in-house standards ($pSiO_2$ or Quartz Merck), which are isotopically similar to the quartz reference material NBS28 (National Institute of Standard and Technology RM #8546) (Abraham et al., 2008). The analytical method was validated by an interlaboratory comparison and the quality of the measurements was controlled by secondary reference materials (diatomite, BHVO-2) along with each samples series, falling on the recommended values (Reynolds et al., 2007; Abraham et al., 2008). Our results were expressed as $\delta^{30}Si$ relative to NBS28 (‰) with an average precision and accuracy on total replicates of ±0.11‰ ($\pm 2\sigma_{SD}$) following:

$$\delta^{30}Si = \left[\frac{\left(\frac{^{30}Si}{^{28}Si} \right)_{sample}}{\left(\frac{^{30}Si}{^{28}Si} \right)_{NBS28}} - 1 \right] * 1000$$

7.3 Results

7.3.1 Soil fractions

The distribution of sand, silt, clay and ASi fractions of the soil layers investigated at the Douglas fir, Black pine and European beech sites is presented in Table 7.1. The acid brown soil mineral fraction was dominated, in average considering all tree species, by the sand fraction (57.5±1.8%) whereas the fraction of silt (24.5±2.1% wt) and clay (18.1±2.3% wt) were less dominant in both 0-7.5 and 30-45 cm layers. The clay-sized fraction in the shallow soil consists of the following minerals: kaolinite (30%) ~ illite (30%) > quartz (20%) > vermiculite (11%) > smectite (4%) > gibbsite (3%) > Fe oxides (2.5%) (Mareschal, 2008). In humus layer (Oh), sand, silt and clay fractions represented, in average considering all tree species, 46.0±8.0, 48.5±8.0 and 5.6±0.5%, respectively of the fine earth dry weight of mineral soil incorporated. The proportion of silt was higher in the humus layer (Oh) relative to the mineral soil layer (0-7.5cm). Through XRD analysis, we identified the following minerals in the clay fraction extracted from humus layer under European beech and

Douglas fir: quartz, kaolinite, illite, illite-vermiculite mixed layers, smectite and chlorite. Calvaruso et al. (2009) also detected these clay minerals in the rhizosphere and bulk soil under Norway spruce and oak from the same experimental site. The SiO_2 content of crystallized minerals ranged from 20% (Douglas fir) to 38% (European beech) of humus dry weight and on average 65.2±4.4% in bulk soil dry weight. The ASi content ranged between 0.5 and 1.4% in humus layers, and between 0.3 and 0.6% in bulk soils. The ASi concentrations in humus and soil layers contribute from 3.0 to 7.0% and from 0.4 to 1.0% of the total crystallized SiO_2, respectively.

Table 7.1 Distribution (% dry weight in fine earth; <2mm) of sand, silt, clay and ASi fractions of humus layers (Oh) and soil layers (0-7.5 and 35-40cm) under Douglas fir, Black pine, and European beech.

	Sand 50-2000µm	Silt 2-50µm	Clay <2µm	ASi[a] 0-2000µm	SiO_2[b] 0-2000µm
	----------	----------	%	----------	----------
			Oh		
Douglas fir	43.5	51.5	5.0	1.4	19.7
Black pine	54.9	39.3	5.8	0.5	37.6
Europ beech	39.5	54.5	6.0	1.2	38.4
			Bulk soil 0-7.5cm		
Douglas fir	57.8	23.0	19.2	0.3	61.7
Black pine	59.2	23.6	17.2	0.5	63.6
Europ beech	57.6	21.8	20.6	0.6	60.6
			Bulk soil 30-45cm		
Douglas fir	53.9	26.3	19.8	0.4	67.3
Black pine	58.5	27.4	14.1	0.3	72.8
Europ beech	57.8	24.7	17.5	0.4	65.2

[a] ASi fraction was quantified by alkaline dissolution with Na_2CO_3 solution (Chapter 6)

[b] The SiO_2 content (%) from crystallized minerals corresponds to the total SiO_2 of bulk soil minus the SiO_2 content from ASi (Chapter 4)

7.3.2 Chemical compositions of solutions

The chemical compositions of forest floor leachates and soil solutions collected at 60 cm depth under each tree species are presented in Table 7.2.

The pH was generally lower in forest floor leachates than in soil solutions (4.6±0.3 and 5.1±0.3, respectively). The concentrations of DOC, Ca^{2+}, K^+, Mg^{2+} and Mn^{2+} were systematically higher in forest floor leachates than in soil solutions. By contrast, the concentrations of Na^+ and Si were higher in soil solutions than in forest floor leachates.

7.3.3 Ge/Si ratios

The Ge/Si ratios measured for the five stands are given in Table 7.3. The Ge/Si ratios of the bedrock, sand and silt fractions were very similar at the European beech site, ranging from 2.3 to 2.5 µmol.mol^{-}1. In contrast, the clay fraction displayed the highest Ge/Si ratio (6.2±0.08 µmol.mol^{-1}, n=2, ±1$\sigma_{SD,}$ two repetitions on two different depths) at this site. The Ge/Si ratios of bulk soils were similar under each tree species, at 2.5±0.1 and 2.6±0.2 µmol.mol^{-1} (n=5, ±1σ_{SD}) for 0-7.5 and 30-45cm bulk soil, respectively. Therefore, we assume that the Ge/Si ratios of sand, silt and clay fractions measured under European beech are also representative for the other sites investigated. The Ge/Si ratios measured in leaves/needles were similar for each species, ranging from 0.1-0.3 µmol.mol-1, except of pine needles with a Ge/Si ratio of 1.5 µmol.mol-1. In organic horizons (Of and Oh), Ge/Si ratios were higher than in leaves/needles with 2.7±0.9 µmol.mol-1 (n=5, ±1σSD) in Of and 3.2±0.2 µmol.mol-1 (n=5, ±1σ_{SD}) in Oh. At each investigated site, the Si concentrations were lower in forest floor leachates than in soil solutions while the forest floor leachates were more enriched in Ge compared to soil solutions. Consequently, Ge/Si ratios were higher in forest floor leachates than in soil solutions collected. More particularly, forest floor leachates under Black pine, European beech and oak displayed higher Ge/Si ratios (2.3-3.7 µmol.mol^{-1}) relative to Douglas fir and Norway spruce (1.6-2.1 µmol.mol^{-1}). In soil solutions, Ge/Si ratios were similar under each tree species (1.2±0.2 µmol.mol$^{-1,}$ n=5, ±1σ_{SD}).

Table 7.2 Chemical compositions of forest floor leachates (0cm) and soil solutions (60 cm) under each tree species.

cm	DOC [a]	pH	F^-	Cl^-	SO_4^{2-}	PO_4^{3-}	NO_3^-	Ca^{2+}	K^+	Na^+	Mg^{2+}	Mn^{2+}	S	Fe	Al	Si
	mg.l-1		μmol.l-1													
							Douglas fir									
0	23.5	4.86	1.1	99.3	23.0	8.0	109.0	63.6	44.5	63.1	28.4	14.4	34.9	3.6	20.0	54.8
60	3.7	4.75	4.2	122.1	19.2	0.2	273.4	12.2	21.0	103.1	15.2	6.9	29.0	0.2	53.4	71.9
							Norway spruce									
0	53.4	4.62	1.1	92.5	21.0	6.7	46.9	31.4	79.3	57.4	16.5	10.4	36.5	8.8	22.2	53.4
60	3.6	5.18	2.6	137.7	55.1	0	17.1	12.0	25.3	97.9	15.6	4.7	59.9	0.2	13.0	60.9
							Black pine									
0	69.0	4.12	1.1	63.8	13.0	0.2	161.4	49.2	109.7	46.1	20.6	18.9	30.3	12.2	64.5	30.6
60	2.4	4.78	3.2	92.8	50.7	0	82.6	12.0	13.0	75.3	9.5	6.0	53.3	0.2	31.9	80.8
							European beech									
0	32.5	4.41	0.5	36.1	11.6	1.2	49.7	29.4	41.2	23.9	9.5	11.6	20.3	7.7	27.4	34.5
60	2.3	5.52	2.1	57.8	38.8	0.2	1.9	3.5	8.7	58.7	6.2	3.3	42.1	0.2	7.8	60.2
							oak									
0	37.0	5.05	0.5	42.0	15.0	5.4	69.7	36.9	39.1	32.2	18.1	10.9	25.9	5.7	39.7	64.5
60	2.6	5.19	1.6	33.3	52.3	0.3	7.6	6.2	4.9	39.1	7.4	1.8	53.3	0.2	10.4	67.0

[a] DOC = dissolved organic carbon

Table 7.3 Si and Ge concentrations and Ge/Si ratios in the compartments of the soil-tree system under five forest stands.

	Si (mmol/g)	Ge (nmol/g)	Ge/Si (µmol/mol)
bedrock	12.6	32.1	2.5
Sand [a]	13.1	29.5	2.3
Silt	12.1	30.4	2.5
Clay1 (from humus)	8.51	53.3	6.3
Clay2 (from soil)	8.30	51.0	6.1
Douglas fir			
Needles	0.21	0.04	0.2
Of	0.83	1.71	2.0
Oh	3.53	11.85	3.4
Forestfloor leachate	0.08	0.158	2.1
Bulk soil 0-7.5	11.13	27.92	2.5
Bulk soil 30-45	11.54	31.97	2.8
Soil solution	0.09	0.11	1.3
Norway spruce			
Needles	0.32	0.03	0.1
Of	0.73	1.06	1.4
Oh	1.72	5.10	3.0
Forestfloor leachate	0.05	0.08	1.6
Bulk soil 0-7.5	10.95	26.90	2.5
Bulk soil 30-45	11.76	29.21	2.5
Soil solution	0.07	0.07	1.0
Black pine			
Needles	0.01	0.02	1.5
Of	1.72	6.02	3.5
Oh	5.68	17.67	3.1
Forestfloor leachate	0.04	0.16	3.7
Bulk soil 0-7.5	10.83	28.17	2.6
Bulk soil 30-45	11.68	31.53	2.7
Soil solution	0.10	0.12	1.2
European beech			
Leaves	0.25	0.05	0.2
Of	2.20	7.55	3.4
Oh	6.03	21.24	3.5
Forest floor leachate	0.043	0.101	2.3
Bulk soil 0-7.5	11.39	26.23	2.3
Bulk soil 30-45	11.81	28.00	2.4
Soil solution	0.067	0.095	1.4
oak			
Leaves	0.17	0.05	0.3
Of	1.09	3.65	3.4
Oh	6.82	20.73	3.0
Forest floor leachate	0.037	0.165	3.7
Bulk soil 0-7.5	11.09	29.52	2.7
Bulk soil 30-45	11.55	29.55	2.6
Soil solution	0.086	0.094	1.1

[a] Sand, silt and clay fractions were separated from soil collected under European beech.

7.3.4 Si-isotopic compositions

The Si-isotopic signatures under Douglas fir and European beech stands are given in Table 7.4 (±1σ_{SD} on replicates n). The sand fraction at the European beech site, mainly containing primary minerals, displayed a δ^{30}Si value of -0.03±0.07‰, which is close to that of granitic bedrock (-0.07±0.03‰). Silt and clay fractions were significantly isotopically lighter than granitic bedrock, with δ^{30}Si values of -0.60±0.28‰ and -1.07±0.32‰, respectively. Bulk soils sampled at 0-7.5 cm and 30-45 cm displayed δ^{30}Si values of -0.06±0.12‰ and +0.08±0.07‰, respectively, which is similar to the signature of the granitic bedrock.

The δ^{30}Si values of the BSi and the humus layer (Oh) at European beech stand were significantly isotopically lighter (-0.64±0.02‰ and -0.68±0.04‰, respectively) than in Douglas fir stand (-0.28±0.11‰ and -0.34±0.08‰, respectively).

The DSi of the forest floor leachates were depleted in heavy Si isotopes compared to the bedrock showing δ^{30}Si values of -1.38±0.17‰ at the Douglas fir site and -2.05±0.12‰ at the European beech site, respectively.

7.4 Discussion

7.4.1 δ^{30}Si and Ge/Si ratios in solid samples

As illustrated in Figure 7.1, unweathered granitic bedrock displays δ^{30}Si signature of -0.07‰, which is in agreement with values previously reported for granitic rocks (average δ^{30}Si value = -0.07±0.05‰ (± 2σ_{SEM}, n = 47; see overview of André et al., 2006)). The Si isotopic and Ge/Si signatures of the bedrock are close to those of granitoid rocks at Luquillo (Puerto Rico) (δ^{30}Si = -0.2‰, Ziegler et al., 2005b; Ge/Si = 2.0 - 2.4 μmol.mol^{-1}, Kurtz et al., 2002, Lugolobi et al., 2010). Clay mineral neoformation produces lighter δ^{30}Si values in secondary clay minerals relative to the bedrock (Ziegler et al., 2005a,b). With increasing soil weathering degree, clay fractions were shown to be increasingly enriched in light Si isotopes (Ziegler et al., 2005b; Opfergelt et al., 2008,2010) with values of -2.2±0.2‰ for kaolinite in the tropical granitic weathering environment at Luquillo (Ziegler et al., 2005b).

Table 7.4 Si-isotopic signatures (δ^{30}Si ± $1\sigma_{SD}$; ‰) of (1) bedrock, soil between 0-7.5cm and 30-45cm depth (<2000µm), sand (>50µm), silt (2-50µm) and clay (<2µm) fractions collected under European beech stand, and (2) biogenic Si (BSi), humus layer (Oh) and forest floor leachates collected under European beech and Douglas fir stands.

	2 σ_{SEM} [b]	δ^{30}Si (‰)	n[a]	$1\sigma_{SD}$
Bedrock	0.12	-0.07	2	0.03
Sand	0.11	-0.03	3	0.07
Silt	0.09	-0.60	4	0.28
Clay	0.14	-1.07	4	0.32
Bulk soil 0-7.5 cm	0.13	-0.06	2	0.12
Bulk soil 30-45 cm	0.11	+0.08	2	0.07
Douglas fir				
BSi	0.09	-0.28	2	0.11
Oh	0.08	-0.34	2	0.08
Forest floor leachate	0.11	-1.38 [c]	4	0.17
European Beech				
BSi	0.10	-0.64	2	0.02
Oh	0.12	-0.68	3	0.04
Forest floor leachate	0.12	-2.05	1	0.12[b]

[a] n = measurement replicates

[b] $2\sigma_{SEM}$ = internal error of the measurement

[c] Repetitions on replicates with two different chemistries = -1.38±0.03‰ (δ^{30}Si ± $1\sigma_{SD}$)

In this latter tropical environment, clay minerals were thus ~2.0‰ more negative than the granitic parent material. This difference is larger than in our temperate ecosystem where the clay fraction displays a δ^{30}Si value 1.0‰ lighter than the granitic bedrock. This difference can be explained by a distinct clay mineralogy mainly composed of kaolinite in the tropical environment (Ziegler et al., 2005b) and of kaolinite and other clay minerals such as illite, vermiculite, and smectite in the present study. Indeed, the clay fraction in Puerto Rico derives from parental granite with a slightly different mineralogy (25% quartz, 56% plagioclase, 10% biotite; Ziegler et al., 2005b) than the granite at our site (34.5% quartz, 24% feldspars, 30.7% albite, 8.5% muscovite, 1.7% biotite and 0.6% chlorite; Ranger et al., 2004; Mareschal, 2008). High Ge/Si ratios in our clay fractions (6.2±0.08 µmol.mol^{-1}), close to that of kaolinite at Luquillo ranging between 4.8 and 6.1 µmol.mol^{-1} (Lugolobi et al., 2010), are due to incongruent weathering reactions leading to an enrichment of Ge in secondary clay minerals relative to primary minerals (Kurtz et al., 2002; Opfergelt et al., 2010).

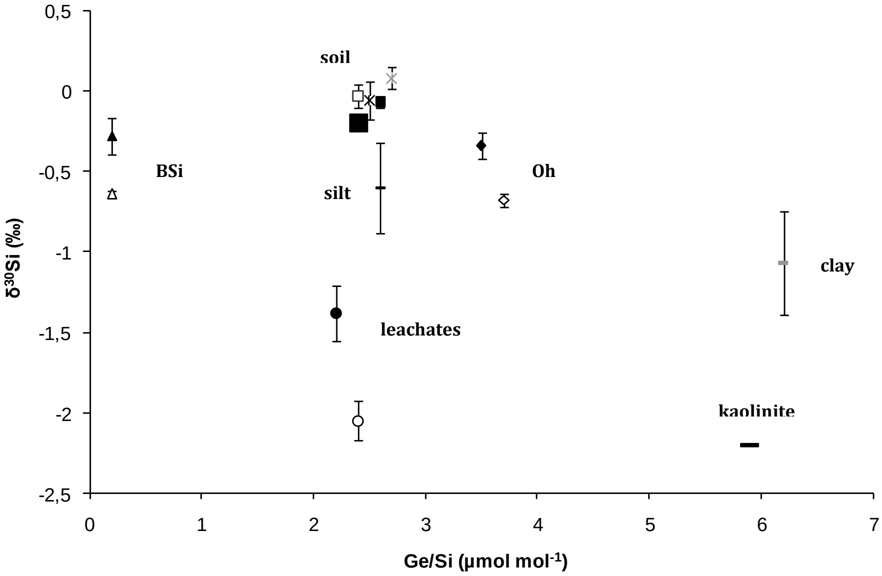

Figure 7.1 δ^{30}Si values plotted versus Ge/Si ratios in bedrock (black square) ; sand (open square), silt (black dash) and clay (grey dash) fractions, 0-7.5 cm bulk soil (black star) and 30-45 cm bulk soil (grey star) under European beech; BSi (triangles), humus layer (diamonds), and forest floor leachates (circles) under European beech (open) and Douglas fir (black). For comparison: Granite = large black square (δ ^{30}Si: Ziegler et al., 2005b; Ge/Si: Kurtz et al., 2002, Lugolobi et al. 2010), Kaolinite from granitic parent material = large black dash (δ ^{30}Si: Ziegler et al., 2005b; Ge/Si: Kurtz et al., 2002).

Si uptake by plants produces lighter δ^{30}Si values in BSi relative to source solution (Ding et al., 2005; Opfergelt et al, 2006a). In trees, the Si-isotopic signatures of BSi from Douglas fir (-0.28‰) and European beech (-0.64‰) are negative, a feature which has also been observed on Downy birch (-0.22‰) from boreal forest (Engström et al., 2008). Since the root biomass is mostly distributed between 0 and 70 cm depth (Ranger et al., 2004), the DSi source for tree uptake is not limited to the DSi from the forest floor leachates, reported to be isotopically lighter than BSi. Except for pine (1.5 µmol.mol^{-1}), leaves and needles display low Ge/Si ratios (0.1-0.3 µmol.mol^{-1}) as reported by Blecker et al. (2007) and Delvigne et al. (2009). The latter authors suggest that Ge is organically trapped in roots.

In our study, the humus layers (Oh) display high Ge/Si ratios. This enrichment in Ge suggests two different processes: (1) an accumulation of secondary clay minerals due to bioturbation (Chapter), and/or (2) the formation of organic complexes between Ge and carboxylic functional groups of the humic acids in the organic-rich horizons (Pokrovski et al., 2000). Considering δ^{30}Si values and Ge/Si ratios of all soil fractions and the proportion of Si in each fraction (sand, silt, clay and ASi fractions) in humus layer of the Douglas fir site, a bulk Si-isotopic and Ge/Si signature of humus layer (Oh) can be calculated by mass balance equation (Opfergelt et al., 2010) (Table 7.5). The calculated δ^{30}Si value of Douglas fir humus layer (-0.43±0.17‰) does not differ significantly from measured δ^{30}Si value (-0.34±0.08‰). This is confirmed by the Ge/Si mass balance: the calculated Ge/Si ratio of Douglas fir Oh (3.1 µmol.mol^{-1}) does not differ from measured Ge/Si (3.4 µmol.mol^{-1}). This suggests that all the Si pools have been identified and that the δ^{30}Si values and Ge/Si ratio in the Oh under Douglas fir are governed by the proportion of biogenic, primary and secondary clay minerals. A similar calculation can be done for the bulk soil at 0-7.5cm depth of the Douglas fir site. The calculated δ^{30}Si value (-0.32±0.17‰) is not significantly different from measured δ^{30}Si value (-0.06±0.12‰), which confirms that all Si pools have been identified. In addition, the calculated Ge/Si ratio (2.3 µmol.mol^{-1}) does not differ from measured Ge/Si (2.5 µmol.mol^{-1}) for the bulk soil at 0-7.5cm depth of the Douglas fir site.

In Chapter 4, we demonstrate that the content of litho/pedogenic minerals in the Oh is strongly influenced by bioturbation rates. Indeed, following bioturbation indexes, the incorporation of soil minerals into organic horizons is less important under Douglas fir and Norway spruce than under Black pine, European beech and oak. This was supported by lower concentration of SiO_2 inherited from soil minerals in Oh under Norway spruce (11.6%) and Douglas fir (20.4%), in comparison with Black pine (37.9%), European beech (39.3%) and oak (43.6%) (Chapter 4).

In the present study, Ge/Si ratios in Of are lower under Douglas fir and Norway spruce (2.0 and 1.4 µmol.mol^{-1}, respectively) than under Black pine, European beech and oak (3.4±0.06 µmol.mol^{-1}, n=3, $1\sigma_{SD}$). These results suggest that the incorporation of clay-sized minerals (characterized by relatively higher Ge/Si ratios) in organic horizons is more important under Black pine, European beech and oak than under Douglas fir and

Table 7.5 Si-isotopic and Ge/Si mass balance calculation to evaluate the bulk Si-isotopic and Ge/Si signatures of Oh and of bulk soil at 0-7.5cm depth under Douglas fir, from all the solid Si pools (% dry weight of humus and fraction < 2mm, respectively).

	Sand Fraction			Silt fraction			Clay fraction			ASi fraction						
	%[a]	SiO_2 %[b]	Proport[c]	%[a]	SiO_2 %[b]	Proport[c]	%[a]	SiO_2 %[b]	Proport[c]	%[a]	SiO_2 %[b]	Proport[c]	$\delta^{30}Si$ calculated[d]	$\delta^{30}Si$ measured	Ge/Si calculated	Ge/Si measured
Oh	14	80	0.54	17	77	0.60	2	47	0.04	0.4	98	0.02	-0.43 (0.17)	-0.34 (0.08)	3.1	3.4
0-7.5 (cm)	58	80	0.68	23	77	0.26	19	47	0.13	0.3	98	0.004	-0.32 (0.17)	-0.06 (0.12)	2.3	2.5

[a] Sand, silt, clay and ASi contents

[b] SiO_2 content in fractions

[c] SiO_2 proportion in sand, silt, clay and ASi fractions calculated as follows [(% fraction * SiO_2% in fraction) / SiO_2% in bulk] / 100. The SiO_2 concentration in bulk Oh and 0-7.5cm soil layer are respectively 21.2% and 68.4%

[d] The contribution of each fractions to the Si-isotopic and Ge/Si bulk soil signature can be calculated by multiplying the $\delta^{30}Si$ or Ge/Si signature of each fraction (from data in Tables 7.3 and 7.4) by the proportion of SiO_2 of each fraction ([c] in this table). The bulk soil signature represents the sum of the contribution of each fraction. The standard deviation ($\pm 1\sigma_{SD}$) is calculated by the method of the propagation of uncertainty.

Norway spruce, driving the lower Ge/Si ratio in the latter group. This is in good agreement with the findings of Cornelis et al. (2010) based on bioturbation.

7.4.2 δ^{30}Si and Ge/Si ratio variations in solutions

The δ^{30}Si values in forest floor leachates collected under Douglas fir and European beech (-1.38‰ and -2.05‰, respectively) are more negative than the isotopically lightest natural waters reported by Georg et al. (2009). The forest floor leachates are isotopically lighter than clay fraction (-1.07 ‰) and than BSi (ranging from -0.28 to -0.64 ‰). For all tree species, the forest floor leachate solutions display higher Ge/Si ratios than soil solutions (Table 7.3). These findings contrast with soil solutions from Hawaii shown to display heavier Si-isotopic signatures relatively to secondary precipitates preferentially incorporating light Si isotopes (Ziegler et al., 2005a).

Our soil solutions display similar Ge/Si ratios for all tree species (1.2±0.2 $\mu mol.mol^{-1}$) suggesting a pedogenic control on DSi (weathering of primary minerals, neoformation of secondary clay minerals and Si adsorption onto Al and Fe (hydr)oxides). Moreover, soil solutions have lower Ge/Si ratios than the bedrock revealing the impact of secondary clay minerals neoformation on the Ge depletion (Kurtz et al., 2002).

To further investigate the origin of these forest floor leachates signatures, the ion concentration of solutions (Table 7.2) was used to calculate the saturation index (PHREEQC Version 2; Parkhurst and Appelo, 1999) with respect to minerals incorporated in the organic horizons by bioturbation. Saturation index calculations show that forest floor leachates are undersaturated with respect to albite, anorthite, chlorites, illite, Ca-montmorillonite, K-feldspar, quartz and amorphous silica and are oversaturated with K-mica and kaolinite (Figure 7.2). Without considering the fact that organic acids promote dissolution of minerals, this simple mineral stability calculation show that clay minerals detected by XRD in the humus layer such as vermiculite, chlorite, illite, and Ca-montmorillonite (smectite) are not stable and could be partially dissolved and transformed in the chemical environment of forest floor. Thus, low pH (4.6±0.3) and high concentration of low molecular organic acids in the organic horizons (DOC = 43.1±18.1 $mg.l^{-1}$) relative to mineral soil (DOC = 2.9±0.7 $mg.l^{-1}$) make it very likely that clay minerals dissolve (Giesler et al., 2000). Indeed clay dissolution favored by the action of organic acids has already been recognized to explain high dissolved element contents in tropical organic-rich rivers (Gaillardet et al., 1995) or soil solutions (Oliva et al., 1999). Barman et al. (1992) also conclude that organic acids dissolve minerals through acid attack and complexation. In organic environment, the hydroxyl inter-layered 2:1 clay minerals lose their Al-interlayers and transform into vermiculite and smectite, which in turn weather, producing large amount of Mg in the solution (Brahy et al., 2000). This process is confirmed in our study by the identification of smectite in the clay fraction from the humus layer and the high content of Mg^{2+} in forest floor leachates relative to soil solution (Table 7.2), which support weathering of Mg-bearing phyllosilicates in humus layers.

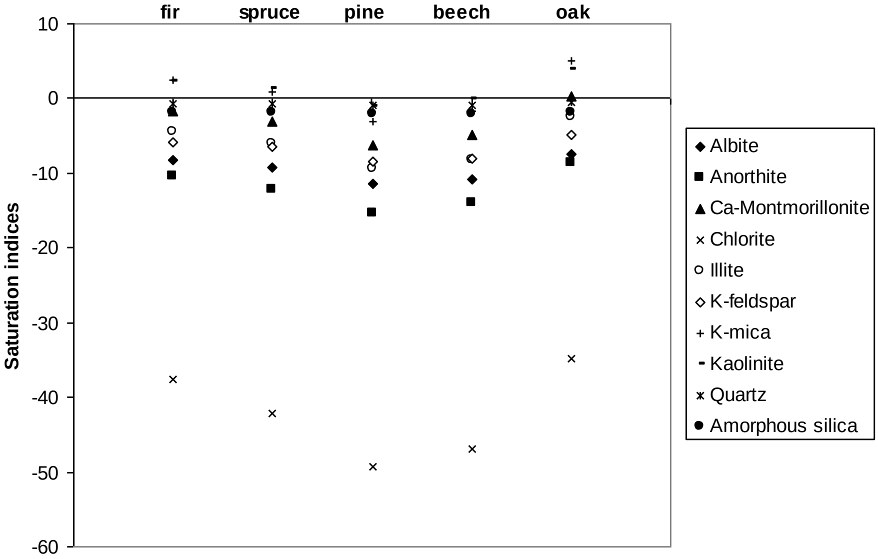

Figure 7.2 Calculated saturation indices (PHREEQC-2) in forest floor leachates for primary and secondary minerals incorporated in humus layer (Oh) by bioturbation under the five tree species: Douglas fir, Norway spruce, Black pine, European beech, and oak.

The δ^{30}Si and Ge/Si data presented above are useful to infer the relative roles of biogenic and inorganic minerals on the release of DSi in forest floor leachate solutions. Indeed, the Si-isotopic composition and Ge/Si ratios of forest floor leachates can be impacted by both biological processes (recycling of biogenic silica in the shallow soil) and by pedogenic processes (weathering of primary minerals and formation/dissolution of secondary clay minerals incorporated in organic horizons by bioturbation). The present study highlights that DSi is controlled by clay dissolution rather than BSi recycling, as supported by Si-isotopically light and Ge-enriched forest floor leachates. In this granitic environment, the stock of ASi, including BSi fraction, seems too low in comparison with the stock of crystallized minerals to significantly influence the DSi release in forest floor leachate and in soil solutions. The Si-isotopic signature and Ge/Si ratio of DSi in the forest floor leachates would represent a bulk signature of the dissolution of sand, silt, clay and ASi fractions (Opfergelt et al., 2010). In our case, the measured Si-isotopic signature of forest floor leachates (-1.38 ‰ and -2.05 ‰) cannot be explained by a congruent dissolution of primary and secondary minerals with an additional contribution from ASi, since the forest floor leachates are isotopically lighter than all components. Moreover, Ge/Si ratios of clay fractions are too high to explain the Ge/Si ratios in the forest floor leachates by congruent dissolution of clay minerals. The ^{28}Si enrichment in forest floor leachates could be explained by the preferential release of light Si isotopes during partial dissolution of clay minerals as seen for BSi (Demarest et al., 2009) and volcanic glass (Ziegler et al., 2005a). Dissolution of clay and silt admixed in the humus layer (Oh) would therefore also release Ge, which could be temporarily organically trapped with organic matter (Delvigne et al., 2009). A release of Ge from clay minerals and Ge-organically trapped could explain high Ge/Si ratio in forest floor leachates.

Based on (1) the contrast between Ge/Si ratios and Si-isotopic compositions, (2) the important pool of soil minerals in humus layer relative to the BSi pool, and (3) the chemical conditions in organic horizons, it seems reasonable to assume that the partial dissolution of clay minerals greatly influences the source of DSi in forest floor leachates.

These combined data suggest that the enrichment in ^{28}Si and Ge in forest floor leachates could be twofold. It could reflect a preferential release of a light Si isotopes and Ge during clay dissolution. Besides, Si adsorbed onto Fe-oxides (2.5% of the clay fraction; Mareschal, 2008) known to be enriched in light Si isotopes (Delstanche et al., 2009; Opfergelt et al., 2009) could be released by desorption. This could explain low δ^{30}Si values of DSi in forest floor leachates.

7.4.3 Implications on biogeochemical Si cycle in forest ecosystem

The Si isotope and Ge/Si signatures in forest soil solutions likely reflect a complex interaction of (i) primary, secondary and biogenic mineral dissolution and mineral transformation, (ii) uptake by forest vegetation, (iii) Si adsorption onto secondary phases, and (iv) Si export from the soil profile. Si isotope data and Ge/Si ratios in forest floor leachates are tree species-dependent mainly through various incorporation of soil minerals in organic horizons by bioturbation (Cornelis et al., 2010; Chapter 4) and only secondarily through the recycling of BSi on topsoil (Table 7.6; Chapter 6). Indeed, Ge/Si ratio in forest floor leachates can be related to Si recycling rate and bioturbation estimated under each tree species. The Ge/Si ratio in forest floor leachates decreases following the sequence Black pine ≥ oak > European beech > Douglas fir > Norway spruce (3.7, 3.7, 2.3, 2.1, 1.6 μmol.mol^{-1}, respectively; Table 7.3). This can be related to a higher bioturbation in Black pine, oak, European beech than in Douglas fir and Norway spruce (Cornelis et al., 2010; Chapter 4), claiming for a decreasing impact of clay dissolution on the DSi from Black pine to Norway spruce. In parallel, recycling of Si increases following the sequence Black pine < oak < European beech < Douglas fir < Norway spruce (2.3, 18.5, 23.3, 30.6, 43.5 kg ha^{-1} yr^{-1}, respectively; Table 7.6). This supports an increasing impact of BSi dissolution from Black pine to Norway spruce (since BSi is depleted in Ge) supporting the lower Ge/Si ratio in forest floor leachate under Norway spruce. δ^{30}Si values in forest floor leachates also support a larger influence of partial clay mineral dissolution in humus layer under European beech than under Douglas fir, as the lighter Si-isotopic signature is under European beech. Besides, even if the Si recycling suggests a higher impact of BSi dissolution under Douglas fir than under European beech, δ^{30}Si of BSi is lighter under European beech (-0.64‰) compared to Douglas fir (-0.28‰). Dissolution of BSi would therefore potentially provide a lighter Si source for DSi in forest floor leachate under European beech.

Table 7.6 Mean values of Si uptake and BSi restitution on topsoil through litterfall in five common tree species studied in same climatic and soil conditions (Cornelis et al., 2010; Chapter 4).

	Si (kg ha^{-1} yr^{-1})				
	Douglas fir	Norway spruce	Black pine	European beech	oak
Uptake	30.6	43.5	2.3	23.3	18.5
Litterfall	29.0	42.2	2.1	19.3	17.8

7.5 Conclusions

This study traced the sources and mechanisms controlling the release of DSi in forest floor leachates and soil solutions using stable Si isotopes and the Ge/Si ratio in well defined soil-tree systems in a temperate granitic environment.

Our results show that Si-isotopic signatures and Ge/Si ratios of forest floor leachates evolve towards lighter δ^{30}Si values (-1.38 and -2.05‰) and higher Ge/Si ratios (2.7±1.0 µmol.mol^{-1}, n=5, 1σ_{SD}), relative to granite bedrock. Sources of dissolved Si in forest floor leachates are influenced by tree species, which determine the extent of mixing of clay minerals in organic horizons by bioturbation while the source of DSi in soil solution is essentially impacted by pedogenic processes. This suggests a difference in the soil mineral weathering regime relative to depth and soil chemistry conditions: more secondary mineral weathering in organic horizons and greater stability of secondary minerals in deeper soil layers.

Although tree species take up to 43.5 kg Si ha^{-1} yr^{-1}, which constitutes a large amount of BSi restituted on topsoil (Cornelis et al., 2010; Chapter 4), dissolution of phytoliths does not seem to mainly influence the DSi composition of the forest floor leachates, even given the high reported dissolution rates for phytoliths (Fraysse et al., 2009). Indeed, the ASi stock, including BSi, in organic horizon is low relative to crystallized Si stock. Our results are consistent with the observations in a tropical granitic catchment (Ziegler et al., 2005b; Lugolobi et al., 2010), but stand in marked contrast either the results of Derry et al. (2005) showing a strong biological control on Si cycling and export in basaltic soils with very low availability of mineral-derived Si.

In order to better assess the relative contributions from biogenic and litho/pedogenic sources to soil solutions, it would be interesting to study the seasonal variations of Si-isotopic signature and Ge/Si ratios in forest floor leachates and soil solutions.

CHAPTER 8:

THE ORIGIN OF DISSOLVED SILICON TRANSFERRED FROM VARIOUS SOIL-PLANT SYSTEMS TOWARDS HYDROSPHERE: PERSPECTIVES*

---

* Adapted from Cornelis JT., Delvaux B., Georg B., Lucas Y., Ranger J., Opfergelt S. Origin of dissolved silicon transferred from various soil-plant systems towards rivers: a review. In preparation to be submitted to *Biogeosciences*.

8.1 Introduction

The silicon (Si) occurs in almost all minerals in the earth surface ranging from values less than 0.5 wt% to almost 47 wt% in the pedosphere (McKeague and Cline, 1963a). As the ultimate source, chemical weathering of silicate minerals liberates dissolved Si (DSi), as monosilicic acid ($H_4SiO_4^0$), which participates in soil formation through biogeochemical reactions on continents - neoformation of secondary minerals (Drees et al., 1989; Wada, 1989; White, 1995), adsorption onto Fe and Al (hydr)oxides (Jones and Handreck, 1963; McKeague and Cline, 1963b) as well as uptake by plants and return of biogenic silica (BSi) on topsoil (Jones and Handreck, 1965) - and is carried from the lithosphere to the hydrosphere (Drever, 1988; Conley, 2002; Sommer et al., 2006; Conley et al., 2006). Over geological time (>10^6 years), weathering of silicate minerals plays an integral role in both the DSi feeding of the oceans and soil development promoting the decreasing of atmospheric CO_2 by consumption of protons from carbonic acid (Chadwick et al., 1994; White and Blum, 1995; Berrner, 1997; Rai and Kittrick, 1989)

The global Si cycle is clearly influenced by the vegetation type (Bartoli, 1983; Alexandre et al., 1997; Blecker et al., 2006; Cornelis et al., 2010; Chapter 4), stage of soil development (Henriet et al., 2008a,b), climate characterized by specifics moisture and temperature (Raven, 1983; White and Blum, 1995), anthropogenic actions (Conley et al., 1993,2002) and orogenesis at the geological timescale (Raymo et al., 1988; Exley, 1998).

Despite Si has (i) a quantitatively important pool in soil, (ii) a vital effect on plant productivity through the physical support and the soil fertility, (iii) a fundamental link with C cycle, and (iv) a beneficial effect for terrestrial plants growing under stress conditions, the role of the type of natural environment on the biogeochemical Si cycle and its strategic importance in the transfer of Si towards the hydrosphere are poorly studied. Sommer et al. (2006) summarize the existing knowledge on Si pools in soils and fluxes into and out of terrestrial biogeosphere. Conley (2002) clearly demonstrates that biological processes in terrestrial ecosystems play an important role in global Si mass balances. However, the impact of contrasting soil-plant systems on the origin of DSi transferred towards the hydrosphere is not integrated and reviewed. The quotation from Trudgill (1983): "*System thinking is a body of ideas concerned with the state of matter and the factors that influence that state*" supports some major challenges for the future: (i) to assess processes governing the transfer of elements from soil-plant system towards rivers, and (ii) more particularly, to compare various soil-plant environments and their impact on the origin of DSi outputs from soils.

Although the drivers of DSi fluxes from land to oceans are identified (Sommer et al., 2006; Chapter 2), the relative proportions of the two different Si pools (biogenic and litho/pedogenic) is still poorly constrained.

8.2 Impact of various soil-plant systems on the origin of dissolved Si transferred towards the hydrosphere

A large variety of Si compounds exists in bio-geosphere (Figure 2.1), and the origin of DSi in soil solution feeding the rivers can be attributed to two main pools: the litho/pedogenic and biogenic Si pools. The litho/pedogenic Si-source represents the primary minerals and the secondary minerals formed by authigenic geochemical precipitation. The biogenic Si-source is mainly constituted by BSi biomineralized as phytoliths.

The impact of environmental factors on the relative contribution of litho/pedogenic and biogenic Si-sources to the DSi export will be deeply influenced by the type of ecosystem and its geographical situation.

Since Si is a ubiquitous element in the biogeosphere, tracing the origin of the DSi output from a soil-plant system requests using (1) Si mass-balance (Bartoli, 1983; Alexandre et al., 1997; Farmer et al., 2005; Gérard et al., 2008; Cornelis et al., 2010; Chapter 4) and (2) geochemical tracers such as Ge/Si ratios (Derry et al., 2005) or stable Si isotopes (Ding et al., 2004; Ziegler et al., 2005a; Georg et al., 2006,2007,2009; Opfergelt et al., 2009, Cornelis et al., in press; Chapter 7).

Through the calculation of Si uptake, Si restitution, Si drainage (Table 1.1; Chapter 4), atmospheric Si inputs and phytolith preservation in soils, a Si mass-balance in specific ecosystems allow to estimate the Si release by primary silicate weathering and by phytolith dissolution, respectively. However, these approximations ignore other important Si sinks in the soil-plant system such as HAS and short-range ordered aluminosilicates formation, neoformation of secondary clay minerals, opaline spheres precipitation and Si adsorption onto Fe and Al (hydr)oxides. Thus, we suggest that Si mass-balance study should be combined with geochemical tracers to make better assumptions about the Si origin in the aqueous phase of well-defined soil-plant systems.

Germanium (Ge) is a trace element with very similar geochemical properties than Si, which substitutes for Si in aluminosilicates mineral lattices. Studying Ge/Si fractionation allows for tracing the weathering of Si-containing phases and the dynamics of DSi produced in soil-plant systems (Kurtz et al., 2002; Derry et al., 2005; Scribner et al., 2006). Secondary clay minerals and biogenic opal display contrasting Ge/Si ratios since clay-sized weathering products are enriched in Ge (Murnane and Stallard, 1990; Kurtz et al., 2002; Kurtz and Derry, 2004; Delvigne et al., 2009; Lugolobi et al. 2010; Cornelis et al., in press; Chapter 7) and biogenic silica (BSi) polymerized in plants as phytoliths is depleted in Ge (Derry et al., 2005; Blecker et al., 2007; Delvigne et al., 2009; Cornelis et al., in press; Chapter 7). The current interpretation of Ge/Si ratio of soil solutions relies on the relative importance of a low-Ge end member derived from incongruent dissolution of fresh rock minerals and biomineralization and a high-Ge end member produced by congruent dissolution of pedogenic minerals (Kurtz et al., 2002).

The stable Si isotopes holds a great potential to assess the relative contribution of Si released from lithogenic and/or biogenic Si pool in the soil solution (Ziegler et al., 2005a; Engström et al., 2008; Georg et al., 2009a; Cornelis et al., in press; Chapter 7). The Si isotopic signature is expressed as δ^{30}Si (‰) as defined in Chapter 7.

The neoformation of secondary precipitates such as clay minerals (Ziegler et al., 2005a,b; Opfergelt at al., 2008,2010; Bern et al., 2010), the plant Si uptake producing biogenic opal (Douthitt, 1982; Ziegler et al., 2005a; Ding et al., 2005,2008; Opfergelt et al., 2006a,b,2008), and the adsorption of Si onto Fe-oxides (Delstanche et al., 2009; Opfergelt et al., 2009) are three processes favouring the incorporation of light Si isotopes, contributing to enrich rivers in heavy Si isotopes (De La Rocha et al., 2000; Ding et al., 2004; Georg et al., 2006,2007). Understanding the contribution of those three processes on DSi output can hardly be done with δ^{30}Si systematics alone. Comparing Ge/Si ratios with Si isotope data (Delvigne et al., 2009; Opfergelt et al., 2010; Lugolobi et al., 2010; Cornelis et al., in press; Chapter 7) may provide a better understanding of the origin of DSi exported from various soil-plant systems towards rivers.

In this regard, the origin of the output of DSi from various soil-plant systems towards rivers will be assessed trough two controlling factors: (i) the weathering ability of the system, and (ii) the impact of vegetation on weathering. The sources of DSi fluxes including litho/pedogenic Si components and/or biogenic Si components can thus be classified more systematically (Figure 8.1). In this classification, it is assumed that some tropical regions still have significant amounts of weatherable minerals available (*Scenario 1*). For *Scenario 2* we assume that many tropical systems have old and highly weathered soils, in which reservoirs of primary minerals are exhausted. In non-tropical regions, the climate is relatively less favorable to silicate weathering while the stock of mineral-derived Si is usually higher than in tropical environments (*Scenario 3*), except for arid climates (*Scenario 4*) where the environmental conditions do not favour silicate weathering, and where no Si soil-plant cycling takes place.

8.2.1 Scenario 1: tropical region with weatherable reserve

In a system with unlimited weathering ability, the release of DSi from land mass to oceans is largely driven by climatic conditions such as temperature and runoff promoting silicate weathering and transport (Gaillardet et al., 1999a; Jennerjahn et al., 2006). However, two recent studies demonstrate the impact of BSi recycling and restitution on topsoil on the mobility of DSi from continents to rivers. The Luquillo stream from a granitic mountains characterized by the fastest measured rates of granitoid weathering (Puerto Rico) is dominated by Si derived from incongruent mineral weathering at the bedrock-saprolite interface as revealed by the positive δ^{30}Si values of soil solution (Ziegler et al., 2005b). The δ^{30}Si signature (-1.5‰) of the pore-water in the top 0.3 m of soil is lighter suggesting the recycling and dissolution of BSi enriched in ^{28}Si. Lugolobi et al. (2010) study the Ge/Si fractionation in the same site and also conclude that biological subcycle should influence Si cycling but does not dominate as in Hawaii (see *Scenario 2*, Derry et al., 2005). In addition, Ding et al. (2004) suggest that growth of rice and grasses have a significant impact on the concentration and Si isotope composition (+0.7 to +3.4‰) of DSi in Yangtze River in China. Indeed, the total DSi taken up by Si-accumulator plants such as rice in the Yangtze River basin is almost 5 times more than the DSi carried out by the Yangtze River to ocean (Ding et al., 2008).

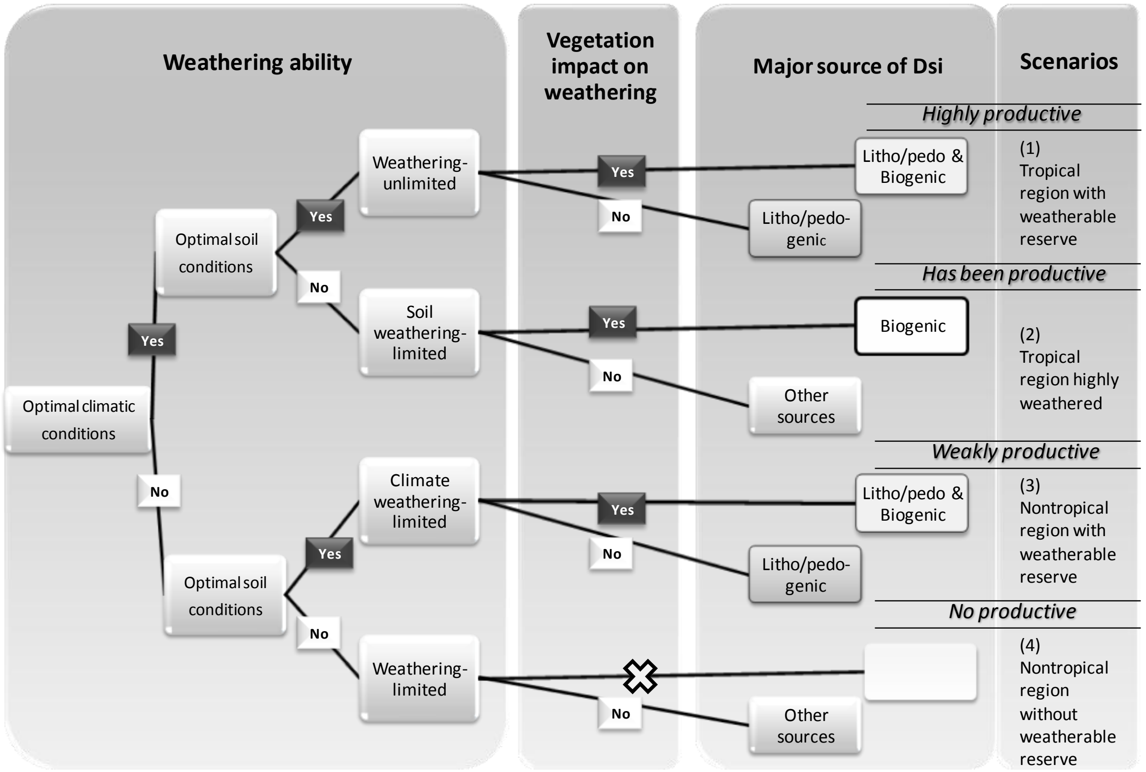

Figure 8.1 Schematic representation of the weathering ability of a system (the ability to release Si from solid phase to aqueous phase) as a function of the climate (runoff and temperature) and soil (presence of weatherable minerals) conditions. The impact of vegetation is included in four scenarios in accordance with the major sources of DSi.

On another hand, the DSi fluxes into the Bay of Bengal equates to approximately 3.5% of the global DSi flux into the oceans where the Si isotope compositions of groundwater varies between +1.3 and -0.2‰ (Georg et al., 2009b) reflecting the change from primary to secondary Si sources, mainly clay minerals and silcretes (Basile-Doelsch et al., 2005; Ziegler et al., 2005a; Georg et al., 2009a).

The relative contribution of weathering and BSi cycling in weathering-unlimited systems is still poorly quantified. Under these conditions, besides the high Si stock of the mineral soils, a high biomass production and turnover should create a relatively large pool of reactive BSi that potentially controls the DSi in shallow soils. This could be redistributed in various Si sinks in the soil profile or exported to stream water.

8.2.2 Scenario 2: tropical region highly weathered

In humid tropical environment, the vegetation will increase the chemical weathering rate without increasing the Si removal from the profile towards regional drainage as a result of the transport limited landscape. Alexandre et al. (1997) illustrate through its model that the Si release from phytolith dissolution is twice that of Si release due to silicate weathering. Indeed ecosystems exhibiting strong depletion of mineral-derived Si and high Si uptake rates by biomass should have strong biological control on Si cycling and export. In highly weathered soils, with optimal climatic conditions, a large fraction of silicic acid is cycling through plants before it is transferred to rivers (Lucas et al., 1993). This implies that the composition of stream water is not controlled by the geochemical processes of the lower soil profile, but rather by the biogeochemical cycling within the plant/surface-soil component of the ecosystem (Markewitz et al., 2001).

Indeed, in a tropical rainforest overlying deeply weathered Hawaiian basalt, Derry et al. (2005) established that the Ge/Si ratios of stream waters can be controlled by (i) a Si-rich component with a relatively low Ge/Si ratio (Ge/Si $\sim 0.25*10^{-6}$) derived from dissolution of BSi in upper soil horizons, and (ii) a Si-poor component with a relatively high Ge/Si ratio (Ge/Si $\sim 2.6*10^{-6}$), originating from dissolution of secondary pedogenic minerals. Therefore on a discharge-weighted basis, they found that BSi contributes to 68–90% of the DSi transported by Hawaiian stream water.

The fact the solubility of bamboo phytoliths is 17 times greater than quartz (Fraysse et al., 2006) supports recent studies suggesting that the clay mineral stability or formation in the upper soil horizons (Lucas et al., 1993; Lucas, 2001; Kleber et al., 2007; Opfergelt et al., 2010) are controlled by phytolith production and recycling rather than by dissolution of quartz or other crystalline mineral phases (Barré et al., 2009).

In environment with very low availability of mineral-derived Si and with significant Si biocycling, we could consider that the DSi fluxes will be deeply influenced by the existing BSi pool. Therefore, DSi fluxes in highly weathered systems without BSi recycling will be insignificant compared to the highly weathered systems biologically active.

8.2.3 Scenario 3: non-tropical region with weatherable reserve

In this climate weathering-limited environment, DSi fluxes from soil-plant systems towards rivers would be impacted by both litho/pedogenic Si pool and biogenic Si pool. It appears that basin lithology and runoff alone are not very reliable indicators of DSi flux in vegetated watersheds where the influence of terrestrial vegetation appears to be important (Fulweiler and Nixon, 2005), promoting silicate weathering and BSi restitution on topsoil. Indeed, the presence of coniferous forest with high productivity and significant concentration of Si in needles can largely contribute to the terrestrial biogeochemical Si cycle even in temperate climate (Gérard et al., 2008).

In a forest site in France, Bartoli (1983) has estimated that 80% of DSi exported from the soil profile derives from the BSi pool in deciduous stands against 20% in coniferous ones arguing for a substantial impact of Si biocycling on the DSi-sources. Moreover, in central Siberia, besides bedrocks and soil minerals, the main sources of DSi from basalt under permafrost conditions can be the litterfall (3.4 kg Si ha^{-1} yr^{-1}) and dissolution of phytoliths (Pokrovsky et al., 2005). Similarly, some fraction of the DSi exported from a deforested temperate ecosystem derive from the dissolution of a biologically derived pool of ASi (phytoliths), which prove the impact of the Si biocycling in this environment (Conley et al., 2008). In a Bohemian forest, the higher leaching of DSi in five glacial lakes despite lower atmospheric deposition of acids could be explained by the decline of Al activity increasing silicate weathering but also by BSi dissolution (Vesely et al., 2005). In the wet climate of the Buenos Aires province, ASi from volcanic or biogenic origin is likely responsible for the high concentration of DSi (1 mM) in the shallow groundwater (Miretzky et al., 2001). Moreover, it has been shown that rivers draining areas with carbonate rocks have surprisingly higher DSi fluxes than silicate rocks, which could be attributed to rapid dissolution of disseminated or interbedded BSi of the carbonate rocks (Bluth and Kump, 2004). Finally, Si biocycling is comparable between forests and grasslands on a watershed scale (Blecker et al., 2006). Since grasslands cover about 40% of terrestrial Earth (White et al., 2000) they likely play an important role in terrestrial Si fluxes, therefore providing interesting ecosystems to use geochemical tracers (Blecker et al., 2007).

For this purpose, the DSi enrichments from the boreal forest areas is associated with an elevated relative concentration of ^{28}Si, suggesting release of isotopically-light plant derived Si mainly during the spring snowmelt. Thus it can be hypothesized that a large fraction of DSi input to the Baltic Sea has a biogenic origin (Engström et al., 2010). On another hand, the lower δ^{30}Si values of dissolved phase for Swiss rivers in high mountain area (+0.84‰, Georg et al., 2006) and for the Iceland Rivers in high latitude area (+0.63‰, Georg et al., 2007) reveal their lower biological Si cycling compared to Asian Yangtze River (+2.13‰, Ding et al., 2004) where the preferential uptake of light Si isotopes by rice plant leads to a progressive enrichment of aqueous phase in heavy Si isotopes. Conversely, in the Yellow River in China, the average δ^{30}Si value of DSi is +1.7‰ (Gao et al., 2006) and suggests the impact of the colder weather and lower precipitation in this agriculture area on the decreasing biochemical activity (Ding et al., 2008). However, in these systems, the role of secondary clay minerals formation/dissolution on the DSi isotope compositions is not clearly determined. Indeed, the Si isotope data combined with the water chemistry of Iceland Rivers show that an average of 50% of the primary weathered Si is precipitated into secondary weathering products within the watersheds (Georg et al., 2007). In this climate weathering-limited environment, the DSi load to rivers seems mainly governed by the litho/pedogenic processes such as silicate weathering and clay minerals neoformation. Moreover, in a temperate granitic forest system, the δ^{30}Si values of DSi in surface soil solution (relatively rich in phytoliths) are the most negative never found in natural aqueous system (-1.38 and -2.05 ‰). The Ge/Si ratios in this surface soil solution are higher than in deeper soil solutions. These findings suggest that forest floor leachate solutions are deeply influenced by the dissolution of ^{28}Si and Ge-enriched secondary clays minerals incorporated by bioturbation in organic-rich horizons, preferentially releasing light Si isotopes (Cornelis et al., in press; Chapter 7). Similarly, in the Navado Sandstone aquifer (Arizona, USA), the negative δ^{30}Si values (-1.42 ‰) could also be due to dissolution of both secondary clay minerals and low-temperature silcretes (Georg et al., 2009). In addition, DSi fluxes in Boreal and Artic rivers seem to be influenced by vegetation only through promoting silicate weathering (Humborg et al., 2006). Indeed, besides the impact of Si recycling and restitution of reactive BSi in topsoil, the Si fluxes exported from vegetated areas seem higher than those measured in bare areas (Moulton et al., 2000).

8.2.4 Scenario 4: non-tropical region without weatherable reserve

In African, Arabian, Asian and Australian deserts, Si can be transported through the atmosphere associated with airborne particles that should be the only form of Si exports from these arid environments (Tegen et al., 2002,2006). However, since the transport of soil-derived dust in the atmosphere is an effective means of redistributing Si in the environment, further studies should focus on their signatures (Ge/Si ratios and δ^{30}Si) in order to assess their impact on the DSi fluxes following dissolution.

8.3 Conclusions

The origin of DSi exported from a soil-plant system is a dynamic balance between the release of DSi from phytoliths (biogenic origin) and from primary and secondary minerals (litho/pedogenic origin). In tropical environments (*Scenarios 1* and *2*), DSi fluxes towards rivers are higher compared with climate weathering-limited environments (*Scenarios 3* and *4*). On another hand, the very low DSi concentration in soil solution of a soil weathering-limited system (*Scenarios 2* and *4*) is responsible of the low DSi output. Thus, the major load of DSi towards rivers is from weathering-unlimited system (*Scenario 1*) where the origin of the Si-sources (litho/pedo or biogenic) needs to be elucidated to better understand the global export of DSi from continents to oceans, and the impact on the global CO_2 consumption rates through silicate weathering.

In the future, more attention should be given to these systems with high ability to weathering and transport, since the recent studies were focused on the biological control on Si cycling and export in highly weathered tropical systems with low availability of mineral-derived Si (Lucas et al., 1993; Alexandre et al., 1997; Derry et al., 2005).

Promising and well-recognized geochemical tracers (Ge/Si ratios and δ^{30}Si) as well as Si mass-balance calculations at watershed scale should be implemented in tropical systems in Asia and Oceania displaying the highest DSi fluxes because of their reactive geology, high runoff and high silicate weathering rates. Further studies in mountains areas of high relief would also improve our knowledge about the global impact of the Si-sources on the DSi fluxes towards rivers.

Finally, tracing mechanisms which control the release of DSi in soil solution in climate weathering-limited environment is of great concern as global warming is believed to be mainly pronounced at high latitudes. It is conceivable that large-scale global change processes will affect global Si cycle as a result of temperature and precipitation perturbations. For example, the enrichment of “greenhouse” gases in the atmosphere has led to an increase in the average global surface temperature of 0.6°C since the late 19th century (IPCC, 2001), and recent studies show that worldwide fresh water runoff from the continent to the ocean increases through the 20th century because plant transpiration decreases with the elevated atmospheric CO_2 (Gedney et al., 2006; Matthews, 2006). As a consequence, since DSi fluxes from continents to oceans are correlated with runoff, temperature and vegetation, we can assume that a change in a climatic variable could disrupt quite rapidly the biogeochemistry of the hydrosphere. The geochemical tracers will help us quantifying these anthropogenic and natural variations that should be incorporated in forecasting models (Garnier et al., 2006; Bernard et al., 2009) predicting DSi loads in rivers.

CHAPTER 9:

CONCLUSIONS AND PERSPECTIVES

In our research on Si cycle in temperate forest ecosystems, we investigated (i) the tree species impact on Si recycling by forest vegetation, (ii) the Si biocycling impact on amorphous silica distribution in forest soil and dissolved Si leached out from soil profile, and (iii) the mechanisms involved in the release of dissolved Si in forest soil solutions. The methods and experimental works allow us to draw the following conclusions about our working hypotheses.

9.1 The Si dynamics in the soil-tree system according to forest tree species

The forest site shows similar acid-brown soils, climatic conditions and parental material but differ in the planted tree species: Douglas fir, Norway spruce, Black pine, European beech and oak. These experimental conditions allow us to isolate tree species impact on the biogeochemical Si cycle. Like other chemical elements such as K, Ca and Mg without a prominent gaseous phase at normal biologic temperature (Likens and Bormann, 1995), Si is crucial to trace the biogeochemical cycles at Earth's surface environment.

In temperate forest ecosystem on a granitic parental material, trees took up a substantial amount of H_4SiO_4 from soil solution, which polymerizes in leaves as amorphous silica (phytoliths). Forest tree species were clearly characterized by contrasting Si uptake, which decreased as the following sequence: Norway spruce (43.5 kg ha^{-1} yr^{-1}) > Douglas fir (30.6 kg ha^{-1} yr^{-1}) > European beech (23.3 kg ha^{-1} yr^{-1}) > oak (18.5 kg ha^{-1} yr^{-1}) >>> Black pine (2.3 kg ha^{-1} yr^{-1}). These contrasting Si uptake rates are due, in part, to different transpiration rates since Si uptake by forest trees is mostly driven by mass-flow of water, as often reported for different plant species and confirmed in our hydroponics experiment. The Si is largely mobile in the soil-tree cycle through litterfall since Si is mainly accumulated in leaves. This results in tree species impact on (i) phytoliths restitution rates on topsoil and (ii) biogenic silica (BSi) pool in organic-rich horizons.

Besides the biological control, the Si content in humus layer (Oh) was mostly influenced by bioturbation, which mixes up silicate minerals from mineral horizons beneath through the action of living organisms. In humus layer, the relative proportion of BSi on the total Si concentration ranged from 1 to 7% depending on tree species. We identified the following minerals in the clay fraction extracted from humus layer under European beech and Douglas fir: quartz, kaolinite, illite, illite-vermiculite mixed layers, smectite and chlorite. Moreover, bioturbation indexes showed that the incorporation of soil minerals into organic horizons is clearly dependent on tree species likely due to contrasted effects on soil biological activity. The bioturbation was less important under Douglas fir and Norway spruce than under Black pine, European beech and oak. This finding confirms the significantly higher Si concentrations inherited from soil minerals in humus layer under Black pine, European beech and oak. Thus, the weathering of silicate minerals incorporated in the forest floor acidic environment should not be neglected. Figure 9.1 summarizes the different tree species impact on the Si concentration in organic-rich horizons.

In mineral soil layers, the relative proportion of ASi (BSi plus the other amorphous silica forms) on the total Si concentration varied between 0.5 and 5% relative to tree species. In this Si-rich soil environment, pedogenic processes could hide tree species impact on ASi concentration in soil. Three major processes were identified to control the ASi concentration in temperate forest soil: biogenic opal translocation, pedogenic formation of opaline spheres and ASi adsorption onto Fe oxides. Using transmission electron microscopy withenergy-dispersive analysis, we proved the presence of opaline spheres in shallow soil although forest floor solutions in our experimental site are not supersaturated with respect to amorphous silica. Such contradiction might be explained by Si saturation in soil microsites or during short periods. Moreover, given the absence of imogolite type material and other allophane compounds, we quantified the (i) ASi adsorbed onto poorly crystallized Fe oxides through oxalate extraction and (ii) the total ASi concentration through Na_2CO_3 extraction. We demonstrated that the increase of ASi concentration in soil is in agreement with the increase of reactive Fe oxides between 7.5 and 45 cm depth. The ASi content adsorbed onto Fe oxides represented 12-26% of total ASi concentration in mineral soil, while the ASi adsorbed onto Fe oxides in humus and 0-7.5 cm layers only represented 1-2 % of total ASi concentration. In the shallow soil we proved that the ASi fraction mainly consists of BSi from tree and understory vegetation as revealed by SEM analysis and by the low concentration of Si extracted by oxalate digestion. Given the high stock of Si-containing crystallized minerals in temperate-granitic environment, biogenic opal-A seems a minor pool, which could be however crucial since it is a ubiquitous soil reactive pool.

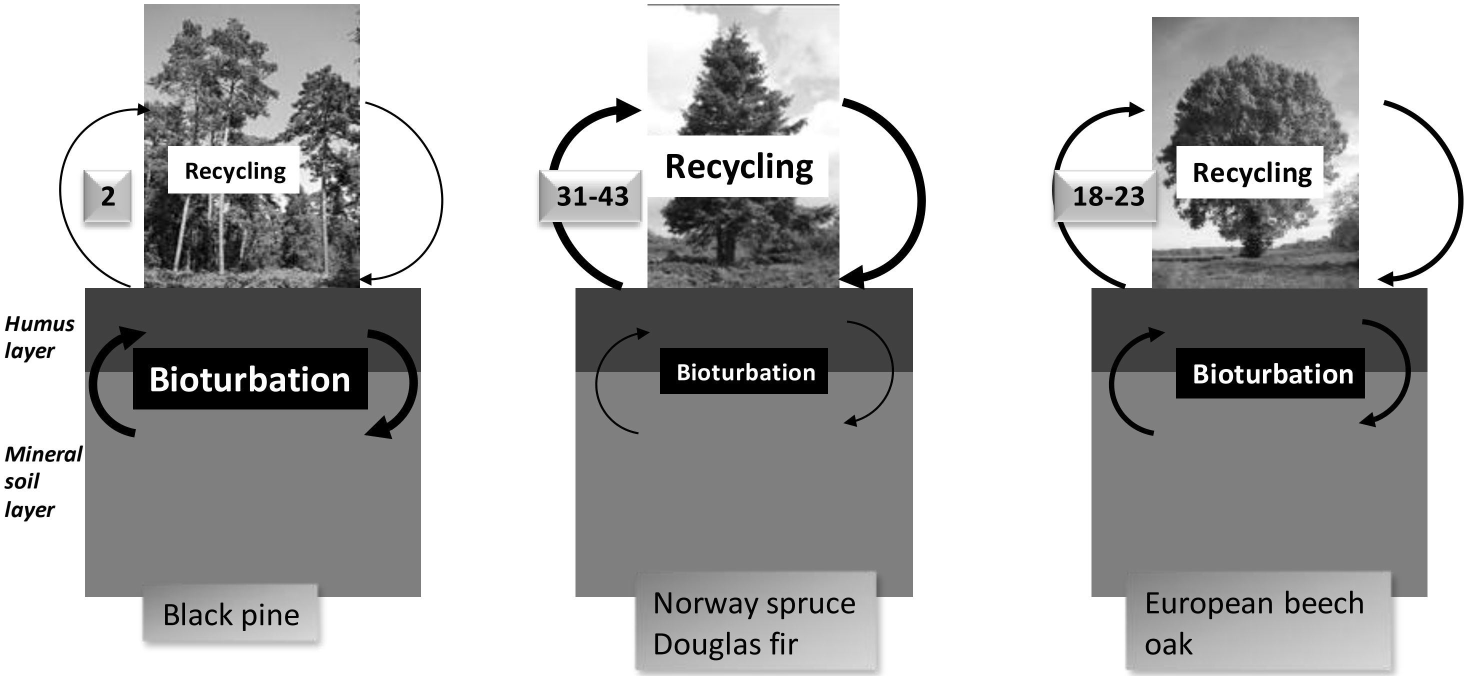

Figure 9.1 Schematic representation of the impact of Si recycling and bioturbation according to tree species. More arrows are thicker, more recycling or bioturabation rates are high. Numbers labeling the recycling arrows show the Si uptake by forest trees (kg Si ha^{-1} yr^{-1}) (Chapter 4).

Based on these findings, we can assume that DSi concentrations in forest floor leachate and soil solutions result from a dynamic and complex balance between (i) dissolution processes involving silicate minerals as well as BSi particles returned on topsoil, and (ii) neoformation of secondary precipitates (mainly phyllosilicates), adsorption of Si onto Fe oxides, tree uptake producing BSi as well as DSi leaching from the soil profile.

9.2 The dissolved Si output in contrasting Si biocycling systems.

The DSi concentration in forest soil solutions is influenced by silicate weathering rates, which are clearly tree species-dependent (Moulton et al., 2000; Johnson-Maynard et al., 2005). In addition, in our PhD we showed that tree species can also strongly impact the Si dynamic in soil-tree cycle through contrasting Si uptake by forest vegetation. Indeed, tree species can affect the DSi transfer from land towards rivers since DSi leaching from the soil profile is negatively correlated to the Si uptake by forest vegetation. Except for Black pine, Si uptake and restitution are largely significant in comparison with the annual DSi leaching (Figure 9.2). In Black pine site, the DSi output exceeds the Si uptake because DSi released by mineral dissolution does not readily contribute to the BSi pool of the vegetation. The Si recycling by forest trees is a major mechanism of Si conservation in the soil-tree system during the growing season. Thus, when tree uptake decreases during winter, DSi is much more leached from soil profile (Gérard et al., 2002; Farmer et al., 2005). Besides the biological processes, the land-rivers fluxes of DSi are also influenced by pedogenic processes.

On the one hand, the decrease of DSi concentration beneath 15 cm depth in each forest sites could reflect the combined effect of root uptake and pedogenic processes acting as Si-sink in soils such as secondary precipitates (phyllosilicates, hydroxyaluminosilicates, opaline spheres) and Si adsorption onto secondary phases (mainly Fe oxides). On the other hand the increase of DSi concentration in soil solution between the humus layer and 15 cm soil depth results from a combined effect of the increase of mineral weathering driven by organic ligands and dissolution of the highly soluble BSi pool.

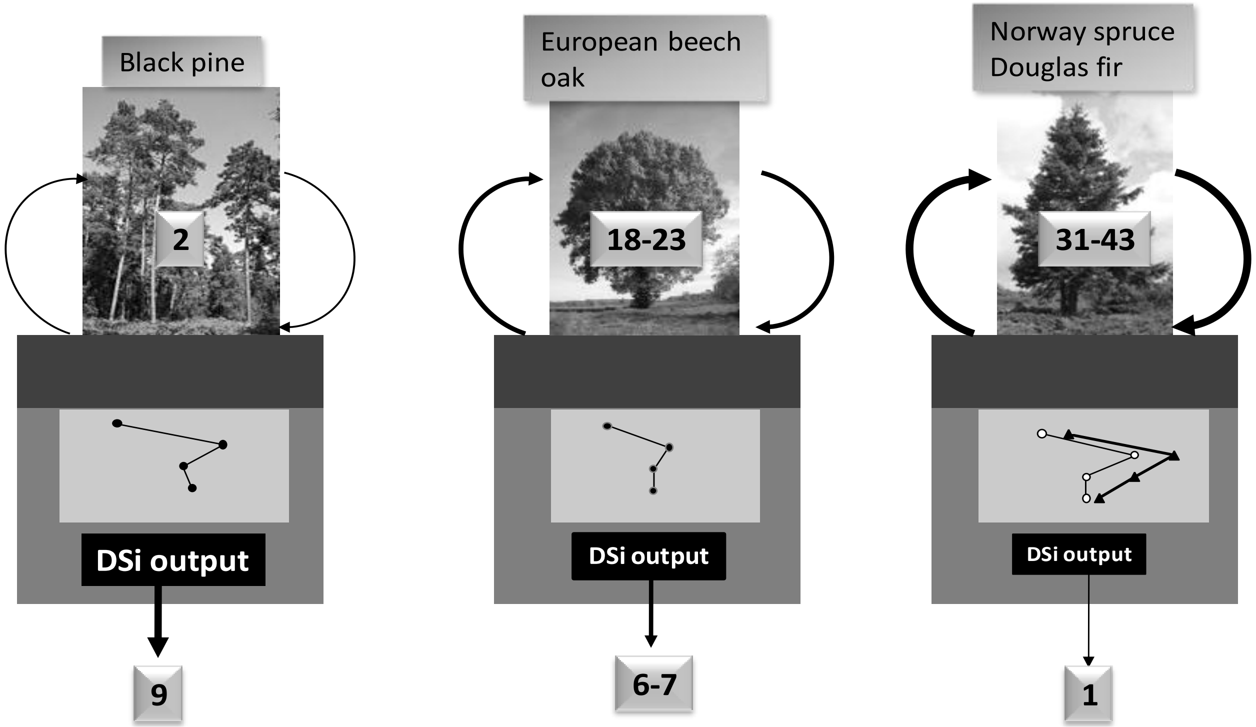

Figure 9.2 Relation between Si uptake and DSi leached from the soil profile according to tree species. Numbers labeling arrows show the Si uptake by forest trees and DSi output (kg Si ha^{-1} yr^{-1}). Graphs inserted in soil represent the mean Si concentrations in soil solutions relative to soil depth (for more details, see Figure 3.5, 3.6 and 3.7).

The quantification of the biological control on the DSi leached out from soil-plant system towards rivers is of great interest as the net DSi inputs in oceans is strongly impacted by the land-rivers fluxes. The ecosystems exhibiting strong Si depletion in soils and high Si uptake rates by biomass have strong biological control on Si cycling and export. It is likely that the mechanisms controlling DSi in forest soil in a temperate-granitic ecosystem would differ. However, based on the findings about Si dynamics in soil-tree system, we cannot provide direct evidence about the relative contribution of litho/pedogenic minerals and biogenic opal to the DSi released in forest soil solutions, hence the usefulness of geochemical tracers.

9.3 The mechanisms controlling the release of DSi in aqueous phase.

The Si isotopic and Ge/Si fractionations in the soil-plant system are due to soil-solution interactions (dissolution of solid phases, neoformation of secondary phases and adsorption onto secondary phases) and biogenic processes (Si uptake by plants and transport within the plant) (Kurtz et al., 2002; Opfergelt et al., 2008; Delvigne et al., 2009; Lugolobi et al., 2010; Cornelis et al., in press; Chapter 7). The Si isotopic compositions and Ge/Si ratios measured in the soil-tree system from Breuil site (France) are compared with available data (summarized in Opfergelt, 2008; Fripiat, 2010) in Figure 9.3 and Figure 9.4, respectively. Measurements on granitic parental material, clay-sized minerals, bulk soil and phytoliths are in good agreement with published data. We provided the first Si isotopic and Ge/Si ratios measurements on forest floor leachates solutions and on humus layer. Moreover, we gave Ge/Si ratio data on each isolated soil fractions for the first time.

In the temperate forest site, clay-sized minerals were enriched in ^{28}Si and had high Ge/Si ratios, while BSi from phytoliths was also enriched in ^{28}Si, but had low Ge/Si ratio as compared to parental material. Such a contrast is crucial to infer the relative contribution of silicate weathering and BSi dissolution on the release of DSi in forest soil solutions.

The δ^{30}Si values in forest floor leachates collected in Douglas fir and European beech sites (-1.38‰ and -2.05‰, respectively) were more negative than the isotopically lightest natural waters reported by Georg et al. (2009a).

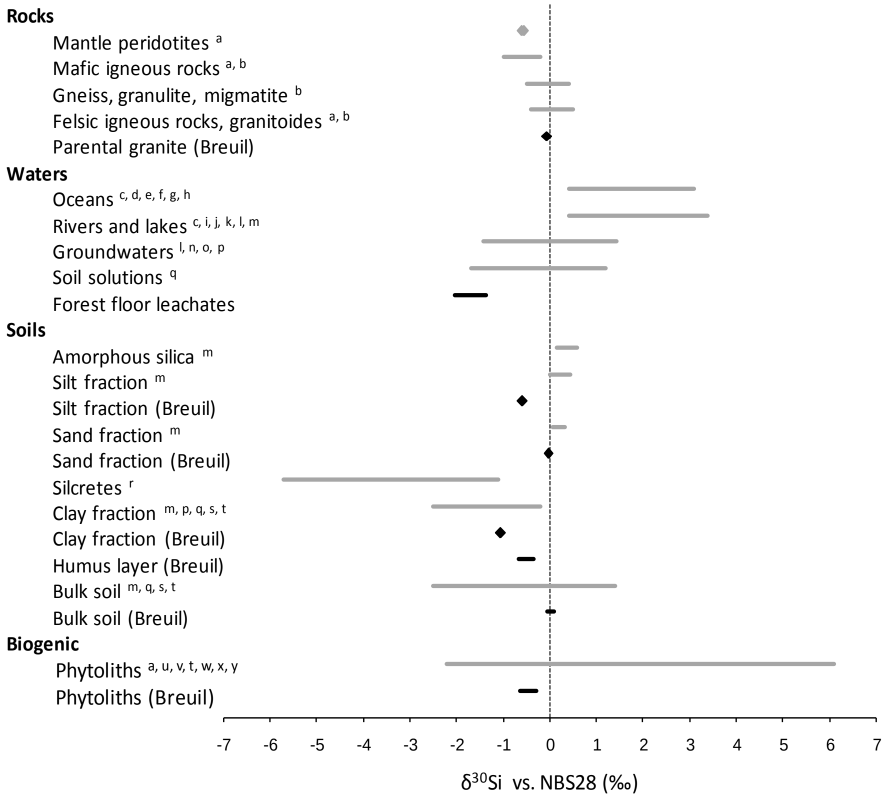

Figure 9.3 Comparison of the Si isotope data in the soil-tree system (black) with the data available in the literature (grey, (a) Douthit, 1982; (b) Ding et al., 1996; (c) De la Rocha et al., 2000; (d) Varela et al., 2004; (e) Cardinal et al., 2005; (f) Reynolds et al., 2006; (g) Beucher et al., 2008; (h) Cavagna et al., in revision; (i) Ding et al., 2004; (j) Alleman et al., 2005; (k) Georg et al., 2006; (l) Georg et al., 2007; (m) Opfergelt et al., 2010; (n) Georg et al., 2005; (o) Georg et al., 2009a; (p) Georg et al., 2009b; (q) Ziegler et al., 2005a; (r) Basile-Doelsch et al., 2005; (s) Ziegler et al., 2005b ; (t) Opfergelt et al., (2008); (u) Ding et al., 2005; (v) Opfergelt et al., 2006; (w) Engström et al., 2008 ; (x) Hodson et al., 2008 ; (y) Ding et al., 2008).

The Ge/Si ratios were higher in forest floor leachates (2.7±1.0 µmol.mol^{-1}) relative to soil solutions (1.2±0.1 µmol.mol^{-1}). The enrichment in ^{28}Si and Ge in forest floor leachates is due to partial dissolution of secondary clay minerals (δ^{30}Si = -1.07‰; Ge/Si = 6.2 µmol.mol^{-1}) which are incorporated by bioturbation in a more acidic environment. Indeed phytoliths, which are characterized by low Ge/Si ratios (0.1-0.3 µmol.mol^{-1}), are not expected to significantly influence the Ge/Si and Si isotopic ratios in forest floor leachates. In addition, since the forest floor leachates are isotopically lighter than silicate minerals, the Si-isotopic composition cannot be explained by a congruent dissolution of silicate minerals. In contrast, a preferential release of light Si isotopes during dissolution of silicate minerals could explain such a negative Si-isotopic signature.

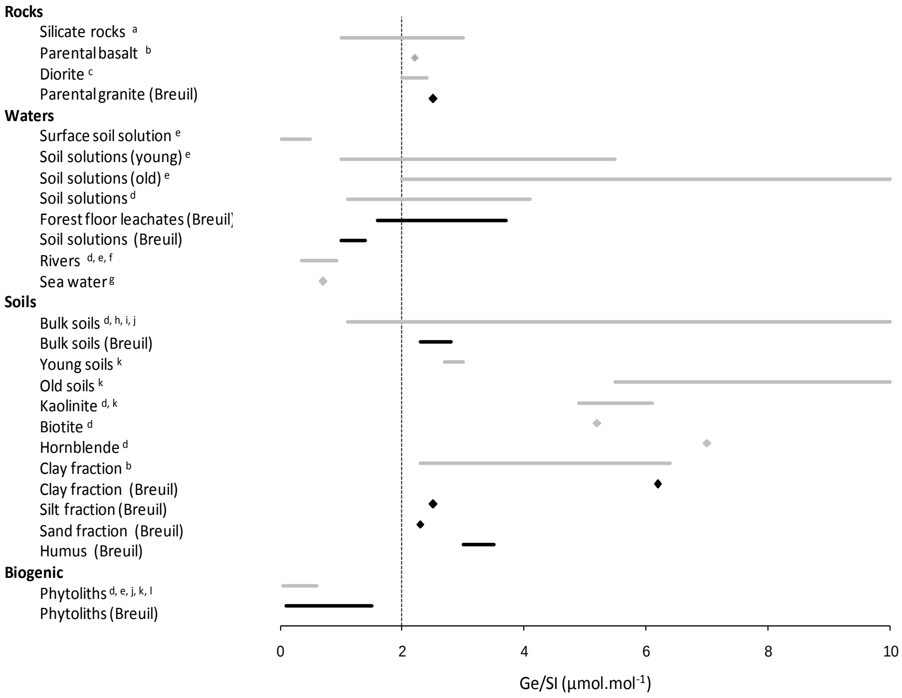

Figure 9.4 Comparison of the Ge/Si ratio measured in the soil-tree system (black) with the data available in the literature (grey, (a) De Argollo and Schilling, 1978; (b) Opfergelt et al., 2010; (c) Kurtz et al., 2002; (d) Lugolobi et al., 2010; (e) Derry et al., 2005; (f) Froelich et al., 1992; (g) Froelich and Andrea, 1981; (h) Murnane and Stallard, 1990; (i) Scribner et al., 2006; (j) Delvigne et al., 2009; (k) Kurtz and Derry, 2004; (l) Blecker et al., 2007).

Based on (i) the contrast between Ge/Si ratios and Si-isotopic compositions, (ii) the important pool of soil minerals in humus layer relative to the BSi pool, and (iii) the chemical conditions in organic horizons, it seems reasonable to assume that the partial dissolution of clay minerals greatly influences the source of DSi in forest floor leachates. These findings suggest that the overall impact of Si biocycling and BSi restitution on the DSi release in shallow soil is minor relative to dissolution of crystallized secondary clay-sized minerals. The preferential release of ^{28}Si from silt-sized minerals could also partly explain the negative δ^{30}Si values in forest floor leachates.

Thus, DSi content in forest floor leachates is tree species-dependent mainly through various incorporation of soil minerals in organic horizons by bioturbation and only secondarily through the recycling of BSi on topsoil. Ge/Si ratio in forest floor leachate solutions can be related to Si recycling and bioturbation rates estimated under each tree species (Figure 9.1). Indeed, the Ge/Si ratio under Black pine (3.7 μmol.mol^{-1}) would be mainly influenced by dissolution of clay minerals since the recycling of Si is very low (2.3 kg ha^{-1} yr^{-1}) and bioturbation is important. On the other hand, under European beech and oak, the Ge/Si ratio (2.3-3.7 μmol.mol^{-1}) seems to be influenced by both clay minerals and BSi dissolution as the uptake of Si (18.5-23.3 kg ha^{-1} yr^{-1}) and bioturbation are both substantial. Finally, the Ge/Si ratio under Douglas fir and Norway spruce (1.6-2.1 μmol.mol^{-1}) could reflect more the dissolution of BSi as the bioturbation is lower and the recycling of Si is large (30.6-43.5 kg ha^{-1} yr^{-1}).

Otherwise, soil solutions display similar Ge/Si ratio for all tree species suggesting a pedogenic control on DSi content, such as weathering of primary minerals, neoformation of secondary phases and Si adsorption onto Fe oxides.

9.4 General conclusions: the biogeochemical Si cycle and pedogenesis.

In highly-weathered environment with very low availability of mineral-derived Si and with significant Si biocycling, the DSi fluxes are deeply influenced by the existing BSi pool. In our temperate weathering-unlimited systems, besides the high Si stock in silicate minerals, a high biomass production and turnover should create a relatively large pool of reactive BSi in shallow soils. Although tree species take up to 43.5 kg Si ha^{-1} yr^{-1}, which constitute a large amount of BSi restituted on topsoil, dissolution of phytoliths does not seem to control the DSi composition of the forest floor leachates, even given the high reported dissolution rates for phytoliths (Fraysse et al., 2009).

In this granitic environment, the ASi pool is likely too low to strongly influence the DSi release in forest floor leachate and soil solutions as compared to the pool of litho/pedogenic crystallized Si. This result contrasts with recent study showing a strong biological control on the Si cycling and export in basaltic soils with very low availability of mineral-derived Si (Derry et al., 2005).

The release of DSi from the BSi pool could be redistributed in various Si sinks in the soil profile or exported to stream water. In our acid brown soil, we observe that the DSi is redistributed in (i) well-crystallized form: secondary clay minerals, and (ii) amorphous forms: opaline spheres, adsorption onto Fe oxides and phytoliths. Besides the substantial pool of phytoliths (BSi) in soil, the ASi adsorption onto Fe oxides is also a significant pool of the ASi fraction in our temperate forest soil. Although Si biocyling does not seem directly impacted the DSi release in aqueous phase of a temperate-granitic environment, BSi re-distribution in forest soil can play a major role in the pedogenesis as (i) DSi source for neoformation of secondary phases which influence the pedogenesis process (*e.g.*, podzolization) through the decrease of metals activity in soil solution, (ii) adsorption surface for fulvic acids which are stabilized through humification process, and (iii) translocation and accumulation of amorphous silica.

9.5 Further perspectives

The soil-plant system…

The impact of biogeochemical Si cycle on the pedogenic processes in forest ecosystem, such as distribution of Si-containing solid phases and DSi chemistry of forest soil solutions, have been partly identified in this PhD thesis.

The biogeochemical cycle of chemical elements is of great interest as the soil-plant relationships relate the effects of soil fertility on biomass nutrition and production and the effects of vegetation on soil processes (Ranger et al., 1995). Identifying the sources and mechanisms of solute contribution to stream waters is necessary for understanding nutrient cycling processes in soil-plant system and the global nutrient balance. Therefore, a better knowledge of the biogeochemical cycles of Si, but also of Ca^{2+}, Mg^{2+}, K^{+}, Mn^{2+} is relevant to better constrain the biological and geochemical controls on the release of elements in stream water. In this respect, we need to assess biomass production according to soil fertility under similar climatic conditions to better advise the farmer and forester. Indeed, some biogeochemical cycles are mainly controlled by the geochemical relationships, while others are controlled by the biological cycling, hence the crucial interest of mulching with organic crop residues. In forest ecosystem, the biological cycle of nutrients largely contributes to maintaining a significant base cation saturation of the adsorbing complex in the upper soil horizons of acidic soils (Ranger and Colin-Belgrand, 1996). When soil nutrient reserves are relatively small as compared to forest nutrient uptake, the biological cycle represents the key process in the maintenance of forest productivity (Ranger et al., 1997). A better assessement of the nutrient needs for plant growth and the nutrient sources would thus be of interest for the future planet food needs.

… and hydrosphere

Firstly, we suggest a modeling of weathering and biocycling processes in order to (i) assess the biogeochemical Si cycle and (ii) identify which component (biogenic or litho/pedogenic) dominates Si dynamics at the catchment scales (Goddéris et al., 2006; Gérard et al., 2008). We would use a numerical model of chemical weathering in soil horizons coupled to a numerical model of water cycle in forest ecosystems to simulate the Si concentrations, and their seasonal variability, within the soil horizon and the stream of the granitic watershed.

We provide direct evidence of clay-sized mineral control on the DSi release in forest floor leachates solutions. However, details are lacking on the relative control of pedogenic and biogenic processes on the DSi release from the soil profile towards rivers. As the impact of ceramic cup lysimeters on the Si isotopes fractionation is unknown, we have to improve the soil solutions sampling to measure Si and other useful isotopes in aqueous phase using, *e.g.* Teflon suction cup or stainless steel suction cup lysimeters.

The separation of soil solutions could be carried out by centrifugation drainage technique according to the procedure described by Gérard et al. (2003). However, the kind of soil solutions collected is very important as it is well known that leaching soil solutions are mobile, solutions collected by ceramic cup lysimeters incorporate the aqueous phase fixed to the solid phase with moderate energy and solutions collected by centrifugation incorporate the aqueous phase energetically fixed to the soil solid phase. Leaching solution is suitable for ecosystem input-output budgets while capillary solution is valuable when the equilibrium soil-solution phase is considered (Marques et al., 1996). A characterization of Ge/Si ratios and Si isotope data in leaching and capillary solutions would thus be of interest to better constrain the chemistry of reactive soil solutions. In addition, it would be interesting to study the seasonal variations of DSi content, Si-isotopic signature and Ge/Si rations in (i) forest floor leachates and (ii) soil solutions leached out from the soil profile.

Finally, in the review, we confirm that the major load of DSi towards rivers is from weathering-unlimited system (tropical rivers in Asia and Oceania) where the origin of the Si-sources (litho/pedo or biogenic) is of great importance for understanding the global export of DSi to oceans and the global CO_2 consumption rates through silicate weathering. Thus, we should give more attention to these systems with high ability to weathering and transport since the recent study focus on the biological control on Si cycling and export in highly weathered tropical systems with low availability of mineral-derived Si (Lucas et al., 1993; Alexandre et al., 1997; Derry et al., 2005).

… and pedogenesis

Through alkaline dissolution (Na_2CO_3), we show that the Si biocycling and BSi restitution largely affect the ASi content in humus layer. Thus we suggest to trace dissolution and input of DSi from phytoliths in secondary minerals comparing $\delta^{30}Si$ and Ge/Si signatures of secondary clay-sized minerals extracted from surface layers and from soil depth. It could be interesting to study the relation between weathering processes, geochemical signature of clay-sized minerals and H^+, DOC and NO_3^- content in the soil profile.

The ASi content in mineral soil layers is mostly affected by pedogenic processes. Although oxalate digestion is known to quantify short-range ordered aluminosilicates (allophane and imogolite) and weakly ordered Fe and Al oxides, we show that oxalate digestion also extract ASi adsorbed onto secondary oxides, thus overestimating the allophane and imogolite content in soils. To further distinguish between ASi and short-range ordered aluminosilicates in soils, the use of a sequential $CaCl_2$-oxalate-Na_2CO_3 in allophanic soil could be efficient to understand the specific dissolution of Si-components in soils. Furthermore, a more specific extractant for polysilicic acid adsorbed onto Fe oxides, which does not dissolve short-range ordered aluminosilicates, would likely permit to gain insights into the factors that control the poorly-crystallized minerals formation. To achieve that, Fe^{3+} should be reduced to Fe^{2+} by a reducing agent such as dithionite. However, the dithionite-citrate-bicarbonate (DCB) extraction (pH = 8.5), commonly used to remove Fe oxides from soil samples, irreversibly alters imogolite and allophane mineral surfaces and modifies surface charge characteristics (Chunming and Harsh, 1996). For instance, it should be interesting to test time-course extraction with NH_4F solution (Delfosse et al., 2005) and other kinds of reducing extractant.

The selective extractions of Fe and Al are widely used to assess the mobility of the metal in soils and are thus of great concern to study the podzolization processes (Titeux, 2005). Moreover, it would allow tracing the organomineral complex as poorly crystalline minerals play a key role in controlling C sequestration in soils (Basile-Doelsch et al., 2007). Indeed, the very low polymerized aluminosilicates such as allophane and imogolite largely control the amount of organic C stabilized in soils. Imogolite and proto-imogolite are mostly reported from podzols, whereas allophane occurs mainly in volcanic soils. In forest ecosystem, further research are needed to trace mechanisms which control the neoformation of secondary phases involved in the long-term stabilization of soil organic C, especially in volcanic areas and in soils with features of a podzol. Therefore, such a study would focus on contrasting soil-tree systems to:

- identify the mechanisms that control the formation of secondary minerals with high capacity to stabilize SOM using geochemical tracers;
- assess the effect of different pedogenic processes on SOM stabilization;
- assess the impact of tree species on the above processes.

In particular, we need to isolate minerals implied in the organomineral complexes (feldspars, gibbsite, poorly crystalline minerals and Fe oxides) through densimetric methods (Basile-Doeslch et al., 2007) to further investigate their geochemical signatures (elemental ratios, Ge/Si ratios and isotopic data) under contrasting tree species and soil conditions. Therefore, a better knowledge of the Si and Al sources for formation of secondary phases with high capacity to stabilize OC is best relevant for assessing the long-term OC stock in soils. Given the crucial role of organomineral complexes in the long-term C cycle, the major questions that remain are whether the formation of secondary poorly crystalline phases is rapid and whether it is geochemically significant.

APPENDIX A:

SOIL PROFILE DESCRIPTION

Table A.1 Description of a soil profile (Alumnic Cambisol) under the native forest. This profile is representative of the acid brown soil at the experimental site of Breuil-Chenue.

Horizon	Depth (cm)	Color†	Description
Humus	10 - 0	Dark	Dysmoder; thickness of Oh > 2cm
A1/E	0-5	7.5YR 2.5/2 (dark)	Gradual and regular boundary; organic-rich; sandy loam; particular structure; bleached quartz, plastic, porous; many fine and medium roots.
A1-A1/'Bp'	5-8	7.5YR 2.5/3 (dark brown)	Diffuse boundary; sandy loam; massive structure; plastic, high porosity; many roots.
SAl 1	8-18	7.5YR 4/4 (brown)	Diffuse boundary; sandy loam; subangular polyhedric structure; homogenous, plastic, porous; many fine and medium roots.
SAl 2	18-35	7.5YR 5/6 (brown)	Diffuse boundary; sandy loam; subangular polyhedric structure; homogenous, plastic, porous; a great many roots.
SAl 3	35-55	7.5YR 4/6 (brown)	Clear abrupt boundary; sandy loam; well developed polyhedric subangular structure; homogenous, slightly plastic, porous; roots.
II SAl 4	55-75	7.5YR 4/6 (brown)	Diffuse boundary; sandy loam; well developed polyhedric subangular structure; homogenous, rigid, porous; roots.
II B/C	75-95	7.5YR 4/6 (brown)	Clear abrupt boundary; loam; well developed polyhedric subangular structure; homogenous, rigid, medium porosity; very few roots.
II C	95-110	7.5YR 4/6 (brown to reddish brown)	Clear regular boundary; sandy loam; well developed polyhedric subangular to angular structure; homogenous, rigid, medium porosity; very few roots

†Munsell colors on dry soil samples

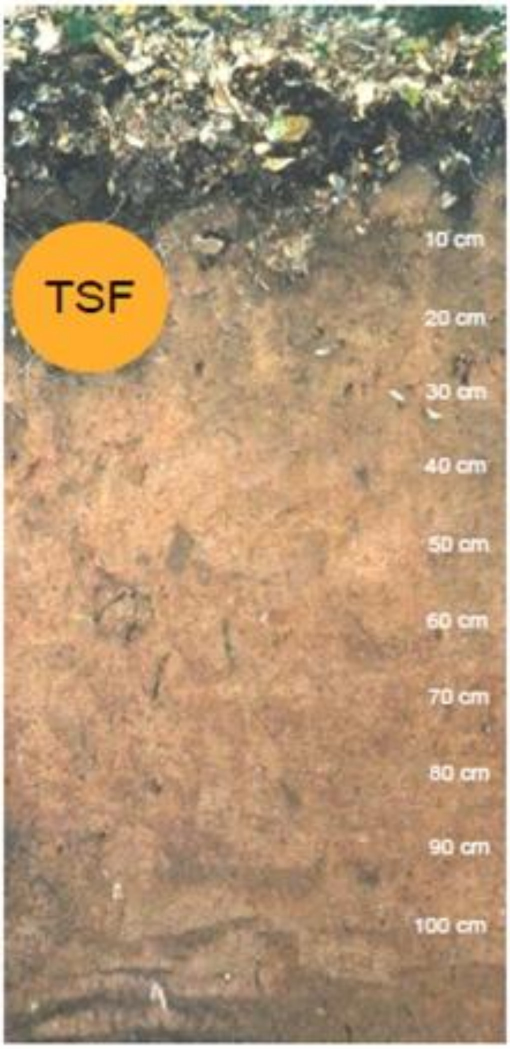
TSF
10 cm
20 cm
30 cm
40 cm
50 cm
60 cm
70 cm
80 cm
90 cm
100 cm

APPENDIX B:
RELEASE AND ADSORPTION OF CHEMICAL ELEMENTS FROM THE CERAMIC CUP LYSIMETERS

Introduction

The chemical composition of soil solutions is the result of primary minerals weathering, neoformation of secondary solid phase, adsorption onto minerals, complexation of chemicals, absorption by vegetation and micro-organisms and leaching from the soil profile. In a biogeochemical approach, the collect and study of soil solutions is of great interest to understand the chemical dynamics between solid and aqueous phases.

According to Marques et al. (1996), zero tension lysimeters, which collect gravitary solution, are the most appropriate to calculate the balance between chemicals input and ouput in a forest ecosystem. Ceramic cup lysimeters, which collect capillary solutions, are valuable in order to assess the chemical reactions between solid and aqueous phases. The physico-chemical properties of materials used for sampling soil solutions greatly differ in their impact on chemistry of soil solutions through the release or adsorption of chemical elements. For instance, Wenzel and Wieshammer (1995) show that adsorption processes can modify substantially the concentrations of heavy metals in solutions collected by suction cup lysimeters.

In this study, we aim at assessing (i) the dissolution and release of elements from the ceramic cup, and (ii) the adsorption of elements onto ceramic cup in controlled conditions with realistic concentrations of soil solutions. The objective is to study how a ceramic cup lysimeter (used at Breuil forest site) can influence the chemistry of solutions collected in the field. More particularly, we will focus on the dynamics of Si, Al and DOC in the aqueous phase.

Materials and methods

Figure B.1 shows the experimental ceramic cup lysimeter. Each part of the device was tested to ensure that the release or adsorption of elements is only influenced by the ceramic cup. We observed that the concentration of Si released by the other parts of the device (vial and column) was below the detection limit of the ICP AES (0.01 mM).

Realistic soil solutions were collected in the forest site of Breuil-Chenue by lysimeters made in polypropylene. Every 8 days, we added 300ml of soil solutions in the column containing the ceramic cup in increasing Si concentrations (Table B.2). We measured the pH, conductivity and concentrations of dissolved elements (Si, Al and DOC) before and after passing through ceramic cup lysimeters.

Figure B.1 the ceramic cup lysimeter is inserted tightly into the column where the realistic soil solution is added to increasing Si concentrations.

Results and Discussion

The chemical composition of the ceramic cup lysimeters (Table B.1) clearly showed that it is mainly constituted of SiO_2 (17.7%) and Al_2O_3 (79.9%).

Table B.1 Total analysis of the ceramic cup (unpublished data INRA-Champenoux).

SiO_2	Al_2O_3	MgO	CaO	Fe_2O_3	Mn_3O_4	TiO_2	BaO	P_2O_5	SrO	Na_2O	K_2O
% dry weight											
17.7	79.9	0.13	*	*	0.011	0.12	*	0.43	*	0.16	0.46

* below the detection limit

In Table B.2, we observed that the concentrations of Al and DOC decrease after percolation through the ceramic cup lysimeter, while the concentration of Si and pH increase after percolation whatever the concentration of the input solution.

Table B.2 Chemical compositions of the solutions to increasing Si, Al and DOC concentrations before and after percolation in the ceramic cup lysimeters.

Solutions	Date	Al mM	Si mM	pH	DOC $mg.l^{-1}$
Input	16-10-07	0.012	0.015	5.49	1.36
Output	23-10-07	0.005	0.062	5.32	1.25
Input	23-10-07	0.029	0.029	4.85	1.81
Output	30-10-07	0.005	0.061	5.06	1.15
Input	30-10-07	0.039	0.036	4.81	1.90
Output	06-11-07	0.005	0.060	4.99	1.21
Input	06-11-07	0.083	0.072	4.65	2.76
Output	13-11-07	0.012	0.093	4.75	1.15
Input	13-11-07	0.179	0.138	4.39	4.57
Output	20-11-07	0.081	0.162	4.39	1.60
Input	20-11-07	0.358	0.242	4.15	9.70
Output	03-12-07	0.316	0.302	4.34	5.22

In addition, the amount of Al and DOC adsorbed by the ceramic cup lysimeter increases with the increase of the input solution concentrations. The release of Si by the ceramic cup decreases with the increase of the input solution concentrations (Figure B.2).

The release of Si from the ceramic cup decreases gradually as the Si activity in the input solution increases. As shown in Figure B.3, for a realistic concentration of 0.14 mM in the input solution (S_{in}), 15% of the Si concentration in the output solution (Si_{out}) is from dissolution of the ceramic cup, which is close to the Si detection limit of ICP-AES (0.01 mM). The relationship between Si_{in} and the ratio Si_{in}/Si_{out} (r = 0.95) allow us to calculate the following logarithmic regression:

$$Si_{in}/Si_{out} = 0.17\times\ln(Si_{in}) + 1.12 \qquad \text{Eq. (B.1)}$$

in which Si_{in} and Si_{out} are in mM and correspond to the input solution in the ceramic cup device and output solution from the ceramic cup device, respectively.

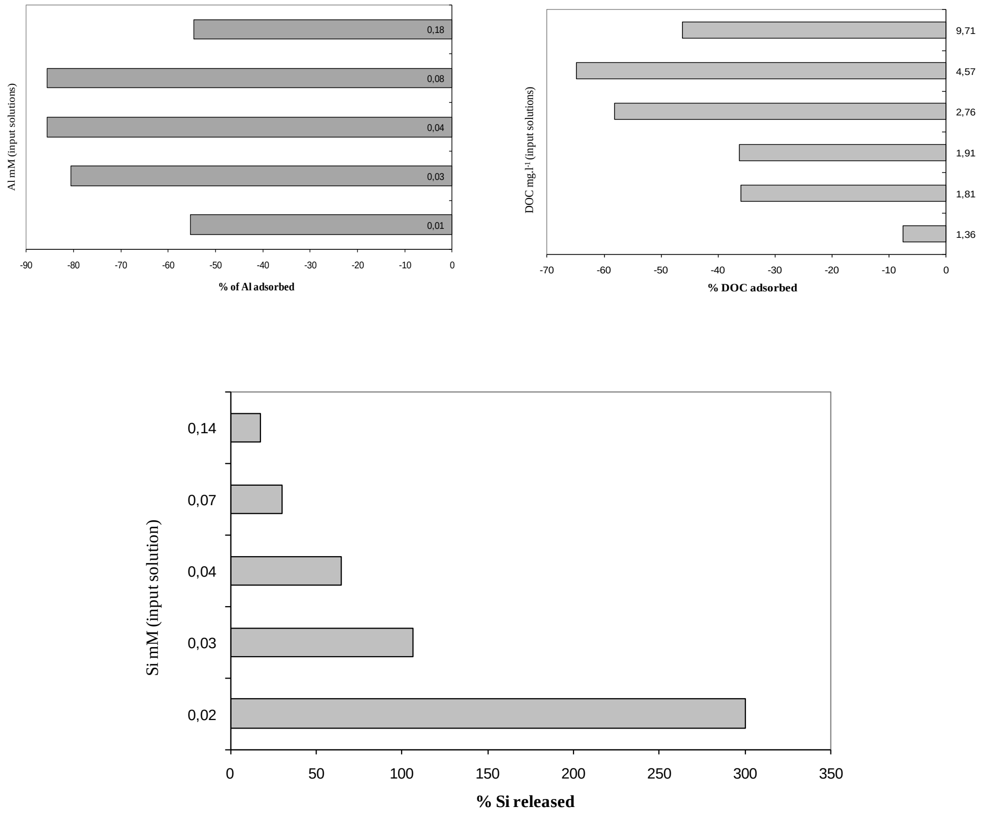

Figure B.2 Proportion of Si, Al and DOC adsorbed onto (negative X-axis) or released from (positive X-axis) the ceramic cup relative to the concentration of the input solution.

Despite different dynamics between ceramic cup and soil solution in the field, we could evaluate the real Si concentration in the forest soil solution using Eq. (B.1).

Our laboratory experiment proves that more attention is needed about contamination of isolated soil solution with ceramic cup when we study the Si dynamics in forest soil solutions with low Si concentrations. In an attempt to understand the adsorption or dissolution mechanisms and thereby also the usefulness of ceramic cups, experiments would carry out to define stability under soil conditions, cation exchange capacity, and reactivity under conditions relevant to the field, as realized for the Al contamination of soil solutions.

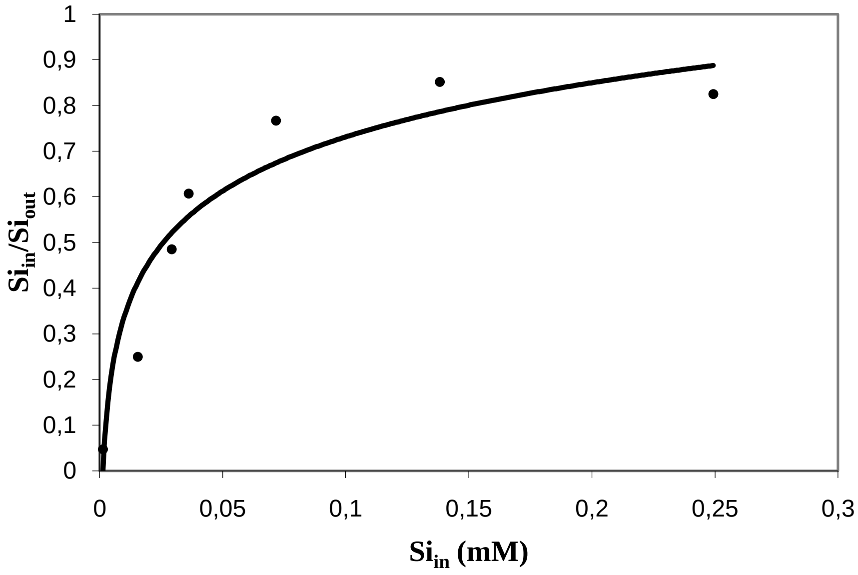

Figure B.3 Relationship between Si_{in}/Si_{out} ratio and Si_{in} concentration of soil solutions collected by ceramic cup lysimeter.

Indeed, Raulund-Rasmussen (1991) concludes that porcelain cup (abbreviated to P.80) is thermodynamically unstable under acidic conditions when the Al activity in the soil solution is below that controlled by the cup materials. This leads to a proton-induced, kinetically-controlled dissolution of the cup material, which depends on (i) the solution intake rate, (ii) the rinsing procedure before sampling, and (iii) the composition of the soil solution (pH and Al activity). However, the ceramic cups can be appropriate for sampling acidic soil solution, provided they are suitably pretreated and then equilibrated in the field before use (Hughes and Reynolds, 1990).

APPENDIX C: CLAY-SIZED MINERAL IDENTIFICATION THROUGH XRD ANALYSIS

In order to quantify the amount of soil minerals incorporated in the humus layers by bioturbation, we isolate sand, silt and clay fractions from humus layer (Oh) (Chapter 4). Thereafter, clay fraction mineralogy was assessed by XRD (X-ray diffraction using CuKα radiation in a Bruker Advance diffractometer) after treatment with Na-citrate at 100°C, K^+ and Mg^{2+} saturation, ethylene glycol (EG) salvation and thermal treatments at 105, 300 and 550°C. Through XRD analysis (Figure C.1), we identified the following minerals in the clay fraction extracted from humus layer under European beech and Douglas fir: quartz (0.33 and 0.43nm), kaolinite (0.71 and 0.35nm), mica (0.99 and 0.49nm), mica-vermiculite mixed layers (basal peak intermediate between 1.00nm and 1.41nm from Mg 20°C -saturated samples), smectite (swelling increases after EG-solvation on Mg 20°C sample) and chlorite (1.41nm and 0.71nm after heating K-saturated samples at 550°C).

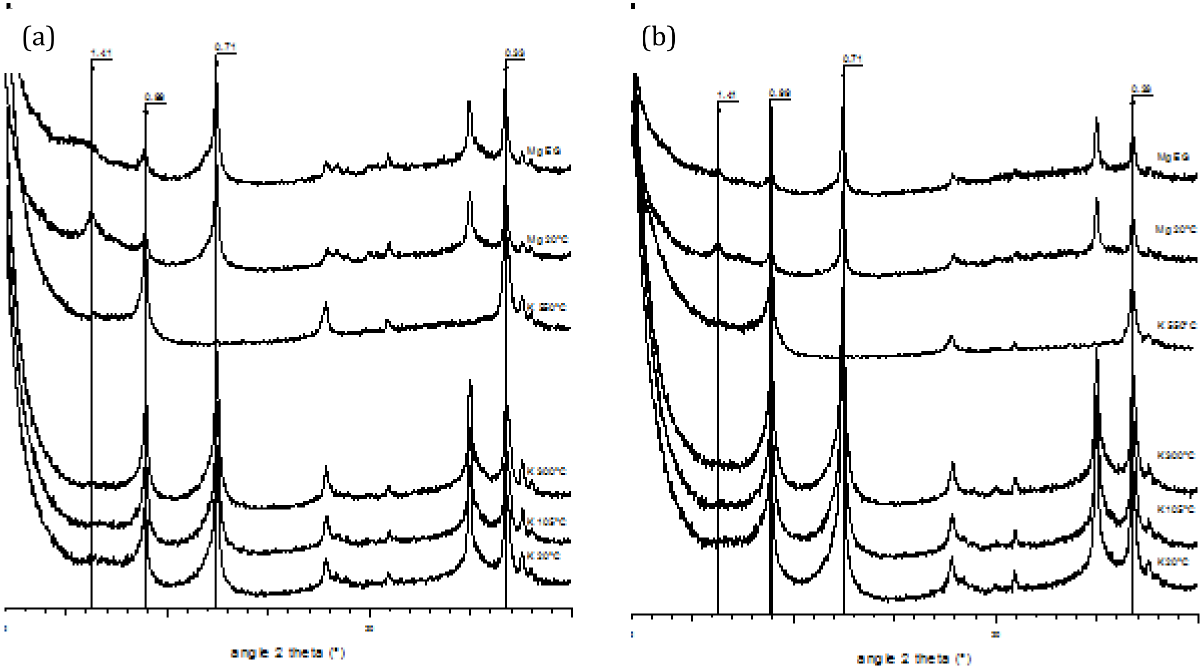

Figure C.1 X-ray diffraction pattern of the clay fractions (<2 µm) extracted from the humus layer (Oh) under (a) European beech and (b) Douglas fir, after saturation with K (K 20°C) and heating at 105, 300 and 550°C, or with Mg (Mg 20°C) and solvation with ethylene glycol (Mg EG). Typical reflections are described in text with first order reflections (nm) highlighted in the figure.

APPENDIX D:

DSI RELEASED FROM PHYTOLITHS VS. ORTHOSE

In order to explore the dissolution of primary minerals (orthose = ISi) relative to amorphous silica (phytolihs from European beech = BSi), we compare the release of DSi from ISi and BSi as a function of pH in solution (Table D.1). In order to have the same quantity of Si atoms in each solid phase, we added 23 mg of BSi and 33 mg of ISi in 80 ml of nutrient solution (see Chapter 4). In table D.1, we observed that the release of DSi from BSi is significantly higher than from orthose (ISi). The BSi dissolution strongly increased with the increase of pH, while the ISi dissolution is low and constant wathever the pH.

Table D.1 Concentration of DSi in a solution slightly shaken for 7 days.

	pH	**DSi mM**
Isi	4	0.006
Bsi	4	0.017
Isi+Bsi *	4	0.022
Isi	5	0.004
Bsi	5	0.033
Isi+Bsi	5	0.033
Isi	7	0.005
Bsi	7	0.349
Isi+Bsi	7	0.480

* ISi+BSi means that 33mg of ISi was mixed with 23mg of BSi in 80 ml of realistic nutrient solution (used for hydroponics experiment with tree seedlings in Chapter 4).

In addition to this preliminary experiment, we test the dissolution of ISi and BSi in a hydroponic experiment with tree seedlings, as described in Chapter 4. Six Douglas fir seedlings were grown in PVC pots containing

2.5 l of nutrient solution in which the same amount of Si atoms in BSi (0.65g) and ISi (1g) was added. Seedlings were placed in a perforated plate of expanded polystyrene which limit water loss by evaporation. The experiment was conducted during 11 weeks in a growth chambers with a 448 µE $m^{-2}s^{-1}$ photon density flux during 8h per day, 75% relative humidity, and day/night temperatures of 20/18°C.

The Si concentration in nutrient solution at the beginning and the end of hydroponic experiment and the Si concentration in Douglas fir leaves after 11 weeks of experiment are presented in Table D.2.

Table D.2 Si concentrations in nutrient solutions at the beginning (B) and the end (E) of hydroponic experiments. Si concentrations in leaves collected after 11 weeks of Douglas fir growth in the nutrient solution.

Solid phase in nutrient solution	Si-conc in nutrient solution (mM)		Si-conc in leaves ($mg.g^{-1}$)
	(B)	(E)	
BSi	0.008	0.073	0.53
ISi	0.003	0.011	0.21

In these conditions, we observe that BSi dissolution released seven times more DSi in aqueous phase than the ISi dissolution. This finding is confirmed by the Si concentration in leaves, which was two times higher in fir leaves growing in a nutrient solution with BSi as DSi source as compared to ISi as DSi source. This should be investigated in more details with a better control on the DSi sources using the contrasting Si isotopic signature of beech phytoliths (-0.64±0.02 ‰, Chapter 6) and feldspar (-0.15±0.01‰, Georg et al., 2005). The Si concentrations and isotopic composition in the nutrient solution would allow us to assess the relative contribution of BSi (amorphous) and ISi (crystalline) to the release of DSi in aqueous phase.

REFERENCES

Abraham K, Opfergelt S, Fripiat F, Cavagna AJ, de Jong JTM, Foley S, André L, Cardinal D (2008) δ^{30}Si and δ^{29}Si determinations on BHVO-1 and BHVO-2 reference materials via new configuration on Nu Plasma Multi Collector (MC)-ICP-MS. *Geostandard Geoanalytical Research* 32:193-202.

Alexander GB, Heston WM, Iler RK (1953) The solubility of amorphous silica in water. *Journal of American Chemical Society* 75:453-455.

Alexandre A, Meunier JD, Colin F, Koud JM (1997) Plant impact on the biogeochemical cycle of silicon and related weathering processes. *Geochimica Et Cosmochimica Acta* 61:677-682.

Alleman LY, Cardinal D, Cocquyt C, Plisnier PD, Descy JP, Kimirei I, Sinyinza D, André L (2005) Silicon isotopic fractionation in lake Tanganyika and its main tributaries. *Journal of Great Lake Research* 31:509-519.

Allen BL, Hajek BF (1989) Mineral occurrence in soil environments. In: Dixon JB, Weed SB (eds) *Minerals in soil environments*. Soil Science Society of America, Madison, pp 199-279.

Anderson SP, Drever JI, Humphrey NF (1997) Chemical weathering in glacial environments. *Geology* 25:399-402.

Anderson SP, Drever JI, Frost CD and Holden P (2000) Chemical weathering in the foreland of a retreating glacier. *Geochimica Et Cosmochimica Acta* 64:1173-1189.

André L, Cardinal D, Alleman LY, Moorbath S (2006) Silicon isotopes in ~3.8 Ga West Greenland rocks as clues to the Eoarchean supracrustal Si cycle. *Earth and Planetary Science Letters* 245:162-173.

Aoki Y, Hoshino M, Matsubara T (2007) Silica and testate amoebae in a soil under pine-oak forest. *Geoderma* 142:29-35.

Augusto L, Ranger J, Binkley D, Rothe A (2002) Impact of several common tree species of European temperate forests on soil fertility. *Annals of Forest Science* 59:233-253.

Aurousseau P (1976) Morphologie et genèse des sols sur granite du Morvan. *PhD Thesis*, Université de Rennes, 210 pp.

References

Azam F, Volcani BE (1981) Germanium-silicon interactions in biological systems. In Simpson TL, Voclani BE (eds) *Silicon and Siliceous Structures in Biological Systems*. Springer-Verlag, New York, pp 43-67.

Barman AK, Varadachari C, Ghosh K (1992) Weathering of silicate minerals by organic acids. I. Nature of cation solubilisation. *Geoderma* 53:45-63.

Barré P, Berger G, Velde B (2009) How element translocation by plants may stabilize illitic clays in the surface of temperate soils. *Geoderma* 151:22-30.

Bartoli F, Souchier B (1978) Cycle et rôle du silicium d'origine végétale dans les écosystèmes forestiers tempérés. *Annales des Sciences Forestières* 35:187-202.

Bartoli F, Wilding LP (1980) Dissolution of biogenic opal as a function of its physical and chemical properties. *Soil Science Society of America Journal* 44:873-878.

Bartoli F (1983) The biogeochemical cycle of silicon in two temperate forest ecosystems. *Environmental Biogeochemistry Ecol Bull* 35:469-476.

Bartoli F (1985) Cristallochemistry and surface-properties of biogenic opal. *Soil Science Society of America Journal* 36:335-350.

Bartoli F, Burtin G, Herbillon AJ (1991) Disaggregation and clay dispersion of oxisols: Na resin, a recommended methodology. *Geoderma* 49:301-317.

Basile-Doelsch I, Meunier JD, Parron C (2005) Another continental pool in the terrestrial silicon cycle. *Nature* 433:399-402.

Basile-Doelsch I (2006) Si stable isotopes in the Earth's surface: a review. *Journal of Geochemical Exploration* 88:252–256.

Basile-Doelsch I, Amundson R, Stone WEE, Borschneck D, Bottero JY, Moustier S, Masin F, Colin F (2007) Mineral control of carbon pools in a volcanic soil horizon. *Geoderma* 137:477-489.

Beckwith RS, Reeve R (1963) Studies on soluble silica in soils. I. The sorption of silicic acid by soils and minerals. *Australian Journal of Soil Research* 1:157-168.

Bélanger RR, Bowen PA, Ehret DL, Menzies JG (1995) Soluble silicon: its role in crop and disease management of greenhouse crops. *Plant Disease* 79:329-336.

Bélanger RR, Benhamou N, Menzies, JG (2003). Cytological evidence of an active role of silicon in wheat resistance to powdery mildew (*Blumeria graminis* f. sp tritici). *Phytopathology* 93:402-412.

Bennet PC, Siegel DI, Hill BM, Glaser PH (1991) Fate of silicate minerals in a peat bog. *Geology* 19:328-331.

Bern CR, Brzezinski MA, Beucher C, Ziegler K, Chadwick OA (2010) Weathering, dust and biocycling effects on soil isotope ratios. *Geochimica et Cosmochimica Acta* 74:876-889.

Berner RA, Lasaga AC, Garrels RM (1983) The Carbonate-silicate geochemical cycle and it's effect on atmospheric carbon dioxide over the past 100 million years. *American Journal of Science* 283:641-683.

Berner RA (1995) Chemical weathering and its effect on the atmospheric CO_2 and climate. In: White AF, Brantley SL (eds) *Chemical weathering rates of silicate minerals. Reviews in mineralogy.* Mineralogical Society of America, Washington, DC, pp 565-583.

Berner RA (1997) The rise of plants and their effect on weathering and atmospheric CO_2. *Science* 276:544.

Beucher CP, Brzezinski MA, Jones JL (2008) Sources and biological fractionation of silicon isotopes in the Eastern Equatorial Pacific. *Geochimica Et Cosmochimica Acta* 72:3063-3073.

Beusen AHW, Bouwman AF, Dürr HH, Dekkers ALM, Hartmann J (2009) Global patterns of dissolved silica export to the coastal zone : results from a spatially explicit global model. *Global biogeochemical cycles* 23.

Binkley D (1995). The influence of Tree Species on Forest Soils : Processes and Patterns. In: Mead DJ, Cornforth IS (eds.) *Proceedings of the Trees and Soil Workshop*, Lincoln University 28 February - 2 March 1994. Lincoln University Press, Canterbury.

Binkley D, Giardina C (1998) Why do tree species affect soils ? The Warp and Woof of tree-soil interactions. *Biogeochemistry* 42:89-106.

Birchall JD (1990) The role of silicon in biology. Chemistry in Britain 26:141-144.

Blecker SW, McCulley RL, Chadwick OA, Kelly EF (2006) Biologic cycling of silica across a grassland bioclimosequence. *Global Biogeochemical Cycles* 20.

Blecker SW, King SL, Derry LA, Chadwick OA, Ippolito JA, Kelly EF (2007) The ratio of germanium to silicon in plant phytoliths: Quantification of biological discrimination under controlled experimental conditions. *Biogeochemistry* 86:189-199.

Bluth GJ, Kump LR (1994) Lithologic and climatologic controls of river chemistry. *Geochimica Et Cosmochimica Acta* 58:2341–2359.

Bonneau M, Brêthes A, Lacaze JF, Lelong F, Levy G, Nys C, Souchier B (1977) Modification de la fertilité des sols sous boisement artificiel de résineux purs. *C.R. Fin d'Etude D.G.R.S.T.*, Nancy-Champenoux, 88 pp.

Bormann BT, Wang D, Bormann FH, Benoit G, April R, Snyder MC (1998) Rapid, plant-induced weathering in an aggrading experimental ecosystem. *Biogeochemistry* 43:129-155.

Brahy V, Deckers J, Delvaux B (2000a) Estimation of soil weathering stage and acid neutralizing capacity in a toposequence Luvisol-Cambisol on loess under deciduous forest in Belgium. *European Journal of Soil Science* 51:1-13.

Brahy V, Titeux H, Delvaux B (2000b) Incipient podzolization and weathering caused by complexation in a forest Cambisol on loess as revealed by a soil solution study. *European Journal of Soil Science* 51:475-484.

Breda N, Soudani K, Bergonzini JC (2002) Mesure de l'indice foliaire en forêt. *Doc GIP ECOFOR* Paris Laballery, Clamecy imp, 157 pp.

Brethes A, Brun JJ, Jabiol B, Ponge J, Toutain F (1995) Classification of forest humus forms: a French proposal. *Annales des Sciences Forestières* 52: 535-546.

Buurman, P, Van Reeuwijk LP (1984) Proto-imogolite and the process of podzol formation: a critical note. *European Journal of Soil Science* 35:447-452.

Bluth GJ, Kump LR (1994) Lithologic and climatologic controls of river chemistry. *Geochimica Et Cosmochimica Acta* 58:2341–2359.

Calvaruso C, Mareschal L, Turpault MP, Leclerc E (2009) Rapid clay weathering in the rhizosphere of Norway spruce and oak in an acid forest ecosystem. *Soil Science Society of America Journal* 73:331-338.

Cardinal D, Alleman LY, De Jong J, Ziegler K, André L (2003) Isotopic composition of silicon measured by multicollector plasma source mass spectrometry in dry plasma mode. *Journal of Analytical Atomic Spectrometry* 18:213-218.

Cardinal D, Alleman LY, Dehairs F, Savoye N, Trull TW, André L (2005) Relevance of silicon isotopes to Si-nutrient utilization and Si-source assessment in Antarctic waters. *Global Biogeochemical Cycles* 19.

Carignan J, Hild P, Mevelle G, Morel J, Yeghicheyan D (2001) Routine analyzes of trace element in geological samples using flow injection and low pressure on-line liquid chromatography coupled to ICP-MS: a study of geochemical reference materials BR, DR-N, UB-N, AN-G and GH. *Geostandards Newsletter* 25:187-198.

Carnelli AL, Madella M, Theurillat JP (2001) Biogenic silica production in selected alpine plant species and plant communities. *Annals of Botany* 87:425-434.

Carnelli AL, Theurillat JP, Madella M (2004) Phytolith types and type-frequencies in subalpine-alpine plant species of the European Alps. *Review of Palaeobotany and Palynology* 129:39-65.

Cary L, Alexandre A, Meunier JD, Boeglin JL, Braun, JJ (2005) Contribution of phytoliths to the suspended load of biogenic silica in the Nyong basin rivers (Cameroon). *Biogeochemistry* 74:101-114.

Casey WH, Kinrade SD, Knight CTG, Rains DW, Epstein E (2003) Aqueous silicate complexes in wheat, Triticum aestivum l. *Plant Cell and Environment* 27:51-54.

Cavagna AJ, Fripiat F, Dehairs F, Wolf-Gladrow D, Savoye N, André L, Cardinal D (2009) Silicon isotopic signal during EIFEX: diatom uptake vs. mixing, biological fractionation and iron fertilization impact. In revision for *Limmology and Oceanography.*

Chadwick OA, Hendricks DM, Nettleton WD (1987). Silica in duric soils 2. Mineralogy. *Soil Science Society of America Journal* 51:982-985.

Chadwick OA, Kelly EF, Merritts DM, Amundson RG (1994) Atmospheric carbon dioxide consumption during soil development. *Biogeochemistry* 24:115-127.

Chadwick OA, Derry LA, Vitousek PM, Huebert BJ, Hedin LO (1999) Changing sources of nutrients during four million years of ecosystem development. *Nature* 397:491-497.

Chao TT, Sanzolone RF (1992) Decomposition techniques. *Journal of Geochemical Exploration* 44:65-106.

Chunming SU, Harsh JB (1996) Alteration of imogolite, allophane, and acidic soil clays by chemical extractants. *Soil Science Society of America Journal* 60:77-85.

Cinotti B (1996) Evolution des surfaces boisées en France: Proposition de reconstruction depuis le début du XIXe siècle. *Revue forestière française* XLVIII:547-562.

Clarke J (2003) The occurrence and significance of biogenic opal in the regolith. *Earth Science Reviews* 60:175-194.

Cochran MF, Berner RA (1996) Promotion of chemical weathering by higher plants : field observations on Hawaiian basalts. *Chemical Geology* 132:71-77.

Cocker KM, Evans DE, Hodson MJ (1998) The amelioration of aluminium toxicity by silicon in higher plants: solution chemistry or an in planta mechanism? *Physiologia Plantarum* 104:608-614.

Conley DJ, Schelske CL (1993) Potential role of sponge spicules in influencing the silicon biogeochemistry of Florida lakes. *Canadian Journal of Fisheries and Aquatic Science* 50:296-302.

Conley DJ (2002) Terrestrial ecosystems and the global biogeochemical silica cycle. *Global Biogeochemical Cycles* 16.

Conley DJ, Sommer M, Meunier JD, Kaczorek D, Saccone L (2006) Silicon in the terrestrial biogeosphere. In: Ittekot V, Unger D, Humborg C, Tac An N (eds.) *The Silicon Cycle. Human perturbations and impacts on aquatic systems*. SCOPE, 66, pp 13-28.

Conley DJ, Likens GE, Buso DC, Saccone L, Bailey SW, Johnson, CE (2008) Deforestation causes increased dissolved silicate losses in the Hubbard Brook Epxerimental Forest. *Global Change Biology* 14:2548-2554.

Conrad CF, Icopini GA, Yasuhara H, Bandstra JZ, Brantley SL, Heaney PJ (2007) Modeling the kinetics of silica nanocolloid formation and precipitation in geologically relevant aqueous solutions. *Geochimica Et Cosmochimica Acta* 71:531-542.

Cornelis JT, Ranger J, Iserentant A, Delvaux B (2010) Tree species impact the terrestrial cycle of silicon through various uptakes. *Biogeochemistry* 97:231-245.

Cornelis JT, Delvaux B, Cardinal D, André L, Ranger J, Opfergelt S (2010) Tracing the mechanisms controlling the release of dissolved silicon in forest soil solutions using Si isotopes and Ge/Si ratios. *Geochimica Et Cosmochimica Acta* (in press), doi 10.1016/j.gca.2010.04.056.

Cornu S, Lucas Y, Ambrosi JP, Desjardins T (1998) Transfer of dissolved Al, Fe and Si in two Amazonian forest environments in Brazil. *European Journal of Soil Science* 49:377-384.

Dahlgren RA, Ugolini FC (1989) Formation and stability of imogolite in e tephritic Spodosol, Cascade Range, Washington, U.S.A. *Geochimica Et Cosmochimica Acta* 53:1897-1904.

Dahlgren RA (1994) Quantification of allophane and imogolite. In Zelzny LW, Amonette JE (eds) *Quantitative methods in soil mineralogy.* Soil Science Society of America, Madison, pp 430-451.

De Argollo R, Schilling JG (1978) Ge-Si and Ga-Al fractionation in Hawaiian volcanic rocks. *Geochimica Et Cosmochimica Acta* 42:623-630.

Dejou J (1966) Le massif granitique à 2 micas de la Pierre qui Vire (Yonne et Nièvre). Etude pétrographique de ses différents fasciès. *Annales agronomiques* 17:99-141.

De La Rocha CL, Brzezinski MA, De Niro MJ (1996) Purification, recovery, and laser-driven fluorination of silicon dissolved and particulate silica for the measurement of natural stable isotope abundances. *Analytical Chemistry* 68:3746-3750.

De La Rocha CL, Brzezinski MA, DeNiro MJ (1997). Fractionation of silicon isotopes by marine diatoms during biogenic silica formation. *Geochimica Et Cosmochimica Acta* 61:5051-5056.

De La Rocha CL, Brzezinski MA, De Niro MJ (2000) A first look at the distribution of the stable isotopes of silicon in natural waters. *Geochimica Et Cosmochimica Acta* 64:2467-2477.

Delfosse T, Delmelle P, Givron C, Delvaux B (2005) Inorganic sulphate extraction from SO_2-impacted Andosols. *European Journal of Soil Science* 56:127-133.

Delstanche S, Opfergelt S, Cardinal D, Elsass F, André L, Delvaux B (2009) Silicon isotopic fractionation during adsorption of aqueous monosilicic acid onto iron oxide. *Geochimica Et Cosmochimica Acta* 73:923-934.

Delvigne C, Opfergelt S, Cardinal D, Delvaux B, André L. (2009) Distinct silicon and germanium pathways in the soil-plant system: evidence from banana and horsetail. *Journal of Geophysical Research – Biogeosciences* 114.

Demarest MS, Brzezinski MA, Beucher CP (2009) Fractionation of silicon isotopes during biogenic silica dissolution. *Geochimica Et Cosmochimica Acta* 73:5572-5583.

DeMaster DJ (1981) The supply and accumulation of silica in the marine environments. *Geochimica Et Cosmochimica Acta* 45:1715-1732.

De Monza JP (1991) L'altlas des forêts de France. de Monza (ed), Ligulé, Poitiers, France.

Derry LA, Kurtz AC, Ziegler K, Chadwick OA (2005) Biological control of terrestrial silica cycling and export fluxes to watersheds. *Nature* 433:728-731.

Desplanques V, Cary L, Mouret JC, Trolard F, Bourrié G, Grauby O, Meunier JD (2006) Silicon transfers in a rice field in Camargue (France). *Journal of Geochemical Exploration* 88:190-193.

Dietzel M (2000) Dissolution of silicates and the stability of polysilicic acid. *Geochimica Et Cosmochimica Acta* 64:3275–3281.

Dietzel M (2002) Interaction of polysilicic and monosilicic acid with mineral surfaces. In Stober I, Bucher K (eds) *Water–Rock Interaction*. Kluwer Academic Publishers, pp 207-235.

Ding TP, Jiang S, Wan D, Li Y, Li J, Song H, Liu Z, Yao X (1996) Silicon Isotope Geochemistry. Geological Publishing House, Bejing, China.

Ding TP, Wan DF, Wang C, Zhang F (2004) Silicon isotope compositions of dissolved silicon and suspended matter in the Yangtse River, China. *Geochimica et Cosmochimica Acta* 68: 205-216.

Ding TP, Ma GR, Shui MX, Wan DF, Li RH (2005) Silicon isotope study on rice plants from the Zhejiang province, China. *Chemical Geology* 218:41-50.

Ding TP, Zhou JX, Wan DF, Chen ZY, Wang CY, Zhang F (2008) Silicon isotope fractionation in bamboo and its significance to the biogeochemical cycle of silicon. *Geochimica Et Cosmochimica Acta* 72:1381-1395.

Doucet FJ, Schneider C, Bones SJ, Kretchmer A, Moss I, Tekely P and Exley C (2001) The formation of hydroxyaluminosilicates of geochemical and biological significance. *Geochimica Et Cosmochimica Acta* 65:2461-2467.

Douthitt CB (1982) The geochemistry of the stable isotopes of silicon. *Geochimica Et Cosmochimica Acta* 46:1449-1458.

Dove PM (1995) Kinetic and thermodynamic controls on silica reactivity in weathering environments. In White AF, Brantley SL (eds.) *Chemical weathering rates of silicate minerals*. *Review in Mineralogy*. Mineralogical Society of America, Washington D. C., pp 235–290.

Dove PM, Han N, Wallace AF, De Yoreo JJ (2008) Kinetics of amorphous silica dissolution and the paradox of the silica polymorphs. *Proceedings of the National Academy of Sciences* 105:9903-9908.

Drees LR, Wilding LP, Smeck NE, Senkayi AL (1989) Silica in soils: quartz and disorders polymorphs. In Dixon JB, Weed SB (eds) *Minerals in soil environments*. Soil Science Society of America, Madison, pp 914–974.

Drénou C (2006) Les racines, face cache des arbres. IDF, Paris

Drever JI (1988) The Geochemistry of Natural Waters. Prentice-Hall, Englewood Cliffs, NJ, USA.

Drever JI (1994) The effect of land plants on weathering rates of silicates minerals. *Geochimica Et Cosmochimica Acta* 58:2325-2332.

Dupré B, Dessert C, Oliva P, Goddéris Y, Viers J, François LM, Millot R, Gaillardet J (2003) Rivers, chemical weathering and Earth's climate. *Comptes Rendus Geoscience* 335:1141-1160.

Emadian SF, Newton RJ (1989) Growth enhancement of loblolly pine (Pinus taeda L.) seedlings by silicon. *Journal of Plant Physiology* 134:98-103.

Engström E, Rodushkin I, Öhlander B, Ingri J, Baxter DC (2008) Silicon isotopic composition of boreal forest vegetation in Northern Sweden. *Chemical Geology* 247:247-256.

Epstein E (1994) The Anomaly of silicon in plant biology. *Proceedings of the National Academy of Sciences of the United States of America* 91:11–17.

Epstein E (1999) Silicon. *Annual Review of Plant Physiology and Plant Molecular biology* 50:641-664.

Epstein E (2001) Silicon in plants: Facts vs. Concepts. In Datnoff LE, Snyder GH, Korndorfer GH (eds.) *Silicon in agriculture*. The Netherlands: Elsevier, pp 1-15.

Exley C (1998) Silicon in life: a bioinorganic solution to bioorganic essentiality. *Journal of Inorganic Biochemistry* 69: 139-144.

FAO (2006) Global Forest Resources Assessment: progress towards sustainable forest management, Forestry paper 147, Rome.

Farmer VC, Russel JD, Berrow ML (1980) Imogolite and proto-imogolite allophane in spodic horizons: evidence for a mobile aluminum silicate complex in Podzol formation. *European Journal of Soil Science* 31:673-684.

Farmer VC, Delbos E, Miller JD (2005) The role of phytolith formation and dissolution in controlling concentrations of silica in soil solutions and streams. *Geoderma* 127:71-79.

Faure G (1991) Principles and application of inorganic geochemistry. New York: MacMillan.

Fitzapatrick RW, Chittleborough DJ (2002) Titanium and Zirconium minerals. In Dixon JB, Schulze SB (eds) *Soil Mineralogy with environmental applications*. Madison, Wisconsin, USA, pp 667-690.

Fraysse F, Pokrovsky OS, Schott J, Meunier JD (2006) Surface properties, solubility and dissolution kinetics of bamboo phytoliths. *Geochimica Et Cosmochimica Acta* 70:1939-1951.

Fraysse F, Pokrovsky OS, Schott J, Meunier JD (2009) Surface chemistry and reactivity of plant phytoliths in aqueous solutions. *Chemical Geology* 258:197-206.

Fripiat F (2010) Isotopic approaches in the silicon cycle: The Southern Ocean case study. *PhD Thesis*, Université Libre de Bruxelles

Froelich PN, Andreae MO (1981) The marine geochemistry of germanium: ekasilicon. *Science* 213:205-297.

Froelich PN, Blanc V, Mortlock RA, Chillrud SN, Dunstan W, Udomkit A, Peng TH (1992) River fuxes of dissolved silica to the ocean were higher during glacials: Ge/Si in diatoms, rivers, and oceans. *Paleoceanography* 7:739-767.

Fulweiler RW, Nixon SW (2005) Terrestrial vegetation and the seasonal cycle of dissolved silica in a Southern New England coastal river. *Biogeochemistry* 74:115-130.

Gaillardet J, Dupré B, Allègre CJ (1995) A global geochemical mass budget applied to the Congo Basin rivers: Erosion rates and continental crust composition, *Geochimica Et Cosmochimica Acta* 59:3469-3485.

Gaillardet J, Dupré B, Allègre CJ, Négrel P (1997) Chemical and physical denudation in the Amazon River Basin. *Chemical Geology* 142:141-173.

Gaillardet J, Dupré B, Allègre CJ (1999a). Geochemistry of large river suspended sediments: Silicate weathering or recycling tracer? *Geochimica Et Cosmochimica Acta* 63:4037-4051.

Gaillardet J, Dupré B, Louvat P, Allègre CJ. (1999b) Global silicate weathering and CO2 consumption rates deduced from the chemistry of large rivers. *Chemical Geology* 159:3-30.

Gao J, Ding T, Tian S (2006) Silicon isotope compositions of dissolved silicon and suspended matter in the Yellow river, China. *Geochimica Et Cosmochimica Acta* 70(18 S): A192.

Garvin CJ (2006) An exploratory study of the terrestrial biogeochemical silicon cycle at a forested watershed in northern Vermon. *Dissertation*, Cornell University

Gedney N, Cox PM, Betts RA, Boucher O, Huntingford C, Stott PA (2006). Detection of a direct carbon dioxide effect in continental river runoff records. *Nature* 439:835-838.

Geis JW (1973) Biogenic silica in selected species of deciduous angiosperms. *Soil Science* 116: 113-119.

Georg RB, Reynolds BC, Frank M, Halliday AN (2006) Mechanisms controlling the silicon isotopic compositions of river waters. *Earth and Planetary Science Letters* 249:290-306.

Georg RB, Reynolds BC, West AJ, Burton KW, Halliday AN (2007) Silicon isotope variations accompanying basalt weathering in Iceland. *Earth and Planetary Science Letters* 261:476-490.

Georg RB, Zhu C, Reynolds BC, Halliday AN (2009a) Stable silicon isotopes of groundwater, feldspars, and clay coatings in the Navajo Sandstone aquifer, Black Mesa, Arizona, USA. *Geochimica Et Cosmochimica Acta* 73:2229-2241.

Georg RB, West AJ, Basu AR, Halliday AN (2009b) Silicon fluxes and isotope composition of direct groundwater discharge into the Bay of Bengal and the effect on the global ocean isotope budget. *Earth and Planetary Science Letters* 283:67-74.

Gérard F, François M, Ranger J (2002) Processes controlling silica concentration in leaching and capillary soil solutions of an acidic brown forest soil (Rhône, France). *Geoderma* 107:197-226.

Gérard F, Ranger J, Menetrier C, Bonnaud P (2003) Silicate weathering mechanisms determined using soil solutions held at high matric potential. *Chemical Geology* 202:443-460.

Gérard F, Mayer KU, Hodson MJ, Ranger J (2008) Modelling the biogeochemical cycle of silicon in soils: Application to a temperate forest ecosystem. *Geochimica Et Cosmochimica Acta* 72:741-758.

Giesler R, Ilvesniemi H, Nyberg L, van Hees P, Starr M, Bishop K, Kareinen T, Lundström US (2000) Distribution and mobilization of Al, Fe and Si in three podzolic soil profiles in relation to the humus layer. *Geoderma* 94:149-263.

Gislason SR, Oelkers EH, Eiriksdottir ES, Kardjilov MI, Gisladottir G, Sigfusson B, Snorrason A, Elefsen S, Hardardottir J, Torssander P, Oskarsson N (2009) Direct evidence of the feedback between climate and weathering. *Earth and Planetary Science Letters* 277:213-222.

Goddéris Y, François LM, Probst A, Schott J, Moncoulon D, Labat D, Viville D (2006) Modelling weathering processes at the catchment scale: the WITCH numerical model. *Geochimica et Cosmochimica Acta* 70: 1128–1147.

Gordeev VV, Martin JM, Sidorov IS, Sidorova MV (1996) A reassessment of the Eurasian river input of water, sediment, major elements, and nutrients to the Arctic Ocean. *American Journal of Science* 296:664-691.

Granier A, Bréda N, Biron P, Villette S (1999) A lumped water balance model to evaluate duration and intensity of drought constraints in forest stands. *Ecological Modelling* 116:269-283.

Hammond KE, Evans DE, Hodson MJ (1995) Aluminium/silicon interactions in barley (Hordeum vulgare L.) seedlings. *Plant and soil* 173:89-95.

Henriet C, Draye X, Oppitz I, Swennen R, Delvaux B (2006) Effects, distribution and uptake of silicon in banana (Musa spp.) under controlled conditions. *Plant and Soil* 287:359-374.

Henriet C, Draye X, Dorel M, Bodarwe L, Delvaux B. (2008a) Leaf silicon content in banana (Musa spp.) reveals the weathering stage of volcanic ash soils in Guadeloupe. *Plant and Soil* 313:71-82.

Henriet C, De Jaeger N, Dorel M, Opfergelt S, Delvaux B (2008b) The reserve of weatherable primary silicates impacts the accumulation of biogenic silicon in volcanic ash soils. *Biogeochemistry* 90:209-223.

Herbauts J, Dehalu FA, Gruber W (1994) Quantitative-determination of plant opal content in soils, using a combined method of heavy liquid separation and alkali dissolution. *European Journal of Soil Science* 45:379-385.

Herbillon AJ (1986) Chemical estimation of weatherable minerals present in the diagnostic horizons of low activity clay soils. In Beinroth F, Camargo M, Eswaran (eds) *Proceedings of the 8th International Soil Classification Workshop: Classification, Characterization and Utilization of Oxisols*, Embrapa, Rio de Janeiro, pp. 39-48.

Hiemstra T, Barnett MO, van Riemsdijk WH (2007) Interaction of silicic acid with goethite. *Journal of Colloid and Interface Science* 310:8-17.

Hinsinger P, Barros ONF, Benedetti MF, Noack Y, Callot G (2001) Plant-induced weathering of a basaltic rock: experimental evidence. *Geochimica Et Cosmochimica Acta* 65:137-152.

Hodson MJ, Evans DE (1995) Aluminium/silicon interactions in higher plants. *Journal of Experimental Botany* 46:161-171.

Hodson MJ, Sangster AG (1999) Aluminium/silicon interactions in conifers. *Journal of Inorganic Biochemistry* 76:89-98.

Hodson MJ, White PJ, Mead A, Broadley MR (2005) Phylogenetic variation in the silicon composition of plants. *Annals of Botany* 96:1027-1046.

Hodson MJ, Parker AG, Leng MJ, Sloane HJ (2008) Silicon, oxygen and carbon isotope composition of wheat (Triticum aestivum L.) phytoliths: implications for palaeoecology and archaeology. *Journal of Quaternary Science* 23:331-339.

Humborg C, Rahm L, Smedberg E, Mörth CM, Danielsson A (2006) Dissolved silica dynamics in boreal and arctic rivers: vegetation control over temperature? In: Ittekot V, Unger D, Humborg C, Tac An N (eds.) *The Silicon Cycle. Human perturbations and impacts on aquatic systems*. SCOPE, 66, pp 53-69.

Hughes S, Reynolds B (1990) Evaluation of porous ceramic cups for monitoring soil-water aluminium in acid soils: comment on a paper by Raulund-Rasmussen (1989). *European Journal of Soil Science* 41:325-328.

Iler RK (1979) The Chemistry of Silica. Wiley-Interscience, New York.

Ingestad T (1971) A definition of optimum nutrient requirements in birch seedlings. II. *Physiologia Plantarum* 24:118-125.

IPCC Intergovernmental Panel on Climate Change, 2001. Climate Change: The Scientific Basis. Cambridge Univ. Press, Cambridge, UK.

Ittekot V, Unger D., Humborg C, Tac An N. (Eds.) *The Silicon cycle. Human Perturbations and impacts on aquatic systems*. SCOPE, 66, 275 pp.

IUSS Working Group WRB (2006) World reference base for soil resources 2006, 2nd edn. World Soil Resources Reports No. 103. FAO, Rome.

Jackson ML, Tyler SA, Willis AL, Bourbeau GA, Pennington RP (1948) Weathering sequence of clay-size minerals in soils and sediments. I. Fundamental generalizations. *Journal of Physical and Colloid Chemistry* 52:1237-1260.

Jackson RB, Canadell J, Ehleringer JR, Mooney HA, Sala OE, Schulze ED (1996) A global analysis of root distributions for terrestrial biomes. *Oecologia* 108:389-411.

Jaffrain J (2006) Effet des essences forestières sur le fonctionnement organo-minéral d'un sol acide: observations et modélisation. *PhD Thesis*, Université Henri Poincarré, Nancy-I.

Jaffrain J, Gérard F, Meyer M, Ranger J (2007) Assessing the quality of dissolved organic matter in forest soils using ultraviolet absorption spectrophotometry. *Soil Science Society of America Journal* 71:1851-1855.

Jennerjahn TC, Knoppers BA, de Souza WFL, Brunskill GJ, Ivan E, Silva L, Adi S (2006) Factors controlling dissolved silica in tropical rivers . In:

Ittekot, V., Unger D, Humborg, C, Tac An N (eds.) T*he Silicon Cycle. Human perturbations and impacts on aquatic systems*. SCOPE, 66, pp. 29-52.

Johnson-Maynard JL, Graham RC, Shouse PJ, Quideau SA (2005) Base cation and silicon biogeochemistry under pine and scrub oak monocultures: implications for weathering rates. *Geoderma* 126:353-365.

Jones LHP Handreck KA (1963). Effects of iron and aluminum oxides on silica in solution in soils. *Nature* 198:852-853.

Jones LHP, Handreck KA (1965) Studies of silica in the oat plant. III. Uptake of silica from soils by plant. *Plant and Soil* 23:79-96.

Jones L HP, Handreck KA (1967) Silica in soils, plants, and animals. *Advancies in Agronomy* 19:107-149.

Kamatani A, Oku O (2000) Measuring biogenic silica in marine sediments. *Marine chemistry* 68:219-229.

Karathanasis AD (2002) Mineral equilibria in environmental soil systems. In Dixon JB, Weed SB (eds.) *Soil Mineralogy with environmental applications*. Madison (USA) Soil Science Society of America, pp 109-151.

Kelly EF (1990) Methods for extracting opal phytoliths from soil and plant material. Workshop on biotic indicators of global change, Seatlle, Washington

Kelly EF, Chadwick OA, Hilinski TE (1998) The effect of plants on mineral weathering. *Biogeochemistry* 42:21-53.

Kleber M, Scwendenmann L, Veldkamp E, Röbner J, Jahn R (2007) Halloysite versus gibbsite: silicon cycling as a pedogenetic process in two lowland neotropical rain forest soils of La Selva, Costa Rica. *Geoderma* 138:1-11.

Klein RL, Geis JW (1978) Biogenic silica in the pinaceae. *Soil Science* 126:145-156.

Knight CTG, Kinrade SD (2001) A primer on the aqueous chemistry of silicon. In Datnoff L E, Snyder GH, Korndorfer GH (eds) *Silicon in agriculture.* Elsevier, The Netherlands, pp 57-84.

Kodama H, Ross GJ (1991) Tiron dissolution method used to remove and characterize inorganic components in soils. *Soil Science Society of America journal* 55:1180–1187.

Koning E, Epping E, Van Raaphorst W, (2002) Determing biogenic silica in marine samples by tracking silicate and aluminium concentrations in alkaline leaching solutions. *Aquatic Geochemistry* 8:37-67.

Korndörfer GH, Lepsch I (2001) Effect of silicon on plant growth and crop yield. In: Datnoff LE, Snyder GH, Korndörfer GH (eds) *Silicon in agriculture*. Elsevier, The Netherlands, pp 133–147.

Kurtz AC, Derry LA, Chadwick OA (2001) Accretion of asian dust to Hawaiian soils : isotopic, elemental and mineral mass balances. *Geochimica Et Cosmochimica Acta* 65:1971-1983.

Kurtz A, Derry LA, Chadwick OA (2002) Germanium-silicon fractionation in the weathering environment. *Geochimica Et Cosmochimica Acta* 66:1525-1537.

Kurtz AC, Derry LA (2004) Tracing silicate weathering and terrestrial silica cycling with Ge/Si ratios, in Wanty RB, Seal RR (eds) *Proceedings of 11th International Symposium on Water Rock Interaction*. A.A. Balkema, Leiden, Netherlands, pp 833– 836.

Lal R (2004) Soil carbon sequestration impacts on global climate change and food security. *Science* 304:1623-1627.

Lal R (2010) Managing soils for a warming earth in a food-insecure and energy starved wolrd. *Journal of Plant Nutrition and Soil Science* 173: 4-15.

Laruelle GG et al. (2009) Anthropogenic perturbations of the silicon cycle at the global scale: key role of the land-ocean transition. *Global biogeochemical cycles* 23.

Levrel G, Ranger J (2006) Effet des substitutions d’essences forestières sur les propriétés physiques d’un Alocrisol (site expérimental de la forêt de Breuil-Chenue/Morvan). *Etude et gestion des sols* 13:71-88.

Liang YC, Yang CG, Shi HH (2001) Effects of silicon on growth and mineral composition of barley grown under toxic levels of aluminium. *Journal of Plant Nutrition* 24:229-243.

Liang Y, Hua H, Zhu Y, Zhang J, Cheng C, Römheld V (2006) Importance of plant species and external silicon concentration to active silicon uptake and transport. *New Phytologist* 172:63-72.

Liang Y, Sun W, Zhu YG, Christie P (2007) Mechanisms of silicon-mediated alleviation of abiotic stresses in higher plants: A review. *Environmental Pollution* 147:422-428.

Likens GE, Pierce RS, Eaton JS, Johnson NM (1977) Biogeochemistry of a forested ecosystem. Springer-Verlag

Likens GE, Bormann FH (1995) Biogeochemistry of a forested ecosystem. Springer-Verlag, second edition.

Lindsay WL (1979). Chemical Equilibria in Soils. Wiley Interscience, New-York.

Lovering TS (1959) Significance of accumulator plants in rock weathering. *Bulletin of the Geological Society of America* 70:781– 800.

Lucas Y, Luizao FJ, Chauvel A, Rouiller J, Nahon D (1993) The relation between biological activity of the rain forest and mineral composition of soils. *Science* 260:521-523.

Lucas Y (2001) The role of plants in controlling rates and products of weathering: importance of biological pumping. Annual Reviews – Earth and Planetary Sciences 29:135-163.

Lugolobi F, Kurtz AC, Derry LA (2010) Germanium-silicon fractionation in a tropical, granitic weathering environment. *Geochimica Et Cosmochimica Acta* 74:1294-1308.

Lundström US, van Breemen N, Bain D (2000) The podzolization process. A review. *Geoderma* 94:91–107.

Lux, A, Luxova M, Abe J, Morita S, Inanaga S (2003a) Silicifcation of bamboo (*Phyllostachys heterocycla* mitf.) root and leaf. *Plant and Soil* 255:85-91.

Lux A, Luxova M, Abe J, Tanimoto E, Hattori T, Inanaga S (2003b) The dynamics of silicon deposition in the sorghum root endodermis. *New Phytologist* 158:437-441.

Ma JF, Miyake Y, Takahashi E (2001) Silicon as a beneficial element for crop plants. In Datnoff LE, Snyder GH, Korndorfer GH (eds) *Silicon in agriculture*. The Netherlands. Elsevier, pp 17-39.

Ma JF, Takahashi E (2002) *Soil, fertilizer, and plant silicon research in Japan*. The Netherlands: Elsevier.

Ma JF (2004) Role of silicon in enhancing the resistance of plants to biotic and abiotic stresses. Soil *Science and Plant Nutrition* 50:11-18.

Ma JF, Yamaji N (2006a) Silicon uptake and accumulation in higher plants. *Trends in Plant Science* 11:392–397.

Ma JF, Tamai K, Yamaji N, Mitani N, Konishi S, Katsuhara M, Ishiguro M, Murata Y, Yano M (2006b) A silicon transporter in rice. *Nature* 440:688-691.

Ma JF, Yamaji N, Mitani N, Tamai K, Konishi S, Fujiwara T, Katsuhara M, Yano M (2007) An efflux transporter of silicon in rice. *Nature* 448:209-212.

Madella M, Powers-Jones AH, Jones MK (1998) A simple method of extraction of opal phytoliths from sediments using a non-toxic heavy liquid. *Journal of Archaeological Science* 25:801-803.

Madella M, Alexandre A, Ball T (2005) International Code for Phytolith Nomenclature 1.0. *Annals of Botany* 96: 253–260.

Mann DG (1999) The species concept in diatoms. *Phycologia* 38:437-495.

Mareschal L. (2008) Effet des substitutions d'essences forestières sur l'évolution des sols et de leur mineralogie. *PhD Thesis*, Université Henri Poincarré, Nancy-I.

Mareschal L, Bonnaud P, Turpault MP, Ranger J (2010) Impact of common European tree species on the chemical and physicochemical properties of fine earth: an unusual pattern. *European Journal of Soil Science* 61:14-23.

Markewitz D, Richter D (1998) The bio in aluminium and silicon geochemistry. *Biogeochemistry* 42:235-252.

Markewitz D, Davidson EA, Figueiredo RO, Victoria RL, Krusche AV (2001) Control of cation concentrations in stream waters by surface soil processes in an Amazonian watershed. *Nature* 410:802-805.

Marques R, Ranger J, Gelhaye D, Pollier B, Ponette Q, Goedert O (1996) Comparison of chemical composition of soil solutions collected by zero-tension plate lysimeters with those from ceramic-cup lysimeters in a forest soil. *European Journal of Soil Science* 47:407-417.

Marschner H (1995) Mineral Nutrition of higher plants. Academic Press, 2nd edition, London

Matichenkov VV, Bocharnikova EA (2001) The relationship between silicon and soil physical and chemical properties. In Datnoff LE, Snyder GH, Korndorfer GH (eds) *Silicon in agriculture*. The Netherlands. Elsevier, pp 209-219.

Matthews D (2006) The water cycle freshens up. *Nature* 439:793-794.

McKeague JA, Cline MG (1963a) Silica in soils. *Advances in Agronomy* 15:339-396.

McKeague JA, Cline MG (1963b) Silica in soil solutions : II. The adsorption of monosilicic acid by soil and by other substances. *Canadian Journal of Soil Science* 43:83-96.

Mehra OP Jackson ML (1960) Iron oxides removal from soils and clays by dithionite-citrate system buffered with sodium bicarbonate. In Proceeding of 7th National Conference Clays Clay Minerals, Washington, pp 317-327.

Meunier JD, Colin F, Alarcon C (1999) Biogenic silica storage in soils. *Geology* 27:835-838.

Meunier JD, Alexandre A, Colin F, Braun JJ (2001) Intérêt de l'étude du cycle biogéochimique du silicium pour interpréter la dynamique des sols tropicaux. *Bulletin de la Société géologique de France* 172:533–538.

Meunier JD (2003). Le rôle des plantes dans le transfert du silicium à la surface des continents. *Comptes Rendus Geoscience* 335:1199-1206.

Meunier JD, Guntzer F, Kirman S, Keller C (2008) Terrestrial plant-Si and environmental changes. *Mineralogical magazine* 72:263-267.

Meybeck M (1979) Concentrations des eaux fluviales en elements majeurs et apports en solution aux oceans. *Revue de Géologie Dynamique et de Géographie Physique* 21:215-246.

Michalopoulos P, Aller RC (2004) Early diagenesis of biogenic silica in the Amazon delta : alteration, authigenic clay formation and storage. *Geochimica Et Cosmochimica Acta* 68:1061-1085.

Millot G. 1979 Les argiles. In: Pour la Science, n°20, juin, pp 61-70.

Milliman JD, Meade RH (1983) World-wide delivery of river sediment to the oceans. *Journal of Geology* 91:1-21.

Milliman JD, Syvitski JPM (1992) Geomorphic/tectonic control of sediment discharge to the ocean : the importance of small mountainous rivers. *Journal of Geology* 100:525-544.

Miretzky P, Conzonno V, Fernandez Cirelli A (2001) Geochemical processes controlling silica concentrations in groundwaters of the Salado River drainage basin, Argentina. *Journal of Geochemical Exploration* 73:155-166.

Mitani N, Ma JF (2005) Uptake system of silicon in different plant species. *Journal of Experimental Botany* 56:1255-1261.

Monger HC, Kelly EF (2002) Silica minerals. In Dixon JB, Weed SB (Eds.) *Soil Mineralogy with environmntal applications*. Madison (USA): Soil Science Society of America, pp 611-636.

Morris RC, Fletcher AB (1987) Increased solubility of quartz following ferrous-ferric iron reactions. *Nature* 330:558-561.

Mortlock RA, Froelich PN (1996) Determination of germanium by isotope dilution-hydride generation inductively coupled plasma mass spectrometry. *Analytical Chimica Acta* 322: 5638-5645.

Moulton KL, West J, Berner RA (2000) Solute flux and mineral mass balance approaches to the quantification of plant effects on silicate weathering. *American Journal of Science* 300:539–570.

Murnane RJ, Stallard RF (1990) Germanium and silicon in rivers of the Orinoco drainage basin. *Nature* 344:749-752.

Nagy KL (1995) Dissolution and precipitation kinetics of sheet silicates. In White AF Brantley SL (eds) *Chemical weathering rates of silicate minerals.* Mineralogical Society of America and the Geochemical Society, Reviews in Mineralogy and Geochemistry, pp 173-233.

Oliva P, Viers J, Dupré B, Fortuné JP, Martin F, Braun JJ, Nahon D, Robain H (1999) The effect of organic matter on chemical weathering: study of a small tropical watershed: Nsimi-Zoétélé site, Cameroon. *Geochimica Et Cosmochimica Acta* 63:4013-4035.

Opfergelt S, Cardinal C, Henriet C, Draye X, André L, Delvaux B (2006a) Silicon isotope fractionation by banana (Musa spp.) grown in a continuous nutrient flow device. *Plant and Soil* 285:333-345.

Opfergelt S, Cardinal D, Henriet C, André L, Delvaux B (2006b) Silicon isotope fractionation between plant parts in banana: In situ vs. in vitro. *Journal of Geochemical Exploration* 88:224-227.

Opferfelt S (2008) Silicon cycle in the soil-plant system: biogeochemical tracing using Si isotopes. *PhD Thesis*, Université catholique de Louvain.

Opfergelt S, Delvaux B, André L, Cardinal D (2008) Plant silicon isotopic signature might reflect soil weathering degree. *Biogeochemistry* 91:163-175.

Opfergelt S, de Bournonville G, Cardinal D, André L, Delstanche S, Delvaux B (2009) Impact of soil weathering degree on silicon isotopic fractionation during adsorption onto iron oxides in basaltic ash soils, Cameroon. *Geochimica Et Cosmochimica Acta* 73:7226-7240.

Opfergelt S, Cardinal D, André L, Delvigne C, Bremond L, Delvaux B (2010) Variations of δ^{30}Si and Ge/Si with weathering and biogenic input in tropical basaltic ash soils under monoculture. *Geochimica Et Cosmochimica Acta* 74:225-240.

Parfitt RL (1978) Anion adsorption by soils and soil materials. *Advances in Agronomy* 30:1-50.

Parkhurst DL, Appelo CAJ (1999) User's guide to PHREEQC (Version 2)—A computer program for speciation, batch-reaction, one-dimensional transport, and inverse geochemical calculations: U.S. Geological Survey Water-Resources Investigations Report 99-4259, 310 pp.

Piperno DR, Stothert KE (2003) Phytolith evidence for early Holocene cucurbita domestication in southwest Ecuador. *Science* 299: 1054-1057.

Pearsall DM, Piperno DR (1993) Current research in phytolith analysis: Applications in archaeology and paleoecology. *Masca Research Papers in Science and Archaeology* 10:212.

Pédro G (1984) La genèse des argiles pédologiques. Ses implications minéralogiques, physico-chimiques et hydriques. *Sci. Géol. Bull.* 37: 333-347.

Peel MC, Finlayson BL, McMahon TA (2007) Updated world map of the Köppen-Geiger climate classification. *Hydrology and Earth System Sciences* 11:1633-1644.

Perry CC, Keeling-Tucker (1998) Aspects of the bioinorganic chemistry of silicon in conjunction with the biometals calcium, iron and aluminium. *Journal of Inorganic Biochemistry* 69:181-191.

Piperno DR (1988) Phytolith Analysis: An Archaeological and Geological Perspective. Academic Press: San Diego

Pokrovski GS, Martin F, Hazemann JL, Schott J (2000) An X-ray absorption fine structure spectroscopy study of germanium-organic ligand complexes in aqueous solution. *Chemical Geology* 163:151-165.

Pokrovski GS, Schott J, Garges F, Hazemann JL (2003) Iron (III)-silica interactions in aqueous solution: Insights from X-ray absorption fine structure spectroscopy. *Geochimica Et Cosmochimica Acta* 67:3559-3573.

Pokrovsky OS, Schott J, Kudryavtzev DI, Dupré B (2005) Basalt weathering in Central Siberia under permafrost conditions. *Geochimica Et Cosmochimica Acta* 69: 5659-5680.

Puhe J (2003) Growth and development of the root system of Norway spruce (Picea abies) in forest stands-a review. *Forest Ecology and Management* 175:253-273.

Ragueneau O, Tréguer P, Leynaert A, Anderson RF, Brezinski, DeMaster DJ, Dugdale RC, Dymond J, Fischer G, François R, Heinze C, Maier-Reimer E, Martin-Jézéquel V, Neslon D, Quéguiner B (2000) A review of the Si cycle in the modern ocean: recent progress and missing gaps in the application of biogenic opal as a paleo-productivity proxy. *Global and Planetary Change* 26:315-366.

Ragueneau O, Conley DJ, Leynaert A, Longphuirt SN, Slomp CP (2006) Responses of coastal ecosystems to anthropogenic perturbations of silicon cycling. In: Ittekot V, Unger D, Humborg C, Tac An N (Eds.) *The Silicon Cycle. Human perturbations and impacts on aquatic systems*. SCOPE, 66, pp. 197-214.

Rai D, Kittrick JA (1989) Mineral equilibria and the soil system. In Dixon J and Weed S (eds) *Minerals in Soil Environments*. Madison, Soil Science Society of America, pp 161-198.

Ranger J, Bonneau M (1984) Effets prévisibles de l'intensification de la production et des récoltes sur la fertilité des sols de forêt. Le cycle biologique en forêt. *Revue Forestière Française* XXXVI :93-122.

Ranger J, Colin-Belgrand M, Nys C (1995) Le cycle biogéochimique des éléments majeurs dans les écosystèmes forestiers. *Etude et Gestion des Sols* 2:119-134.

Ranger J, Marques R, Colin-Belgrand M, Flammang N, Gelhaye D (1995) The dynamics of biomass and nutrient accumulation in a Douglas-fir (Pseudotsuga menziesii Franco) stand studied using a chronosequence approach. *Forest Ecology and Management* 72:167–183.

Ranger J, Colin-Belgrand M (1996) Nutrient dynamics of chestnut tree (*Castanea sativa* Mill.) coppice stands. *Forest Ecology and Management* 86:259-277.

Ranger J, Marques R, Colin-Belgrand M (1997) Nutrients dynamics during the development of a Douglas fir (Pseudotsuga menziesii Mirb.) stand. *Acta Oecologica* 18:73-91.

Ranger J, Andreux F et al. (2004) Effet des substitutions d'essence sur le fonctionnement organo-minéral de l'écosystème forestier, sur les communautés microbiennes et sur la diversité des communautés fongiques mycorhiziennes et saprophytes (cas du dispositif experimental de Breuil – Morvan). Rapport final du contrat INRA-GIP Ecofor 2001-24, n°INRA 1502A Nancy : INRA-Champenoux, Biogéochimie des écosystèmes forestiers, 202 pp.

Raulund-Rasmussen K (1991) Aluminium contamination of acid soil solution isolated by means of porcelain suction cups: a reply to a paper by Hughes and Reynolds (1990) and an interpretation of aluminium release. *European Journal of Soil Science* 42:271-276.

Raven JA (1983) The transport and function of silicon in plants. *Biological Review of the Cambridge Philosophical Society* 58:179-207.

Raven, J.A. (2001) Silicon transport at the cell and tissue level. In Datnoff LE, Snyder GH, Korndorfer GH (eds.) *Silicon in agriculture.*The Netherlands: Elsevier, pp 41-55.

Raymo ME, Ruddiman WF, Froelich P (1988) Influence of late Cenozoic mountain building on ocean geochemical cycles. *Geology* 16:649-653.

Reynolds, BC, Frank M, Halliday AN (2006) Silicon isotope fractionation during nutrient utilization in the North Pacific. *Earth and Planetary Science Letters* 244:431-443.

Reynolds BC, et al. (2007) An inter-laboratory comparison of Si isotope reference materials. *Journal of Analytical Atomic Spectrometry* 22:561-568.

Richmond KE, Sussman M (2003). Got silicon? The non-essential beneficial plant nutrient. *Current Opinion in Plant Biology* 6:268-272.

Robert M, Tessier D (1974) Méthode de préparation des argiles des sols pour des études minéralogiques. *Annales Agronomiques* 25:859-882.

Rouiller J, Burtin G, Souchier B (1972) La dispersion des sols dans l'analyse granulométrique. Méthode utilisant les résines échangeuses d'ions. ENSAIA Nancy 14 : 194-205

Rustad LE, Cronan CS (1995) Biogeochemical controls of aluminium chemistry in the O horizon of a red spruce (Picea rubens Sarg.) stand in central Maine, USA. *Biogeochemistry* 29:107-129.

Saccone L, Conley DJ, Koning E, Sauer D, Sommer M, Kaczorek D, Blecker SW, Kelly EF (2007) Assessing the extraction and quantification of amorphous silica in soils of forest and grassland ecosystems. *European Journal of Soil Science* 58:1446–1459.

Saccone L, Conley DJ, Likens GE, Bailey SW, Buso DC, Johnson CE (2008). Factors that control the range and variability of amorphous silica in soils in the Hubbard Brook experimental Forest. *Soil science society of America journal* 72:1637-1644.

Saint-André L, Thongo M'Bou, Mabiala A, Mouvondy W, Jourdan C, Roupsard O, Deleporte Ph, Hamel O, Nouvellon Y (2005) Age-related equations for above- and below-ground biomass of a Eucalyptus hybrid in Congo. *Forest Ecology and Management* 205:199-214.

Sangster AG, Hodson MJ (1986) Silica in higher plants. In Evered D, O'Connor M (eds) *Silicon Biochemistry.* Ciba Foundation Symposium, John Wiley: Chichester, pp 90-107.

Sangster AG, Hodson MJ, Tubb HJ (2001) Silicon deposition in higher plants. In Datnoff LE, Snyder GH, Korndörfer GH (eds) *Silicon in Agriculture*. Amsterdam. Elsevier, pp 85-113.

Sangster AG, Ling L, Gérard F, Hodson MJ (2007) X-ray microanalysis of needles from Douglas fir growing in environments of contrasting acidity. *Water Air Soil Pollution* 7:143-149.

Sauer D, Saccone L, Conley DJ, Herrmann L, Sommer M (2006) Review of methodologies for extracting plant-available and amorphous Si from soils and aquatic sediments. *Biogeochemistry* 80:89-108.

Schwertmann U, Taylor RM (1989) Iron oxides. In Dixon JB, Weed SB (eds) *Minerals in soil environments*. Madison, Wisconsin, U.S. Soil Science Society of America, pp 379-438.

Schulze, DG (2002) An introduction to soil mineralogy. In Dixon JB, Schulze DG (eds) *Soil mineralogy with environmental applications*. Madison. Soil Science Society of America, pp 1-35.

Schwertmann U, Cornell RM (1991) Iron oxides in the laboratory. Preparation and characterization. VCH, Weinhein, 204p.

Scribner AM, Kurtz AC, Chadwick OA (2006) Germanium sequestration by soil: Targeting the roles of secondary clays and Fe-oxyhydroxides. *Earth and Planetary Science Letters* 243:760-770.

Seddoh FK (1973) Altération des roches cristallines du Morvan (granite, granophyres,rhyolites). Etude minéralogique, géochimique et micro-morphologique. *PhD Thesis*. University of Dijon, France.

Sicard C, Saint-Andre L, Gelhaye D, Ranger J (2005) Effect of initial fertilization on biomass and nutrientcontent of Norway spruce and Douglas fir plantations at the same site. *Trees-structure and Function* 20:229-246.

Siever R, Woodford N (1973) Sorption of silica by clay minerals. *Geochimica Et Cosmochimica Acta* 37:1851-1880.

Simonson RW (1995) Airborne dust and its significance to soils. *Geoderma* 65:1-43.

Smetacek V (1998) Diatoms and the silicate factor. *Nature* 391:25-32.

Smetacek V (1999) Diatoms and the ocean carbon cycle. *Protist* 150: 25-32.

Smithson F (1956) Plant opal in soil. *Nature* 178:107.

Sommer M, Kaczorek D, Kuzyakov Y, Breuer J (2006) Silicon pools and fluxes in soils and landscapes-a review. *Journal of Plant Nutrition and Soil Science* 169:310–329.

Street-Perrott FA, Barker P (2008) Biogenic silica: a neglected component of the coupled global continental biogeochemical cycles of carbon and silicon. *Earth Surface Processes and Landforms* 33:1436-1457.

Struyf E, Opdekamp W, Backx H, Jacobs S, Conley DJ, Meire P (2009) Vegetation and proximity to the river control amorphous silica storage in a riparian wetland (Biebrza National Park, Poland). *Biogeosciences Discussions* 6:895-918.

Stumm W, Morgan JJ (1996) Aquatic chemistry-chemical equilibria and rates in natural waters. Wiley, New York, 1022 p.

Summerfield MA, Hulton NJ (1994) Natural controls of fluvial denudation rates in major world drainage basins. *Journal of Geophysical Research* 99:13871-13883.

Takahashi E, Ma JF, Miyake Y (1990) The possibility of silicon as an essential element for higher plants. *Comments Agricultural and Food Chemistry* 2:99-122.

Tegen I, Harrison SP, Kohfeld KE, Prentice IC, Coe MC, Heimann M (2002) The impact of vegetation and preferential source areas on global dust aerosol: Results from a model study. *Journal of Geophysical Research* 107.

Tegen I, Kohfeld KE (2006) Atmospheric transport of silicon. In: Ittekot V, Unger D, Humborg C, Tac An N (Eds.) *The Silicon Cylce. Human perturbations and impacts on aquatic systems*. SCOPE, 66, pp 81-92.

Titeux H (2005) Influence du fonctionnemnet de la litière et des réserves minérales du sol. PhD Thesis, Université catholique de Louvain.

Tréguer P, Pondaven P (2000) Silica control of carbon dioxide. *Nature* 406:358-359.

Tréguer P, Nelson DM, Van Bennekom AJ, De Master DJ, Leynaert A, Quéguiner B (1995) The silica balance in the world ocean: a reestimate. *Science* 268:375-379.

Trudgill ST (1983) Soil and vegetation systems – Contempary problems in geography. 2nd editions, 209 pp.

Turner RE, Rabalais NN, Justic D, Dortch Q (2003) Global patterns of dissolved N, P and Si in large rivers. *Biogeochemistry* 64:297-317.

Turpault MP, Trotigon L (1994) The dissolution of biotite single crystals in dilute HNO_3 at 24°C: evidence of an anisotropic corrosion process of micas in acidic solutions. *Geochimica Et Cosmochimica Acta* 58:2761-2775.

Van Cappellen P (2003) Biomineralization and global biogeochemical cycles. *Review in Mineralogy and Geochemistry* 54:357-381.

Varela DE, Pride CJ, Brzezinski MA (2004) Biological fractionation of silicon isotopes in Southern Ocean surface waters. *Global Biogeochemical Cycles* 18.

Vesely J, Majer V, Kopacek J, Safanda J, Norton SA (2005) Increasing silicon concentrations in Bohemian Forest lakes. *Hydrology and Earth System Sciences* 9:699-706.

Vialette Y (1965) Granitisation hercynienne dans le massif central français. *Sciences de la Terre* 369-382.

Volk T (1987) Feedbacks between weathering and atmospheric CO_2 over the last 100 million years. *American Journal of Science* 287:763-779.

Vuai SAH, Tokuyama A (2007) Solute generation and CO_2 consumption during silicate weathering under subtropical, humid climate, northern Okinawa Island, Japan. *Chemical geology* 236:199-216.

Wada K (1989) Allophane and imogolite. In Dixon JB, Weed SB (eds) *Minerals in Soil Environments*. Soil Science Society of America Book Series No. 1, Madison, WI, pp. 1051-1087.

Walker JCJ, Hays PB, Kasting JF (1981) A negative feedback mechanism for thelong term stabilization of the earth's surface temperature. *Journal of Geophysical Research* 86:9766-9782.

Watteau F, Villemin G (2001) Ultrastructural study of the biogeochemical cycle of silicon in the soil and litter of a temperate forest. *European Journal of Soil Science* 52:385-396.

Wedepohl KH (1995) The composition of the continental crust. *Geochimica Et Cosmochimica Acta* 59:1217-1232.

Wenzel WW, Wieshammer G (1995) Suction cup materials and their potential to bias trace metal analyses of soil solutions: a review. *International Journal of Environmental Analytical Chemistry* 59:277-290.

White AF, Blum AE (1995): Effects of climate on chemical weathering in watersheds. *Geochimica Et Cosmochimica Acta* 59 :1729-1747.

White AF (1995). Chemical weathering rates of silicate minerals in soils. In White AF, Brantley SL (eds) *Chemical weathering rates of silicate minerals.* Mineralogical Society of America and the Geochemical Society, Reviews in Mineralogy and Geochemistry, pp 407-460.

White R, Murray S, Rohweder M (2000), Pilot analysis of global ecosystems: Grassland ecosystems, report, World Resour. Inst., Washington, D. C.

Wilding LP, Drees LR (1974) Contributions of forest opal and associated crystalline phases to fine silt and clay fractions of soils. *Clays and Clay Minerals* 22:295-306.

Wonisch H, Gérard F, Dietzel M, Jaffrain J, Nestroy O, Boudot JP (2008) Occurrence of polymerized silicic acid and aluminium species in two forest soil solutions with different acidity. *Geoderma* 144:435-445.

Wüst RAJ, Bustin RM (2003) Opaline and Al–Si phytoliths from a tropical mire system of West Malaysia: abundance, habit, elemental composition, preservation and significance. *Chemical Geology* 200:267–292.

Wyttenbach A, Tobler L (1998) Effet of surface contamination on results of plant analysis. *Communications in Soil Science and Plant Analysis* 29:809-823.

Yamaji N, Mitani N, Ma JF (2008) A transporter regulating silicon distribution in rice shoots. *Plant Cell* 20:1381-1389.

Yeghicheyan D, Carignan J, et al. (2001) A compilation of silicon and thirty one trace elements measured in the natural river water reference material SLRS-4 (NRC-CNRC). *Geostandards Newsletter: The Journal of Geostandards and Geoanalysis* 25:465-474.

Zhao Z, Pearsall DM (1998) Experiments for improving phytolith extraction from soils. *Journal of Archaeological Science* 25:587-598.

Ziegler K, Chadwick OA, Brzezinski MA, Kelly EF (2005a) Natural variations of δ^{30}Si ratios during progressive basalt weathering, Hawaiian Islands. *Geochimica Et Cosmochimica Acta* 69:4597-4610.

Ziegler K, Chadwick OA, White AF, Brzezinski MA (2005b) δ^{30}Si systematics in a granitic saprolite, Puerto Rico. *Geology* 33:817-820.

LIST OF PUBLICATIONS

International peer-reviewed journals

Cornelis JT., Ranger J., Iserentant A. and Delvaux B. (2010) Tree species impact the terrestrial cycle of silicon through various uptakes, *Biogeochemistry* 97:231-245.

Cornelis JT., Ranger J., Titeux H. and Delvaux B. Distribution of amorphous silica in a temperate forest soil under three common tree species. Submitted to *European Journal of Soil Science*.

Cornelis JT., Delvaux B., Cardinal D., André L., Ranger J. and Opfergelt S. (2010) Tracing the mechanisms controlling the release of dissolved silicon in forest soil solutions using Si isotopes and Ge/Si ratios. *Geochimica et Cosmochimica Acta*, in press, doi 10/1016/j.gca.2010.04.056.

Cornelis JT., Delvaux B. and Titeux H. The contrasting silicon uptakes by coniferous trees: a hydroponic experiment. Accepted with minor modifications in *Plant and Soil*.

Cornelis JT., Delvaux B., Ranger J. and Titeux H. The release of dissolved silicon in forest floor leachates is influenced by tree species. *Geoderma***,** in preparation.

Cornelis JT., Delvaux B., Georg B., Lucas Y., Ranger J. and Opfergelt S. The origin of dissolved silicon transferred from various soil-plant systems towards rivers: a review. *Biogeosciences,* in preparation.

Conference proceedings

Cornelis JT., Ranger J. and Delvaux B. Impact of tree species on the distribution of amorphous silica in an acid brown soil. *World congress of soil science*, 2010, Brisbane, Australia. Accepted

Van Ranst E., Alemayehu R., Dumon M., **Cornelis JT**., Diels J., Deckers J. On the origin of Planosols – the process of ferrolysis revisited. *World congress of soil science 2010*, Brisbane, Australia. Accepted

Cornelis JT., Delvaux B., Cardinal D., André L., Ranger J. and Opfergelt S. Ge/Si ratios and Si isotopes tracing mechanisms controlling the release of dissolved silicon in forest soil solutions. *ENVITAM PhD Day*, 2010, Namur, Belgium

Cornelis JT., Delvaux B., Cardinal D., André L., Ranger J. and Opfergelt S. Ge/Si ratios and Si isotopes tracing mechanisms controlling the release of dissolved silicon in forest soil solutions. *3rd workshop on the aqueous chemistry and biochemistry of silicon – Silicon by the sea*, 2009, San Diego, USA

Cornelis M. and **Cornelis JT.** Public debate, collective learning process and soil-plant system expertise: when scientific knowledge become socially distributed. *International Symposium - Change in governance as collective learning process: management, politics and ethics in forestry*, 2009, Nancy, France

Cornelis JT., Ranger J. and Delvaux B. Impact of tree species on the distribution of amorphous silica in an acid brown soil. *International conference geologica belgica – Challenge for the planet: earth science's prespective*, 2009, Ghent, Belgium

Cornelis JT., Ranger J., Iserentant A. and Delvaux B**.** Evaluation of silicon stocks and uptake in five forest stands on an acid brown soil. *Eurosoil congress, Soil-society-environment*, 2008, Vienna, Austria

Cornelis JT, Ranger J. and Delvaux B. Forest tree species impacts plant uptake of Si. *Silicon in Agriculture conference*, 2008, Port Edwards, South Africa

Cornelis JT., Ranger J., Lambin A., Delvaux B. Distribution of biogenic and inorganic silicon in three distinct forest floors from an acid brown soil. *ENVITAM PhD Day*, 2008, Liège, Belgium

Cornelis JT., Lambin A., Ranger J. and Delvaux B. Distribution of biogenic and inorganic silicon in three distinct forest floors from an acid brown soil. *International symposium on forest soils and ecosystem health*, 2007, Noosa, Australia